2015

Mathematical models for tumour invasion

Andrew Brett Holder
University of Wollongong

Mathematical Models for Tumour Invasion

A thesis submitted in fulfilment of the requirements for the award of the degree

Doctor of Philosophy

from

University of Wollongong

by

Andrew Brett Holder

B. Mathematics (Advanced) Honours Class 1

School of Mathematics and Applied Statistics

Certification

I, Andrew B. Holder, declare that this thesis, submitted in fulfilment of the requirements for the award of Doctor of Philosophy, in the School of Mathematics and Applied Statistics, University of Wollongong, is wholly my own work unless otherwise referenced or acknowledged. The document has not been submitted for qualifications at any other academic institution.

Andrew B. Holder

February 13, 2015

To Kirsten

Abstract

Mathematical modelling of tumour invasion and cancer development has grown dramatically in recent years, with mathematics being applied to understand more complex and specific tumour mechanisms such as angiogenesis and metastasis. One such mechanism that has gained attention is aerobic glycolysis due to the association of this mechanism with increased tissue invasion, increases in angiogenesis and metastasis and some evidence suggesting it causes an increase in chemoresistance. Aerobic glycolysis is an altered metabolism that results in the extracellular tumour environment becoming acidic. This acidity has been hypothesised to be a mechanism for invasion termed the acid-mediation hypothesis. This is the hypothesis that the acidification of the tumour and surrounding microenvironment causes destruction of normal tissue ahead of the tumour-host interface, removing competitive forces and allowing the tumour to invade. This thesis looks to develop mathematical models and methods for examining tumour invasion with these models and methods being applied to the acid-meditation hypothesis. Through the examination we hope to gain a better understanding of the implications of the acid-mediation hypothesis and potential methods that can be used to counteract this invasion. Our analysis will also provide a greater insight in to certain models for invasion and their limitations, as well as providing methods for the analysis of similar models.

Acknowledgements

I would like to sincerely thank my supervisor Marianito Rodrigo for his support, advice, encouragement and for agreeing to supervise a student he had only just met. Your work ethic, attention to detail and rigor have been invaluable in helping me complete this venture.

My thanks go to James McCoy for encouraging me to pursue a PhD and getting me started on my research journey.

To all my mathematics teachers at Bomaderry High School and my Lecturers at the University of Wollongong, you all helped me to fall in love with mathematics and started me on this road, for that I am truly grateful.

To Noel Cressie, you have been truly inspirational and I have learnt so much from working for you, I am very thankful for the opportunity you gave me.

My thanks go to my friends and fellow PhD students, Luke, Carson, Mitch, James, Scott, Chris and Koen, you have been a great support network. Thanks for all the coffee breaks, lunch breaks, occasional dinners and for allowing me to hijack your time with random conversations. I have learnt something from everyone of you and would not have come this far without you guys being there.

Sincerest gratitude to my parents, Margaret and Nigel Holder, for your love and support no matter the circumstances. You are there in the good times and the bad; without your hard work and support for the family I would not be where I am today.

Finally, to my beautiful, loving and intelligent partner, Kirsten Ricetti. Thank you for believing in me, for your encouragement and for being my motivation to complete my PhD. I met you when I started this mammoth task and you stuck with me the whole way through. I love you and you are my best friend, you helped make this possible.

Contents

List of Figures v

List of Tables vii

List of Abbreviations ix

1 Introduction 1

1.1 Tumours and their characteristics . . . 2

1.1.1 Avascular and vascular tumours . . . 2

1.1.2 Tumour-induced angiogenesis . . . 3

1.1.3 Metastasis . . . 6

1.1.4 Enhanced ability to sustain growth . . . 7

1.1.5 The Warburg effect . . . 8

1.1.6 Treatment methods . . . 11

1.2 Mathematical modelling of tumour growth . . . 13

1.2.1 Early growth models . . . 13

1.2.2 Angiogenesis . . . 14

1.2.3 Metastasis . . . 15

1.2.4 Warburg effect and the acid-mediation hypothesis . . . 16

1.2.5 Treatment . . . 18

1.3 Mathematical methods . . . 20

1.3.1 ODE models, steady-state solutions and periodic solutions . . . 20

1.3.2 Reaction-diffusion models and travelling waves . . . 20

1.3.3 Parameter estimation . . . 22

1.4 Aims of thesis . . . 25

2 AMTI with nonlinear acid production term **27**

2.1 Introduction 27

2.2 Model formulation 28

2.3 Fast travelling waves 33

2.3.1 Leading-order approximations 33

2.3.2 Stability 34

2.3.3 Statement of results for fast waves 38

2.4 Slow travelling waves 38

2.4.1 Outer solutions 40

2.4.2 Inner solutions 41

2.4.3 Uniform approximations 43

2.4.4 An estimate for the interstitial gap 45

2.4.5 Statement of results for slow waves 51

2.5 Numerical results 52

2.6 Discussion and concluding remarks 54

2.A Auxillary results 60

2.B Properties of interstitial gap estimate 64

2.C Speed estimation 67

3 AMTI with chemotherapy intervention: I **69**

3.1 Introduction 69

3.2 Model formulation 70

3.3 Constant infusion of chemotherapy drug 76

3.3.1 Steady-state analysis 76

3.3.2 A reduced model with constant infusion 79

3.4 Periodic infusion of chemotherapy drug 80

3.4.1 Existence, uniqueness and stability of the periodic solution of a reduced system 82

3.4.2 Existence of co-existence periodic solution 91

3.4.3 Special periodic solutions of the full system 94

3.4.4 Stability of special periodic solutions to the full system 96

3.5 Discussion 99

3.6 Concluding remarks . . . 102
3.A Auxiliary definitions and results . . . 103
3.B Results for specific ODEs and corresponding periodic solutions . . . 105
3.C Details of steady-state analysis . . . 111

4 AMTI with chemotherapy intervention: II **121**
4.1 Introduction . . . 121
4.2 Model formulation . . . 122
4.3 Numerical simulations . . . 128
4.3.1 Constant infusion . . . 128
4.3.2 Periodic infusion . . . 135
4.4 Asymptotic analysis . . . 142
4.4.1 Analysis for invading tumour . . . 142
4.4.2 Analysis for receding tumour . . . 156
4.5 Discussion and concluding remarks . . . 162
4.A Auxiliary results . . . 165
4.B Tables of parameter values . . . 165

5 Integration-based parameter estimation **169**
5.1 Introduction . . . 169
5.2 Method . . . 170
5.3 Applications . . . 172
5.3.1 Bernoulli's smallpox model . . . 172
5.3.2 HIV dynamic model . . . 173
5.3.3 Tumour cell and chemotherapy drug interaction model . . . 177
5.4 Discussion and concluding remarks . . . 183

6 Conclusions **185**

List of Symbols **189**

Bibliography **191**

List of Figures

1.1 Hemotoxylin and Eosin staining of an avascular human neuroendocrine multicellular tumour spheroid section 4

1.2 Mammalian cell glucose metabolism 9

1.3 Tumour displaying Warburg effect and invasion 16

1.4 Comparison of typical profiles of "front" and "pulse" TW solutions 23

2.1 Fast TW solutions given by (2.3.3)–(2.3.6) 35

2.2 Asymptotic approximations given by (2.4.16)–(2.4.19) in the case ($\gamma = 2\alpha$) . . . 46

2.3 Initial conditions for numerical simulations 53

2.4 Numerical approximations of (2.2.4)–(2.2.6) with $\eta_2 = 4 \times 10^{-5}$ 55

2.5 Comparison of numerical and asymptotic ($\gamma = 2\alpha$) solutions of (2.2.4)–(2.2.6) with $\eta_2 = 4 \times 10^{-5}$ 56

2.6 Region of uniform solutions for the slow TWs in the α–γ plane 58

3.1 Simulation of (3.2.7) for $\alpha_1 = 1$, $\alpha_2 = 0.5$, $\beta_2 = 1$, $\beta_3 = 70$, $\beta_4 = 20$, $\delta_1 = 12.5$, $\delta_2 = 1.1$, $\delta_4 = 0.6$ 81

3.2 Simulation of (3.2.7) for $\alpha_1 = 1$, $\alpha_2 = 0.5$, $\beta_2 = 1$, $\beta_3 = 70$, $\beta_4 = 20$, $\delta_1 = 12.5$, $\delta_2 = 0.1$, $\delta_4 = 1$ 81

3.3 Simulation of (3.2.7) for $\alpha_1 = 0.25$, $\alpha_2 = 0.25$, $\beta_2 = 1$, $\beta_3 = 70$, $\beta_4 = 20$, $\delta_1 = 0.25$, $\delta_2 = 0.25$, $\delta_4 = 1$ 82

3.4 Diagram showing solutions $\mathbf{u}$ initially in $S \subset \mathbb{R}^3$ will be in S at time ρ 84

4.1 Initial conditions used for the numerical solutions 129

4.2 Contour plots u_1 and u_2 from simulations of (4.2.7)–(4.2.10) with parameters $\alpha_1 = 1$, $\alpha_2 = 0.5$, $\beta_2 = 1$, $\beta_3 = 70$, $\beta_4 = 20$, $\delta_1 = 12.5$, $\delta_2 = 1.1$, $\delta_4 = 0.6$ 130

4.3 Contour plots u_1 and u_2 from simulations of (4.2.7)–(4.2.10) with parameters $\alpha_1 = 1$, $\alpha_2 = 0.5$, $\beta_2 = 1$, $\beta_3 = 70$, $\beta_4 = 20$, $\delta_1 = 12.5$, $\delta_2 = 3$, $\delta_4 = 11$ 132

4.4 Contour plots u_1 and u_2 from simulations of (4.2.7)–(4.2.10) with parameters $\alpha_1 = 1$, $\alpha_2 = 3$, $\beta_2 = 1$, $\beta_3 = 70$, $\beta_4 = 20$, $\delta_1 = 5$, $\delta_2 = 1.25$, $\delta_4 = 3.5$ 133

4.5 Contour plots u_1 and u_2 from simulations of (4.2.7)–(4.2.10) with parameters $\alpha_1 = 1$, $\alpha_2 = 0.5$, $\beta_2 = 1$, $\beta_3 = 70$, $\beta_4 = 20$, $\delta_1 = 12.5$, $\delta_2 = 0.1$, $\delta_4 = 1$ 134

4.6 Contour plots u_1 and u_2 from simulations of (4.2.7)–(4.2.10) with parameters $\alpha_1 = 0.25$, $\alpha_2 = 0.25$, $\beta_2 = 1$, $\beta_3 = 70$, $\beta_4 = 20$, $\delta_1 = 0.25$, $\delta_2 = 0.25$, $\delta_4 = 1$ 135

4.7 Contour plots u_1 and u_2 from simulations of (4.2.7)–(4.2.10) with periodic infusion and parameters $\alpha_1 = 1$, $\alpha_2 = 0.5$, $\beta_2 = 1$, $\beta_3 = 70$, $\beta_4 = 20$, $\delta_1 = 12.5$, $\delta_2 = 1.1$, $\delta_4 = 0.6$ 137

4.8 Contour plots u_1 and u_2 from simulations of (4.2.7)–(4.2.10) with periodic infusion and parameters $\alpha_1 = 1$, $\alpha_2 = 0.5$, $\beta_2 = 1$, $\beta_3 = 70$, $\beta_4 = 20$, $\delta_1 = 12.5$, $\delta_2 = 3$, $\delta_4 = 11$ 138

4.9 Contour plots u_1 and u_2 from simulations of (4.2.7)–(4.2.10) with periodic infusion and parameters $\alpha_1 = 1$, $\alpha_2 = 3$, $\beta_2 = 1$, $\beta_3 = 70$, $\beta_4 = 20$, $\delta_1 = 5$, $\delta_2 = 1.25$, $\delta_4 = 3.5$ 139

4.10 Contour plots u_1 and u_2 from simulations of (4.2.7)–(4.2.10) with periodic infusion and parameters $\alpha_1 = 1$, $\alpha_2 = 0.5$, $\beta_2 = 1$, $\beta_3 = 70$, $\beta_4 = 20$, $\delta_1 = 12.5$, $\delta_2 = 0.1$, $\delta_4 = 1$ 140

4.11 Contour plots u_1 and u_2 from simulations of (4.2.7)–(4.2.10) with periodic infusion and parameters $\alpha_1 = 0.25$, $\alpha_2 = 0.25$, $\beta_2 = 1$, $\beta_3 = 70$, $\beta_4 = 20$, $\delta_1 = 0.25$, $\delta_2 = 0.25$, $\delta_4 = 1$ 141

4.12 Comparison of asymptotic and numerical solutions of (4.2.7)–(4.2.10) with parameters $\alpha_1 = 1$, $\alpha_2 = 0.5$, $\beta_2 = 1$, $\beta_3 = 70$, $\beta_4 = 20$, $\delta_1 = 12.5$, $\delta_2 = 0.1$, $\delta_4 = 1$, $\theta = 0.0122$ 153

5.1 Comparison of data observed by Halley with solution to Bernoulli's model 174

5.2 Comparison of simulated data with noise, model solution and model solution with estimated parameters 181

List of Tables

2.1 Table of parameters and estimated values for (2.2.1)–(2.2.3) 31

2.2 Table of non-dimensionalised parameters (2.2.4)–(2.2.6) 32

3.1 Table of parameters and estimated values for (3.2.1)–(3.2.4) 72

3.2 Table of non-dimensionalised parameters for (3.2.7) 75

4.1 Table of parameters and estimated values 166

4.2 Table of non-dimensionalised parameters 167

5.1 Means and standard deviations of estimated parameters values from 500 simulations of the HIV model with noise for time-step 0.1 177

5.2 Means and standard deviations of estimated parameters values from 500 simulations of the HIV model with noise for time-step 0.2 177

5.3 Means and standard deviations of estimated parameters values from 500 simulations of the HIV model with noise for time-step 0.4 178

5.4 Means and standard deviations of estimated parameter values from 500 simulations of the tumour cell and chemotherapy drug interaction model with noise for time-step 0.1 180

5.5 Means and standard deviations of estimated parameter values from 500 simulations of the tumour cell and chemotherapy drug interaction model with noise for time-step 0.2 180

5.6 Means and standard deviations of estimated parameter values from 500 simulations of the tumour cell and chemotherapy drug interaction model with noise for time-step 0.4 182

5.7 Means and standard deviations of MAE of simulated data and solution obtained with estimated parameters and MAV of noise from simulated data for time-step 0.1 182

5.8 Means and standard deviations of MAE of simulated data and solution obtained with estimated parameters and MAV of noise from simulated data for time-step 0.2 183

5.9 Means and standard deviations of MAE of simulated data and solution obtained with estimated parameters and MAV of noise from simulated data for time-step 0.4 183

List of Abbreviations

AMTI	Acid-mediated tumour invasion
APC	Antigen-presenting cell
ATP	Adenosine 5'-triphosphate
BC	Boundary condition
CTL	Cytotoxic T lymphocytes
DNA	Deoxyribonucleic acid
FdG	Fluorodeoxyglucose
HIV	Human immunodeficiency virus
LS	Least squares
MAE	Mean absolute error
MAV	Mean absolute value
MOP	Mitochondrial oxidative phosphorylation
ODE	Ordinary differential equation
PDE	Partial differential equation
PET	Positron-emission tomography
RD	Reaction-diffusion
SD	Standard deviation
SS	Steady-state

TPTW Time-periodic travelling wave

TSP Thrombospondin

TW Travelling wave

VEGF Vascular endothelial growth factor

Chapter 1

Introduction

As at 2012, the global risk of dying from cancer before the age of 75 was 10.4% and the risk of developing cancer before the age of 75 was 18.5% [103]. We can therefore see that cancer represents a significant health challenge for the world and that is why in 2008 the World Health Organization launched its Noncommunicable Disease Action Plan which includes cancer-specific interventions [208]. One of the key points of the plan is to coordinate and conduct research on the causes of human cancer and the mechanisms of carcinogenesis. Mathematical modelling has the capability to generate data, guide new research and understanding that would not otherwise be possible via traditional biological research techniques. Mathematics has the capability to inform researchers about what drives certain biological processes as well as distinguish between different control factors that cannot be determined by intuition or observation.

The amount of mathematical literature concerning the modelling of cancer and tumour growth has increased significantly in recent years and also developed in its complexity. Much of the literature concerns itself with solid avascular tumour growth and there is also a growing amount of articles concerned with modelling the growth of vascularised tumours, angiogenesis and metastasis, a key factor in malignancy. These mechanisms, along with many other aspects of cancer have generated interest from the mathematical community. However due to the complex nature and number of variables associated with *in vivo* tumour growth, the task of mathematically modelling cancer still remains a monumental challenge.

Due to the overwhelming diversity of cancer it is only possible to provide a selective review of the biological aspects of this disease. As such we will confine our discussion to some of the biological aspects of tumour growth and cancer that are of particular interest to mathematicians. This discussion will be a basic overview of different stages of tumour growth and an explanation

of mechanisms that drive them. There will then be a discussion of past and current mathematical models that have been proposed to examine the diverse aspects of tumour growth as well as some discussion of the challenges that still remain. A discussion of a selection of mathematical techniques relevant to tumour modelling and this thesis will then be presented.

1.1 Tumours and their characteristics

In vivo cancer growth is a complex phenomenon involving many interrelated processes with different types of cancers utilising their own unique combinations of biological mechanisms. As a result there are a multitude of important processes utilised by invading tumours that can be characterised. Here, summaries of biological characteristics of tumours that have particular interest to mathematicians will be presented.

1.1.1 Avascular and vascular tumours

An avascular tumour is one in which the cell population has no direct connection to the vascular system and as a result obtains all nutrients through diffusion from a nearby blood vessel. Due to the natural limitations resulting from obtaining nutrients from diffusion alone the growth of the tumour is very limited in this stage. In fact, tumours do not grow beyond two millimetres in diameter in this phase of growth due to this limitation [29]. The avascular growth phase is the early stage of tumour growth [34] which can be effectively studied *in vitro* by culturing three-dimensional multicellular spheroids from cancer cells [56, 192]. Avascular tumours typically develop to have three different cell layers that have a small amount of blending at their respective boundaries. The tumour will have an outer layer of proliferating cells that are exposed to the highest concentrations, available in this stage of growth, of nutrients required for normal cellular function. Hence the growth of the tumour is driven by this outer layer of proliferating cells. Note that the thickness of the outer layer is often small in comparison to the radius of the tumour spheroid. Below this layer is a quiescent layer consisting of cells that are in a static phase due to the reduced availability of nutrients as a result of consumption of nutrients by the proliferating layer. These cells no longer divide to generate new cells but rather their population only increases if a proliferating cell transition to this static state. In the centre of these tumours there exists a necrotic core made up of dead tumour cells that result from the nutrients available for live cells decreasing below a survival threshold or through mechanisms such as apoptosis. The necrotic core can often account for a majority of the tumour cell mass.

Note that cells can transition between being proliferative and quiescent in both directions whereas clearly the transition to necrosis is unidirectional. In Figure 1.1 the cross-section of an avascular multicellular tumour spheroid is shown that clearly displays the different cell layers.

Due to the natural limitations associated to the avascular stage of growth, tumours utilise mechanisms, that are discussed in the following section, to advance to vascular tumours. This stage of growth is, as the name suggests, when the tumour has obtained a direct connection to the vascular system and as such has an almost limitless and abundant supply of nutrients. Hence removing the impediments of low levels of nutrients experienced in the avascular stage, so much so that a vascular tumour can grow up to 16000 times the avascular size [25]. Whilst vascularisation of a tumour can result in almost exponential growth, it does not necessarily imply that the tumour is malignant. A tumour becoming vascular is however an important step in enabling a tumour to achieve malignancy as this is required for the process of metastasis [34], a common trait of malignant tumours. Hence much research is focused on preventing the process that allows tumours to transition from the avascular to vascular stage; this process is known as tumour-induced angiogenesis. It was noted that avascular tumours can effectively be studied *in vitro* whereas the same level of confidence cannot be assigned to *in vitro* analysis of vascular tumours due to the complex nature of the many processes required *in vivo* [36].

1.1.2 Tumour-induced angiogenesis

In Chaplain and Anderson [35] it is explained that primary tumour growth is initially as a result of division of cells. As is discussed in the previous section, this growth is limited by the availability of oxygen and nutrients diffused from nearby blood vessels. In fact, for cells located further than $100\mu\mathrm{m}$ from a capillary blood vessel, normal cellular function, survival and growth is uncommon [89]. Therefore this stage of growth provides significant growth barriers and as such tumours require further mechanisms to enable growth within the surrounding tissue. One such mechanism is the production of angiogenic substances to encourage the growth of blood vessels towards the tumour in order to obtain a richer source of nutrients than that obtained through diffusion alone. Angiogenesis is the process of sprouting new blood vessels from existing ones [90], this is in contrast to vasculogenesis which is the process of birth of new endothelial cells and their assembly into vascular tubes. It should be noted that inducing angiogenesis is a trait that is not unique to tumours and rather it is a normal cellular function, however in tumours the way angiogenesis is characterised is unique. Inducing angiogenesis is also a key component for tumours to transition

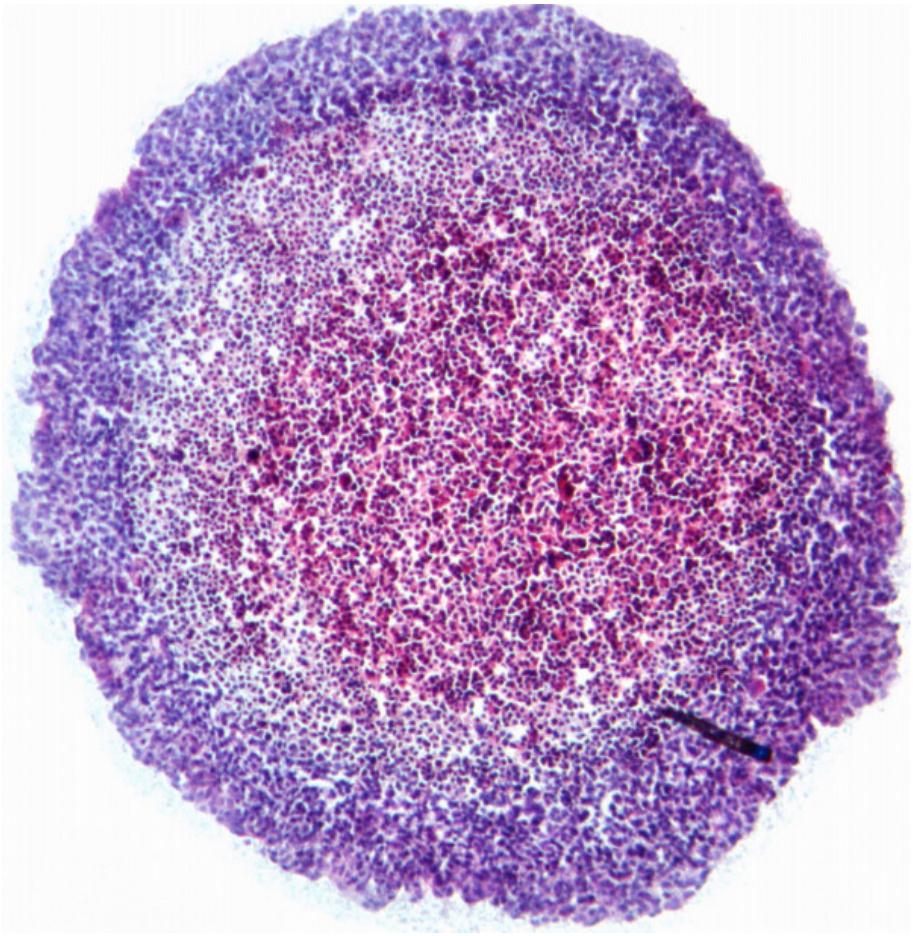

Figure 1.1: Hemotoxylin and Eosin staining of an avascular human neuroendocrine multicellular tumour spheroid section (by Monazzam et al. [143, Figure 9])

from the avascular stages of growth to the vascular stage and furthermore to achieve malignancy.

Angiogenesis is an evolution that occurs very early in the development of cancers. This has been shown by analysis of premalignant lesions including dysplasias and *in situ* carcinomas revealing early activation of angiogenesis [88, 170], however activation of the "angiogenic switch" can occur at any stage of tumour development [18].

In normal cells the angiogenic switch is only turned on when required, meaning normal angiogenesis is a well-regulated and transitory process leading to a well-ordered vasculature. In contrast, during tumour growth the angiogenic switch is almost always on. Therefore, as described by Hanahan and Weinberg [90] and the references therein, tumour vasculature is marked by precocious capillary sprouting, complicated and excessive vessel branching, distorted and enlarged vessels, abnormal blood flow, microhemorrhaging, leakiness, and unusual levels of endothelial cell proliferation and apoptosis. One advantage, for the tumour, of this irregularity and leakiness in the vasculature is that it enables metastasis by making it easier for metastatic cells to enter the vasculature [46]. Now in the case of tumours, the angiogenic switch appears to be regulated by encouraging mechanisms that induce angiogenesis and suppressing measures that oppose angiogenesis. A prominent angiogenesis inducer is vascular endothelial growth factor-A (VEGF-A). The genes that regulate VEGF-A work by encoding ligands that manage the development of new blood vessel growth in embryonic and postnatal development, in endothelial survival and in physiological and pathological situations in adulthood [90]. Such physiological and pathological situations in adulthood include tissue-repair and wound healing [7]. The VEGF gene expression is commonly upregulated by hypoxia and oncogene signalling [32, 46, 65, 130] leading to high production of ligands that promote angiogenesis in tumours. A common inhibitor of angiogenesis is thrombospondin-1 (TSP-1) which works by binding endothelial cells' receptors which causes suppressive signals to counter the signals that promote angiogenesis. Experiments with cultured cells from Li–Fraumeni patients show that tumour cells display a decline in TSP expression [86] and hence a decrease in the suppressive angiogenic signalling. Hence it can be seen that a combination of increased promotive and decreased suppressive chemical signals are produced to cause far more unregulated blood vessel development in tumour populations to enable invasion through greater availability of resources and increased ability to metastasize.

1.1.3 Metastasis

Metastasis is the mechanism in which primary tumour colonies disseminate cancer cells to distant tissues where those cells subsequently adapt to these foreign tissue microenvironments and form secondary colonies at these sites. The process of invasion and metastasis is often described by a series of distinct steps known as the invasion-metastasis cascade [193, 196]. The series of steps starts with local invasion by the primary tumour, then intravasation[a] of cancer cells into nearby blood and lymphatic vessels, then transport and survival from immune clearance of these cells through these systems until the extravasation[b] of these cells into secondary tissue sites, the cells then form small nodules of cancer cells (micrometastases) and then undergo the final step, known as colonisation, in which the micrometastases grow into macroscopic tumours.

Successful colonisation does not necessarily follow from cell dissemination as in many patients micrometastases have successfully disseminated but never develop into secondary tumour colonies [141, 193]. However some tumours produce suppression factors that make micrometastases dormant as shown by the sudden metastatic growth after removal of the primary tumour [52]. Other forms of cancer may remain dormant for a period of decades until such time as the micrometastases have adapted to the foreign micro environment and successfully colonise [12]. Metastatic dissemination is traditionally thought of as the final stage of tumour development, however there is evidence of early stage tumours disseminating cells with premalignant lesions in both mice and humans disseminating cells [39, 111]. Whilst there is evidence of early dissemination, the evidence is lacking for the ability of these cells to colonise in secondary locations.

Most disseminated cancer cells are unlikely to be adapted to the microenvironment they travel to and as such will need to develop adaptations if they are to colonise [87]. The adaptations will be determined by the type of disseminated cell and the microenvironment to which the cells have travelled. Certain disseminated cancers may be better adapted to certain tissue microenvironments which contributes to why some cancers have a predisposition to form secondary colonies in particular sites, e.g. colorectal and pancreatic cancers typically metastasise in the liver and lungs [147]. These secondary tumours may then begin a process of metastasis and due to the specific adaptations of the tumour cells may reseed the location of the primary tumour. As such the successful progression of the primary tumour in this environment may not be from usual tumour invasion mechanisms but rather from emigrants that have returned to the initial tumour location [109].

[a] The invasion of cancer cells through the basal membrane into a blood or lymphatic vessel [196]
[b] Escape of cells from the lumina of blood or lymphatic vessels [90]

Whilst the process of metastasis can be effectively described by this series of systematic steps and the physical behaviours that occur are well understood, many of the underlying mechanisms that govern metastasis are less well understood. This area of research represents what is still an emerging field, however there have been some significant steps made in determining important mechanisms governing metastasis.

1.1.4 Enhanced ability to sustain growth

Tumour cells utilise a combination of mechanisms that enable the populations to sustain accelerated growth. This includes mechanisms that both increase creation of new cells and decrease cell death. A fundamental trait of tumours is sustained proliferative signaling [90]. In normal cells the production of growth promoting signals that instruct cells to begin a cell-division (mitosis) cycle is a well-regulated process where cell growth has a high dependence on exogenous growth promotion factors. Due to this external dependence the mechanisms controlling mitogenic signalling of normal cells are poorly understood. Tumours deregulate this process to decrease their dependence on external signals and subsequently produce many of their own growth promotion signals [89] thus liberating them from their dependence on the normal tissue microenvironment. Furthermore, these signals often influence other cellular properties such as cell survival and metabolism [90]. Interestingly, since the mitogenic signalling controlling tumour cells are far more internalised the mechanisms underlying this are better understood [17, 61, 80, 101, 119].

Cancer cells achieve independent sustained proliferative signalling by utilising a number of techniques. The tumour cells may produce the growth factor ligands themselves resulting in self stimulation. Cells may also signal normal cells in the tumour stroma to produce growth promotion factors that are supplied to the tumour [37]. Tumour cells may also increase the number of cell surface receptors that respond to growth signalling making them far more responsive to lower amounts of growth factor. Cancer cells also sustain proliferative signalling by disrupting negative-feedback loops designed to dampen and regulate various types of signalling.

Sustained proliferative signalling is not without costs: studies suggest that excessive signalling can provoke counter measures from cells such as inducing senescence[a] and apoptosis[b] [40, 129, 216]. Due to this response to excessive growth signalling, oncogenic signalling may represent either a compromise or an optimisation between maximising mitogenic signalling and minimising anti-proliferative responses [90]. Some tumours however avoid this requirement by reprogramming

[a] The process of cell aging and degradation where cells enter into an irreversible non-proliferative state
[b] Programmed cell death

the mechanisms governing senescence and apoptosis.

The process of avoiding cell death is another mechanisms by which tumours enhance their growth. Apoptosis is induced by stresses such as elevated oncogene signalling, DNA damage and excessive proliferation [216]. By avoiding apoptosis a single tumour cell has the potential to undergo far more cycles of mitosis thus generating a far greater number of daughter cells with the same resistance to apoptosis. Hence this avoidance of apoptosis is often found in highly malignant tumours that are resistant to therapy [1, 120, 129]. This avoidance of cell death is closely related to cells becoming immortalised.

A further part of the story around tumour's enhanced ability to sustain growth is to transition to immortalisation. Most normal cells have a limited number of mitosis cycles, where this limitation occurs as a result of senescence and apoptosis. Should cells reproduce excessively they first enter into senescence and then, for cells that avoid this, they enter into apoptosis in which a large majority of the cell population dies. Should cells survive this crisis phase they can exhibit unlimited mitogenic potential and are seen as having transitioned into immortalisation. This transition to immortality is associated with the ability to protect telomeres on the ends of chromosomes which in turn prevents damage to chromosomal DNA caused by end-to-end fusion [23, 41, 184].

Tumour cells not only enhance growth by increasing growth promotion signals, they also decrease and evade growth suppressing signals and mechanisms. Many of these growth suppression programs are as a result of tumour suppressor genes that operate in various ways to limit cell growth and proliferation. These suppressor genes encode proteins that operate as part of the cellular circuitry that controls the decisions to proliferate, or to activate senescence or apoptosis [90].

1.1.5 The Warburg effect

A common characteristic of observable solid tumours is a lowered extracellular pH when compared to that of normal tissue [33, 158, 202, 203]. Normal tissue typically exhibits pH levels of 7.4 [81, 191] whereas tumour tissue has been observed regularly with an extracellular pH as low as 6.3 [33, 158]. It has been speculated that this lower than normal extracellular pH is a key mechanical reason for the malignancy and morbidity associated with tumour development [203]. This lowered extracellular pH is caused by an increased reliance on the process of glycolysis (lysis of glucose) for energy production. Normal cellular tissue relies primarily on the process of mitochondrial oxidative phosphorylation (MOP) to generate adenosine 5'-triphosphate (ATP) which corresponds to energy produced [200]. Whilst normal tissue can utilise the process of glycolysis for

ATP production, MOP is favoured since this is a far more efficient mechanism than glycolysis with complete MOP producing 36 ATP per glucose molecule whereas glycolysis produces only 2 ATP per glucose molecule [73, 200]. As such normal tissue tends to only utilise glycolysis when rapid energy production is required or there is insufficient oxygen to produce the energy requirements such as during strenuous physical exercise. Glycolysis involves first the conversion of glucose to pyruvate and then this is converted into lactic acid. In most mammalian cells, glycolysis is inhibited by the presence of oxygen as this enables cell mitochondria to oxidize pyruvate to carbon dioxide and water and hence not produce lactic acid. Conversion of glucose to lactic acid in the presence of oxygen is known as aerobic glycolysis or the "Warburg effect", named after Otto Warburg who made the observation of the distinct metabolism of cancers in 1924 [203, 204]. See Figure 1.2 for an illustration of MOP and glycolysis.

Interest in glycolysis and cancer metabolism has waned over the years since its initial discovery however more recently there has been a resurgence in research and interest in this phenomenon. A primary example of this is the inclusion of glycolysis as part of the "Hallmarks of Cancer" described by Hanahan and Weinberg [90], noting that it was absent from the previous list provided by the same authors 11 years earlier [89].

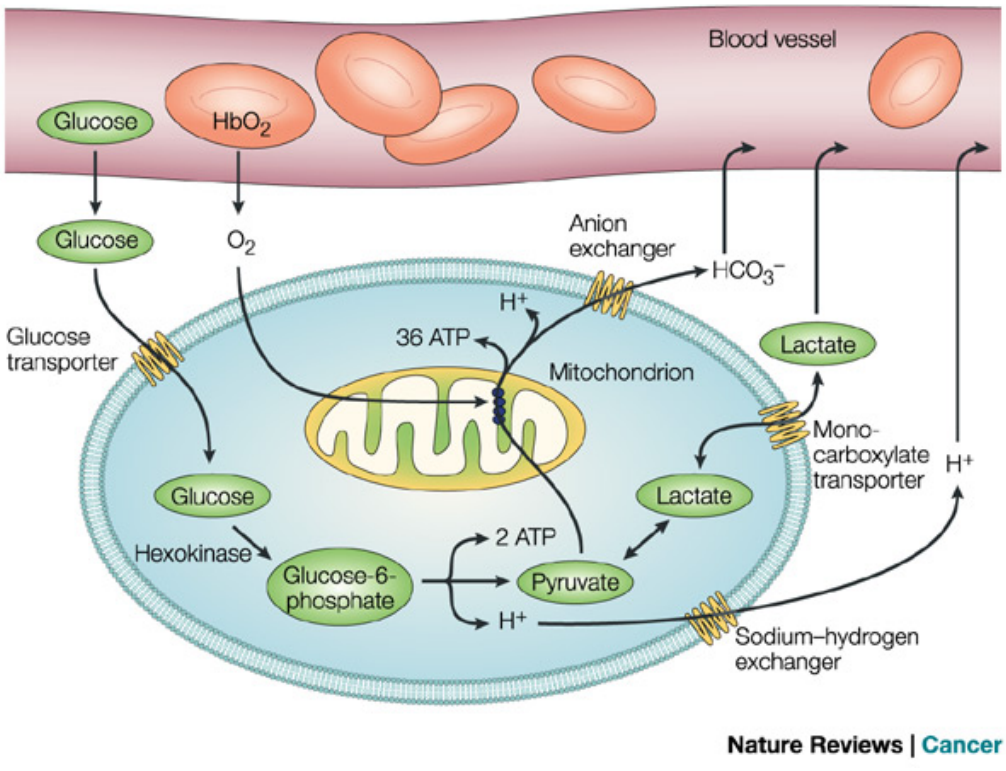

Figure 1.2: Mammalian cell glucose metabolism (Reprinted by permission from Macmillan Publishers Ltd: Nature Reviews Cancer [73], copyright 2004)

Due the fact that glycolysis is far less efficient at ATP production per glucose molecule than MOP it seems, on the surface, counter intuitive that tumours would have such an increased reliance on glycolysis to meet their ATP production requirements. However as noted in [204] the rate of MOP in cancer cells remains within a standard error to that of normal tissue and rather the rate of aerobic glycolysis can be up to ten times higher than that of the normal tissue such that for every 13 glucose molecules taken up one is used for MOP and the rest are processed using glycolysis causing an additional 24 ATP to be produced in the same time period. This results in a large uptake of glucose which allows cancerous tissue to be imaged by positron-emission tomography (PET) using the glucose analogue tracer fluorodeoxyglucose (FdG) [68, 91, 199, 205]. As a result of this behaviour a definitive explanation of the Warburg effect still eludes the biological community. The primary speculation for the cause of the Warburg effect is that it provides an evolutionary advantage to that of the neighbouring cells that utilise primarily MOP. This speculation is made as carcinogenesis can be describe by somatic evolution in which phenotypical adaptations occur due to factors such as barriers present in the microenvironment [24, 26, 61, 74, 75, 118, 190]. Various hypotheses have been provide as to what evolutionary advantage this provides and as to the conditions that form this evolution. Gatenby along with other authors have proposed that this evolution to aerobic glycolysis is the result of an adaptation to intermittent hypoxia in pre-malignant lessions [73, 74, 78]. This hypothesis suggests that this evolution initially occurs as a result of lowered oxygen conditions in regions of the host tissue and as such cells that have a greater capacity to utilise glycolysis will survive and therefore this trait will be passed on to subsequent daughter cells. After subsequent repetitions of this process the cells that are left represent cells that exhibit the Warburg effect. Gatenby further hypothesised that due to the production of lactic acid as a byproduct of glycolysis, the cells that have evolved require a resistance to apoptosis caused by acidosis, giving a competitive advantage over cells without this resistance to acid in the extracellular environment [71, 73, 74]. Furthermore, the lactic acid produced by aerobic glycolysis diffuses into the surrounding normal tissue creating an inhospitable environment for normal cells, which subsequently causes the destruction of these normal cells. Hence, this reduces population competition for the tumour cells resistant to acid and allows cellular invasion, this is known as the acid-mediation hypothesis [60, 63, 71, 140].

The proposed hypothesis that the Warburg effect is caused by intermittent hypoxia is challenged by Vander Heiden et al. [200] since cancers have been shown to develop this unique metabolism prior to exposure to hypoxic conditions. Examples of this include leukemic cells that reside within the bloodstream at high oxygen levels yet are still glycolytic [58, 83] and lung tumours in the air-

ways in highly aerobic conditions which still exhibits the Warburg effect [38, 148]. Due to these observations it has lead to the hypothesis that aerobic glycolysis is utilised to meet the energy requirements for cell proliferation [200]. This hypothesis is derived from noting that many unicellular organisms utilise fermentation, the microbial equivalent of aerobic glycolysis, in order to proliferate thus demonstrating the capability for aerobic glycolysis to meet the energy requirements for proliferation. Vander Heiden et al. [200] provide an alternative hypothesis based on the biomass requirements for cell proliferation. It is noted that in order to produce two viable daughter cells at mitosis a cell must replicate its entire cellular contents causing a large requirement for nucleotides, amino acids and lipids. For most mammalian cells only glucose and glutamine are utilised in significant quantities hence these molecules must supply most of the components required for cell growth and division. Considering this, Vander Heiden et al. [200] note that the complete oxidation of glucose via MOP is counter to the needs of the proliferating cell. Aerobic glycolysis allows for the diversion of the components required to produce the required biomass and therefore partially explains the selective advantage of the Warburg effect.

Whilst the hypotheses vary to the cause of the Warburg effect the common trait still remains in that there is increased extracellular acidification. Hence there is still the requirement for these cells to also have an increased resistance to apoptosis caused by acidosis and therefore an evolutionary advantage. This increased acidification results in further benefits such as enabling mutagenesis and clastogenesis [144], resistance to anthracyclines[a] as a result of greater phenotypic diversity [64] which is enabled by the mutagenic/clastogenic effect of acidosis. We also note that there have been several articles that have noted a link between increased acidity and decreased efficacy of host immune functions, e.g. [113, 117, 127, 128, 173–175, 183]. Examples include decreased lysis function of cytotoxic T lymphocyte (CTL) cells [175], decreased lymphocyte motility in highly acidic environments [173, 174] and inhibition of IL-2-stimulated lymphocyte proliferation [128]. Acidosis has also been shown to accelerate malignant invasion [60, 71, 135] and stimulate metastasis [180, 182].

1.1.6 Treatment methods

There exist two sides to the treatment of cancer and tumours. The first side is the treatment that looks to eradicate or manage the disease itself and the second side looks to treat issues associated with the health problems caused by the disease and often the treatment for the disease itself.

[a] A class of chemotherapy drug that prevents DNA replication during mitosis

This review will look at the former of these, however the latter topic does present many problems worth considering. Treatment methods for cancer are almost as diverse as cancer itself with methods that include targeted radiation therapies [57, 124, 154], surgical methods [185, 206], cytotoxic chemotherapy [22, 42, 57], immunotherapy [55, 186], antiangiogenic drugs [46, 176] and other cellular function specific treatments [165, 184, 213]. For the purpose of this review, immunotherapy and chemotherapy will be discussed as they are the most relevant to the mathematical modelling of treatment methods and the aims of this thesis.

Current and developing immunotherapies try to utilise the host's own immune system to manage the cancer and as such are an attractive means of treatment due to their potential for low toxicity to normal cells. A popular method for immunotherapy focuses on the activation/creation of antigen-specific T cells (T lymphocytes) through the use of bacterial and viral vectors or with DNA-based vaccines [55]. The bacterial and viral vectors work by loading vectors with a specific antigen, unique to the cancer, to be targeted, which then infects certain cells where a proportion of which undergo cell death. The cellular debris and the antigens contained within are taken up by antigen-presenting cells (APCs) which when activated present these antigens to T cells [55]. One drawback of using viral and bacterial vectors is the immune system may react to the presence of the vector rather than the antigen the vector is trying to deliver and as a result prime the immune system to attack the vectors rather than the cancers with the specific antigen [43, 55]. Another antigen-specific method is to use DNA-based vaccines as strains of DNA are able to be easily synthesised making it simple to target any antigen required [177]. The difficulty with DNA-based vaccines is that they have low immunogenicity[a] compared to viral and bacterial vectors. This is compensated for by incorporating molecules in the DNA-based vaccines that illicit a response from the immune system such as Toll-like receptor[b] antagonists that activate APCs.

Cytotoxic chemotherapy is a systemic treatment that involves the use of drugs that are administered either orally or intravenously which aim to kill cancer cells. The drugs target cells that rapidly divide and as such utilising cancers enhanced ability to grow [164]. Different cytotoxic drugs achieve this in different ways: anthracyclines and epipodophyllotoxins prevent DNA replication during mitosis; alkylating agents damage DNA and interfere with mitosis; antimetabolites which prevent cells from obtaining the nutrients they require to reproduce; plant alkaloids prevent mitosis by binding to proteins necessary for cell division; antitumour antibiotics bind to DNA to interfere with replication and transcription of DNA. Since these cytotoxic drugs target cells during

[a] The ability of a particular substance to provoke an immune response

[b] Class of proteins that recognise microbes and then activate immune cell responses [2]

cell division they also affect normal cells resulting in a level of toxicity that needs to be balanced when considering dosages. In particular, the cells affected most are those that divide most frequently such as bone marrow, gastrointestinal mucosa, hair follicles and gonads [42]. A common problem that can occur with chemotherapy is that of chemoresistance, which is a preexisting or acquired resistance of tumour cells to the cytotoxic drugs used [42]. Mechanisms for drug resistance include reduced drug uptake, up-regulation of DNA repair and enhanced detoxification by the cells [53]. An increased understanding of these mechanisms and ways to overcome them are an important and developing area of research.

1.2 Mathematical modelling of tumour growth

Given the above review of the biological characteristics of tumour growth, tumour invasion and methods for treatment this review will now proceed to discuss significant contributions to the mathematical modelling of these aspects of tumour growth. It will not be possible to provide a review of mathematical modelling of cancer that can do the field of research justice, however excellent summaries of work conducted in the area include Araujo and McElwain [6], Bellomo and Adam [13] and Preziosi [168].

1.2.1 Early growth models

The first models to consider the growth of tumours focused purely on the growth dynamics. In an article by Mayneord [138] the effect of X-radiations on the growth of the Jensen's rat sarcoma was observed. It was noticed that a linear law governed the rate of growth and that a necrotic core developed inside a thin proliferating outer shell of the tumour that could explain this linear rate of growth. The effect of this necrotic core was considered by Mayneord by developing a mathematical model for the growth of a tumour that considered the effect of different distributions of proliferating cells. It was shown that if the entire tumour was proliferating then exponential growth would be observed and as the region of proliferating cells was reduced to an outer shell the rate of growth also reduced. Studies of the effects of radiation on tumour cells were undertaken that lead to a paper by Gray et al. [84] in which the effect of the concentration of dissolved oxygen on radiotherapy was investigated. The articled resulted in radiotherapy being attempted at increased oxygen pressures.

In an attempt to model the initial exponential growth and then eventual exponential retardation of a tumour, Laird [115] applied the Gompertzian equation given by (1.2.1). Originating from an

actuarial model developed by Gompertz [82], Laird applied the model to tumour growth of primary and implanted tumours in the mouse, rat and rabbit. The model was shown to have great success modelling the observed tumour growth over a large range of tumour sizes. The Gompertz model considers the tumour population, $N(t)$, as a function of time, t, and is governed by:

$$\frac{\mathrm{d}N}{\mathrm{d}t} = rN\ln(N/K), \quad N(0) = N_0, \tag{1.2.1}$$

where r is the static growth rate, K is the carrying capacity and N_0 is the initial population size. Other popular phenomenological models for the dynamic growth of tumours include the logistic equation and the von Bertalanffy equation [25, Chapter 8].

Some of the early models of avascular tumour growth that considered the effect of the distribution of nutrients are attributed to Burton [28] and Greenspan [85]. Burton considered the development of tumours when nutrients are supplied to the tumour cells by diffusion from the periphery. Burton showed through this model that a necrotic core develops at a critical radius. It was further shown that under "diffusion-limitation", retardation of growth is experienced and that tumour growth fits the Gompertzian prediction.

Greenspan [85] developed a model for the nutrient concentration within a tumour and the surrounding tissue coupled with the internal pressure on the cells within the tumour. This model was for a three-dimensional tumour of an arbitrary shape, with proliferating, quiescent and necrotic layers. Greenspan formed a model that was given by a system of partial differential equations (PDEs) with moving boundary, which was then reduced to a system of ordinary differential equations (ODEs) by assuming that the tumour was spherically symmetric. From this reduction, an ODE was also found for the moving boundary which was investigated by a steady-state analysis. This article also considered a perturbation analysis to determine under what conditions a tumour slightly perturbed from spherical symmetry would return to a sphere. Greenspan did not continue to develop a governing equation for the motion of a point on the surface of an arbitrary tumour, and this still appears to be an open problem.

1.2.2 Angiogenesis

Angiogenesis has been considered mathematically in many articles, prominent examples include [34, 105, 132, 166] in which various factors responsible for this mechanism are analysed. Chaplain [34] focused on the effect of the migration of endothelial cells and of the concentration profile between

a tumour and nearby blood vessel of a tumour angiogenesis factor secreted by the tumour. Jones and Sleeman [105] looked at angiogenesis in general, not specifically for tumour growth, in an attempt to gain a better understanding of this normal bodily function. They modelled the response of endothelial cells to growth factors, the motion of the endothelial cells through the idea of reinforced random walks and capillary sprouting angiogenesis due to it being the predominant type of angiogenesis involved in tumourigenesis. Mantzaris et al. [132] and Plank and Sleeman [166] conducted a thorough review of the processes involved in tumour-induced angiogenesis and some mathematical models are presented in Mantzaris et al. [132]. Angiogenesis is significant as not only does it enable tumours to grow beyond the limitations of diffusion-limited growth but it is also a key factor in invasion and enabling tumours to reach the metastatic stage of growth.

The research into tumour-induced angiogenesis is still developing and is an area of research in which significant contributions can be made.

1.2.3 Metastasis

The mechanism of metastasis represents an important and challenging area of research. It is receiving ever increasing focus from those in the field of cancer and moreover, in the mathematical community. Recognition of this phenomenon was noted as early as 1829 with work conducted by Cruveilier [44], however mathematical models for this phenomenon only began to appear in the 1970s; some examples include [125, 126, 181]. The article by Saidel et al. [181] produced a model for the haematogenous metastatic process from a solid tumour. A compartmental model was considered that contained five subpopulations: tumour cells, vascular surfaces, invading tumour cells on the inner vessel surface, viable tumour cells arrested in pulmonary vessels and pulmonary metastatic foci. This framework developed by Saidel et al. [181] was extended by Liotta et al. [126] to a diffusion model which attempted to describe temporal changes in tumour cell and blood vessel radial distributions. A set of coupled diffusion equations with source and sink terms, in a spherically symmetric system, was proposed to describe both tumour density and surface area of tumour vessels as functions of time and radius.

More recent articles considering metastasis focus on specific aspects of the metastatic cascade. In the articles by Anderson et al. [5] and Orme and Chaplain [150] the assumption that tumour cells react to presence of blood vessels and move up a blood vessel gradient was considered. The assumption is also made that a necrotic core will develop as a result of overcrowding of tumour cells and a resulting collapse of blood vessels. Gerisch and Chaplain [79] examined the process of

cell invasion of tissue by considering cell–cell and cell–matrix adhesion. Painter [155] considered tumour invasion through the extracellular matrix by cellular shape changes and remodelling of the matrix.

Similarly to tumour induced angiogenesis, the mathematical modelling of metastasis is an emerging area of research which presents many challenges for mathematics.

1.2.4 Warburg effect and the acid-mediation hypothesis

Mathematical modelling related to the Warburg effect has been primarily concerned with examining the consequences of the Warburg effect rather than the Warburg effect itself. In one of the first models to examine these consequences, Gatenby and Gawlinski [71] proposed a set of reaction-diffusion (RD) equations to model the growth of tumours that produce excess H^+ ions, as a result of the Warburg effect, to create an acidic region that destroys surrounding healthy tissue. This then gives a region devoid of normal tissue into which the tumour can grow and thus acts as a mechanism for invasion. This process of invasion is called the acid-mediation hypothesis. This has been observed experimentally [60] and the model in [71] aimed to examine the effect of this mechanism on the growth of the tumour. An example of this effect is displayed in Figure 1.3.

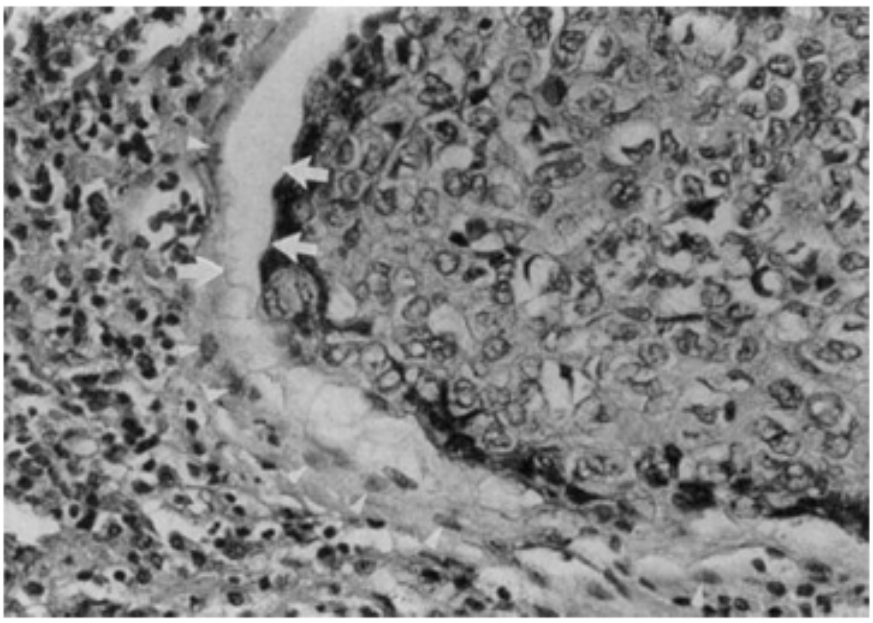

Figure 1.3: Tumour displaying Warburg effect and invasion (Reprinted from [71, p. 5750] with permission from AACR)

This mechanism has also been considered by Smallbone et al. [187] in which a model is derived similar to that of Greenspan [85] to consider the effect of a layer of excess H^+ ions at the

tumour surface. The acid-mediation hypothesis was examined by Patel et al. [159] with a cellular automaton based model that considered the effect vascular densities and tumour metabolism had in determining optimal conditions for tumour invasion. Interaction of the extracellular matrix and matrix metalloproteinases was considered in [134] where it was suggested there exists an optimal level of tumour aggressiveness. Other interesting articles modelling this phenomenon include Bianchini and Fasano [21], Fasano et al. [63] and Smallbone et al. [188]. Gatenby and Gawlinski's model consists of a system of three coupled RD equations that determines the spatial distribution and temporal evolution of three fields: the density of normal tissue $N_1(\mathbf{x}, t)$, the density of tumour tissue $N_2(\mathbf{x}, t)$ and the concentration of excess H^+ ions $L(\mathbf{x}, t)$ [71]. The model considers that N_1 and N_2 are governed by logistic growth, with a population competition relationship, as well as diffusion of the respective tissue particles with a diffusion coefficient that is determined by the other respective tissue density. The model accounts for loss of normal tissue due to interaction with the H^+ ions produced by the tumour tissue. The H^+ ions are considered to be produced relative to the density of the tumour tissue and to diffuse chemically. An uptake term is incorporated to take account of mechanisms for increasing pH. The model proposed in [71] is given by

$$\begin{aligned}
\frac{\partial N_1}{\partial t} &= r_1 N_1 \left(1 - \frac{N_1}{K_1} - \alpha_{12}\frac{N_2}{K_2}\right) - d_1 L N_1 + \nabla \cdot [D_{N_1}(N_2)\nabla N_1], \\
\frac{\partial N_2}{\partial t} &= r_2 N_2 \left(1 - \frac{N_2}{K_2} - \alpha_{21}\frac{N_1}{K_1}\right) + \nabla \cdot [D_{N_2}(N_1)\nabla N_2], \\
\frac{\partial L}{\partial t} &= r_3 N_2 - d_3 L + D_L \nabla^2 L,
\end{aligned}$$

where r_1 and r_2, and K_1 and K_2, are the logistic growth rates and carrying capacities of N_1 and N_2, respectively; α_{12} and α_{21} are the population competition parameters of N_1 and N_2, respectively; d_1 is the death rate due to H^+ ions-normal tissue interaction; D_{N_1} and D_{N_2} are the diffusion coefficients of N_1 and N_2, respectively; r_3 is the production rate of H^+ ions; d_3 is the reabsorption rate of the H^+ ions; and D_L is the diffusion coefficient of the H^+ ions.

Gatenby and Gawlinski [71] examined this model for $\alpha_{12} = \alpha_{21} = 0$ by a combination of numerical and analytical approximation techniques and found for certain parameter values an interstitial gap developed, that is, an area of high H^+ ion concentration almost entirely devoid of tumour and normal tissue. The existence of an interstitial gap was confirmed experimentally and can be seen in Figure 1.3. This model was further analysed by Fasano et al. [63] where an asymptotic analysis was performed in which it was found the model admits a fast wave solution and a slow wave solution. The fast wave solution was found to be linearly stable for all parameter values. The

slow wave solution predicted the existence of an interstitial gap and from this solution an estimate for the size of the gap was found. McGillen et al. [139] further extended this model to consider the effect of an acid buffer, such as sodium bicarbonate, on the advancement of the tumour. In a further article, McGillen et al. [140] considered the model in [71] with the assumption that tumour cells are also destroyed by the presence of acid but at a smaller rate than the acid destroys normal cells. This model demonstrated that the acid prevents the tumour population from obtaining the carrying capacity and furthermore, should the normal cell competition and destruction of tumour cells as a result of acid interaction be sufficiently strong, the tumour can be removed from the system. This suggests that the level of acidity, that established tumours develop, represents either a compromise or an optimisation to ensure the greatest chance of successfully invading. The solutions for the concentration of excess H^+ ions obtained in the models of Fasano et al. [63], Gatenby and Gawlinski [71] and McGillen et al. [140] present as a fronts due to the assumption of production of acid as a linear function of the tumour cell density. These solutions suggest that the concentration of acid will be highest inside the tumour, with an almost homogeneous concentration, rather than at the tumour-host interface. Tumours tend to present with very spatially heterogeneous acid profiles [92, 117] and there are experimental observations of higher acid concentration near the region of the interstitial gap [51, 92, 133]. Hence it still remains to consider a RD model that captures this nonuniform acid production, the resulting acid profile and the affect this has on the growth of the tumour.

We remark that the majority of articles that consider the acid-mediation hypothesis have examined the process as a relatively closed system, that is, without considering some form of external intervention such as treatment of the tumour with chemotherapy. An exception to this is McGillen et al. [139] that incorporates the effect of an acid buffer such as sodium bicarbonate into the model of Gatenby and Gawlinski [71]. Due to this gap in the literature we wish to propose and subsequently analyse a model for acid-mediated tumour invasion whilst treatment for the tumour is being administered.

1.2.5 Treatment

Mathematical modelling of treatment mechanisms largely focuses on the host's immune cells and on drug therapies such as cytotoxic chemotherapy. An immune response will usually utilise CTL and natural killer cells [49, 114, 136]. There are many models that consider the interaction between this aspect of the immune system and the corresponding effect on the growth of solid tumours.

Continuum models have been proposed in which the dynamics of total cell populations (i.e. tumour, normal and immune cell populations) have been considered by employing the use of ODEs, some examples include [14, 15, 48, 49, 114, 137]. These models, among other important results, showed that the immune response can explain both short-term and long-term variations in the growth of tumours such as oscillations and tumour relapse. Mallet and de Pillis [131] proposed a model that was a hybrid cellular automata–partial differential equation model to describe the interactions between a growing tumour near a nutrient source and the host immune system. A more recent model utilising a similar method was a hybrid agent based–delay differential equation model examined by Kim and Lee [110] that considered the effect of immune cell signalling to recruit further immune cells to attack the target tumour. Matzavinos et al. [136] considered a spatio-temporal model of the response of CTL cells to the growth of a solid tumour. This model included the dynamics of chemokine production that induces an immune response which includes the infiltration of T-cells capable of rejecting immunogenic tumours. Modelling of tumour-macrophage dynamics has been considered in spatio-temporal models proposed in [151–153]. These models attempt to display the effect that macrophages have on both the promotion and inhibition of the growth of tumours at the early stages of development.

There are many models that consider chemotherapy and the corresponding effect on the growth of solid tumours. Continuum models have been consider in which the dynamics of total cell populations and average chemotherapy drug concentration have been examined by employing the use of ODEs, some examples include [30, 31, 47, 157]. The example considered by Byrne [30] partly extends an earlier model by Tyson and Novak [198] to consider the dynamics of a tumour growing under the influence of a cytotoxic treatment that is administered periodically. There are other models that consider the addition of an immune response in a tumour cell and chemotherapy model [47, 49, 50] encouraged by experimental results suggesting an important impact of the host immune response on the effectiveness of a chemotherapy treatment. The model considered in [50] is an optimal control problem, similar to [27, 67, 156], designed to determine the optimal treatment given that the treatment was considered to have an adverse effect on immune cells.

It is noted that the effects of normal cell populations in models that consider chemotherapy have largely been neglected. Noted in Section 1.1.5 is a link between increased acidity and decreased efficacy of host immune functions, however there has yet to be a mathematical model considered to examine these observations, hence this has the potential for examination. Moreover, as mentioned in Section 1.1.5, highly acidic tumours have been shown to be resistent to anthracyclines as a result

of greater phenotypic diversity; this chemoresistance remains to be examined theoretically through the use of a mathematical model.

1.3 Mathematical methods

Here we present a brief description of some of the mathematical methods relevant to mathematical modelling of tumour invasion and to this thesis.

1.3.1 ODE models, steady-state solutions and periodic solutions

Ordinary differential equations regularly arise in the modelling of tumour growth; several examples have already been mentioned. These equations often arise when modelling average concentrations and densities or when it is assumed that the populations being considered are spatially homogeneous (i.e. are well mixed). Typically many of the models considered are first-order nonlinear systems, that is, of the form

$$\frac{\mathrm{d}\mathbf{u}}{\mathrm{d}t} = \mathbf{F}(t, \mathbf{u}),$$

where $\mathbf{u} : \mathbb{R}_+ \to \mathbb{R}^m$ and $\mathbf{F} : \mathbb{R}_+ \times \mathbb{R}^m \to \mathbb{R}^m$. Should this system be autonomous (i.e. $\mathbf{F}$ has no dependence on t), then a standard method for examining the properties of the solutions is a steady-state (SS) analysis in which the solutions for $\mathbf{u}$ are found that correspond to the derivative of $\mathbf{u}$ being zero, that is, when the solution is fixed (i.e. constant). Hence these solutions are found by solving $\mathbf{F}(\mathbf{u}) = 0$. A stability analysis is carried out to determine under what conditions these solutions are attractors or repellers to ascertain what the long-term behaviour of solutions to this system will be.

Should the system be periodic (i.e. $\mathbf{F}(t + T, \cdot) = \mathbf{F}(t, \cdot)$ for some $T > 0$ and for all $t \in \mathbb{R}_+$), then a standard method for analysis is to look for periodic solutions, where the period is that of the function $\mathbf{F}$ (i.e. $\mathbf{u}(t + T) = \mathbf{u}(t)$ for all $t \in \mathbb{R}_+$). In an analogous fashion to a SS analysis, it can then be determined under what conditions these solutions are attractors or repellers. For further information on SS analysis or periodic solutions see [62, 201] and the references therein.

1.3.2 Reaction-diffusion models and travelling waves

Systems of RD equations are popular in the modelling of ecology, biology, chemistry and physics to name a few. This is due to the fact that these equations combine the dynamics associated to the

interaction of relevant populations/substances within the model as well as the spatial motility that these populations/substances possess.

Consider $\mathbf{u} : \mathbb{R}_+ \times \mathbb{R}^n \to \mathbb{R}^m$ which represent state variables at time $t \in \mathbb{R}_+$ and position $\mathbf{x} \in \mathbb{R}^n$. A general system of RD equations is of the form

$$\frac{\partial \mathbf{u}}{\partial t} = L\mathbf{u} + F(t, \mathbf{x}, \mathbf{u}),$$

where L is a second order elliptic operator. As can be seen the system considered by Gatenby and Gawlinski [71], discussed in Section 1.2.4, is a system of RD equations. Other well known RD equations include the Fisher–KPP equation [66, 112], the equations for the Belousov–Zhabotinskii reaction [197], the Fitzhugh–Nagumo RD equations [178], the diffusive Lotka–Volterra equations [69, 106] and the time-periodic competition-diffusion equations [3, 10].

Autonomous system

Many of the RD systems that are considered are autonomous, that is, there are no terms in the governing equations that are explicit functions of time and position. An example of this is the Fisher–KPP equation given by

$$\frac{\partial u}{\partial t} = \eta \frac{\partial^2 u}{\partial x^2} + \beta u(1-u). \tag{1.3.1}$$

Autonomous systems are commonly observed to have travelling wave (TW) solutions. In the simplest case, a TW solution is a function of the form $u(x,t) = \varphi(x - \theta t)$, which is fixed profile that propagates along the real line with constant speed θ, where the sign of θ determines the direction the wave travels. Moreover, SSs of the corresponding reaction system form the boundary conditions (BCs) for the system. Knowledge of the properties of these SSs enables us to predict the direction in which the respective waves will travel and enables potential estimation and bounds on the speed at which these waves can propagate.

The Fisher–KPP equation is perhaps the most famous RD equation to exhibit TW solutions. The equation given by (1.3.1) has a solution of the form $u(x,t) = \varphi(x - \theta t)$ for $\theta \geq 2\sqrt{\eta\beta}$, where $\varphi(-\infty) = 1$ and $\varphi(\infty) = 0$. The TW solution for the Fisher-KPP equation is known as a "front"; these occur when the BCs of the solution are different. Should a TW solution have the same values for the BCs then the solution is known as a "pulse"; examples of a front solution and a pulse solution can be seen in Figures 1.4a and 1.4b, respectively. Note that fronts and pulses are

only particular cases of travelling waves; depending on the nature of the underlying biological or physical problem and the space dimension involved, one could also consider "target", "spiral" and "scroll" waves [108, 207].

Non-autonomous time-periodic coefficients

Another particular class of RD equations that are popular for modelling invasion of species are systems of RD equations with time-periodic coefficients. These arise as many processes vary seasonally, such as births, or are artificially performed in repeated cycles, such as treatment for diseases. A particular example of such a RD system is the time-periodic Lotka–Volterra RD system given by

$$\begin{aligned}\frac{\partial u_1}{\partial t} &= d_1(t)\frac{\partial^2 u_1}{\partial x^2} + u_1[a_1(t) - b_1(t)u_1 - c_1(t)u_2],\\ \frac{\partial u_2}{\partial t} &= d_2(t)\frac{\partial^2 u_2}{\partial x^2} + u_2[a_2(t) - b_2(t)u_1 - c_2(t)u_2],\end{aligned}$$

where a_i, b_i, c_i, d_i for $i = 1, 2$ are Hölder continuous and are T-periodic (i.e. $(a_i, b_i, c_i, d_i)(t) = (a_i, b_i, c_i, d_i)(t + T)$ for all $t \in \mathbb{R}_+$ and some $T > 0$, for $i = 1, 2$).

In an analogous fashion to many autonomous systems of RD equations permitting TW solutions, RD equations with time-periodic coefficients often permit time-periodic travelling wave (TPTW) solutions. A TPTW is a fixed surface that can be parameterised above a cylinder of infinite length; the surface propagates in the direction of the real line $z = x - \theta t$ with constant speed θ, where the sign of θ determines the direction the wave travels. Moreover, TPTWs connect periodic solutions of the corresponding spatially homogeneous system, which is analogous to how TWs connect the SS solutions of a corresponding kinetic system. Hence knowledge of the periodic solutions to the spatially homogeneous system enables predictions to be made about the direction in which the respective waves will travel and the speed of propagation. The time-periodic Lotka–Volterra RD system is a particular system that permits TPTW solutions, as was confirmed recently in [10, 212].

1.3.3 Parameter estimation

It has been commonplace for many years to use ODEs to model the physical world. The practice of using these models to predict and determine the behaviour of certain state variables is prolific in mathematical and scientific literature. The inverse problem of predicting the parameter values that appear in an ODE, based on observed data, has been studied considerably less and traditionally

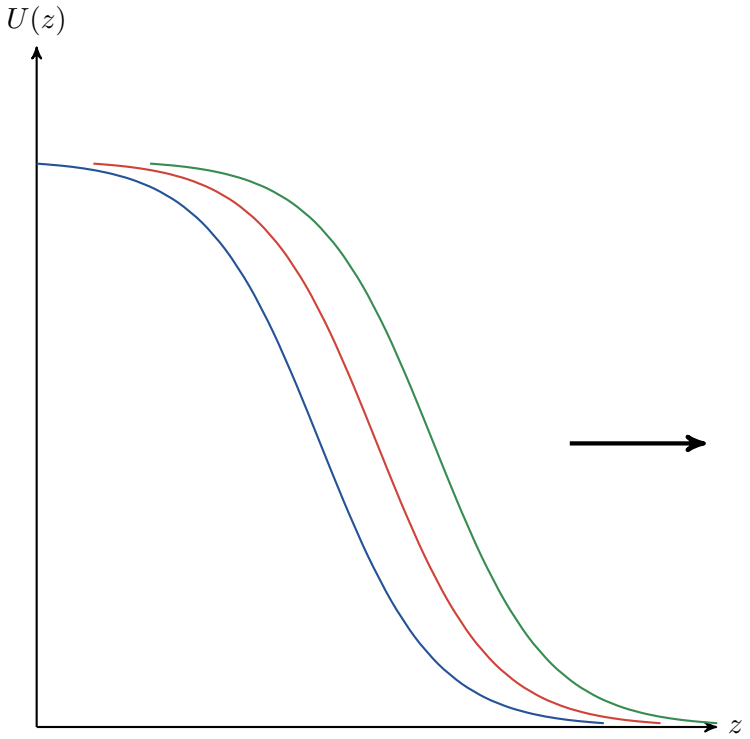

(a) An example of a "front" wave

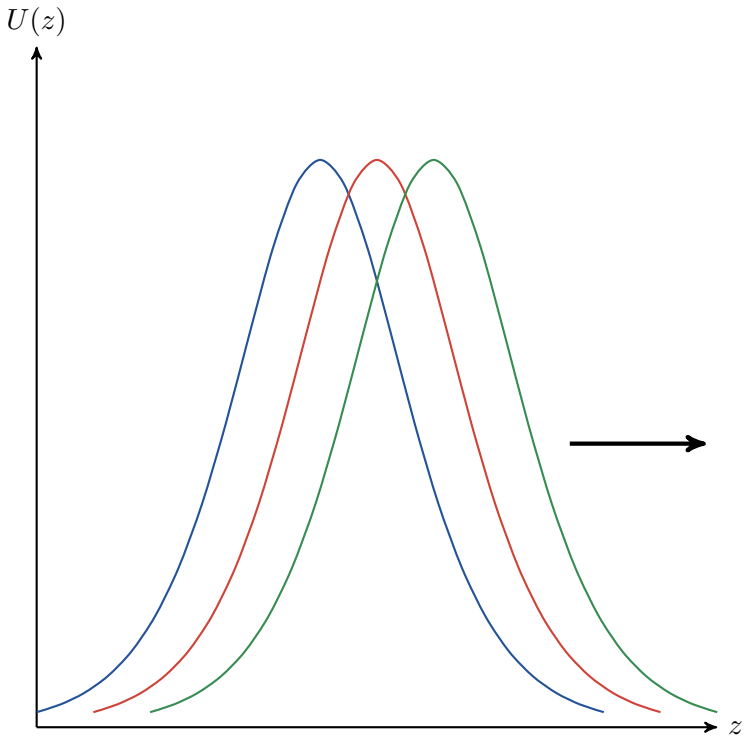

(b) An example of a "pulse" wave

Figure 1.4: Comparison of typical profiles of "front" and "pulse" TW solutions

only a few methods have been used, many of which approach the problem via a least squares (LS) fit method (see for example, [8, 11, 93, 121] and the references therein). The ability to estimate parameters accurately and efficiently is very important for areas such as tumour modelling as the future behaviour and treatment of a tumour is determined by various parameter values. We also note the ability to effectively estimate parameters is useful for the analysis of RD equations in which TW solutions arise. Travelling wave solutions transform the governing system of PDEs into a system of ODEs with an introduced paramater which needs to be determined. Using a parameter estimation technique and the solution obtained from solving the PDE system, with a sufficiently large time domain, the introduced parameter can be estimated.

The LS fit methods are based on minimising the distance between the observed data and values predicted by the model at discrete points in time. If the model can be solved analytically, then the exact solution is used to generate a distance function which is minimised with respect to the system parameters. Since many of these equations have many local minima, an algorithm must be used to find the global minimum [59]. Alternatively, when the model can only be solved numerically, a trial set of parameters is used to generate a solution in which the LS distance is calculated between the solution and the data. A trajectory is then found by altering the parameters and resolving the system numerically and comparing the LS distances. This method can be very inefficient and is not guaranteed to return the global minimum, hence much of the focus is on creating stable and efficient algorithms to optimise this approach [59, 172]. More recently some statistical based methods have been considered. These include a hierarchical Bayesian approach which is used to estimate dynamic parameters in HIV models [9, 100, 169], as well as a local kernel smoothing-based method to estimate constant parameters considered in [122]. Estimation of dynamic parameters was also considered in [171] using a technique known as principal differential analysis. This technique involves taking discrete data obtained from several sources and fitting a spline to each data set, then the approximations are substituted into an ODE and the dynamic parameters are then found by a LS procedure. A spline-based smoothing approach has also been considered in [172] to estimate constant parameters. An approach based on integrator theory has been considered in [160] in which a condition is placed on the integral of a particular function within the ODE to ensure convergence to the true parameter values.

1.4 Aims of thesis

This thesis aims to develop and extend both mathematical models and mathematical techniques for the study of tumour growth and invasion. The modelling will focus primarily on developing further understanding of the effects of the tumour metabolism on the interaction between tumour cells and normal cells. Moreover, it is an aim to develop understanding of how a tumour's metabolism can alter the effectiveness of a cytotoxic chemotherapy agent for treatment of an invading tumour. The thesis aims to develop and provide a reference for how asymptotic techniques can be utilised in the modelling of invasion. Moreover, a novel parameter estimation technique will be developed that can be used for the estimation of what are often difficult parameters to obtain.

In Chapter 2 a model for acid-mediated tumour invasion (AMTI) will be developed based on the work of Gatenby and Gawlinski [71] that considers the production of acid from the tumour metabolism as a nonlinear function of the tumour cell density[a]. The model will be given by a system of autonomous RD equations for which we will look for TW solutions. The system will by analysed utilising both numerical and asymptotic techniques in a similar fashion to [63].

Chapter 3 will see the development of a model for AMTI with the addition of a cytotoxic treatment response[b]. This model will assume well mixed populations and consider the infusion of a cytotoxic drug as a function of time leading to a non-autonomous system of ODEs. This model will be considered using steady-state analysis techniques and techniques for periodic solutions such as those provided in [62].

The work of Chapter 4 will extend the model developed in the previous chapter by removing the assumption that the populations are well mixed, leading to a model given by a system of RD equations[c]. By utilising the results of Chapter 3, the model will be analysed to try determine when it exhibits TW and TPTW solutions. The model will be analysed using a combination of numerical and asymptotic techniques.

A novel and computationally efficient parameter estimation technique will be developed and tested in Chapter 5[d]. The technique will utilise integration methods to provide estimates for parameters that arise in a class of systems of ODEs from discrete observations of the state variables.

A summary of the results and findings of the thesis will be presented in Chapter 6. This chapter will also contain discussions of potential further work.

[a] The content of Chapter 2 is based on the work of Holder et al. [98]
[b] The content of Chapter 3 is based on the work of Holder and Rodrigo [96]
[c] The content of Chapter 4 is based on the work of Holder and Rodrigo [97]
[d] The content of Chapter 5 is based on the work of Holder and Rodrigo [95]

Chapter 2

Acid-mediated tumour invasion with nonlinear acid production term

2.1 Introduction

Mathematical modelling of tumour growth has steadily increased in popularity in recent years with a range of growth mechanisms being considered through the application of various modelling techniques. One such technique is the use of RD equations due to their ability to capture invasive processes. Here we will utilise this technique to derive a model for tumour invasion.

In Chaplain and Anderson [35] it is explained that primary tumour growth is initially a result of division of cells. However once a critical size is reached, tumours require a further mechanism to enable growth within the surrounding tissue. One such mechanism, discussed in Chapter 1, is to alter the standard cellular metabolism to utilise glycolysis in aerobic conditions to increase energy production and the availability of the components required for mitosis and cell survival. This altered metabolism was first observed by Warburg [202] and has since been termed the "Warburg effect".

Recall from Chapter 1 that the Warburg effect causes acidification of the tumour and surrounding microenvironment, which is hypothesised to facilitate local invasion by destroying normal tissue at the tumour-host interface allowing the tumour to invade in the vacant region. This is termed the acid-mediation hypothesis and was first examined using a RD model by Gatenby and Gawlinski [71, 72]. The situation considered by Gatenby and Gawlinski [71, 72] corresponds to a one-dimensional setting and was later extended to consider higher-dimensional geometries, as well as

the occurrence of necrotic cores [187], glucose dynamics [21] and tumour cell death due to the acidic environment [140]. A key feature of their model is that for certain parameters an "interstitial gap" is observed, i.e. a region practically depleted of cells located right ahead of the invading tumour front. This phenomenon has been observed experimentally and was also discussed in [71]. The Gatenby and Gawlinski [71] model produced TW solutions in which the tumour invades the region occupied by normal tissue. The model's solution for the concentration of excess H^+ ions presents as a front [63, 71], which suggests that the concentration of acid will be highest inside the tumour, with an almost homogeneous concentration, rather than at the tumour-host interface. Tumours tend to present with very heterogeneous acid profiles [92, 117] and there is experimental observations of higher acid concentration near the region of the interstitial gap [51, 92, 133]. A cause for this pH gradient could be a large region of necrosis [71]. This localised acid concentration phenomenon has also been predicted mathematically in [188]. Therefore we propose to model the acid concentration as a pulse. In this way it will then be possible for the highest concentration of H^+ ions to be observed at or close to the tumour-host interface. Should we observe an interstitial gap in which the concentration of H^+ ions is greatest in or near this region, we would have a solution in line with experimental results and thus confirm the validity of this as an alternative model to that of Gatenby and Gawlinski for acid-mediated tumour invasion.

This chapter is organised as follows. In Section 2.2 we provide the details of the formulation of the model. In Section 2.3 we consider fast TWs and derive leading-order asymptotic formulas for these waves and analyse their stability. In Section 2.4 we look at slow TWs and derive asymptotic formulas for these waves. We also estimate the width of the interstitial gap. Section 2.5 shows the results of numerical simulations where we compare the solution of the RD system with our asymptotical formulas. Finally, we give some brief concluding remarks in Section 2.6. To keep the flow of our main arguments, the proofs of several results needed in Sections 2.3 and 2.4 are postponed to 2.A and 2.B at the end of the chapter.

2.2 Model formulation

We will now describe our model in detail. Let the populations at time s (in s) and position $\mathbf{y}$ (in cm) be denoted by:

- $N_1(\mathbf{y}, s)$, normal cell density (in $\mathrm{cells\,cm^{-3}}$);
- $N_2(\mathbf{y}, s)$, tumour cell density (in $\mathrm{cells\,cm^{-3}}$);

- $L(\mathbf{y}, s)$, excess H^+ ion concentration (in M).

We present the following hypotheses to govern our model:

(i) Both normal and tumour cells are governed by logistic growth in the absence of any kind of intervention [49, 71];

(ii) A population competition relationship exists between the normal and tumour cells [71];

(iii) The normal and tumour cells undergo cell diffusion and are assumed to have a diffusion coefficient proportional to the other respective cell density, i.e. the diffusion coefficients for the normal tissue and tumour tissue are $D_1(N_2)$ and $D_2(N_1)$, respectively [71];

(iv) The tumour tissue produces H^+ ions as a result of aerobic glycolysis [71] at a rate proportional to a function of the tumour cell density;

(v) The normal tissue interacts with the excess H^+ ions, leading to a death rate proportional to the concentration of H^+ ions [71, 140];

(vi) The excess H^+ ions diffuse chemically and are produced at a rate proportional to the tumour cell density until the latter reaches a threshold, after which the production rate decreases as the tumour tissue attains its carrying capacity. Moreover, an uptake term is included to take account of mechanisms for increasing extracellular pH [71].

The above hypotheses lead to the following system of partial differential equations:

$$\frac{\partial N_1}{\partial s} = \underbrace{\nabla \cdot [D_1(N_2)\nabla N_1]}_{\text{cell movement}} + \underbrace{r_1 N_1 \left(1 - \frac{N_1}{K_1} - a_1 \frac{N_2}{K_2}\right)}_{\substack{\text{logistic growth with cellular} \\ \text{competition}}} - \underbrace{d_1 L N_1}_{\substack{\text{normal cell} \\ \text{death by acid}}}, \tag{2.2.1}$$

$$\frac{\partial N_2}{\partial s} = \underbrace{\nabla \cdot [D_2(N_1)\nabla N_2]}_{\text{cell movement}} + \underbrace{r_2 N_2 \left(1 - \frac{N_2}{K_2} - a_2 \frac{N_1}{K_1}\right)}_{\substack{\text{logistic growth with cellular} \\ \text{competition}}}, \tag{2.2.2}$$

$$\frac{\partial L}{\partial s} = \underbrace{D_3 \nabla^2 L}_{\text{acid diffusion}} + \underbrace{r_3 N_2 \left(1 - \frac{N_2}{K_2}\right)}_{\text{acid production}} - \underbrace{m_3 L}_{\text{acid uptake}}. \tag{2.2.3}$$

As in [71], with a slight abuse of notation, we let the diffusion coefficients D_1 and D_2 be given by

$$D_1(N_2) = 0, \qquad D_2(N_1) = D_2\left(1 - \frac{N_1}{K_1}\right)$$

where D_2 (in $\mathrm{cm}^2 \cdot \mathrm{s}^{-1}$) is constant. The convention has been used of the subscripts for each parameter corresponding to the relevant equation: r represents growth rate; K represents carrying capacity; a represents population competition strength; d represents rate of decrease due to interaction; D is diffusion coefficient; m represents decrease through system mechanisms. We will make the assumption that the competition coefficient $a_2 = 0$ as we wish to consider a system in which a tumour is invading. Hence it is reasonable to assume that the death of tumour cells due to interaction with normal tissue will be negligible, provided the tumour is not less efficient at consuming available nutrients than the nearby normal tissue as a consequence of acid resistance. Note that Gatenby and Gawlinski [71] assumed that both $a_1 = 0$ and $a_2 = 0$. A recent article by McGillen et al. [140] considered a generalisation of the Gatenby and Gawlinski model with non-zero competition parameters and a destruction term for the tumour by the presence of acid. Gatenby and Gawlinksi also assumed that the excess H^+ ions are produced at a rate proportional to the tumour cell density throughout, i.e. in (2.2.3) they had the term $r_3 N_2$ instead of the logistic-type term $r_3 N_2(1 - N_2/K_2)$. This represents a notable difference in our approach to that used in the models considered by Gatenby and Gawlinski [71] and McGillen et al. [140]. For simplicity we will consider the system given by (2.2.1)–(2.2.3) only in one spatial dimension, i.e. $\mathbf{y} = y \in \mathbb{R}$. The parameters used in the model, their interpretation and potential values/range of values have been provided in Table 2.1.

Making the substitutions

$$u_1 = \frac{N_1}{K_1}, \quad u_2 = \frac{N_2}{K_2}, \quad u_3 = \frac{d_1}{a_1 r_1} L, \quad t = r_1 s, \quad x = y\sqrt{\frac{r_1}{D_3}}$$

and letting

$$\delta_1 = a_1, \quad \beta_2 = \frac{r_2}{r_1}, \quad \beta_3 = \frac{d_1 r_3 K_2}{r_1^2 a_1}, \quad \eta_2 = \frac{D_2}{D_3}, \quad \delta_3 = \frac{a_1 m_3 r_1}{d_1 r_3 K_2},$$

Table 2.1: Table of parameters and estimated values for (2.2.1)–(2.2.3)

Parameter	Units	Description	Value	Source
r_1	s^{-1}	normal cell growth rate	$O(10^{-6})$	[49, 71]
r_2	s^{-1}	tumour cell growth rate	$O(10^{-6})$	[49, 71]
r_3	$\mathrm{M\,cm^3\,s^{-1}cells^{-1}}$	$\mathrm{H^+}$ ion production rate	2.2×10^{-17}	[133]
d_1	$\mathrm{M^{-1}\,s^{-1}}$	fractional normal cell kill by $\mathrm{H^+}$ ions	$O(1)$	[71]
m_3	s^{-1}	$\mathrm{H^+}$ ion removal rate	$O(10^{-4})$	[71]
K_1	$\mathrm{cells\,cm^{-3}}$	normal cell carrying capacity	5×10^7	[195]
K_2	$\mathrm{cells\,cm^{-3}}$	tumour cell carrying capacity	5×10^7	[195]
D_2	$\mathrm{cm^2\,s^{-1}}$	tumour cell diffusion coefficient	2×10^{-10}	[45]
D_3	$\mathrm{cm^2\,s^{-1}}$	$\mathrm{H^+}$ ion diffusion coefficient	5×10^{-6}	[123]
a_1	none	fractional normal cell death due to tumour cell	$O(1)$	chosen freely

we obtain the non-dimensionalised form of (2.2.1)–(2.2.3) given by

$$\frac{\partial u_1}{\partial t} = u_1(1-u_1) - \delta_1 u_1(u_2+u_3), \tag{2.2.4}$$

$$\frac{\partial u_2}{\partial t} = \eta_2 \frac{\partial}{\partial x}\left[(1-u_1)\frac{\partial u_2}{\partial x}\right] + \beta_2 u_2(1-u_2), \tag{2.2.5}$$

$$\frac{\partial u_3}{\partial t} = \frac{\partial^2 u_3}{\partial x^2} + \beta_3[u_2(1-u_2) - \delta_3 u_3]. \tag{2.2.6}$$

In the quantitative discussions presented in [71], η_2 was assumed to be a small parameter, i.e.

$$0 < \eta_2 \ll 1, \tag{2.2.7}$$

an assumption which is to be retained throughout this chapter. The motivation for (2.2.7) comes from the fact that η_2 is shown to be of the form $\eta_2 = D_2/D_3$, where D_2 and D_3 are the respective static diffusion coefficients of the tumour tissue and $\mathrm{H^+}$ ions. It is therefore natural to assume that D_3 is much larger than D_2. The parameter δ_1 in (2.2.4) measures the destructive influence of tumour tissue and the $\mathrm{H^+}$ ions on the healthy tissue, and therefore its value can be taken as an indicator of tumour aggressiveness. Note that unlike the system examined by Gatenby and Gawlinski [71], invasion is still possible if the acid concentration is sent to zero due to population competition. This is possible provided the tumour cell density is non-zero everywhere or if the normal cell density is below its respective carrying capacity due to the nonlinear diffusion term in (2.2.4). Whilst invasion is possible through competition alone, we wish to focus on the implications of acid-mediation on the system due to the increased ability to invade as a result of removal of the

aforementioned restrictions and effective increase in tumour aggressiveness. The parameter β_2 measures the growth rate of tumour tissue relative to the growth rate of the normal tissue. Hence, having $\beta_2 > 1$ implies tumour cells reproduce faster than normal cells and $\beta_2 < 1$ implies the converse. The parameter β_3 can be thought of as a production rate of H^+ ions, with a large value for β_3 representing a high production of acid. Lastly, the parameter δ_3 can be thought of as representing the strength of the uptake mechanisms for increasing extracellular pH relative to the production rate of the H^+ ions. The uptake of acid is mainly through the vasculature, so δ_3 changes primarily as a result of the density and proximity of blood vessels in and around the tumour and normal tissue. A summary of potential non-dimensional parameter values/range of values and interpretation of their meaning has been provided in Table 2.2.

Table 2.2: Table of non-dimensionalised parameters (2.2.4)–(2.2.6)

Parameter	Interpretation	Value/Range
δ_1	tumour aggressiveness	$O(1)$
δ_3	relative strength of pH uptake	$O(10^{-1})$
η_2	relative tumour-H^+ ion diffusion rate	$O(10^{-5})$
β_2	relative tumour growth rate	1.0
β_3	relative H^+ ion production rate	$O(10^2)$

The set of equations (2.2.4)–(2.2.6) is a RD system, and it should be noted that this type of system typically has TW solutions connecting some of their steady-states. This is especially true here since we are considering invasive processes. Let

$$(u_1, u_2, u_3)(x, t) = (\varphi_1, \varphi_2, \varphi_3)(z)$$

where $z = x - \theta t$ is a real number and θ is the wave speed. Substituting into (2.2.4)–(2.2.6) we obtain

$$0 = \theta\varphi_1' + \varphi_1(1 - \varphi_1) - \delta_1\varphi_1(\varphi_2 + \varphi_3), \tag{2.2.8}$$

$$0 = \eta_2[(1 - \varphi_1)\varphi_2'' - \varphi_1'\varphi_2'] + \theta\varphi_2' + \beta_2\varphi_2(1 - \varphi_2), \tag{2.2.9}$$

$$0 = \varphi_3'' + \theta\varphi_3' + \beta_3[\varphi_2(1 - \varphi_2) - \delta_3\varphi_3], \tag{2.2.10}$$

where $(\,)'$ represents differentiation with respect to z. Since we are modelling invasion we note that $\theta > 0$ and we are solving (2.2.8)–(2.2.10) with respect to the BCs

$$(\varphi_1, \varphi_2, \varphi_3)(-\infty) = (0, 1, 0),\ (\varphi_1, \varphi_2, \varphi_3)(\infty) = (1, 0, 0) \tag{2.2.11a}$$

when $\delta_1 \geq 1$, and

$$(\varphi_1, \varphi_2, \varphi_3)(-\infty) = (1 - \delta_1, 1, 0),\ (\varphi_1, \varphi_2, \varphi_3)(\infty) = (1, 0, 0) \tag{2.2.11b}$$

when $0 < \delta_1 < 1$. These BCs are obtained by observing that $(1, 0, 0)$, $(0, 1, 0)$ and $(1 - \delta_1, 1, 0)$ (when $0 < \delta_1 < 1$) are the relevant steady-states of the associated kinetic system.

2.3 Fast travelling waves

2.3.1 Leading-order approximations

We consider the case of the fast TW solution, i.e. $\theta = O(1)$ as $\eta_2 \to 0^+$. Define

$$(\varphi_{10}, \varphi_{20}, \varphi_{30})(z) = (\varphi_1, \varphi_2, \varphi_3)(z; 0).$$

Letting $\eta_2 \to 0^+$ in (2.2.8)–(2.2.10) yields the system of equations

$$0 = \theta\varphi_{10}' + \varphi_{10}(1 - \varphi_{10}) - \delta_1\varphi_{10}(\varphi_{20} + \varphi_{30}), \tag{2.3.1}$$

$$0 = \theta\varphi_{20}' + \beta_2\varphi_{20}(1 - \varphi_{20}), \tag{2.3.2}$$

$$0 = \varphi_{30}'' + \theta\varphi_{30}' + \beta_3[\varphi_{20}(1 - \varphi_{20}) - \delta_3\varphi_{30}],$$

with BCs given by (2.2.11). We see that (2.3.2) is a Bernoulli equation and can be solved explicitly to give

$$\varphi_{20}(z) = \frac{1}{2}\left(1 - \tanh\frac{\beta_2 z}{2\theta}\right). \tag{2.3.3}$$

Note that the boundary conditions $\varphi_{20}(-\infty) = 1$ and $\varphi_{20}(\infty) = 0$ are satisfied. To fix the phase of the TW, we assume that $\varphi_{20}(0) = 1/2$ without loss of generality. For later use we observe that

$$\varphi_{20}(z)[1 - \varphi_{20}(z)] = \frac{1}{4}\mathrm{sech}^2\frac{\beta_2 z}{2\theta}. \tag{2.3.4}$$

Invoking Lemma 2.A.1 in Appendix 2.A, and recalling (2.3.4), we have

$$\varphi_{30}(z) = \frac{1}{4}\frac{\beta_3}{\varrho_1 - \varrho_2}\left[\int_z^\infty \mathrm{e}^{\varrho_1(z-s)}\mathrm{sech}^2\frac{\beta_2 s}{2\theta}\,\mathrm{d}s + \int_{-\infty}^z \mathrm{e}^{\varrho_2(z-s)}\mathrm{sech}^2\frac{\beta_2 s}{2\theta}\,\mathrm{d}s\right], \tag{2.3.5a}$$

where

$$\varrho_1 = \frac{-\theta + \sqrt{\theta^2 + 4\delta_3\beta_3}}{2}, \quad \varrho_2 = \frac{-\theta - \sqrt{\theta^2 + 4\delta_3\beta_3}}{2}. \tag{2.3.5b}$$

We also obtain from Lemma 2.A.3 in Appendix 2.A that

$$\varphi_{10}(z) = \frac{\theta\Phi_0(z)}{\int_z^\infty \Phi_0(s)\,\mathrm{d}s}, \quad \Phi_0(z) = \mathrm{e}^{-\int_0^z [1-\delta_1\varphi_{20}(s)-\delta_1\varphi_{30}(s)]/\theta\,\mathrm{d}s}. \tag{2.3.6}$$

Therefore we have the following result:

Proposition 2.3.1. *Suppose that $\theta = O(1)$ as $\eta_2 \to 0^+$. Then, to leading order, we have*

$$\varphi_1(z;\eta_2) \simeq \frac{\theta\Phi_0(z)}{\int_z^\infty \Phi_0(s)\,\mathrm{d}s},$$

$$\varphi_2(z;\eta_2) \simeq \frac{1}{2}\left(1 - \tanh\frac{\beta_2 z}{2\theta}\right)$$

and

$$\varphi_3(z;\eta_2) \simeq \frac{1}{4}\frac{\beta_3}{\varrho_1 - \varrho_2}\left[\int_z^\infty \mathrm{e}^{\varrho_1(z-s)}\mathrm{sech}^2\frac{\beta_2 s}{2\theta}\,\mathrm{d}s + \int_{-\infty}^z \mathrm{e}^{\varrho_2(z-s)}\mathrm{sech}^2\frac{\beta_2 s}{2\theta}\,\mathrm{d}s\right],$$

where

$$\Phi_0(z) = \mathrm{e}^{-\int_0^z [1-\delta_1\varphi_{20}(s)-\delta_1\varphi_{30}(s)]/\theta\,\mathrm{d}s}.$$

Note that we have a regular perturbation problem since the solution of the reduced system satisfies all of the BCs [16]. Plots of the fast TW solutions for particular parameter values are displayed in Figures 2.1a and 2.1b. Note the pulse-like nature of the acid variable.

2.3.2 Stability

We now show that the solution (2.3.3), (2.3.5) and (2.3.6) is linearly stable. Let

$$(u_1, u_2, u_3)(x, t; \eta_2) = (\tilde{\varphi}_1, \tilde{\varphi}_2, \tilde{\varphi}_3)(z, \tau; \eta_2),$$

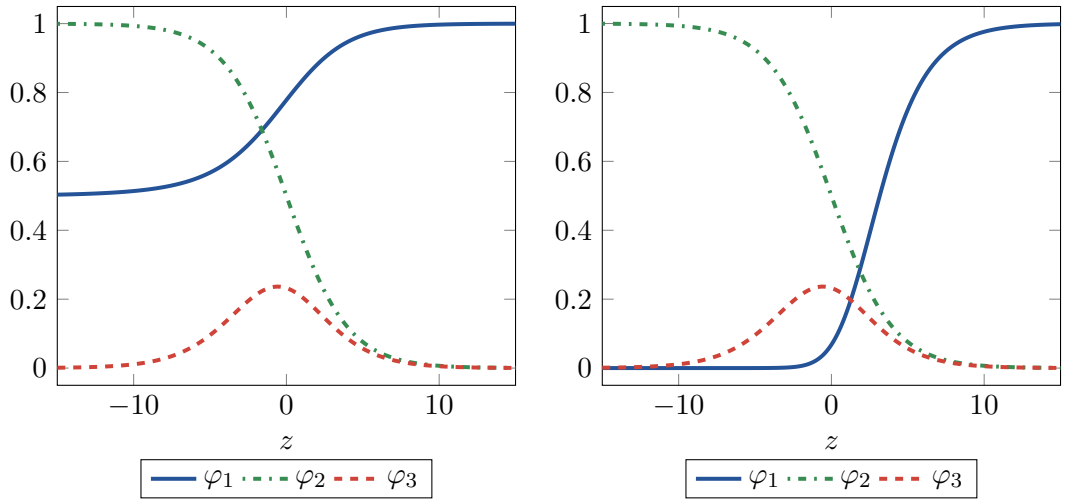

(a) $(\delta_1, \beta_2, \beta_3, \delta_3, \theta) = (0.5, 1, 3, 1, 2)$ **(b)** $(\delta_1, \beta_2, \beta_3, \delta_3, \theta) = (4, 1, 3, 1, 2)$

Figure 2.1: Fast TW solutions given by (2.3.3)–(2.3.6): (a) A solution with BCs given by (2.2.11b). (b) A solution with BCs given by (2.2.11a)

where $z = x - \theta t$, $\tau = t$ and $\theta > 0$ is a fixed wave speed. Noting that

$$\frac{\partial}{\partial t} = \frac{\partial}{\partial z}\frac{\partial z}{\partial t} + \frac{\partial}{\partial \tau}\frac{\partial \tau}{\partial t} = -\theta\frac{\partial}{\partial z} + \frac{\partial}{\partial \tau}, \quad \frac{\partial}{\partial x} = \frac{\partial}{\partial z}\frac{\partial z}{\partial x} = \frac{\partial}{\partial z}$$

and substituting this into (2.2.4)–(2.2.6), we obtain

$$\frac{\partial \tilde{\varphi}_1}{\partial \tau} = \theta\frac{\partial \tilde{\varphi}_1}{\partial z} + \tilde{\varphi}_1(1 - \tilde{\varphi}_1) - \delta_1\tilde{\varphi}_1(\tilde{\varphi}_2 + \tilde{\varphi}_3), \tag{2.3.7}$$

$$\frac{\partial \tilde{\varphi}_2}{\partial \tau} = \eta_2\frac{\partial}{\partial z}\left[(1 - \tilde{\varphi}_1)\frac{\partial \tilde{\varphi}_2}{\partial z}\right] + \theta\frac{\partial \tilde{\varphi}_2}{\partial z} + \beta_2\tilde{\varphi}_2(1 - \tilde{\varphi}_2), \tag{2.3.8}$$

$$\frac{\partial \tilde{\varphi}_3}{\partial \tau} = \frac{\partial^2 \tilde{\varphi}_3}{\partial z^2} + \theta\frac{\partial \tilde{\varphi}_3}{\partial z} + c[\tilde{\varphi}_2(1 - \tilde{\varphi}_2) - \delta_3\tilde{\varphi}_3]. \tag{2.3.9}$$

We look for a solution of (2.3.7)–(2.3.9) of the form

$$\tilde{\varphi}_1 = \varphi_1(z; \eta_2) + \varepsilon e^{-\lambda\tau}\phi_1(z) + \dots, \tag{2.3.10}$$

$$\tilde{\varphi}_2 = \varphi_2(z; \eta_2) + \varepsilon e^{-\lambda\tau}\phi_2(z) + \dots, \tag{2.3.11}$$

$$\tilde{\varphi}_3 = \varphi_3(z; \eta_2) + \varepsilon e^{-\lambda\tau}\phi_3(z) + \dots. \tag{2.3.12}$$

Here, $0 < \varepsilon \ll 1$, $(\varphi_1, \varphi_2, \varphi_3)$ is the TW solution with fixed speed θ for (2.2.8)–(2.2.11) and (ϕ_1, ϕ_2, ϕ_3) represent eigenfunctions. Substitute (2.3.10)–(2.3.12) into (2.3.7)–(2.3.9) and gather up the $O(1)$ terms. Since the leading order terms of (2.3.10)–(2.3.12) depend only the spatial variable z, the $O(1)$ terms give a system equivalent to (2.2.8)–(2.2.10), and thus $(\varphi_1, \varphi_2, \varphi_3)$ satisfies

this automatically. Collecting the $O(\varepsilon)$ terms gives the system

$$\theta\phi_1' + [1 + \lambda - 2\varphi_1 - \delta_1(\varphi_2 + \varphi_3)]\phi_1 = \delta_1\varphi_1(\phi_2 + \phi_3), \tag{2.3.13}$$

$$\theta\phi_2' + [\beta_2(1 - 2\varphi_2) + \lambda]\phi_2 = -\eta_2[(1 - \varphi_1)\phi_2' - \varphi_2'\phi_1]', \tag{2.3.14}$$

$$\phi_3'' + \theta\phi_3' - (\delta_3\beta_3 - \lambda)\phi_3 = -\beta_3(1 - 2\varphi_2)\phi_2. \tag{2.3.15}$$

We assume for the BCs that

$$\phi_i(\pm\infty) = 0 \quad \text{for } i = 1, 2, 3.$$

If we can find a nontrivial solution (ϕ_1, ϕ_2, ϕ_3) for some $\lambda > 0$ to the eigenvalue problem (2.3.13)–(2.3.15), then the fast TW solution will be linearly stable as the small perturbation will decay to zero.

Assume that $\lambda = O(1)$ as $\eta_2 \to 0^+$ and define

$$(\phi_{1,0}, \phi_{2,0}, \phi_{3,0})(z) = (\phi_1, \phi_2, \phi_3)(z; 0).$$

Setting $\eta_2 = 0$ in (2.3.13)–(2.3.15) gives

$$\theta\phi_{1,0}' + [1 + \lambda - 2\varphi_{10} - \delta_1(\varphi_{20} + \varphi_{30})]\phi_{1,0} = \delta_1\varphi_{10}(\phi_{2,0} + \phi_{3,0}), \tag{2.3.16}$$

$$\theta\phi_{2,0}' + [\beta_2(1 - 2\varphi_{20}) + \lambda]\phi_{2,0} = 0, \tag{2.3.17}$$

$$\phi_{3,0}'' + \theta\phi_{3,0}' - (\delta_3\beta_3 - \lambda)\phi_{3,0} = -\beta_3(1 - 2\varphi_{20})\phi_{2,0}. \tag{2.3.18}$$

Before continuing, it is easy to see that

$$\int_0^z [1 - 2\varphi_{20}(s)]\,\mathrm{d}s = \int_0^z \tanh\frac{\beta_2 s}{2\theta}\,\mathrm{d}s = \frac{2\theta}{\beta_2}\ln\cosh\frac{\beta_2 z}{2\theta}.$$

As (2.3.17) is a first-order separable equation we can solve it explicitly to give

$$\phi_{2,0}(z) = C\mathrm{e}^{-\lambda z/\theta}\mathrm{sech}^2\frac{\beta_2 z}{2\theta} = \frac{C}{[\mathrm{e}^{(\lambda+\beta_2)z/(2\theta)} + \mathrm{e}^{(\lambda-\beta_2)z/(2\theta)}]^2}$$

where C is an arbitrary constant. If $0 < \lambda < b$, then we have $\phi_{2,0}(\pm\infty) = 0$. So for any $C \neq 0$ this represents a nontrivial solution for $\phi_{2,0}(z)$.

We can now solve (2.3.18) by noting that it is in the form of (2.A.1) in Lemma 2.A.1 in Appendix 2.A, where $\kappa = \delta_3\beta_3 - \lambda$ and $f(s) = -\beta_3[1 - 2\varphi_{20}(s)]\phi_{2,0}(s)$. We can see that

$f(\pm\infty) = 0$. Thus if we set $0 < \lambda < \delta_3\beta_3$, then $I_1(\pm\infty) = I_2(\pm\infty) = 0$ and $\phi_{3,0}(\pm\infty) = 0$, where

$$\phi_{3,0}(z) = \frac{\beta_3}{\rho_1 - \rho_2}\left\{\int_z^\infty \mathrm{e}^{\rho_1(z-s)}[1 - 2\varphi_{20}(s)]\phi_{2,0}(s)\,\mathrm{d}s + \int_{-\infty}^z \mathrm{e}^{\rho_2(z-s)}[1 - 2\varphi_{20}(s)]\phi_{2,0}(s)\,\mathrm{d}s\right\}$$

and

$$\rho_1 = \frac{-\theta + \sqrt{\theta^2 + 4(\delta_3\beta_3 - \lambda)}}{2}, \quad \rho_2 = \frac{-\theta - \sqrt{\theta^2 + 4(\delta_3\beta_3 - \lambda)}}{2}.$$

We now consider (2.3.16) and note that it is a first-order linear ODE with solution given by

$$\phi_{1,0}(z) = -\frac{\delta_1}{\theta}\frac{\int_z^\infty \varphi_{10}(s)[\phi_{2,0}(s) + \phi_{3,0}(s)]\Phi(s)\,\mathrm{d}s}{\Phi(z)}, \tag{2.3.19}$$

where

$$\Phi(z) = \mathrm{e}^{-\int_0^z [2\varphi_{10}(s) + \delta_1\varphi_{20}(s) + \delta_1\varphi_{30}(s) - 1 - \lambda]/\theta\,\mathrm{d}s}.$$

We now find the positive values for λ that allows (2.3.19) to be consistent with the BCs. Applying Lemma 2.A.2 in Appendix 2.A with

$$g(s) = \frac{1}{\theta}[2\varphi_{10}(s) + \delta_1\varphi_{20}(s) + \delta_1\varphi_{30}(s) - 1 - \lambda]$$

we have $g(\infty) = (1 - \lambda)/\theta$. If we set $0 < \lambda < 1$, then $g(\infty) > 0$ and $\Phi(\infty) = 0$; hence we need to apply L'Hôpital's Rule to obtain the value for $\phi_{1,0}(\infty)$:

$$\lim_{z\to\infty} \phi_{1,0}(z) = \frac{\delta_1}{\theta}\lim_{z\to\infty} \frac{\varphi_{10}(z)[\phi_{2,0}(z) + \phi_{3,0}(z)]\Phi(z)}{-g(z)\Phi(z)} = 0.$$

To find $\phi_{1,0}(-\infty)$ we need to consider cases. When $\delta_1 > 1$ we have $g(-\infty) = (\delta_1 - 1 - \lambda)/\theta$. Hence if $0 < \lambda < \delta_1 - 1$, then we have $g(-\infty) > 0$ and $\Phi(-\infty) = \infty$. If $0 < \delta_1 < 1$, then $g(-\infty) = (1 - \delta_1 - \lambda)/\theta$. Therefore if $0 < \lambda < 1 - \delta_1$, then we have $g(-\infty) > 0$ and $\Phi(-\infty) = \infty$. Hence for $\delta_1 > 0$ and $\delta_1 \neq 1$ we have conditions on $\lambda > 0$ such that $\Phi(-\infty) = \infty$. If $\int_{-\infty}^\infty \varphi_{10}(s)[\phi_{2,0}(s) + \phi_{3,0}(s)]\Phi(s)\,\mathrm{d}s$ is finite, then $\phi(\pm\infty) = 0$; otherwise if it is infinite, then we apply L'Hôpital's Rule to obtain

$$\lim_{z\to-\infty} \phi_{1,0}(z) = \frac{\delta_1}{\theta}\lim_{z\to-\infty} \frac{\varphi_{10}(z)[\phi_{2,0}(z) + \phi_{3,0}(z)]\Phi(z)}{-g(z)\Phi(z)} = 0.$$

Thus, if $0 < \delta_1 < 1$ and $0 < \lambda < \min\{\beta_2, \delta_3\beta_3, 1-\delta_1\}$ or if $\delta_1 > 1$ and $0 < \lambda < \min\{\beta_2, \delta_3\beta_3, \delta_1 - 1\}$, then $(\phi_{1,0}, \phi_{2,0}, \phi_{3,0})(\pm\infty) = 0$ as required. This implies that the fast TW solution is stable. Note that we can not make any conclusions about the stability of the fast TW solution when $\delta_1 = 1$ as the above argument breaks down.

2.3.3 Statement of results for fast waves

The results of this section can be summarised as follows:

If the speed $\theta = O(1)$ as $\eta_2 \to 0^+$, then we obtain the following leading-order asymptotic approximations for $(\varphi_1, \varphi_2, \varphi_3)(z)$:

$$\varphi_1(z;\eta_2) \simeq \frac{\theta\Phi_0(z)}{\int_z^\infty \Phi_0(s)\,\mathrm{d}s},$$

$$\varphi_2(z;\eta_2) \simeq \frac{1}{2}\left(1 - \tanh\frac{\beta_2 z}{2\theta}\right)$$

and

$$\varphi_3(z;\eta_2) \simeq \frac{1}{4}\frac{\beta_3}{\varrho_1 - \varrho_2}\left[\int_z^\infty \mathrm{e}^{\varrho_1(z-s)}\mathrm{sech}^2\frac{\beta_2 s}{2\theta}\,\mathrm{d}s + \int_{-\infty}^z \mathrm{e}^{\varrho_2(z-s)}\mathrm{sech}^2\frac{\beta_2 s}{2\theta}\,\mathrm{d}s\right],$$

where

$$\varrho_1 = \frac{-\theta + \sqrt{\theta^2 + 4\delta_3\beta_3}}{2}, \quad \varrho_2 = \frac{-\theta - \sqrt{\theta^2 + 4\delta_3\beta_3}}{2}$$

and

$$\Phi_0(z) = \mathrm{e}^{-\int_0^z [1-\delta_1\varphi_{20}(s)-\delta_1\varphi_{30}(s)]/\theta\,\mathrm{d}s}.$$

A linear stability analysis showed that these solutions are linearly stable for $\delta_1 \neq 1$, with no conclusion able to be made about the stability in the case $\delta_1 = 1$.

2.4 Slow travelling waves

In this section we consider slow TWs. By this we mean that their wave speed is such that

$$\theta = \theta_0\eta_2^\alpha \qquad (\theta_0, \alpha > 0) \tag{2.4.1}$$

where $\theta_0 = O(1)$ as $\eta_2 \to 0^+$. We remark that if no other parameter assumptions are made our first-order asymptotic solution for φ_3 becomes trivial, i.e. $\varphi_3 \simeq 0$. In order to obtain a significant

matched asymptotic solution, we require the assumption that β_3 is large. This assumption corresponds physically to a high rate of acid production which would suggest a very high dependence on the process of glycolysis for energy production. The validity of this assumption is also confirmed when finding numerical solutions to (2.2.4)–(2.2.6) as in order to obtain a solution for φ_3 that is not "small", a value of β_3 must be used that is sufficiently large (e.g. see Figures 2.4c and 2.4d). Our assumption can also be seen to be plausible by using estimated parameter values (as stated in [63]) for the dimensional parameters that constitute β_3 to show that it is typically large. Hence we let

$$\beta_3 = \beta_{30}\eta_2^{-\gamma} \qquad (\beta_{30}, \gamma > 0) \tag{2.4.2}$$

where $\beta_{30} = O(1)$ as $\eta_2 \to 0^+$. As in [63], our analysis will utilise matched asymptotic expansions such as those found in [16].

Substituting (2.4.1) and (2.4.2) into (2.2.8)–(2.2.10) we obtain the system of equations

$$0 = \theta_0\eta_2^{\alpha}\varphi_1' + \varphi_1(1-\varphi_1) - \delta_1\varphi_1(\varphi_2+\varphi_3), \tag{2.4.3}$$

$$0 = \eta_2[(1-\varphi_1)\varphi_2'' - \varphi_1'\varphi_2'] + \theta_0\eta_2^{\alpha}\varphi_2' + \beta_2\varphi_2(1-\varphi_2), \tag{2.4.4}$$

$$0 = \eta_2^{\gamma}\varphi_3'' + \theta_0\eta_2^{\alpha+\gamma}\varphi_3' + \beta_{30}[\varphi_2(1-\varphi_2) - \delta_3\varphi_3], \tag{2.4.5}$$

with the BCs given by (2.2.11). Introducing the stretched inner variable $\xi = z/\eta_2^{\alpha}$ into (2.4.3)–(2.4.5), and letting

$$(\varphi_1, \varphi_2, \varphi_3)(z;\eta_2) = (\psi_1, \psi_2, \psi_3)(\xi;\eta_2),$$

we have the equivalent system

$$0 = \theta_0\dot{\psi}_1 + \psi_1(1-\psi_1) - \delta_1\psi_1(\psi_2+\psi_3), \tag{2.4.6}$$

$$0 = \eta_2^{1-2\alpha}[(1-\psi_1)\ddot{\psi}_2 - \dot{\psi}_1\dot{\psi}_2] + \theta_0\dot{\psi}_2 + \beta_2\psi_2(1-\psi_2), \tag{2.4.7}$$

$$0 = \eta_2^{\gamma-2\alpha}\ddot{\psi}_3 + \theta_0\eta_2^{\gamma}\dot{\psi}_3 + \beta_{30}[\psi_2(1-\psi_2) - \delta_3\psi_3], \tag{2.4.8}$$

where $\dot{(\,)}$ denotes differentiation with respect to ξ.

The outer and inner solutions are defined by

$$(\varphi_{1\text{out}}, \varphi_{2\text{out}}, \varphi_{3\text{out}})(z) = (\varphi_1, \varphi_2, \varphi_3)(z;0)$$

and

$$(\varphi_{1\text{in}}, \varphi_{2\text{in}}, \varphi_{3\text{in}})(\xi) = (\psi_1, \psi_2, \psi_3)(\xi; 0),$$

respectively. We require that the outer and inner solutions satisfy the matching conditions

$$(\varphi_{1\text{in}}, \varphi_{2\text{in}}, \varphi_{3\text{in}})(\pm\infty) = (\varphi_{1\text{out}}, \varphi_{2\text{out}}, \varphi_{3\text{out}})(0\pm).$$

2.4.1 Outer solutions

The outer solution $\varphi_{2\text{out}}$ is found by taking $\eta_2 \to 0^+$ in (2.4.4) and hence is governed by the algebraic equation

$$\beta_2 \varphi_{2\text{out}} (1 - \varphi_{2\text{out}}) = 0$$

where $\varphi_{2\text{out}}(-\infty) = 1$ and $\varphi_{2\text{out}}(\infty) = 0$. We can see that a function that satisfies these conditions is

$$\varphi_{2\text{out}}(z) = \begin{cases} 1 & \text{if } z < 0, \\ 0 & \text{if } z > 0. \end{cases} \tag{2.4.9}$$

Note that the discontinuity at $z = 0$ is not an issue as this is the outer solution only and we will find an inner solution valid for a small region about the point $z = 0$.

We find the governing equation for the outer solution $\varphi_{3\text{out}}$ by taking $\eta_2 \to 0^+$ in (2.4.5) to give us the algebraic equation

$$\beta_{30}[\varphi_{2\text{out}}(1 - \varphi_{2\text{out}}) - \delta_3 \varphi_{3\text{out}}] = 0$$

subject to $\varphi_{3\text{out}}(-\infty) = 0$ and $\varphi_{3\text{out}}(\infty) = 0$. Using (2.4.9) gives

$$\varphi_{3\text{out}}(z) = 0 \quad (z \neq 0). \tag{2.4.10}$$

Finally, consider (2.4.3) and take $\eta_2 \to 0^+$ to obtain

$$\varphi_{1\text{out}}(1 - \varphi_{1\text{out}}) - \delta_1 \varphi_{1\text{out}}(\varphi_{2\text{out}} + \varphi_{3\text{out}}) = 0, \tag{2.4.11}$$

where $\varphi_{1\text{out}}(-\infty) = 1 - \delta_1$ and $\varphi_{1\text{out}}(\infty) = 1$ for $0 < \delta_1 < 1$, while $\varphi_{1\text{out}}(-\infty) = 0$ and $\varphi_{1\text{out}}(\infty) = 1$ for $\delta_1 \geq 1$. Using (2.4.9) and (2.4.10), we solve (2.4.11) and obtain for $0 < \delta_1 < 1$

that

$$\varphi_{1\text{out}}(z) = \begin{cases} 1-\delta_1 & \text{if } z<0, \\ 1 & \text{if } z>0, \end{cases} \tag{2.4.12a}$$

while for $\delta_1 \geq 1$ we have

$$\varphi_{1\text{out}}(z) = \begin{cases} 0 & \text{if } z<0, \\ 1 & \text{if } z>0. \end{cases} \tag{2.4.12b}$$

2.4.2 Inner solutions

We proceed to the inner solutions by letting $\eta_2 \to 0^+$ in (2.4.6)–(2.4.8). Now, if $\alpha > 1/2$ in (2.4.7) we have

$$(1-\varphi_{1\text{in}})\ddot{\varphi}_{2\text{in}} - \dot{\varphi}_{1\text{in}}\dot{\varphi}_{2\text{in}} = 0,$$

which cannot satisfy the corresponding boundary conditions. Furthermore, if $\alpha = 1/2$ in (2.4.7) and take $\eta_2 \to 0^+$ we obtain an equation for $\varphi_{2\text{in}}$ given by

$$(1-\varphi_{1\text{in}})\,\ddot{\varphi}_{2\text{in}} - \dot{\varphi}_{1\text{in}}\dot{\varphi}_{2\text{in}} + \theta_0\dot{\varphi}_{2\text{in}} + \beta_2\varphi_{2\text{in}}\,(1-\varphi_{2\text{in}}) = 0.$$

However due to the fact that this equation is part of a coupled system of equations that cannot be solved easily, the asymptotic analysis cannot be completed for this case. Note also that if $\gamma < 2\alpha$ and we take $\eta_2 \to 0^+$ in (2.4.8) we have $\ddot{\varphi}_{3\text{in}} = 0$ and only the trivial solution can satisfy the boundary conditions. With these restrictions in mind we will therefore assume from this point onwards that

$$0 < \alpha < 1/2, \quad \gamma \geq 2\alpha.$$

Taking $\eta_2 \to 0^+$ in (2.4.7) yields an equation equivalent to (2.3.2); hence the inner solution for the tumour tissue is given by

$$\varphi_{2\text{in}}(\xi) = \frac{1}{2}\left(1 - \tanh\frac{\beta_2\xi}{2\theta_0}\right). \tag{2.4.13}$$

It is clear that $\varphi_{2\text{in}}$ satisfies

$$\varphi_{2\text{in}}(-\infty) = 1 = \varphi_{2\text{out}}(0-), \quad \varphi_{2\text{in}}(\infty) = 0 = \varphi_{2\text{out}}(0+).$$

For the H^+ ion concentration we need to consider two cases: $\gamma > 2\alpha$ and $\gamma = 2\alpha$.

Suppose first that $\gamma > 2\alpha$ and take $\eta_2 \to 0^+$ in (2.4.8). Then the governing equation for $\varphi_{3\text{in}}$ is

$$\beta_{30}[\delta_3\varphi_{3\text{in}} - \varphi_{2\text{in}}\,(1 - \varphi_{2\text{in}})] = 0.$$

Solving this algebraic equation gives

$$\varphi_{3\text{in}}(\xi) = \frac{1}{\delta_3}\varphi_{2\text{in}}(\xi)\,[1 - \varphi_{2\text{in}}(\xi)]\,,$$

which simplifies to

$$\varphi_{3\text{in}}(\xi) = \frac{1}{4\delta_3}\operatorname{sech}^2\frac{\beta_2\xi}{2\theta_0} \tag{2.4.14}$$

from (2.4.13) and (2.3.4).

In the case $\gamma = 2\alpha$, when we take $\eta_2 \to 0^+$, (2.4.8) becomes

$$\ddot{\varphi}_{3\text{in}} + \beta_{30}[\varphi_{2\text{in}}(1 - \varphi_{2\text{in}}) - \delta_3\varphi_{3\text{in}}] = 0,$$

which can be rewritten as

$$\ddot{\varphi}_{3\text{in}} - \delta_3\beta_{30}\varphi_{3\text{in}} = -\beta_{30}\varphi_{2\text{in}}(1 - \varphi_{2\text{in}}) = -\frac{\beta_{30}}{4}\operatorname{sech}^2\frac{\beta_2\xi}{2\theta_0} \tag{2.4.15}$$

using (2.3.4). We solve this equation subject to

$$\varphi_{3\text{in}}(-\infty) = \varphi_{3\text{out}}(0-) = 0, \quad \varphi_{3\text{in}}(\infty) = \varphi_{3\text{out}}(0+) = 0.$$

Applying Lemma 2.A.1 in Appendix 2.A to (2.4.15) yields

$$\varphi_{3\text{in}}(\xi) = \frac{1}{8}\sqrt{\frac{\beta_{30}}{\delta_3}}\left[\int_\xi^\infty \mathrm{e}^{\sqrt{\delta_3\beta_{30}}(\xi-s)}\operatorname{sech}^2\frac{\beta_2 s}{2\theta_0}\,\mathrm{d}s + \int_{-\infty}^{\xi} \mathrm{e}^{-\sqrt{\delta_3\beta_{30}}(\xi-s)}\operatorname{sech}^2\frac{\beta_2 s}{2\theta_0}\,\mathrm{d}s\right].$$

Lastly, we find the inner solution for the normal tissue. We consider (2.4.6) and take $\eta_2 \to 0^+$ to obtain

$$\theta_0\dot{\varphi}_{1\text{in}} + \varphi_{1\text{in}}\,(1 - \varphi_{1\text{in}}) - \delta_1\varphi_{1\text{in}}\,(\varphi_{2\text{in}} + \varphi_{3\text{in}}) = 0,$$

where

$$\varphi_{1\text{in}}(-\infty) = \varphi_{1\text{out}}(0-), \quad \varphi_{1\text{in}}(\infty) = \varphi_{1\text{out}}(0+).$$

Then using (2.4.12a) ((2.4.12b), respectively) for $0 < \delta_1 < 1$ ($\delta_1 \geq 1$, respectively) we obtain

limits for $\varphi_{1\mathrm{in}}$ at $\pm\infty$ such that the governing equation for $\varphi_{1\mathrm{in}}$ is in the same form as (2.3.1). Therefore a similar application of Lemma 2.A.3 gives

$$\varphi_{1\mathrm{in}}(\xi) = \frac{\theta_0 \Phi(\xi)}{\int_\xi^\infty \Phi(s)\,\mathrm{d}s},$$

where

$$\Phi(z) = \mathrm{e}^{-\int_0^z [1-\delta_1\varphi_{2\mathrm{in}}(s)-\delta_1\varphi_{3\mathrm{in}}(s)]/\theta_0\,\mathrm{d}s}.$$

2.4.3 Uniform approximations

Given that we have obtained our outer and inner solutions, we can look for uniform approximations for φ_1, φ_2 and φ_3. This is the result of the following proposition:

Proposition 2.4.1. *Suppose that*

$$\theta = \theta_0\eta_2^\alpha, \quad \beta_3 = \beta_{30}\eta_2^{-\gamma}$$

where $\theta_0, \beta_{30} = O(1)$ *as* $\eta_2 \to 0^+$ *and*

$$0 < \alpha < 1/2, \quad \gamma \geq 2\alpha.$$

Define

$$\phi(z;\eta_2) = \frac{1}{\theta_0}\int_0^z \left[\delta_1\varphi_{2\mathrm{in}}\left(\frac{s}{\eta_2^\alpha}\right) + \delta_1\varphi_{3\mathrm{in}}\left(\frac{s}{\eta_2^\alpha}\right) - 1\right]\mathrm{d}s. \tag{2.4.16}$$

Then uniform approximations for φ_1, φ_2 *and* φ_3 *are respectively given by*

$$\varphi_1(z;\eta_2) \simeq \frac{\theta_0\eta_2^\alpha \mathrm{e}^{\phi(z;\eta_2)/\eta_2^\alpha}}{\int_z^\infty \mathrm{e}^{\phi(s;\eta_2)/\eta_2^\alpha}\,\mathrm{d}s}, \tag{2.4.17}$$

$$\varphi_2(z;\eta_2) \simeq \frac{1}{2}\left(1 - \tanh\frac{\beta_2 z}{2\theta_0\eta_2^\alpha}\right) \tag{2.4.18}$$

and

$$\varphi_3(z;\eta_2) \simeq \begin{cases} \dfrac{1}{4\delta_3}\mathrm{sech}^2\dfrac{\beta_2 z}{2\theta_0\eta_2^\alpha} & \text{if } \gamma > 2\alpha, \\ \dfrac{1}{8}\sqrt{\dfrac{\beta_{30}}{\delta_3}}\left[\displaystyle\int_{z/\eta_2^\alpha}^\infty \mathrm{e}^{\sqrt{\delta_3\beta_{30}}(z/\eta_2^\alpha - s)}\mathrm{sech}^2\frac{\beta_2 s}{2\theta_0}\,\mathrm{d}s\right. & \\ \qquad\left. + \displaystyle\int_{-\infty}^{z/\eta_2^\alpha} \mathrm{e}^{-\sqrt{\delta_3\beta_{30}}(z/\eta_2^\alpha - s)}\mathrm{sech}^2\frac{\beta_2 s}{2\theta_0}\,\mathrm{d}s\right] & \text{if } \gamma = 2\alpha. \end{cases} \tag{2.4.19}$$

Proof. Uniform approximations for φ_1, φ_2 and φ_3 are obtained by adding the corresponding outer and inner solutions and then subtracting the common values in the overlap region. For the tumour tissue we have

$$\varphi_{2c} = \begin{cases} \varphi_{2\text{in}}(-\infty) = \varphi_{2\text{out}}(0-) = 1 & \text{if } z < 0, \\ \varphi_{2\text{in}}(\infty) = \varphi_{2\text{out}}(0+) = 0 & \text{if } z > 0, \end{cases}$$

while for the H^+ ion concentration it is

$$\varphi_{3c} = \begin{cases} \varphi_{3\text{in}}(-\infty) = \varphi_{3\text{out}}(0-) = 0 & \text{if } z < 0, \\ \varphi_{3\text{in}}(\infty) = \varphi_{3\text{out}}(0+) = 0 & \text{if } z > 0. \end{cases}$$

For the normal tissue the common value when $0 < \delta_1 < 1$ is

$$\varphi_{1c} = \begin{cases} \varphi_{1\text{in}}(-\infty) = \varphi_{1\text{out}}(0-) = 1 - \delta_1 & \text{if } z < 0, \\ \varphi_{1\text{in}}(\infty) = \varphi_{1\text{out}}(0+) = 1 & \text{if } z > 0, \end{cases}$$

while for $\delta_1 \geq 1$ it is

$$\varphi_{1c} = \begin{cases} \varphi_{1\text{in}}(-\infty) = \varphi_{1\text{out}}(0-) = 0 & \text{if } z < 0, \\ \varphi_{1\text{in}}(\infty) = \varphi_{1\text{out}}(0+) = 1 & \text{if } z > 0. \end{cases}$$

Therefore a uniform approximation for the tumour tissue is given by

$$\varphi_2(z;\eta_2) \simeq \varphi_{2\text{out}}(z) + \varphi_{2\text{in}}\left(\frac{z}{\eta_2^\alpha}\right) - \varphi_{2c} = \frac{1}{2}\left(1 - \tanh\frac{\beta_2 z}{2\theta_0\eta_2^\alpha}\right).$$

A uniform approximation for the H^+ ion concentration when $\gamma > 2\alpha$ is

$$\varphi_3(z;\eta_2) \simeq \varphi_{3\text{out}}(z) + \varphi_{3\text{in}}\left(\frac{z}{\eta_2^\alpha}\right) - \varphi_{3c} = \frac{1}{4\delta_3}\operatorname{sech}^2\frac{\beta_2 z}{2\theta_0\eta_2^\alpha},$$

while for $\gamma = 2\alpha$ it is

$$\begin{aligned}\varphi_3(z;\eta_2) &\simeq \varphi_{3\text{out}}(z) + \varphi_{3\text{in}}\left(\frac{z}{\eta_2^\alpha}\right) - \varphi_{3c} \\ &= \frac{1}{8}\sqrt{\frac{\beta_{30}}{\delta_3}}\left[\int_{z/\eta_2^\alpha}^{\infty} \mathrm{e}^{\sqrt{\delta_3\beta_{30}}(z/\eta_2^\alpha - s)}\operatorname{sech}^2\frac{\beta_2 s}{2\theta_0}\,\mathrm{d}s + \int_{-\infty}^{z/\eta_2^\alpha} \mathrm{e}^{-\sqrt{\delta_3\beta_{30}}(z/\eta_2^\alpha - s)}\operatorname{sech}^2\frac{\beta_2 s}{2\theta_0}\,\mathrm{d}s\right].\end{aligned}$$

For the normal tissue a uniform approximation is given by

$$\varphi_1(z;\eta_2) \simeq \varphi_{1\text{out}}(z) + \varphi_{1\text{in}}\left(\frac{z}{\eta_2^\alpha}\right) - \varphi_{1c} = \frac{\theta_0\Phi(z/\eta_2^\alpha)}{\int_{z/\eta_2^\alpha}^\infty \Phi(s)\,\mathrm{d}s},$$

where

$$\Phi(z) = \mathrm{e}^{-\int_0^z [1-\delta_1\varphi_{2\text{in}}(s)-\delta_1\varphi_{3\text{in}}(s)]/\theta_0\,\mathrm{d}s}.$$

By an appropriate substitution for s we obtain

$$\int_{z/\eta_2^\alpha}^\infty \Phi(s)\,\mathrm{d}s = \frac{1}{\eta_2^\alpha}\int_z^\infty \Phi\left(\frac{s}{\eta_2^\alpha}\right)\,\mathrm{d}s.$$

Similarly, if we define

$$\phi(z;\eta_2) = \frac{1}{\theta_0}\int_0^z \left[\delta_1\varphi_{2\text{in}}\left(\frac{s}{\eta_2^\alpha}\right) + \delta_1\varphi_{3\text{in}}\left(\frac{s}{\eta_2^\alpha}\right) - 1\right]\,\mathrm{d}s,$$

then

$$\Phi\left(\frac{z}{\eta_2^\alpha}\right) = \mathrm{e}^{\phi(z;\eta_2)/\eta_2^\alpha}.$$

Hence

$$\varphi_1(z;\eta_2) \simeq \frac{\theta_0\eta_2^\alpha \mathrm{e}^{\phi(z;\eta_2)/\eta_2^\alpha}}{\int_z^\infty \mathrm{e}^{\phi(s;\eta_2)/\eta_2^\alpha}\,\mathrm{d}s}.$$

□

Plots of the slow TW solutions for particular parameter values are displayed in Figures 2.2a and 2.2b. In Section 2.5 these solutions will be compared to corresponding numerical solutions of the PDE model (2.2.4)–(2.2.6).

2.4.4 An estimate for the interstitial gap

Here we wish to estimate the width of the interstitial gap. To do so we need to approximate the following generalised Laplace integral appearing in the uniform approximation for φ_1:

$$\int_z^\infty \mathrm{e}^{\phi(s;\eta_2)/\eta_2^\alpha}\,\mathrm{d}s, \tag{2.4.20}$$

where ϕ is given by (2.4.16). The next lemma provides information about the behaviour of $\varphi_{3\text{in}}$ that will be utilised for the approximation of the generalised Laplace integral.

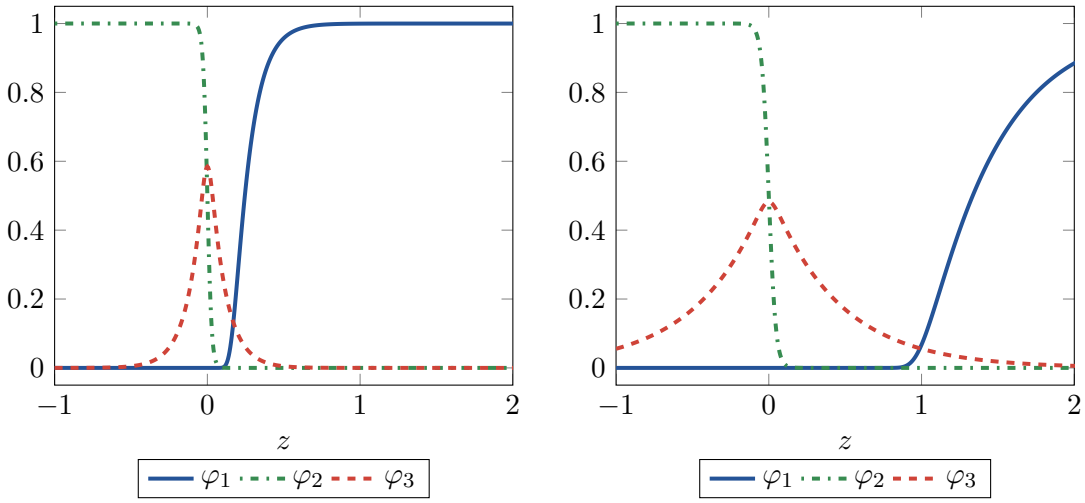

(a) $(\delta_1, \beta_2, \beta_3, \eta_2, \delta_3, \theta) = (10, 1, 1000, 4 \times 10^{-5}, 0.1, 0.0140)$

(b) $(\delta_1, \beta_2, \beta_3, \eta_2, \delta_3, \theta) = (20, 0.5, 100, 4 \times 10^{-5}, 0.05, 0.0116)$

Figure 2.2: Asymptotic approximations given by (2.4.16)–(2.4.19) in the case ($\gamma = 2\alpha$)

Lemma 2.4.2. *Define*

$$\varphi_{3\text{in}}(\xi) = \begin{cases} \dfrac{1}{4\delta_3}\operatorname{sech}^2\dfrac{\beta_2\xi}{2\theta_0} & \text{if } \gamma > 2\alpha, \\ \dfrac{1}{8}\sqrt{\dfrac{\beta_{30}}{\delta_3}}\left[\displaystyle\int_\xi^\infty \mathrm{e}^{\sqrt{\delta_3\beta_{30}}(\xi-s)}\operatorname{sech}^2\frac{\beta_2 s}{2\theta_0}\,\mathrm{d}s\right. & \\ \qquad \left. + \displaystyle\int_{-\infty}^\xi \mathrm{e}^{-\sqrt{\delta_3\beta_{30}}(\xi-s)}\operatorname{sech}^2\frac{\beta_2 s}{2\theta_0}\,\mathrm{d}s\right] & \text{if } \gamma = 2\alpha. \end{cases} \tag{2.4.21}$$

Then $\dot\varphi_{3\text{in}}(\xi) > 0$ *for* $\xi < 0$ *and* $\dot\varphi_{3\text{in}}(\xi) < 0$ *for* $\xi > 0$. *Thus* $\varphi_{3\text{in}}$ *has a unique global maximum at* $\xi = 0$.

Proof. The case when $\gamma > 2\alpha$ is trivial. Suppose that $\gamma = 2\alpha$. Since (2.4.21) is an even function, it has a turning point at $\xi = 0$ (i.e. $\dot\varphi_{3\text{in}}(0) = 0$). We see that

$$\dot\varphi_{3\text{in}}(\xi) = \frac{\beta_{30}}{8}\left[\int_\xi^\infty \mathrm{e}^{\sqrt{\delta_3\beta_{30}}(\xi-s)}\operatorname{sech}^2\frac{\beta_2 s}{2\theta_0}\,\mathrm{d}s - \int_{-\infty}^\xi \mathrm{e}^{-\sqrt{\delta_3\beta_{30}}(\xi-s)}\operatorname{sech}^2\frac{\beta_2 s}{2\theta_0}\,\mathrm{d}s\right]. \tag{2.4.22}$$

We can view (2.4.21) and (2.4.22) as a linear system with the improper integrals as the unknowns. Solving this system gives

$$\dot\varphi_{3\text{in}}(\xi) = -\sqrt{\delta_3\beta_{30}}\varphi_{3\text{in}}(\xi) + \frac{\beta_{30}}{4}\int_\xi^\infty \mathrm{e}^{\sqrt{\delta_3\beta_{30}}(\xi-s)}\operatorname{sech}^2\frac{\beta_2 s}{2\theta_0}\,\mathrm{d}s,$$

To proceed further, we shall use Lemma 2.A.4 in Appendix 2.A. If we let

$$F(\xi, W) = -\sqrt{\delta_3\beta_{30}}W + \frac{\beta_{30}}{4}\int_\xi^\infty \mathrm{e}^{\sqrt{\delta_3\beta_{30}}(\xi-s)}\mathrm{sech}^2\frac{\beta_2 s}{2\theta_0}\,\mathrm{d}s$$

with $J = [0, \infty)$, then

$$D_1F(\xi, W) = \frac{\beta_{30}}{4}\left[-\mathrm{sech}^2\frac{\beta_2\xi}{2\theta_0} + \sqrt{\delta_3\beta_{30}}\int_\xi^\infty \mathrm{e}^{\sqrt{\delta_3\beta_{30}}(\xi-s)}\mathrm{sech}^2\frac{\beta_2 s}{2\theta_0}\,\mathrm{d}s\right].$$

For $0 \le \xi < s$, sech^2 is strictly decreasing; hence

$$\begin{aligned}\int_\xi^\infty \mathrm{e}^{\sqrt{\delta_3\beta_{30}}(\xi-s)}\mathrm{sech}^2\frac{\beta_2 s}{2\theta_0}\,\mathrm{d}s &< \int_\xi^\infty \mathrm{e}^{\sqrt{\delta_3\beta_{30}}(\xi-s)}\mathrm{sech}^2\frac{\beta_2\xi}{2\theta_0}\,\mathrm{d}s\\ &= \frac{1}{\sqrt{\delta_3\beta_{30}}}\mathrm{sech}^2\frac{\beta_2\xi}{2\theta_0}.\end{aligned}$$

This shows that $D_1F(\xi, W) < 0$ for all $(\xi, W) \in J \times \mathbb{R}$. From Lemma 2.A.4 (with $\xi_0 = \xi^* = 0$) we deduce that $\dot\varphi_{3\mathrm{in}}(\xi) < 0$ for all $\xi > 0$.

On the other hand, since $\varphi_{3\mathrm{in}}(\xi)$ is even, we therefore know that $\dot\varphi_{3\mathrm{in}}(\xi)$ is odd. As $\dot\varphi_{3\mathrm{in}}(\xi) < 0$ for $\xi > 0$, the fact that $\dot\varphi_{3\mathrm{in}}(\xi)$ is odd implies $\dot\varphi_{3\mathrm{in}}(\xi) > 0$ for $\xi < 0$. □

We now show that for certain values of δ_1, the function ϕ defined in (2.4.16) achieves a unique maximum.

Lemma 2.4.3. *Let ϕ be defined by* (2.4.16)*. If $\delta_1 \ge 2$, then there exists a unique maximum of ϕ attained at a value $z_+ > 0$. Here, z_+ is the unique positive solution of*

$$\delta_1\varphi_{2\mathrm{in}}\left(\frac{z_+}{\eta_2^\alpha}\right) + \delta_1\varphi_{3\mathrm{in}}\left(\frac{z_+}{\eta_2^\alpha}\right) - 1 = 0. \tag{2.4.23}$$

Proof. Suppose that $\delta_1 \ge 2$. First we claim that $\phi'(z; \eta_2) > 0$ for $z \le 0$. Consider

$$\theta_0\phi'(z;\eta_2) = \delta_1\varphi_{2\mathrm{in}}\left(\frac{z}{\eta_2^\alpha}\right) + \delta_1\varphi_{3\mathrm{in}}\left(\frac{z}{\eta_2^\alpha}\right) - 1 > \delta_1\varphi_{2\mathrm{in}}\left(\frac{z}{\eta_2^\alpha}\right) - 1$$

as $\varphi_{3\mathrm{in}}(\xi) > 0$ for all $\xi \in \mathbb{R}$. Note that $\dot\varphi_{2\mathrm{in}}(\xi) < 0$ for all $\xi \in \mathbb{R}$, therefore for $z \le 0$

$$\varphi_{2\mathrm{in}}\left(\frac{z}{\eta_2^\alpha}\right) \ge \varphi_{2\mathrm{in}}(0) = \frac{1}{2}.$$

Hence

$$\theta_0\phi'(z;\eta_2) > \frac{\delta_1}{2} - 1 \geq 0,$$

proving that $\phi'(z;\eta_2) > 0$ for $z \leq 0$.

Next we claim that ϕ has a unique turning point at some $z_+ > 0$. Define

$$G(z) = \delta_1\varphi_{2\text{in}}\left(\frac{z}{\eta_2^\alpha}\right) + \delta_1\varphi_{3\text{in}}\left(\frac{z}{\eta_2^\alpha}\right) - 1 \quad (z \geq 0).$$

We see that

$$G(0) = \frac{\delta_1}{2} + \delta_1\varphi_{3\text{in}}(0) - 1 > 0$$

and

$$G(\infty) = \lim_{z\to\infty} G(z) = -1.$$

Therefore there exists $M > 0$ such that $|G(z) + 1| < 1/2$ for all $z \geq M$, i.e.

$$-\frac{3}{2} < G(z) < -\frac{1}{2} \quad (z \geq M).$$

Hence $G(M) < -1/2 < 0$ and $G(0) > 0$. By Bolzano's Theorem there exists a value $z_+ \in (0, M)$ such that

$$G(z_+) = \delta_1\varphi_{2\text{in}}\left(\frac{z_+}{\eta_2^\alpha}\right) + \delta_1\varphi_{3\text{in}}\left(\frac{z_+}{\eta_2^\alpha}\right) - 1 = 0$$

(i.e. $\phi'(z_+;\eta_2) = G(z_+)/\theta_0 = 0$). To prove that this point is unique we consider

$$G'(z) = \frac{\delta_1}{\eta_2^\alpha}\left[\dot{\varphi}_{2\text{in}}\left(\frac{z}{\eta_2^\alpha}\right) + \dot{\varphi}_{3\text{in}}\left(\frac{z}{\eta_2^\alpha}\right)\right].$$

We note that $\dot{\varphi}_{2\text{in}}(z/\eta_2^\alpha) < 0$ and $\dot{\varphi}_{3\text{in}}(z/\eta_2^\alpha) < 0$ for $z > 0$ by Lemma 2.4.2. Hence $G'(z) < 0$ for all $z > 0$, i.e. $G(z)$ is strictly decreasing for all $z > 0$. Therefore there can exist only one zero of the function G on $(0, \infty)$, and this occurs at $z = z_+$. Note that this implies that $G(z) > 0$ for all $0 \leq z < z_+$ and $G(z) < 0$ for all $z > z_+$ (i.e. $\phi'(z;\eta_2) = G(z)/\theta_0 > 0$ for all $0 \leq z < z_+$ and $\phi'(z;\eta_2) = G(z)/\theta_0 < 0$ for all $z > z_+$).

Finally, we claim that ϕ has a unique maximum at z_+. We showed that $\phi'(z;\eta_2) > 0$ for $z \leq 0$ and $\phi'(z;\eta_2) > 0$ for all $0 \leq z < z_+$, thus $\phi'(z;\eta_2) > 0$ for all $z < z_+$. Also, we showed that $\phi'(z_+) < 0$ for all $z > z_+$. Therefore $\phi(z;\eta_2)$ has a unique global maximum at $z = z_+$. □

We can apply Lemma 2.A.5 in Appendix 2.A to approximate (2.4.20) for $\delta_1 \geq 2$. Note that

(2.4.16) implies

$$|\phi(z;\eta_2)| \leq \frac{\delta_1 + \delta_1\varphi_{3\text{in}}(0) + 1}{\theta_0}|z|$$

for all z. Thus ϕ remains bounded as $\eta_2 \to 0^+$.

We first consider (2.4.20) for $z > z_+$. For $z_+ < z \leq s < \infty$ (i.e. $s > z_+$) we have by Lemma 2.4.3 that $\phi'(s;\eta_2) < 0$ for all $z \leq s < \infty$. Hence by Lemma 2.A.5 (i) we have for (2.4.20) that

$$\int_z^\infty \mathrm{e}^{\phi(s;\eta_2)/\eta_2^\alpha}\,\mathrm{d}s \simeq -\frac{\eta_2^\alpha \mathrm{e}^{\phi(z;\eta_2)/\eta_2^\alpha}}{\phi'(z;\eta_2)}.$$

Therefore (2.4.17) gives

$$\begin{aligned}\varphi_1(z;\eta_2) &\simeq -\theta_0\phi'(z;\eta_2)\\ &= 1 - \delta_1\varphi_{2\text{in}}\left(\frac{z}{\eta_2^\alpha}\right) - \delta_1\varphi_{3\text{in}}\left(\frac{z}{\eta_2^\alpha}\right)\end{aligned} \tag{2.4.24}$$

for $z > z_+$.

Now we consider (2.4.20) for $z < z_+$. We note from Lemma 2.4.3 that ϕ has a unique maximum at z_+, where $z < z_+ < \infty$. Hence from Lemma 2.A.5 (iii) we obtain

$$\int_z^\infty \mathrm{e}^{\phi(s;\eta_2)/\eta_2^\alpha}\,\mathrm{d}s \simeq \frac{\sqrt{2\pi}\eta_2^{\alpha/2}\mathrm{e}^{\phi(z_+;\eta_2)/\eta_2^\alpha}}{\sqrt{-\phi''(z_+;\eta_2)}}.$$

Therefore (2.4.17) gives

$$\varphi_1(z;\eta_2) \simeq \frac{\theta_0}{\sqrt{2\pi}}\eta_2^{\alpha/2}\sqrt{-\phi''(z_+;\eta_2)}\mathrm{e}^{[\phi(z;\eta_2)-\phi(z_+;\eta_2)]/\eta_2^\alpha} \tag{2.4.25}$$

for $z < z_+$. Then combining (2.4.24) and (2.4.25) we have

$$\varphi_1(z;\eta_2) \simeq \begin{cases} 1 - \delta_1\varphi_{2\text{in}}\left(\dfrac{z}{\eta_2^\alpha}\right) - \delta_1\varphi_{3\text{in}}\left(\dfrac{z}{\eta_2^\alpha}\right) & \text{if } z > z_+,\\ \dfrac{\theta_0}{\sqrt{2\pi}}\eta_2^{\alpha/2}\sqrt{-\phi''(z_+;\eta_2)}\mathrm{e}^{[\phi(z;\eta_2)-\phi(z_+;\eta_2)]/\eta_2^\alpha} & \text{if } z < z_+. \end{cases}$$

We claim that the interstitial gap is approximately given by $(0, z_+)$. Mathematically, we characterise this gap as a region where $\varphi_1(z;\eta_2) + \varphi_2(z;\eta_2) \ll 1$ for all $z \in (0, z_+)$ and η_2 small. Fix

$z \in (0, z_+)$. Then from (2.4.18) we see that

$$\lim_{\eta_2 \to 0^+} \varphi_2(z; \eta_2) = 0.$$

Since $0 < z < z_+$, and ϕ is bounded as $\eta_2 \to 0^+$ and strictly increasing on $(0, z_+)$, it follows that $\phi(z; \eta_2) < \phi(z_+; \eta_2)$ and so

$$\lim_{\eta_2 \to 0^+} \mathrm{e}^{[\phi(z;\eta_2) - \phi(z_+;\eta_2)]/\eta_2^\alpha} = 0.$$

Consider

$$\phi''(z_+; \eta_2) = \frac{\delta_1}{\theta_0 \eta_2^\alpha} \left[\dot{\varphi}_{2\mathrm{in}} \left(\frac{z_+}{\eta_2^\alpha} \right) + \dot{\varphi}_{3\mathrm{in}} \left(\frac{z_+}{\eta_2^\alpha} \right) \right].$$

Then

$$\eta_2^{\alpha/2} \sqrt{-\phi''(z_+; \eta_2)} = \sqrt{\frac{\delta_1}{\theta_0}} \sqrt{-\dot{\varphi}_{2\mathrm{in}} \left(\frac{z_+}{\eta_2^\alpha} \right) - \dot{\varphi}_{3\mathrm{in}} \left(\frac{z_+}{\eta_2^\alpha} \right)}.$$

We have

$$|\dot{\varphi}_{2\mathrm{in}}(\xi)| = \left| -\frac{\beta_2}{4\theta_0} \mathrm{sech}^2 \frac{\beta_2 \xi}{2\theta_0} \right| \leq \frac{\beta_2}{4\theta_0},$$

so that $\dot{\varphi}_{2\mathrm{in}}(z_+/\eta_2^\alpha)$ remains bounded as $\eta_2 \to 0^+$. When $\gamma > 2\alpha$

$$|\dot{\varphi}_{3\mathrm{in}}(\xi)| = \left| -\frac{\beta_2}{4\delta_3\theta_0} \mathrm{sech}^2 \frac{\beta_2 \xi}{2\theta_0} \tanh \frac{\beta_2 \xi}{2\theta_0} \right| \leq \frac{\beta_2}{4\delta_3\theta_0},$$

while for $\gamma = 2\alpha$ we have

$$\begin{aligned} |\dot{\varphi}_{3\mathrm{in}}(\xi)| &= \left| \frac{\beta_{30}}{8} \left[\int_\xi^\infty \mathrm{e}^{\sqrt{\delta_3\beta_{30}}(\xi - s)} \mathrm{sech}^2 \frac{\beta_2 s}{2\theta_0} \, \mathrm{d}s - \int_{-\infty}^\xi \mathrm{e}^{-\sqrt{\delta_3\beta_{30}}(\xi - s)} \mathrm{sech}^2 \frac{\beta_2 s}{2\theta_0} \, \mathrm{d}s \right] \right| \\ &\leq \frac{\beta_{30}}{8} \left[\int_\xi^\infty \mathrm{e}^{\sqrt{\delta_3\beta_{30}}(\xi - s)} \, \mathrm{d}s + \int_{-\infty}^\xi \mathrm{e}^{-\sqrt{\delta_3\beta_{30}}(\xi - s)} \, \mathrm{d}s \right] \\ &= \frac{1}{4} \sqrt{\frac{\beta_{30}}{\delta_3}}. \end{aligned}$$

In either case $\dot{\varphi}_{3\mathrm{in}}(z_+/\eta_2^\alpha)$ remains bounded as $\eta_2 \to 0^+$. Hence we deduce from (2.4.25) that

$$\lim_{\eta_2 \to 0^+} \varphi_1(z; \eta_2) = 0,$$

thus proving the claim that the interstitial gap can be approximated by $(0, z_+)$ with width z_+.

When $\gamma > 2\alpha$, we can actually find z_+ explicitly. Indeed, using (2.4.13) and (2.4.14) in

(2.4.23), we obtain

$$\tanh^2 \frac{\beta_2 z_+}{2\theta_0 \eta_2^\alpha} + 2\delta_3 \tanh \frac{\beta_2 z_+}{2\theta_0 \eta_2^\alpha} + 4\delta_3 \left(\frac{1}{\delta_1} - \frac{1}{2} \right) - 1 = 0.$$

This is a quadratic equation in $\tanh$ and whose roots are

$$\tanh \frac{\beta_2 z_+}{2\theta_0 \eta_2^\alpha} = -\delta_3 \pm \sqrt{\delta_3^2 - 2\delta_3(2-\delta_1)/\delta_1 + 1}.$$

Note that the discriminant is always positive since $\delta_1 \geq 2$. Taking the positive root since $z_+ > 0$ gives

$$z_+ = \frac{2\theta_0 \eta_2^\alpha}{\beta_2} \tanh^{-1} \left(-\delta_3 + \sqrt{\delta_3^2 - 2\delta_3(2-\delta_1)/\delta_1 + 1} \right).$$

Differentiating with respect to the parameters yields

$$\frac{\partial z_+}{\partial \delta_1} > 0, \quad \frac{\partial z_+}{\partial \beta_2} < 0, \quad \frac{\partial z_+}{\partial \eta_2} > 0, \quad \frac{\partial z_+}{\partial \delta_3} < 0$$

for $\delta_1 \geq 2$. When $\gamma = 2\alpha$, it is not possible to solve for z_+ explicitly but differentiating (2.4.23) implicitly with respect to the parameters δ_1, β_2, η_2 and δ_3 gives the same relations as for $\gamma > 2\alpha$ (see 2.B for details).

2.4.5 Statement of results for slow waves

The results of this section can therefore be summarised as follows:

If we assume that $\theta = \theta_0 \eta_2^\alpha$ and $\beta_3 = \beta_{30} \eta_2^{-\gamma}$ where $\theta_0, \beta_{30} = O(1)$ as $\eta_2 \to 0^+$ and

$$0 < \alpha < 1/2, \quad \gamma \geq 2\alpha,$$

then we obtain the following uniform approximations for $(\varphi_1, \varphi_2, \varphi_3)(z)$:

$$\varphi_2(z; \eta_2) \simeq \frac{1}{2} \left(1 - \tanh \frac{\beta_2 z}{2\theta_0 \eta_2^\alpha} \right),$$

$$\varphi_1(z; \eta_2) \simeq \frac{\theta_0 \eta_2^\alpha \mathrm{e}^{\phi(z;\eta_2)/\eta_2^\alpha}}{\int_z^\infty \mathrm{e}^{\phi(s;\eta_2)/\eta_2^\alpha} \, \mathrm{d}s},$$

and

$$\varphi_3(z;\eta_2) \simeq \begin{cases} \dfrac{1}{4\delta_3}\operatorname{sech}^2\dfrac{\beta_2 z}{2\theta_0\eta_2^\alpha} & \text{if } \gamma > 2\alpha, \\ \dfrac{1}{8}\sqrt{\dfrac{\beta_{30}}{\delta_3}}\left[\displaystyle\int_{z/\eta_2^\alpha}^{\infty} \mathrm{e}^{\sqrt{\delta_3\beta_{30}}(z/\eta_2^\alpha - s)}\operatorname{sech}^2\frac{\beta_2 s}{2\theta_0}\,\mathrm{d}s\right. & \\ \qquad\left. + \displaystyle\int_{-\infty}^{z/\eta_2^\alpha} \mathrm{e}^{-\sqrt{\delta_3\beta_{30}}(z/\eta_2^\alpha - s)}\operatorname{sech}^2\frac{\beta_2 s}{2\theta_0}\,\mathrm{d}s\right] & \text{if } \gamma = 2\alpha. \end{cases}$$

Here,

$$\phi(z;\eta_2) = \frac{1}{\theta_0}\int_0^z \left[\delta_1\varphi_{2\mathrm{in}}\left(\frac{s}{\eta_2^\alpha}\right) + \delta_1\varphi_{3\mathrm{in}}\left(\frac{s}{\eta_2^\alpha}\right) - 1\right]\mathrm{d}s,$$

where

$$\varphi_{2\mathrm{in}}(\xi) = \frac{1}{2}\left(1 - \tanh\frac{\beta_2\xi}{2\theta_0}\right)$$

and

$$\varphi_{3\mathrm{in}}(\xi) = \begin{cases} \dfrac{1}{4\delta_3}\operatorname{sech}^2\dfrac{\beta_2\xi}{2\theta_0} & \text{if } \gamma > 2\alpha, \\ \dfrac{1}{8}\sqrt{\dfrac{\beta_{30}}{\delta_3}}\left[\displaystyle\int_{\xi}^{\infty} \mathrm{e}^{\sqrt{\delta_3\beta_{30}}(\xi - s)}\operatorname{sech}^2\frac{\beta_2 s}{2\theta_0}\,\mathrm{d}s\right. & \\ \qquad\left. + \displaystyle\int_{-\infty}^{\xi} \mathrm{e}^{-\sqrt{\delta_3\beta_{30}}(\xi - s)}\operatorname{sech}^2\frac{\beta_2 s}{2\theta_0}\,\mathrm{d}s\right] & \text{if } \gamma = 2\alpha. \end{cases}$$

If $\delta_1 \geq 2$ then we obtain an estimate for the size of the interstitial gap, $z_+ > 0$, given by the solution to the following implicit equation

$$\delta_1\varphi_{2\mathrm{in}}\left(\frac{z_+}{\eta_2^\alpha}\right) + \delta_1\varphi_{3\mathrm{in}}\left(\frac{z_+}{\eta_2^\alpha}\right) - 1 = 0.$$

In the case $\gamma > 2\alpha$ we obtain the explicit formula

$$z_+ = \frac{2\theta_0\eta_2^\alpha}{\beta_2}\tanh^{-1}\left(-\delta_3 + \sqrt{\delta_3^2 - 2\delta_3(2-\delta_1)/\delta_1 + 1}\right).$$

Differentiating z_+ with respect to the parameters yields

$$\frac{\partial z_+}{\partial\delta_1} > 0, \quad \frac{\partial z_+}{\partial\beta_2} < 0, \quad \frac{\partial z_+}{\partial\eta_2} > 0, \quad \frac{\partial z_+}{\partial\delta_3} < 0.$$

2.5 Numerical results

We performed a numerical simulation of our model to obtain an idea of important variables and terms affecting the development of the model and also to confirm the validity of the asymptotic ap-

proximations. We solved the system of partial differential equations (2.2.4)–(2.2.6), for a large time domain, by applying a forward finite-difference scheme. Due to boundary conditions at infinity we made the assumption that for values of x at a large enough distance from where the cell densities and acid concentration perform a rapid change, our solution will remain approximately constant for a very large period of time. Without loss of generality we make this rapid change occur initially about $x = 0$. Hence under this assumption the gradients of u_1, u_2 and u_3, at x far enough from $x = 0$, will be zero, and as such we applied a homogeneous Neumann boundary condition at large values $x = -L_1$ and $x = L_2$, where $L_1, L_2 \gg 1$. The initial conditions are given by piecewise linear functions as shown in Figure 2.3. The initial conditions show that the tumour population is at carrying capacity and then decreases to zero within the domain, whereas the normal tissue is initially present at a low density in the tumour region and then increases to carrying capacity in the tumour vacant region. The acid concentration is initially zero. Examples of the solutions obtained for different parameter values can be seen in Figures 2.4a–2.4e. Note that for each of these figures there is a given speed. This speed was not used in the calculation of these solutions, rather the speed has been obtained via a parameter estimation technique that determines a value for θ by matching the data obtained from solving the system of partial differential equations (2.2.4)–(2.2.6) at the final timestep to the ordinary differential equation (2.2.8). The technique used is an integration-based estimation technique outlined in Chapter 5 (see 2.C for further details). As a result we were able to plot the asymptotic approximations, given by Figures 2.2a and 2.2b, respectively, for the parameter values used to obtain the numerical solutions displayed in Figures 2.4a and 2.4b, respectively.

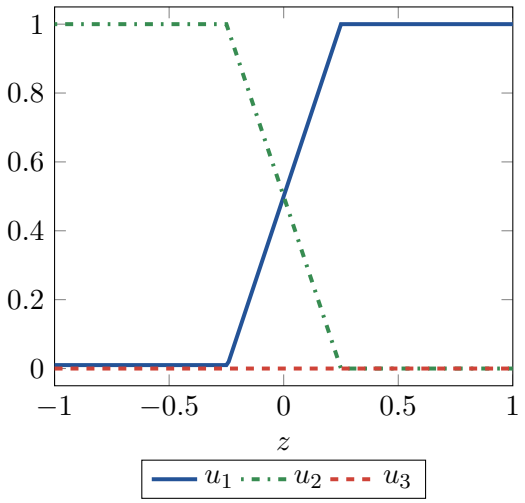

Figure 2.3: Initial conditions for numerical simulations

We observe from Figures 2.4c, and 2.4d that for small values of β_3 we attain solutions of the

H^+ ions that represent low concentrations at any point thus giving justification to the assumption made in the analysis of the slow TWs that β_3 must be large. In Figure 2.4b we have an example of an interstitial gap predicted by the numerical modelling for certain parameter values. The analytical analysis of our estimate for the gap, in Section 2.4, suggests that along with the parameter assumptions $\eta_2 \ll 1$ and $\beta_3 \gg 1$ that if δ_1 is sufficiently large (i.e. $\delta_1 \geq 2$) and β_2 and δ_3 are sufficiently small then the numerical solutions should display an interstitial gap.

In Figures 2.5a and 2.5b we compare the solutions in Figures 2.2a and 2.2b to Figures 2.4a and 2.4b, respectively, and note that the asymptotic approximations produced in the case $\gamma = 2\alpha$ are in excellent agreement with the numerically obtained solutions. In order to compare the solutions, a value was selected from the front of the numerical solution for φ_2 and matched to the position where the asymptotic solution for φ_2 obtains that value. The asymptotic solution was then subtracted from the numerical solution to obtain the error. The maximum difference obtained between the numerical and asymptotic solutions for these parameter values are $O(10^{-3})$–$O(10^{-2})$. When we consider the value used for $\eta_2 = 4 \times 10^{-5}$ to produce these solutions, we note the errors are $O(\eta_2^{\alpha})$ for $0 < \alpha < 1/2$ with $\alpha \approx 1/2$. This is in the range of the expected error as the asymptotic approximation consists of the $O(1)$ terms and we have truncated the $O(\eta_2^{\alpha})$ terms. There is also the possibility of small numerical errors in both the asymptotic and numerical solutions that have contributed to the errors depicted. However the consistency of the numerical solutions and size of the errors suggest this is not a significant influence. We note that in the case $\gamma > 2\alpha$ the asymptotic solutions produced did not provide a good fit to the numerical solutions for the parameter values considered. This would suggest that the values for β_3 used in the numerical simulations were not sufficiently large so that this would provide a good approximation. However when larger values of β_3 were used, the numerical simulations were unstable and hence we were unable to confirm this hypothesis.

2.6 Discussion and concluding remarks

In this chapter we proposed a RD model for the process of acid-mediated tumour growth that is an altered version of the model originally proposed by Gatenby and Gawlinski [71]. While the models appear similar, their dynamics and solutions are significantly different. The model proposed by Gatenby and Gawlinski [71] postulates that an excess of H^+ ions is produced by the tumour cells due to aerobic glycolysis. The excess of H^+ ions is concentrated at the tumour-normal tissue interface.

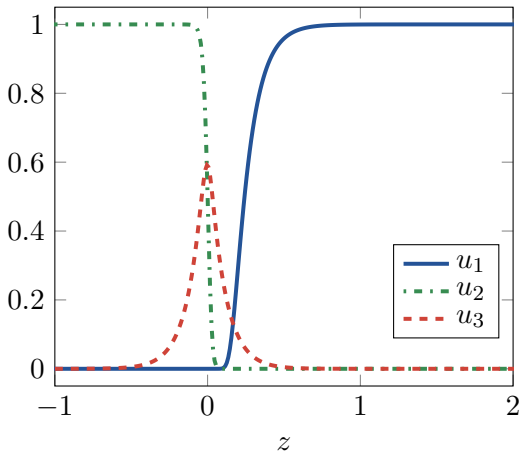

(a) $(\delta_1, \beta_2, \beta_3, \delta_3, \theta) = (10, 1, 1000, 0.1, 0.0140)$

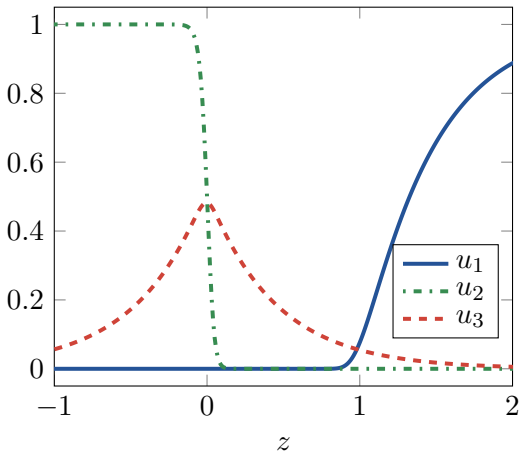

(b) $(\delta_1, \beta_2, \beta_3, \delta_3, \theta) = (20, 0.5, 100, 0.05, 0.0116)$

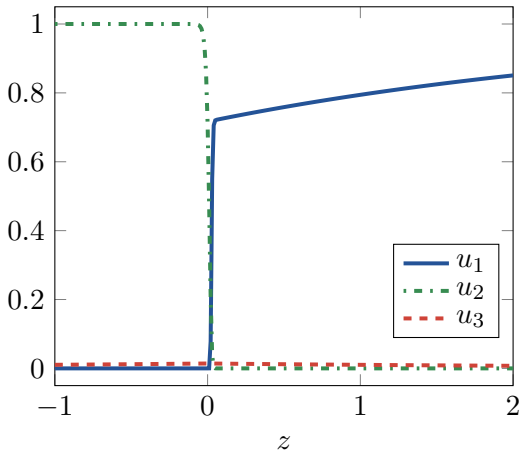

(c) $(\delta_1, \beta_2, \beta_3, \delta_3, \theta) = (20, 1, 1, 0.1, 0.0088)$

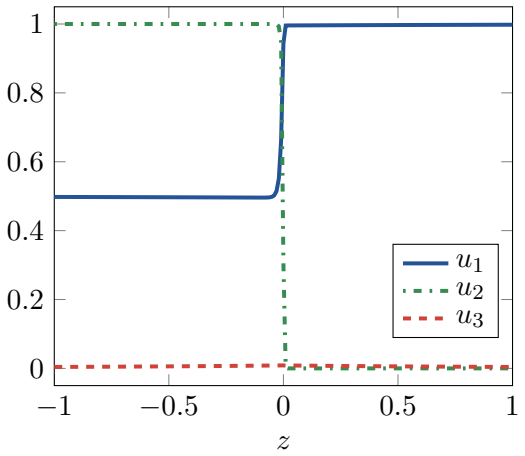

(d) $(\delta_1, \beta_2, \beta_3, \delta_3, \theta) = (0.5, 2, 5, 0.1, 0.0043)$

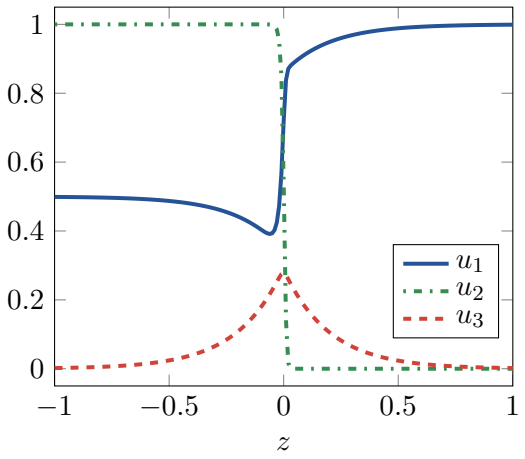

(e) $(\delta_1, \beta_2, \beta_3, \delta_3, \theta) = (0.5, 1, 500, 0.05, 0.0058)$

Figure 2.4: Numerical approximations of (2.2.4)–(2.2.6) with $\eta_2 = 4 \times 10^{-5}$: In (c) and (d) a low value of β_3 is used resulting in production of low levels of acid that diffuses over a wide region. Consequently, normal cell destruction is primarily due to competition at the tumour-host interface, resulting in a sharp change in the normal cell density when the tumour cell density undergoes a steep change. In (c), δ_1 is large and as a result of the low acid concentration over a wide region, normal cell destruction decreases gradually in the tumour vacant region.

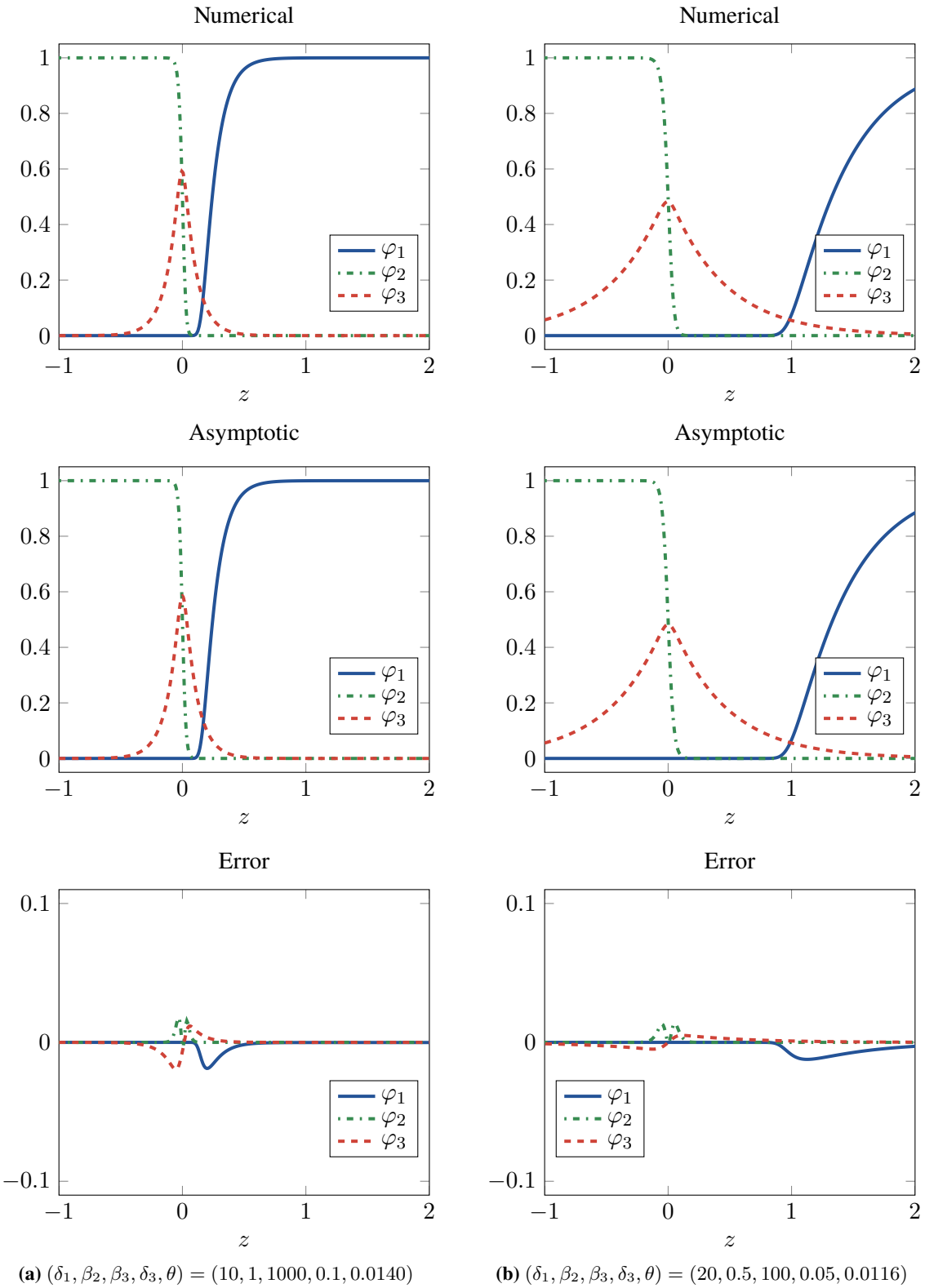

(a) $(\delta_1, \beta_2, \beta_3, \delta_3, \theta) = (10, 1, 1000, 0.1, 0.0140)$

(b) $(\delta_1, \beta_2, \beta_3, \delta_3, \theta) = (20, 0.5, 100, 0.05, 0.0116)$

Figure 2.5: Comparison of numerical and asymptotic ($\gamma = 2\alpha$) solutions of (2.2.4)–(2.2.6) with $\eta_2 = 4\times10^{-5}$: In (b) and (a) the top and centre figures represent the numerical and asymptotic ($\gamma = 2\alpha$) approximations, respectively. The bottom figures display the difference between the numerical and asymptotic solutions (i.e., numerical minus asymptotic). In (a) the absolute maximum errors for each solution are $E_1 = 0.0187$, $E_2 = 0.0178$, $E_3 = 0.0196$. In (b) the maximum absolute errors for each solution are $E_1 = 0.0122$, $E_2 = 0.0137$, $E_3 = 0.0050$.

This creates a region of lowered pH ahead of the advancing tumour. Moreover, for certain parameter values, healthy tissue could be destroyed prior to the arrival of malignant cells. This would result in the formation of an interstitial gap, where the concentrations of tumour and normal tissue are close to zero. The most noticeable difference between the proposed model and that of Gatenby and Gawlinski's is that concentration of H^+ ions is in the form of a pulse and not a front. This difference is due to the hypothesis that the production of H^+ ions is considered to be proportional to the tumour cell density until the latter reaches a threshold, after which the production rate decreases as the tumour cell density reaches its saturation level. This creates a localised region of acid production and concentration. As a consequence of this hypothesis we find that a high production rate of H^+ ions is required, which would indicate a high dependence on glycolysis. We note the results in [77] suggest this highly localised acid production, characterised by the formation of a pulse, may not represent the best model for the acid profile. However, in contrast to the results originally obtained by Gatenby and Gawlinski [71], which suggest an almost spatially homogeneous acid concentration in the tumour region, the results of [77] show a more spatially heterogeneous acid concentration often with greater concentrations of acid near the tumour front. This suggests that the best possible model for acid production lies somewhere in between that originally proposed by Gatenby and Gawlinski and that proposed here. Our conducted analysis was unable to lead to an analytical estimate of the wave speed. Hence a potential analytical estimation of the speed of the TWs and effect of parameters in the system on the speed would enlighten us further to the effects of the localised acid production hypothesis and allow us to better compare our model with Gatenby and Gawlinski's original model [71] and that proposed by McGillen et al. [140]. This analysis of the speed and the factors that cause it to change would provide predictions that potentially could be tested experimentally assuming the relevant predictions and factors affecting them are able to be observed and quantified. We note that our investigation puts a greater importance on population competition than that proposed by Gatenby and Gawlinski [71] and we find that our hypothesis requires competition whereas Gatenby and Gawlinski's does not. Competition is a requirement in this model as without it the tumour will not be able to achieve an invasive state solely from acid-mediation and rather only the coexistence behaviour would be observed. Furthermore, comparing the model presented here to that proposed by McGillen et al. [140] in which the model permits conditions on the system such that the tumour population does not invade but is cleared from the system, our model only considers invasion as in [71].

We undertook an analytical and preliminary numerical analysis of the proposed model (2.2.1)–

(2.2.3). We showed that this model is compatible with various types of fast and slow TW solutions. The biological significance and interpretation of the fast TW solutions is unclear and would seem to represent a purely mathematical feature due to the fact that fast speeds are biologically unrealistic. We note the slow solution is dependent on two introduced parameters α and γ, such that the uniform approximation is obtained for $0 < \alpha < 1/2$ and $\gamma \geq 2\alpha$. This restriction on the parameters has been visualised in Figure 2.6 in which we can see the blue region represents the area for which we found asymptotic solutions in the α–γ plane. The white region in the positive cone represents a region in which our analysis did not give a uniform solution.

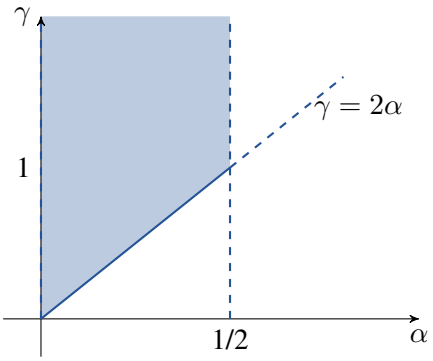

Figure 2.6: Region of uniform solutions for the slow TWs in the α–γ plane

We also characterised conditions under which an interstitial gap, that is, a region almost devoid of tumour and normal cells, exists and have given an implicit formula for calculating an approximation of the gap width. This formula can be made explicit when $\gamma > 2\alpha$. Our results point to the existence of a gap when $\delta_1 \geq 2$ with the estimate for its width being the value z_+ given by solving (2.4.23). This condition is consistent with the prediction made by Gatenby and Gawlinski [71] and Fasano et al. [63] that an interstitial gap can only be achieved by a sufficiently aggressive tumour. We further found that this estimate for the gap would increase with respect to the parameters δ_1 and η_2 and decreases with respect to the parameters β_2 and δ_3. Specifically, the prediction that the gap increases with respect δ_1 implies that the greater the destructive influence of the tumour, the greater the size of interstitial gap as is predicted in Fasano et al. [63]. The increase in z_+ with respect to η_2 suggests that as the cell motility decreases, so too does the size of the interstitial gap. The prediction that the gap decreases with respect to β_2 suggests that if the production of tumour cells is faster than the normal cells, then the interstitial gap should be decreased and if the tumour cell production rate decreases or the normal cell production rate increases the converse would be true. We see that z_+ decreasing with respect to δ_3 predicts that if the uptake of acid increases then the size of the interstitial gap should decrease and if the uptake decreases the converse would be

true. This analysis suggests that an examination, either mathematically or experimentally, of the distribution and density of blood vessels in the tumour region and the resulting effect that these have on acid-mediated growth would be valuable. This would represent a challenging exercise due to other system dynamics that would change as a result of changed blood vessel distribution such as nutrient dynamics. This model predicts an influence on the interstitial gap from a greater number of the parameters within this model than of that described in Fasano et al. [63]. However, as is noted in [63, 140], from the experimental results in [71] the size of interstitial gaps observed are the size of a few cells in width, which when we consider rescaled in terms of our non-dimensionalised spatial variable is of $O(10^{-3})$–$O(10^{-2})$. Hence observed gap sizes are small in comparison to the scale that our continuum model considers. We note that very aggressive tumours produce wider interstitial gaps and mildly aggressive tumours produce gaps in the observable range and as such this may indicate that there is a small upper bound on the level of aggressiveness which is biologically realistic or that usefulness of the prediction of an interstitial gap from this model may be more qualitative rather than quantitative. Alternatively, the sizes of gaps that are experimentally observable may be outside the range of sensitivity for which our model is viable and rather the formation of a gap in our model may represent a mathematical consequence of the model rather than a biological one. This issue of making predictions at the cellular scale is a common problem with continuum models, such as those for spheroid growth (e.g. [85, 188]), that utilise scales much larger than that of individual tumour cells however often predict small proliferating rims on the scale of a few cells in width.

The linear stability of the fast TWs was shown to hold when $\delta_1 \neq 1$ for all strictly positive parameter values. A mathematical analysis of the linear stability of the slow TWs is more involved due to the use of matched asymptotic solutions in order to obtain our approximations. However from numerical simulations conducted we would expect these solutions to be linearly stable. We note also the excellent fit of these asymptotic solutions obtained in the case $\gamma = 2\alpha$ to the data obtained from solving the system (2.2.4)–(2.2.6) numerically. The case where $\gamma = 2\alpha$ implies that the acid production is small enough in relation to the speed of the wave that acid diffusion is still an important factor in the system's dynamics. The case in which $\gamma > 2\alpha$ suggests that acid diffusion becomes less significant and hence is not a factor in determining the leading order approximation.

The model herein presented is a first attempt at considering nonlinear acid-production mechanisms. A possible extension could be carried out within the framework proposed in McGillen et al. [140], with the inclusion of strong competition between normal and tumour tissue, as well as

potential negative acid effect on tumour progression. We also note that the model we have proposed has the potential to be extended to include further growth promoting and inhibiting mechanisms such as haptotaxis and an immunotherapeutic response. This analysis could illuminate how to improve or develop treatment strategies for acid-mediated tumour growth. It could also guide future experimental analyses and research into the mechanisms behind acid-mediated tumour growth. An analysis in higher dimensional geometries remains to be conducted as well as a rigorous proof of existence. However both the asymptotic and numerical analysis conducted in this chapter suggests the existence of a stable and unique class of solutions.

2.A Auxillary results

Lemma 2.A.1. *Consider the equation*

$$W'' + \theta W' - \kappa W = f(z), \tag{2.A.1}$$

where $\theta \geq 0$, $\kappa > 0$ and f is a bounded piecewise continuous function. Let

$$W(z) = \frac{1}{\varrho_2 - \varrho_1} \left[I_1(z) + I_2(z) \right], \tag{2.A.2}$$

where

$$\varrho_1 = \frac{-\theta + \sqrt{\theta^2 + 4\kappa}}{2} > 0, \quad \varrho_2 = \frac{-\theta - \sqrt{\theta^2 + 4\kappa}}{2} < 0 \tag{2.A.3}$$

and

$$I_1(z) = \int_z^\infty \mathrm{e}^{\varrho_1 (z-s)} f(s)\, \mathrm{d}s, \quad I_2(z) = \int_{-\infty}^z \mathrm{e}^{\varrho_2 (z-s)} f(s)\, \mathrm{d}s. \tag{2.A.4}$$

Then (2.A.2)–(2.A.4) *solves* (2.A.1)*. Moreover, should f possess bounded limits at infinity, i.e. if $f(\pm\infty) = \lim_{z \to \pm\infty} f(z)$ both exist, then*

$$
\begin{aligned}
I_1(\infty) &= \frac{f(\infty)}{\varrho_1}, \\
I_1(-\infty) &= \begin{cases} 0 & \text{if } \int_{-\infty}^{\infty} \mathrm{e}^{-\varrho_1 s} f(s)\,\mathrm{d}s \text{ is finite,} \\ \dfrac{f(-\infty)}{\varrho_1} & \text{if } \int_{-\infty}^{\infty} \mathrm{e}^{-\varrho_1 s} f(s)\,\mathrm{d}s \text{ is infinite,} \end{cases} \\
I_2(\infty) &= \begin{cases} 0 & \text{if } \int_{-\infty}^{\infty} \mathrm{e}^{-\varrho_2 s} f(s)\,\mathrm{d}s \text{ is finite,} \\ -\dfrac{f(\infty)}{\varrho_2} & \text{if } \int_{-\infty}^{\infty} \mathrm{e}^{-\varrho_2 s} f(s)\,\mathrm{d}s \text{ is infinite,} \end{cases} \\
I_2(-\infty) &= -\frac{f(-\infty)}{\varrho_2}.
\end{aligned}
$$

Proof. See [63] for a proof. □

Lemma 2.A.2. *For a continuous function g with bounded limits at infinity, let*

$$\Phi(z) = \mathrm{e}^{-\int_0^z g(s)\,\mathrm{d}s}.$$

Then the following statements hold:

(i) *If $g(\infty) > 0$, then $\Phi(\infty) = 0$;*

(ii) *If $g(\infty) < 0$, then $\Phi(\infty) = \infty$;*

(iii) *If $g(-\infty) > 0$, then $\Phi(-\infty) = \infty$;*

(iv) *If $g(-\infty) < 0$, then $\Phi(-\infty) = 0$.*

Proof. See [63] for a proof. □

Lemma 2.A.3. *Let $(\varphi_1, \varphi_2, \varphi_3) = (\varphi_1, \varphi_2, \varphi_3)(z; \eta_2)$ denote a solution to* (2.2.8)–(2.2.11)*, if any. Then the problem* (2.2.8)–(2.2.11) *is equivalent to the following:*

$$0 = \eta_2[(1-\varphi_1)\varphi_2'' - \varphi_1'\varphi_2'] + \theta\varphi_2' + \beta_2\varphi_2(1-\varphi_2),\ \varphi_2(-\infty;\eta_2) = 1,\ \varphi_2(\infty;\eta_2) = 0, \quad \text{(2.A.5)}$$

where

$$\varphi_2(z;\eta_2) = \frac{\theta\Phi(z;\eta_2)}{\int_z^{\infty} \Phi(s;\eta_2)\,\mathrm{d}s},\ \Phi(z;\eta_2) = \mathrm{e}^{-\int_0^z [1-\delta_1\varphi_2(s;\eta_2)-\delta_1\varphi_3(s;\eta_2)]/\theta\,\mathrm{d}s}, \quad \text{(2.A.6)}$$

$$\varphi_3(z;\eta_2) = \frac{\beta_3}{\varrho_1-\varrho_2}\left\{\int_z^\infty \mathrm{e}^{\varrho_1(z-s)}\varphi_2(s;\eta_2)[1-\varphi_2(s;\eta_2)]\,\mathrm{d}s + \int_{-\infty}^z \mathrm{e}^{\varrho_2(z-s)}\varphi_2(s;\eta_2)[1-\varphi_2(s;\eta_2)]\,\mathrm{d}s\right\} \tag{2.A.7a}$$

and

$$\varrho_1 = \frac{-\theta+\sqrt{\theta^2+4\delta_3\beta_3}}{2} > 0,\ \varrho_2 = \frac{-\theta-\sqrt{\theta^2+4\delta_3\beta_3}}{2} < 0. \tag{2.A.7b}$$

Proof. Equation (2.A.5) is the same as (2.2.9) with corresponding boundary conditions for φ_2. We can apply Lemma 2.A.1 to (2.2.10) where $\kappa = \delta_3\beta_3$ and $f(s) = -\beta_3\varphi_2(s;\eta_2)[1-\varphi_2(s;\eta_2)]$ to obtain (2.A.7). Since $f(\pm\infty) = -\beta_3\varphi_2(\pm\infty;\eta_2)[1-\varphi_2(\pm\infty;\eta_2)] = 0$ we see that $I_1(\pm\infty) = I_2(\pm\infty) = 0$ from Lemma 2.A.1. Therefore $\varphi_3(\pm\infty;\eta_2) = 0$ and the corresponding BCs in (2.2.11) hold. Equation (2.2.8) is a Bernoulli-type equation and can be solved explicitly to formally give (2.A.6).

Let

$$g(s) = \frac{1-\delta_1\varphi_2(s;\eta_2)-\delta_1\varphi_3(s;\eta_2)}{\theta}.$$

Then $g(\infty) = 1/\theta$ and therefore $\Phi(\infty;\eta_2) = 0$ by Lemma 2.A.2. Using L'Hôpital's Rule in (2.A.6) verifies that $\varphi_1(\infty;\eta_2) = 1$. Similarly, $g(-\infty) = (1-\delta_1)/\theta$.

When $\delta_1 > 1$ we have $g(-\infty) < 0$; hence $\Phi(-\infty;\eta_2) = 0$ by Lemma 2.A.2. Since $0 < \int_{-\infty}^{\infty}\Phi(s;\eta_2)\,\mathrm{d}s \le \infty$ we infer from (2.A.6) that $\varphi_1(-\infty;\eta_2) = 0$. In the case $0 < \delta_1 < 1$ we have $g(-\infty) > 0$, and so $\Phi(-\infty;\eta_2) = \infty$. Applying L'Hôpital's Rule to (2.A.6) gives $\varphi_1(-\infty;\eta_2) = 1-\delta_1$. When $\delta_1 = 1$ we note that $g(-\infty) = 0$, so that $0 < \Phi(-\infty;\eta_2) \le \infty$ and as a result $\int_{-\infty}^{\infty}\Phi(s;\eta_2)\,\mathrm{d}s = \infty$. So if $\Phi(-\infty;\eta_2)$ is finite, then it follows that $\varphi_1(-\infty;\eta_2) = 0$. However if $\Phi(-\infty;\eta_2)$ is infinite, then L'Hôpital's Rule in (2.A.6) again gives $\varphi_1(\infty;\eta_2) = 0$. □

Lemma 2.A.4. *Let $J = [z_0,\infty)$ and assume that W solves an equation of the form*

$$W'(z) = F(z,W(z)),$$

where $F \in C^1(J\times W(J))$. Suppose that

$$D_1F(z,p) < 0$$

for all $(z,p) \in J\times W(J)$.

(i) *If* $W'(z^*) = 0$ *for some* $z^* \in J$*, then* $W'(z) > 0$ *for all* $z \in [z_0, z^*)$ *and* $W'(z) < 0$ *for all* $z \in (z^*, \infty)$*;*

(ii) *If* $W'(z_0) < 0$*, then* $W'(z) < 0$ *for all* $z > z_0$*.*

Proof. We see that

$$W''(z) = D_1F(z, W(z)) + D_2F(z, W(z))W'(z).$$

Therefore at any point $z \in J$ where $W'(z) = 0$ we have

$$W''(z) = D_1F(z, W(z)) < 0,$$

i.e. W would have a local maximum at z. Now suppose that $W'(z^*) = 0$ for some $z^* \in J$. It then follows that W has a local maximum at z^*.

(i) Suppose that there exists $z_1 \in (z^*, \infty)$ such that $W'(z_1) \geq 0$. If $W'(z_1) = 0$, then W will also have a local maximum at z_1. Since there are two local maxima at z^* and z_1 there must exist a local minimum at some $z_2 \in (z^*, z_1)$. This implies that $W'(z_2) = 0$, which would mean that W will have a local maximum at z_2, a contradiction. On the other hand, suppose that $W'(z_1) > 0$. Since W has a local maximum at z^* we can find $\epsilon_1 > 0$ small enough (e.g. $\epsilon_1 < z_1 - z^*$) such that $W'(z) < 0$ for all $z \in (z^*, z^* + \epsilon_1)$. In particular, $W'(z^* + \epsilon_1/2) < 0$. Over the interval $[z^* + \epsilon_1/2, z_1]$ we therefore have $W'(z^* + \epsilon_1/2)W'(z_1) < 0$. By Bolzano's Theorem there exists $z_3 \in (z^* + \epsilon_1/2, z_1)$ such that $W'(z_3) = 0$. But this brings us back to case above when $W'(z_1) = 0$. Therefore $W'(z) < 0$ for all $z \in (z^*, \infty)$. An almost identical argument can be given to show that $W'(z) > 0$ for all $z \in [z_0, z^*)$.

(ii) Suppose that there exists $z_4 \in (z_0, \infty)$ such that $W'(z_4) \geq 0$. If $W'(z_4) = 0$, then W has a local maximum at z_4. Then there exists $\epsilon_2 > 0$ small enough (e.g. $\epsilon_2 < z_4 - z_0$) such that $W'(z) > 0$ for all $z \in (z_4 - \epsilon_2, z_4)$. In particular, $W'(z_4 - \epsilon_2/2) > 0$. Hence, over the interval $[z_0, z_4 - \epsilon_2/2]$, we have $W'(z_0)W'(z_4 - \epsilon_2/2) < 0$. By Bolzano's Theorem there exists $z_5 \in (z_0, z_4 - \epsilon_2/2)$ such that $W'(z_5) = 0$. This implies that W has a local maximum at z_5; hence $W'(z_5) = 0$. Since we have two local maxima at z_4 and z_5, there must exist a local minimum of W at some $z_6 \in (z_4, z_5)$. Necessarily it follows that $W'(z_6) = 0$. But we saw that this implies that W has a local maximum at z_6, a contradiction. On the other hand, if $W'(z_4) > 0$, then $W'(z_0)W'(z_4) < 0$ and Bolzano's Theorem again implies that there exists $z_7 \in (z_0, z_4)$ such that

$W'(z_7) = 0$. But this brings us back to case above when $W'(z_4) = 0$. Therefore if $W'(z_0) < 0$, then $W'(z) < 0$ for all $z > z_0$. □

Lemma 2.A.5. *Let $\phi(\cdot;\epsilon)$ be a continuous function, $-\infty \leq s_L < s_R \leq \infty$ and $\alpha > 0$. Consider the integral*

$$I(\epsilon) = \int_{s_L}^{s_R} \mathrm{e}^{\phi(s;\epsilon)/\epsilon^\alpha}\,\mathrm{d}s$$

as $\epsilon \to 0^+$. If $\phi(\cdot;d)$ is bounded as $\epsilon \to 0^+$, then the following statements hold:

(i) *If $\phi'(s;\epsilon) < 0$ for $s_L \leq s < s_R$, then*

$$I(\epsilon) \simeq -\frac{\epsilon^\alpha \mathrm{e}^{\phi(s_L;\epsilon)/\epsilon^\alpha}}{\phi'(s_L;\epsilon)};$$

(ii) *If $\phi'(s;\epsilon) > 0$ for $s_L < s \leq s_R$, then*

$$I(\epsilon) \simeq \frac{\epsilon^\alpha \mathrm{e}^{\phi(s_R;\epsilon)/\epsilon^\alpha}}{\phi'(s_R;\epsilon)};$$

(iii) *Suppose that ϕ has a unique maximum at some $s_L < s^* < s_R$. Then*

$$I(\epsilon) \simeq \frac{\sqrt{2\pi}\epsilon^{\alpha/2}\mathrm{e}^{\phi(s^*;\epsilon)/\epsilon^\alpha}}{\sqrt{-\phi''(s^*;\epsilon)}}.$$

Proof. We use Laplace's method to approximate integrals containing a large parameter [16, pp. 266–267]. Note that a small adjustment of the proof provided in [16] needs to be made due to the dependence of ϕ on ϵ. □

2.B Properties of interstitial gap estimate

We wish to show that for z_+ obtained from solving (2.4.23) in the case $\gamma = 2\alpha$, we have that differentiating with respect to the parameters yields

$$\frac{\partial z_+}{\partial \delta_1} > 0, \quad \frac{\partial z_+}{\partial \beta_2} < 0, \quad \frac{\partial z_+}{\partial \eta_2} > 0, \quad \frac{\partial z_+}{\partial \delta_3} < 0$$

for $\delta_1 \geq 2$.

Suppose that $\delta_1 \geq 2$, then from Lemma 2.4.3 we know that $z_+ > 0$. We determine the derivatives of z_+ with respect to the parameters by differentiating (2.4.23) implicitly. We first

consider the derivative with respect to δ_1, noting that $\varphi_{2\text{in}}(\xi)$ and $\varphi_{3\text{in}}(\xi)$ do not depend on δ_1; differentiating (2.4.23) with respect to δ_1 gives,

$$\varphi_{2\text{in}}\left(\frac{z_+}{\eta_2^\alpha}\right) + \varphi_{2\text{in}}\left(\frac{z_+}{\eta_2^\alpha}\right) + \frac{\delta_1}{\eta_2^\alpha}\frac{\partial z_+}{\partial \delta_1}\left[\dot{\varphi}_{2\text{in}}\left(\frac{z_+}{\eta_2^\alpha}\right) + \dot{\varphi}_{3\text{in}}\left(\frac{z_+}{\eta_2^\alpha}\right)\right] = 0.$$

Rearranging this gives

$$\frac{\partial z_+}{\partial \delta_1} = -\frac{\eta_2^\alpha}{\delta_1}\frac{\varphi_{2\text{in}}\left(z_+/\eta_2^\alpha\right) + \varphi_{2\text{in}}\left(z_+/\eta_2^\alpha\right)}{\dot{\varphi}_{2\text{in}}\left(z_+/\eta_2^\alpha\right) + \dot{\varphi}_{3\text{in}}\left(z_+/\eta_2^\alpha\right)}.$$

We know that $\varphi_{2\text{in}}(\xi), \varphi_{3\text{in}}(\xi) > 0$ and $\dot{\varphi}_{2\text{in}}(\xi), \dot{\varphi}_{3\text{in}}(\xi) < 0$ for all $\xi > 0$ and that $z_+ > 0$, therefore we can conclude

$$\frac{\partial z_+}{\partial \delta_1} > 0$$

for $\delta_1 \geq 2$.

We consider the derivative of z_+ with respect to β_2, noting that $\varphi_{2\text{in}}(\xi)$ and $\varphi_{3\text{in}}(\xi)$ depend on β_2: Differentiating (2.4.23) with respect to β_2 gives,

$$\delta_1 \left.\frac{\partial}{\partial \beta_2}\left(\varphi_{2\text{in}} + \varphi_{3\text{in}}\right)\right|_{z_+/\eta_2^\alpha} + \frac{\delta_1}{\eta_2^\alpha}\frac{\partial z_+}{\partial \beta_2}\left[\dot{\varphi}_{2\text{in}}\left(\frac{z_+}{\eta_2^\alpha}\right) + \dot{\varphi}_{3\text{in}}\left(\frac{z_+}{\eta_2^\alpha}\right)\right] = 0.$$

Rearranging this gives

$$\frac{\partial z_+}{\partial \beta_2} = -\eta_2^\alpha \frac{\left.\frac{\partial}{\partial \beta_2}\left(\varphi_{2\text{in}} + \varphi_{3\text{in}}\right)\right|_{z_+/\eta_2^\alpha}}{\dot{\varphi}_{2\text{in}}(z_+/\eta_2^\alpha) + \dot{\varphi}_{3\text{in}}(z_+/\eta_2^\alpha)}.$$

We see that

$$\frac{\partial \varphi_{2\text{in}}}{\partial \beta_2} = -\frac{\xi}{2\theta_0}\operatorname{sech}^2\frac{\beta_2 \xi}{2\theta_0}$$

which is less than zero for all $\xi > 0$. We also have

$$\frac{\partial \varphi_{3\text{in}}}{\partial \beta_2} = -\frac{1}{8\theta_0}\sqrt{\frac{\beta_{30}}{\delta_3}}\left[\int_\xi^\infty \mathrm{e}^{\sqrt{\delta_3\beta_{30}}(\xi - s)} s \tanh\frac{\beta_2 s}{2\theta_0}\operatorname{sech}^2\frac{\beta_2 s}{2\theta_0}\,\mathrm{d}s + \int_{-\infty}^\xi \mathrm{e}^{-\sqrt{\delta_3\beta_{30}}(\xi - s)} s \tanh\frac{\beta_2 s}{2\theta_0}\operatorname{sech}^2\frac{\beta_2 s}{2\theta_0}\,\mathrm{d}s\right].$$

We note that

$$s \mapsto s \tanh\frac{\beta_2 s}{2\theta_0}\operatorname{sech}^2\frac{\beta_2 s}{2\theta_0},$$

is a positive even function and this implies

$$\frac{\partial \varphi_{3\mathrm{in}}}{\partial \beta_2} < 0 \quad \text{for all } \xi \in \mathbb{R}.$$

Since $z_+ > 0$, we conclude for $\delta_1 \geq 2$ that

$$\frac{\partial z_+}{\partial \beta_2} < 0.$$

We consider the derivative of z_+ with respect to η_2, noting that $\varphi_{2\mathrm{in}}(\xi)$ and $\varphi_{3\mathrm{in}}(\xi)$ do not depend on η_2: Differentiating (2.4.23) with respect to η_2 gives,

$$\delta_1 \left[\frac{1}{\eta_2^\alpha}\frac{\partial z_+}{\partial \eta_2} - \frac{\alpha z_+}{\eta_2^{1+\alpha}}\right]\left[\dot{\varphi}_{2\mathrm{in}}\left(\frac{z_+}{\eta_2^\alpha}\right) + \dot{\varphi}_{3\mathrm{in}}\left(\frac{z_+}{\eta_2^\alpha}\right)\right] = 0.$$

Since $\dot{\varphi}_{2\mathrm{in}}(\xi), \dot{\varphi}_{3\mathrm{in}}(\xi) < 0$ for $\xi > 0$ and $z_+ > 0$ we have that

$$\frac{\partial z_+}{\partial \eta_2} = \frac{\alpha}{\eta_2} z_+,$$

and hence for $\delta_1 \geq 2$

$$\frac{\partial z_+}{\partial \eta_2} > 0.$$

We consider the derivative of z_+ with respect to δ_3, noting that $\varphi_{2\mathrm{in}}(\xi)$ does not depend on δ_3 where as $\varphi_{3\mathrm{in}}(\xi)$ does: Differentiating (2.4.23) with respect to δ_3 gives,

$$\delta_1 \left.\frac{\partial \varphi_{3\mathrm{in}}}{\partial \delta_3}\right|_{z^+/\eta_2^\alpha} + \frac{\delta_1}{\eta_2^\alpha}\frac{\partial z_+}{\partial \delta_3}\left[\dot{\varphi}_{2\mathrm{in}}\left(\frac{z_+}{\eta_2^\alpha}\right) + \dot{\varphi}_{3\mathrm{in}}\left(\frac{z_+}{\eta_2^\alpha}\right)\right] = 0.$$

Rearranging this gives

$$\frac{\partial z_+}{\partial \delta_3} = -\eta_2^\alpha \frac{\left.\frac{\partial \varphi_{3\mathrm{in}}}{\partial \delta_3}\right|_{z^+/\eta_2^\alpha}}{\dot{\varphi}_{2\mathrm{in}}(z_+/\eta_2^\alpha) + \dot{\varphi}_{3\mathrm{in}}(z_+/\eta_2^\alpha)}.$$

We see that

$$\begin{aligned}\frac{\partial \varphi_{3\mathrm{in}}}{\partial \delta_3} = &-\frac{1}{16\delta_3}\sqrt{\frac{\beta_{30}}{\delta_3}}\left[\int_\xi^\infty \mathrm{e}^{\sqrt{\delta_3\beta_{30}}(\xi-s)}\mathrm{sech}^2\frac{\beta_2 s}{2\theta_0}\,\mathrm{d}s + \int_{-\infty}^\xi \mathrm{e}^{-\sqrt{\delta_3\beta_{30}}(\xi-s)}\mathrm{sech}^2\frac{\beta_2 s}{2\theta_0}\,\mathrm{d}s\right]\\ &-\frac{1}{16}\frac{\beta_{30}}{\delta_3}\left[\int_\xi^\infty \mathrm{e}^{\sqrt{\delta_3\beta_{30}}(\xi-s)}(s-\xi)\mathrm{sech}^2\frac{\beta_2 s}{2\theta_0}\,\mathrm{d}s\right.\\ &\left.+\int_{-\infty}^\xi \mathrm{e}^{-\sqrt{\delta_3\beta_{30}}(\xi-s)}(\xi-s)\mathrm{sech}^2\frac{\beta_2 s}{2\theta_0}\,\mathrm{d}s\right].\end{aligned}$$

Since for all $\xi \in \mathbb{R}$, we have $(s-\xi) > 0$ for $s > \xi$ and $(\xi - s) > 0$ for $s < \xi$, we then have

$$\left.\frac{\partial \varphi_{3\text{in}}}{\partial \delta_3}\right|_{z_+/\eta_2^\alpha} < 0$$

for all $\xi \in \mathbb{R}$ and hence we conclude for $\delta_1 \geq 2$ that

$$\frac{\partial z_+}{\partial \delta_3} < 0.$$

2.C Speed estimation

We outline the details of the parameter estimation technique used to estimate the speed of the TWs from the numerically generated solutions in Section 2.5. Following the procedure outlined in Chapter 5, we consider equation (2.2.8) to obtain our estimate for θ. We assume that $(\varphi_1, \varphi_2, \varphi_3)(z)$ are observed over some interval $I \subset \mathbb{R}$ and we consider a weight function $\phi : I \to \mathbb{R}$ where ϕ and ϕ' exist and are integrable. We note that (2.2.8) was chosen since it is first order and hence makes the application of this method slightly simpler (if we were to choose (2.2.9) or (2.2.10) to estimate θ we would require estimates for the relevant derivatives of $(\varphi_1, \varphi_2, \varphi_3)$ at the endpoints of the interval or, alternatively, in the case of (2.2.10) we would require ϕ be zero at the endpoints of the interval I). Multiply (2.2.8) by the weight function $\phi(z)$ and integrate over the interval I using integration by parts to obtain

$$\left[\phi(z)\varphi_1(z)|_I - \int_I \phi'(z)\varphi_1(z)\,\mathrm{d}z\right]\theta + \int_I \phi(z)\varphi_1(z)[1-\varphi_1(z)-\delta_1\varphi_2(z)-\delta_1\varphi_3(z)]\,\mathrm{d}z = 0. \tag{2.C.1}$$

Since we are estimating just one parameter we choose $\phi(z) = 1$ for simplicity. Therefore rearranging (2.C.1), we obtain

$$\theta = -\frac{\int_I \varphi_1(z)[1-\varphi_1(z)-\delta_1\varphi_2(z)-\delta_1\varphi_3(z)]\,\mathrm{d}z}{\varphi_1(z)|_I}. \tag{2.C.2}$$

If we have observed data for $\varphi_1, \varphi_2, \varphi_3$ on some interval I, then we can then estimate the value for θ by evaluating the integrals contained in (2.C.2) numerically. Since our solutions for (2.2.4)–(2.2.6) are TWs, the profile of the solutions are therefore time invariant. Hence we can use the values obtained from solving this system numerically (with a sufficiently large time domain) as our observed values for $\varphi_1, \varphi_2, \varphi_3$ and the domain of our numerical solution as our interval I.

Chapter 3

Acid-mediated tumour invasion with chemotherapy intervention: spatially homogeneous populations

3.1 Introduction

This chapter considers the acid-mediation hypothesis with the added interaction of a tumour treatment protocol. As explained in Chapter 1, the acid-mediation hypothesis is the assumption that tumour invasion is facilitated by acidification of the region around the tumour-host interface caused by the Warburg effect [202]. This acidification creates an inhospitable environment and results in the destruction of the normal-tissue ahead of the acid resistant tumour thus enabling the tumour to invade into the vacant region. This hypothesis was first examined by Gatenby and Gawlinski [71] with a system of RD equations that considers the interaction between the tumour, normal tissue and acid. This chapter examines the acid-mediation hypothesis with the inclusion of population competition as considered in [140] and also the effect of tumour treatment from a cytotoxic agent such as used for chemotherapy. This will be considered here in a spatially homogeneous environment to gain an understanding of the reaction dynamics that could predict behaviour of an arguably more realistic spatially heterogeneous setting. The spatially heterogeneous setting will be considered in the following chapter, where a system of RD equations similar to those considered in [71, 72, 140] will be utilised.

The effect of chemotherapy treatment has yet to be considered in a model that utilises the acid-mediation hypothesis. We wish to present a model that addresses this unexamined question of the

interaction of the low extracellular pH of the tumour microenvironment and a cytotoxic tumour treatment. There are however many models that consider chemotherapy and the corresponding effect on the growth of solid tumours. Continuum models have been used in which the dynamics of total cell populations and average chemotherapy drug concentration are considered by employing the use of ODEs, some examples include [30, 49, 50]. There are recent models that consider the addition of an immune response in a tumour cell and chemotherapy model [47, 49] encouraged by experimental results suggesting an important impact of the host immune response on the effectiveness of a chemotherapy treatment. Gatenby and Gillies [73] note that highly acidic tumours have been shown to be resistent to anthracyclines as a result of greater phenotypic diversity [64] which is enabled by mutagenic/clastogenic effects of acidosis. The effects of normal cell populations in a model that considers chemotherapy have largely been neglected. Hence it is an aim of this analysis is to determine whether the presence of normal cells can alter the perceived effectiveness of chemotherapy.

This chapter is organised in the following manner. Section 3.2 describes the assumptions made by the model and provides the formulation of the mathematical model being considered. In Section 3.3 the results are presented of a steady-state analysis for the model when treatment characterised by a constant infusion of the chemotherapy drug is considered. The analysis of the model considering regularly scheduled treatments occurring in cycles is presented in Section 3.4. A discussion of the results of the analysis of the model considering treatment cycles is given in Section 3.5. Concluding remarks have been provided in Section 3.6. Additional results and some of the more laborious calculations required for Sections 3.3 and 3.4 have been provided in Appendices 3.A–3.C.

3.2 Model formulation

The basic assumptions taken into account to develop the model are

(i) Both normal and tumour cells are governed by logistic growth in the absence of any kind of intervention [48, 49, 71];

(ii) A population competition relationship exists between the normal and tumour cells [140];

(iii) The tumour tissue produces H^+ ions as a result of aerobic glycolysis [71, 140] at a rate proportional to a function of the tumour cell density;

(iv) The normal tissue interacts with the excess H^+ ions, leading to a death rate proportional to the concentration of H^+ ions [71, 140];

(v) The excess H^+ ions are produced at a rate proportional to the tumour cell density and an uptake term is included to take account of mechanisms for increasing pH [71];

(vi) The chemotherapy drug is infused at a rate given by a function of time. A term is included for removal of drug from the system by metabolic processes [30, 49];

(vii) The tumour tissue interacts with the chemotherapy drug leading to destruction of tumour tissue at a rate proportional to the concentration of drug [30, 49];

(viii) The chemotherapy drug concentration is decreased as a result of interaction with the tumour tissue [30].

Let the populations at time s (in s) be denoted by:

- $N_1(s)$, normal cell density (in $\text{cells}\,\text{cm}^{-3}$),
- $N_2(s)$, tumour cell density (in $\text{cells}\,\text{cm}^{-3}$),
- $L(s)$, excess H^+ ion concentration (in M),
- $C(s)$, chemotherapy drug concentration (in M).

Consider the following model

$$\frac{\mathrm{d}N_1}{\mathrm{d}s} = \underbrace{r_1 N_1\left(1-\frac{N_1}{K_1}-\alpha_1\frac{N_2}{K_2}\right)}_{\text{logistic growth with cellular competition}} - \underbrace{d_1 L N_1}_{\substack{\text{normal cell}\\ \text{death by acid}}}, \tag{3.2.1}$$

$$\frac{\mathrm{d}N_2}{\mathrm{d}s} = \underbrace{r_2 N_2\left(1-\frac{N_2}{K_2}-\alpha_2\frac{N_1}{K_1}\right)}_{\text{logistic growth with cellular competition}} - \underbrace{d_2 C N_2}_{\substack{\text{tumour death}\\ \text{by drug}}}, \tag{3.2.2}$$

$$\frac{\mathrm{d}L}{\mathrm{d}s} = \underbrace{r_3 f(N_2)}_{\text{acid production}} - \underbrace{m_3 L}_{\text{acid uptake}}, \tag{3.2.3}$$

$$\frac{\mathrm{d}C}{\mathrm{d}s} = \underbrace{r_I(s)}_{\text{drug infusion}} - \underbrace{m_4 C}_{\text{drug decomposition}} - \underbrace{d_4 C N_2}_{\substack{\text{drug-tumour}\\ \text{interaction removal}}}. \tag{3.2.4}$$

The conventions used here are that the subscript for each parameter corresponds to the relevant equation; r represents growth rate; K represents carrying capacity; α represents population competition strength; d represents rate of decrease due to interaction; m represents decrease through

system mechanisms. The parameters used in the model, their interpretation and potential values/range of values have been provided in Table 3.1. Note that we have assumed the use of a stage-specific drug that targets rapidly dividing cells, as discussed in Section 1.2.5, which will primarily target tumour cells. Since normal cell division is a well regulated process [90] we have assumed that the chemotherapeutic effect on the normal tissue can be approximated by reducing the normal tissue's competitive effect and resistance to the presence of acid.

Table 3.1: Table of parameters and estimated values for (3.2.1)–(3.2.4)

Parameter	Units	Description	Value	Source
r_1	s^{-1}	normal cell growth rate	$O(10^{-6})$	[49, 71]
r_2	s^{-1}	tumour cell growth rate	$O(10^{-6})$	[49, 71]
r_3	$\mathrm{M\,cm^3\,s^{-1}cells^{-1}}$	H^+ ion production rate	2.2×10^{-17}	[133]
d_1	$\mathrm{M^{-1}\,s^{-1}}$	fractional normal cell kill by H^+ ions	$O(1)$	[71]
d_2	$\mathrm{M^{-1}\,s^{-1}}$	fractional tumor cell kill by chemotherapy	9.3×10^{-6}	[50]
d_4	$\mathrm{cells^{-1}\,s^{-1}}$	fractional chemotherapy removal by tumour interaction	10^{-13}–10^{-12}	estimated
m_3	s^{-1}	H^+ ion removal rate	$O(10^{-4})$	[71]
m_4	s^{-1}	chemotherapy removal rate	$O(10^{-5})$	[49, 104]
K_1	$\mathrm{cells\,cm^{-3}}$	normal cell carrying capacity	5×10^7	[195]
K_2	$\mathrm{cells\,cm^{-3}}$	tumour cell carrying capacity	5×10^7	[195]
α_1	none	fractional normal cell death due to tumour cell	$O(1)$	chosen freely
α_2	none	fractional tumour cell death due to normal cell	$O(1)$	chosen freely

A question arises: What do we choose for $f(N_2)$ and $r_I(s)$? In the model considered by Gatenby and Gawlinski [71] and McGillen et al. [140] it was assumed that acid was produced as a linear function of the tumour cell density, i.e. $f(N_2) = N_2$. In the model considered in Chapter 2 a nonlinear acid production term was used as a result of the hypothesis that when the tumour cell density was small, acid was produced at a rate proportional to the tumour cell density until a tumour cell saturation was reached at which point acid production would decrease to zero. With this in mind, the function $f(N_2) = N_2(1-N_2/K_2)$ was used. For simplicity we wish to use the acid production term considered in [71] and [140], as such we have $f(N_2) = N_2$. However the term utilised in Chapter 2 or some other nonlinear production term could still be utilised in this or further models.

As for $r_I(s)$, we will choose appropriate functions to represent various treatment protocols. Hence the most obvious, and perhaps most realistic, choice would be to chose a function that is periodic, i.e. $r_I(s) = r_I(s+P)$, where P represents the length of the treatment cycle, or

period, as this would represent a treatment that occurs in repeated cycles such as taking pills or an intravenous administration made in regularly scheduled doses. However to enable a greater potential for analysis we can choose $r_I(s)$ to be constant which would represent a constant infusion of chemotherapy drug, i.e. via a device such as an intravenous pump. No matter the choice of $r_I(s)$ we will naturally require it to meet the conditions that $r_I(s) \geq 0$ for all $s \geq 0$ and that $r_I(s)$ is bounded almost everywhere. These represent natural limitations on a treatment since a negative infusion rate would represent removal of drug from the system and an unbounded infusion rate would represent an infinite amount of drug to be infused.

In the case of administration by pills the use of periodic Dirac delta functions (i.e. $\delta(s)$) can be used to approximate this method of delivery: Let P be the length of the treatment cycle and N being the total number of treatment cycles, then

$$r_I(s) = r_4 \sum_{n=0}^{N-1} \delta(s - nP). \tag{3.2.5}$$

In the case of intravenous infusion occurring in periodic cycles we can approximate this method of delivery with periodic uses of a boxcar function: Let P denote the cycle period and s_0 denote the infusion time, then

$$r_I(s) = r_4 \sum_{n=0}^{N-1} [H(s - nP) - H(s - nP - s_0)], \tag{3.2.6}$$

where r_4 represents the constant rate of intravenous infusion and $H(s)$ is the Heaviside function.

Considering the function $r_I(s)$ with period P we let

$$\bar{r} = \frac{1}{P} \int_0^P r_I(s)\,\mathrm{d}s$$

and then utilise the value $\bar{r}$ to non-dimensionalise the equations given by (3.2.1)–(3.2.4). We remark that this choice of parameter to non-dimensionalise the model enables us to effectively compare the model when utilising different infusion functions. This is because under this non-dimensionalisation the constant infusion rate is equal to the average infusion rate in the periodic case and this will imply that the same amount of drug is infused per cycle no matter the infusion function used. Hence we can compare the models that use the same non-dimensional parameter values.

Make the following substitutions

$$u_1 = \frac{N_1}{K_1}, \quad u_2 = \frac{N_2}{K_2}, \quad u_3 = \frac{m_3}{r_3 K_2} L, \quad u_4 = \frac{m_4}{\bar{r}} C, \quad t = r_1 s,$$

with

$$\beta_2 = \frac{r_2}{r_1}, \quad \beta_3 = \frac{m_3}{r_1}, \quad \beta_4 = \frac{m_4}{r_1}, \quad \delta_1 = \frac{r_3 K_2 d_1}{r_1 m_3}, \quad \delta_2 = \frac{d_2 \bar{r}}{r_2 m_4}, \quad \delta_4 = \frac{d_4 K_2}{m_4}$$

and

$$i(t) = \frac{r_I(t/r_1)}{\bar{r}}, \quad \rho = r_1 P.$$

We then obtain the following system of non-dimensionalised equations

$$\mathbf{u}' = \begin{bmatrix} u_1' \\ u_2' \\ u_3' \\ u_4' \end{bmatrix} = \begin{bmatrix} u_1(1 - u_1 - \alpha_1 u_2 - \delta_1 u_3) \\ \beta_2 u_2(1 - u_2 - \alpha_2 u_1 - \delta_2 u_4) \\ \beta_3(u_2 - u_3) \\ \beta_4[i(t) - u_4 - \delta_4 u_4 u_2] \end{bmatrix} =: \mathbf{F}(t, \mathbf{u}), \tag{3.2.7}$$

where $(\,)'$ denotes differentiation with respect to t. Note that

$$\bar{i} = \frac{1}{\rho} \int_0^\rho i(t)\, \mathrm{d}t = 1$$

and thus the average rate of infusion over each treatment cycle has been normalised to be equal to one. Moreover, under this non-dimensionalisation, the functions (3.2.5) and (3.2.6) become

$$i(t) = \rho \sum_{n=0}^{N-1} \delta(t - n\rho)$$

and

$$i(t) = \frac{\rho}{\tau} \sum_{n=0}^{N-1} [H(t - n\rho) - H(t - n\rho - \tau)]; \quad \tau = r_1 s_0, \tag{3.2.8}$$

respectively.

A summary of potential non-dimensional parameter values/range of values and interpretation of their meaning has been provided in Table 3.2. Note that the primary control parameter is δ_2 since an increase in the amount of drug infused will cause δ_2 to increase.

Table 3.2: Table of non-dimensionalised parameters for (3.2.7)

Parameter	Interpretation	Value/Range
α_1	fractional normal death due to tumour competition	$O(1)$
α_2	fractional tumour death due to normal competition	$O(1)$
δ_1	tumour aggressiveness	$O(1)$
δ_2	chemotherapy aggressiveness	$O(10^{-1})$–$O(1)$
δ_4	fractional removal due to interaction strength	$O(10^{-1})$–$O(1)$
β_2	relative tumour growth rate	1.0
β_3	relative H^+ ion production rate	$O(10^2)$
β_4	relative chemotherapy rate of increase	$O(10)$

Note we define $\mathbb{R}_+ := [0, \infty)$ and the convention is used that if $\mathbf{u}, \mathbf{v} \in \mathbb{R}^n$, then $\mathbf{u} \leq (<)\mathbf{v}$ implies that $u_j \leq (<)v_j$ for all $j \in \{1, \ldots, n\}$. Moreover, if $c \in \mathbb{R}$, then $\mathbf{u} \geq (>)c$ implies that $u_j \geq (>)c$ for all $j \in \{1, \ldots, n\}$.

Theorem 3.2.1. *Let $i \in C(\mathbb{R}_+, [0, i_M])$, where $i_M \in \mathbb{R}$ and $i_M > 0$. If $\mathbf{u}(0) \in \mathbb{R}^4_+$, then* (3.2.7) *has a unique solution $\mathbf{u}$ that satisfies $\mathbf{u}(t) \in \mathbb{R}^4_+$ for all $t \in \mathbb{R}_+$.*

Proof. We utilise Theorem 3.A.7 that requires the existence of an invariant set, as given by Definition 3.A.3 in Appendix 3.A. Clearly, $\mathbf{F} \in C(\mathbb{R}_+ \times S, \mathbb{R}^4)$ and $\mathbf{F}'_{\mathbf{u}} \in C(\mathbb{R}_+ \times S, \mathbb{R}^{4^2})$, where S is any compact set in $\mathbb{R}^4$. This implies that $\mathbf{F}$ is Lipschitz continuous with respect to $\mathbf{u}$ in any compact set $S \subset \mathbb{R}^4$, that is, there exists a constant $L > 0$ such that for any $\mathbf{u}_1, \mathbf{u}_2 \in S \subset \mathbb{R}^4$ and $t \in \mathbb{R}_+$, the following inequality holds:

$$\|\mathbf{F}(t, \mathbf{u}_1) - \mathbf{F}(t, \mathbf{u}_2)\| \leq L\|\mathbf{u}_1 - \mathbf{u}_2\|. \tag{3.2.9}$$

The Cauchy–Schwarz inequality and (3.2.9) are now used to show that the one-sided Lipschitz condition in Theorem 3.A.7 in Appendix 3.A is satisfied on any compact set $S \subset \mathbb{R}^4$. For any $\mathbf{u}_1, \mathbf{u}_2 \in S \subset \mathbb{R}^4$ and $t \in \mathbb{R}_+$,

$$\langle \mathbf{u}_1 - \mathbf{u}_2, \mathbf{F}(t, \mathbf{u}_1) - \mathbf{F}(t, \mathbf{u}_2) \rangle \leq \|\mathbf{u}_1 - \mathbf{u}_2\| \|\mathbf{F}(t, \mathbf{u}_1) - \mathbf{F}(t, \mathbf{u}_2)\| \leq L\|\mathbf{u}_1 - \mathbf{u}_2\|^2.$$

An invariant set, as given by Definition 3.A.3 in Appendix 3.A, is now constructed in $\mathbb{R}^4_+$. A set $S \subset \mathbb{R}^4$ will be invariant with respect to (3.2.7) if

$$\langle \mathbf{n}(\mathbf{u}), \mathbf{F}(t, \mathbf{u}) \rangle \leq 0 \quad \text{for all} \quad t \in \mathbb{R}_+, \quad \mathbf{u} \in \partial S,$$

where $\mathbf{n}(\mathbf{u})$ is the outer normal to S at $\mathbf{u}$. This invariance condition tells us that if $\mathbf{u}(0) \in S$, then the whole path of the solution $\mathbf{u}(t)$ will remain in S. Let $S = E_1 \times E_2 \times E_3 \times E_4$, where $E_1 = [0, \max\{1, u_1(0)\}]$, $E_2 = [0, \max\{1, u_2(0)\}]$, $E_3 = [0, \max\{1, u_2(0), u_3(0)\}]$ and $E_4 = [0, \max\{i_M, u_4(0)\}]$. Clearly, $S \subset \mathbb{R}^4_+$, $\mathbf{u}(0) \in S$ and S is compact. Hence $\mathbf{F}$ will satisfy the one-sided Lipschitz condition on S. The boundary of S (i.e. ∂S) can be written as the union of eight simple sets that have a simple outer normal. Let $\partial S_{i1} = \{\mathbf{u} \in S : u_i = \inf E_i\}$ and $\partial S_{i2} = \{\mathbf{u} \in S : u_i = \sup E_i\}$ for $i = 1, 2, 3, 4$, then $\partial S = \bigcup_{i=1}^4 \partial S_{i1} \cup \partial S_{i2}$. Furthermore, each ∂S_{ij} for $i = 1, 2, 3, 4$, $j = 1, 2$, has outer normal $\mathbf{n}_{ij} = (-1)^j \mathbf{e}_i$, where $\mathbf{e}_i$ for $i = 1, 2, 3, 4$ are the standard basis vectors in $\mathbb{R}^4$. Then, it is straightforward to show that

$$\langle \mathbf{n}_{ij}, \mathbf{F}(t, \mathbf{u}) \rangle = (-1)^j F_i(t, \mathbf{u}) \leq 0, \text{ for } t \in \mathbb{R}_+, \ \mathbf{u} \in \partial S_{ij}, \ i = 1, 2, 3, 4, \ j = 1, 2.$$

Hence the set S is invariant and $\mathbf{F}$ satisfies the one-sided Lipschitz condition on S. Therefore by Theorem 3.A.7 in Appendix 3.A, there exists a unique solution for all time to (3.2.7) with initial condition $\mathbf{u}(0) \in S \subset \mathbb{R}^4_+$, where the path of the solution remains in S. □

Note by a similar argument to the above proof, solutions $\mathbf{u}(t)$ of (3.2.7) are invariant on the sets $\Gamma_1 = \{0\} \times \mathbb{R}^3$ and $\Gamma_2 = \mathbb{R} \times \{0\} \times \mathbb{R}^2$. Hence if there exists $t_1 \in \mathbb{R}_+$ such that $u_1(t_1) = 0$, then $u_1(t) = 0$ for all $t \in [t_1, \infty)$, similarly if there exists $t_2 \in \mathbb{R}_+$ such that $u_2(t_2) = 0$, then $u_2(t) = 0$ for all $t \in [t_2, \infty)$.

3.3 Constant infusion of chemotherapy drug

If we consider (3.2.7) with constant infusion (i.e. $i(t) = 1$), we obtain the system of equations

$$\mathbf{u}' = \begin{bmatrix} u_1' \\ u_2' \\ u_3' \\ u_4' \end{bmatrix} = \begin{bmatrix} u_1(1 - u_1 - \alpha_1 u_2 - \delta_1 u_3) \\ \beta_2 u_2(1 - u_2 - \alpha_2 u_1 - \delta_2 u_4) \\ \beta_3(u_2 - u_3) \\ \beta_4(1 - u_4 - \delta_4 u_4 u_2) \end{bmatrix}. \tag{3.3.1}$$

3.3.1 Steady-state analysis

The natural method for analysis of a system of first-order nonlinear autonomous ODEs is through the use of a SS analysis to determine the long-term behaviour of the system. A summary of the results of the SS analysis and stability analysis for system (3.3.1) is presented below. For full details

of the analysis see Lemma 3.C.1 in Appendix 3.C.

System (3.3.1) has SS solutions:

SS1. $\mathbf{u}^* = (0, 0, 0, 1)$;

SS2. $\mathbf{u}^* = (1, 0, 0, 1)$;

SS3. $\mathbf{u}^* = (0, \hat{u}_2, \hat{u}_2, [1 + \delta_4 \hat{u}_2]^{-1})$, where $\hat{u}_2$ solves

$$\delta_4 \hat{u}_2^2 + (1 - \delta_4)\hat{u}_2 + \delta_2 - 1 = 0;$$

SS4. $\mathbf{u}^* = (1 - (\alpha_1 + \delta_1)\tilde{u}_2, \tilde{u}_2, \tilde{u}_2, [1 + \delta_4 \tilde{u}_2]^{-1})$, where $\tilde{u}_2$ solves

$$\delta_4[1 - \alpha_2(\alpha_1 + \delta_1)]\tilde{u}_2^2 + [1 - \alpha_2(\alpha_1 + \delta_1) + \delta_4(\alpha_2 - 1)]\tilde{u}_2 + \delta_2 + \alpha_2 - 1 = 0.$$

However note that the zero population SS (i.e. SS1) is unconditionally unstable and as a result the solution should always tend towards containing a population of either normal-tissue or tumour-tissue. We see that the tumour free SS (i.e. SS2) is stable provided $\alpha_2 + \delta_2 > 1$. Therefore assuming there is a tumour population, we at the least require this condition to remove the tumour from the system. This condition corresponds to a sufficiently strong treatment in combination with a sufficiently strong population competition provided by the normal-tissue. This state represents the desired state of existence for the system from the point of view of the patient. Hence it is an aim to discover how the system can be altered to make SS2 the most likely long term solution.

It can be seen from Lemma 3.C.1(iii) in Appendix 3.C that the normal-tissue free SS (i.e. SS3) is stable provided certain parameter conditions are met: these being if

$$\delta_2 < \frac{(\alpha_1 + \delta_1 + \delta_4)(\alpha_1 + \delta_1 - 1)}{(\alpha_1 + \delta_1)^2},$$

or if

$$\frac{(\alpha_1 + \delta_1 + \delta_4)(\alpha_1 + \delta_1 - 1)}{(\alpha_1 + \delta_1)^2} \leq \delta_2 < \frac{(1 + \delta_4)^2}{4\delta_4} \quad \text{and} \quad \frac{1}{\delta_4} < \frac{\alpha_1 + \delta_1 - 2}{\alpha_1 + \delta_1}.$$

This state corresponds to an invasive tumour population in which all normal-tissue in the region is destroyed and replaced by the advancing tumour. Note that from the stability conditions, for the normal-tissue free population to be stable it is a necessary condition that $\alpha_1 + \delta_1 > 1$, otherwise the SS will be unconditionally unstable. This means that the tumour needs to provide sufficiently strong

population competition and destructive influence of the acid to potentially be stable. Furthermore, the destructive influence of the treatment (δ_2) needs to be sufficiently small or, alternatively, the removal of chemotherapy drug from interaction with tumour cells (δ_4) needs to be sufficiently large to ensure that SS2 is stable. We remark that if $\delta_2 > (1+\delta_4)^2/4\delta_4$, then the normal-tissue free state does not exist (i.e. $\hat{u}_2 \notin \mathbb{R}$). Hence this condition represents a scenario in which the tumour will be completely removed from the system by the treatment alone. As δ_2 directly relates to the strength of the treatment dose, to obtain a value of δ_2 that will ensure the removal of the tumour by treatment alone may present safety and health concerns for the patient [53, 164]. However from the stability conditions, should the tumour-tissue population competition, the destructive influence of the acid or the removal of drug by interaction with the tumour be decreased, then this could enable the tumour to be removed without using a dangerous treatment dose. As noted in [60, 73] the use of an acid buffer to decrease the acidity could be a potential method to increase the efficacy of the treatment without further increasing doses of strong cytotoxic drugs.

The normal-tissue free state can be stable when the tumour-tissue free state is either unstable or stable. In the case the normal-tissue free state is stable when the tumour-tissue free state is unstable, the long term behaviour would be for the tumour to establish a fixed population that cannot be eradicated by the current treatment protocol. This would suggest that the normal-tissue and chemotherapy treatment would be weak in relation to the tumour-tissue and would potentially correspond to a very aggressive tumour. In the case that both the tumour-tissue free state and the normal-tissue free state are stable, the question of whether the treatment will be effective or the tumour population will successfully invade is dependent on the initial conditions. Therefore the suggestion is that the effectiveness of the treatment will be determined by the size of the initial tumour population. This is consistent with the decreased probability of a cure associated with larger and more established tumour cell populations [164].

The coexistence of tumour- and normal-tissue SS (i.e. SS4) is stable and exists for a complicated, yet still calculable, set of parameter conditions given in Lemma 3.C.1(iv) in Appendix 3.C. These parameter conditions suggest that in order for the coexistence state to exist, the system requires unaggressive tumour- and normal-tissue in combination with a weak treatment response. That is, there needs to be very low population competition, tumour aggressiveness and destructive influence of the chemotherapy treatment. As in [71], this suggests that the SS would represent a benign state of existence. The coexistence SS can potentially change to either the tumour-tissue free SS or the normal-tissue free SS provided a sufficient change occurs in the parameters. Should

the tumour aggressiveness or the tumour-tissue population competition increase, then the tumour would transition to the invasive state, where the normal-tissue free state is stable. Similarly, should the normal-tissue population competition or the destructive influence of the treatment increase, then the tumour will be eradicated from the system.

3.3.2 A reduced model with constant infusion

If we consider the situation originally examined in [30] we have the system of equations

$$\mathbf{x}' = \begin{bmatrix} x_1' \\ x_2' \end{bmatrix} = \begin{bmatrix} \beta_2 x_1(1 - x_1 - \delta_2 x_2) \\ \beta_4(1 - x_2 - \delta_4 x_1 x_2) \end{bmatrix}, \tag{3.3.2}$$

where x_1 represents non-dimensionalised tumour cell density, x_2 represents non-dimensionalised drug concentration and the parameters are as given in (3.3.1). If $\alpha_2 = 0$ in (3.3.1), then the reduced system (3.3.2) provides the governing dynamics for the tumour-tissue density and cytotoxic drug concentration. Analysing this system we can obtain the conditions under which it is sufficient to obtain tumour clearance from the system by chemotherapy drug without the assistance of population competition. The results for this model are considered in [30], however we provide them here in the current parameters for the convenience of the reader and easy reference for further results in this chapter. Moreover, the details of the relevant SS analysis is provided in Appendix 3.C. As in [30], see that this system has the SS solutions:

RS1. $\mathbf{x}^* = (0, 1)$;

RS2. $\mathbf{x}^* = \left(\hat{u}_2, [1 + \delta_4 \hat{u}_2]^{-1}\right)$, where $\delta_4 \hat{u}_2^2 + (1 - \delta_4)\hat{u}_2 + \delta_2 - 1 = 0$.

Note that these are the same values for the tumour density and drug concentration obtained for SS2 and SS3, respectively. Hence we have that this quadratic equation has the solutions

$$\hat{u}_{2\pm} = \frac{\delta_4 - 1 \pm \sqrt{(1 - \delta_4)^2 + 4\delta_4(1 - \delta_2)}}{2\delta_4},$$

where $\hat{u}_{2\pm} \in \mathbb{R}$ if and only if $\delta_2 \leq (1 + \delta_4)^2/4\delta_4$.

As is shown by Byrne [30], RS1 is stable for $\delta_2 > 1$, and RS2 is stable if

$$\delta_2 < 1, \quad \text{or if} \quad 1 \leq \delta_2 < \frac{(1 + \delta_4)^2}{4\delta_4} \text{ and } \delta_4 > 1.$$

Note that the SS $\mathbf{x}^* = (\hat{u}_{2-}, 1/(1+\delta_4\hat{u}_{2-}))$ is unconditionally unstable. In the case $1 < \delta_2 < (1+\delta_4)^2/4\delta_4$ and $\delta_4 > 1$ this SS is positive and represents a point on which the separatrix lies.

Furthermore, it can be shown that if $\delta_2 \geq 1$ and $\delta_4 < 1$, or if $\delta_2 > (1+\delta_4)^2/4\delta_4$, that the long term behaviour of the model will be for the tumour to be eradicated from the system, since not only is RS2 unstable but also biologically meaningless. Moreover, note that under this parameter condition in the case of the full system (3.3.1) we similarly get that the tumour-tissue free SS (i.e. SS2) is the only stable solution and as a result the tumour will be eradicated from the system. We remark that in the case of the parameter condition $\delta_2 > (1+\delta_4)^2/4\delta_4$, RS2 does not exist as $\hat{u}_2 \notin \mathbb{R}$. This would suggest that if this condition is satisfied, then the chemotherapy treatment alone will be sufficient to eradicate the tumour without the assistance of the normal cell population to weaken the tumour cells through competition. We can see that under these conditions that the tumour will always be eradicated since should the population of normal cells be zero, the governing dynamics of the system will reduce to that given by (3.3.2). Therefore this indicates that there is a sufficient scenario under which a tumour will be cleared from the system regardless of the interactions between normal and tumour-tissue. Whilst this observation is an ideal aim to achieve, it is not always feasible or possible due to the fact that this may require doses which would potentially kill the host or require the interaction between the treatment and tumour-tissue to be sufficiently weighted in favour of the treatment.

In the case $\delta_2 < 1$ we have a situation in which the tumour free solution is unstable and hence this would suggest that the tumour is not able to be removed from the system by chemotherapy. However if we are considering the system given by (3.3.1), provided a condition on population competition is satisfied (i.e. $\alpha_2 + \delta_2 > 1$), the tumour free solution will become stable. Furthermore, should tumour aggressiveness and competition be sufficiently small (see Lemma 3.C.1(i)) we will have that the normal-tissue free SS will become unstable. Therefore under these conditions we will have that the tumour will be eradicated from the system by the combined strength of population competition and chemotherapy treatment.

3.4 Periodic infusion of chemotherapy drug

In Section 3.2 we stated that a more realistic function for the infusion of drug is a periodic function such as considered in [49, 50]. Hence assume that $i(t+\rho) = i(t) \geq 0$ for all $t \in \mathbb{R}_+$. Some preliminary numerical simulations of (3.2.7) were run, with $i(t)$ given by (3.2.8), using the `ode15s`

command in MATLAB with parameter values consistent with Table 3.2. The values $\rho = 2.8$ (P approximately 1 week), $\tau = 1.2$ (s_0 approximately 3 days) and total time $T = 40$ (approximately 3-4 months) were used with initial values $\mathbf{u}(0) = (0.9, 0.1, 0.1, 0)$. In these simulations three different behaviours occurred: the eradication of the tumour from the system; the "invasion" of the tumour and subsequent destruction of the normal-tissue; the coexistence of the tumour and normal-tissue. Examples of these behaviours are displayed in Figures 3.1–3.3, respectively.

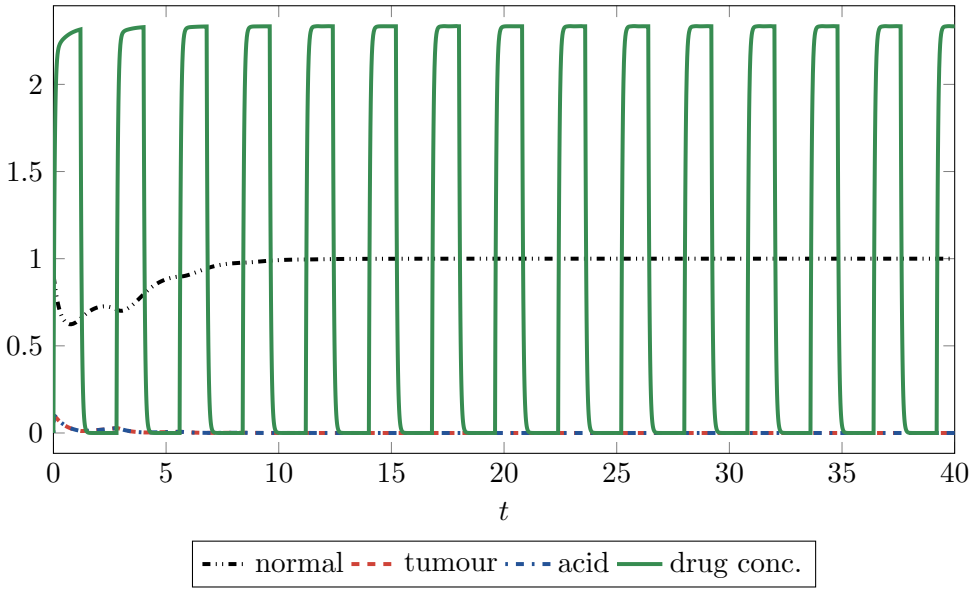

Figure 3.1: Simulation of (3.2.7) for $\alpha_1 = 1$, $\alpha_2 = 0.5$, $\beta_2 = 1$, $\beta_3 = 70$, $\beta_4 = 20$, $\delta_1 = 12.5$, $\delta_2 = 1.1$, $\delta_4 = 0.6$

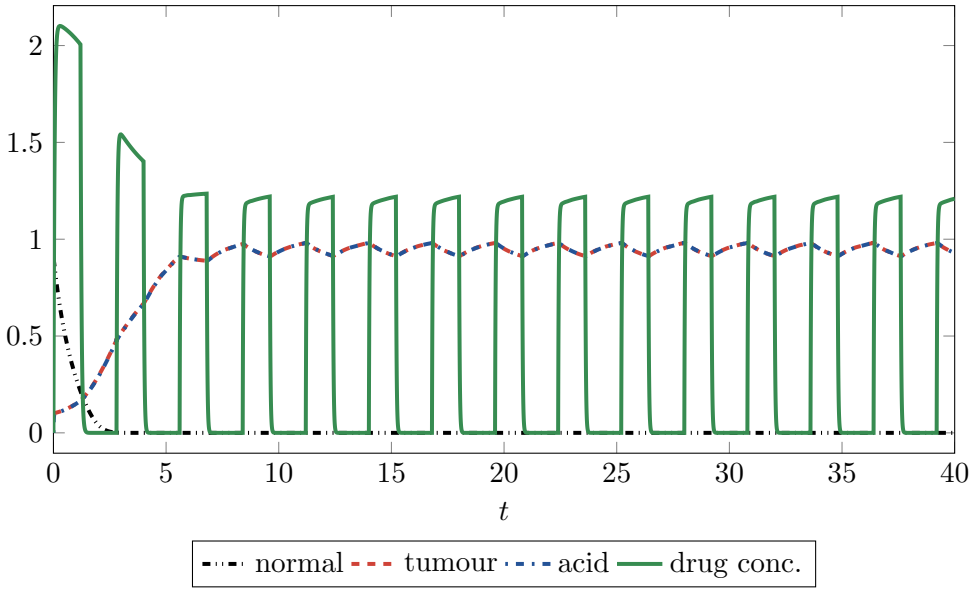

Figure 3.2: Simulation of (3.2.7) for $\alpha_1 = 1$, $\alpha_2 = 0.5$, $\beta_2 = 1$, $\beta_3 = 70$, $\beta_4 = 20$, $\delta_1 = 12.5$, $\delta_2 = 0.1$, $\delta_4 = 1$

Notice in each of these figures that the solutions evolve towards stable ρ-periodic solutions (i.e.

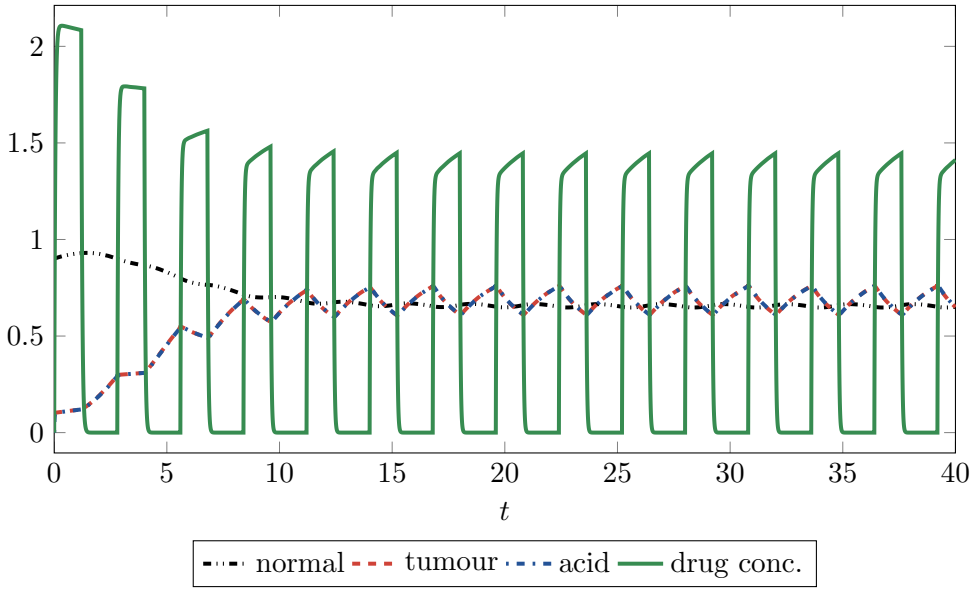

Figure 3.3: Simulation of (3.2.7) for $\alpha_1 = 0.25$, $\alpha_2 = 0.25$, $\beta_2 = 1$, $\beta_3 = 70$, $\beta_4 = 20$, $\delta_1 = 0.25$, $\delta_2 = 0.25$, $\delta_4 = 1$

$\mathbf{u}(t) = \mathbf{u}(t+\rho)$). Therefore to analyse this model we look for time-periodic solutions to (3.2.7) with period ρ (i.e. $\mathbf{u}(t+\rho) = \mathbf{u}(t)$ for all $t \in \mathbb{R}_+$) and analyse the stability of these solutions to determine the long term behaviour of the system. This is analogous to a steady-state analysis or limit-cycle analysis for an autonomous system of equations.

A reduced version of system (3.2.7) is considered first that corresponds to when the solution for $u_1 \equiv 0$. The system considered will be analogous to the reduced system considered in Section 3.3.2. Moreover, the reduced system corresponds to that originally proposed in [30]. Byrne [30] however did not analyse the system in this form, but rather made the simplifying assumption that the drug concentration was equivalent to the infusion function which was given by (3.2.8). This reduced the system to a single explicitly solvable Bernoulli equation. Here we present a more thorough analysis of this model for general ρ-periodic functions $i \in C(\mathbb{R}_+)$.

3.4.1 Existence, uniqueness and stability of the periodic solution of a reduced system

Consider the system

$$\mathbf{x}' = \begin{bmatrix} x_1' \\ x_2' \end{bmatrix} = \begin{bmatrix} \beta_2 x_1(1 - x_1 - \delta_2 x_2) \\ \beta_4[i(t) - x_2 - \delta_4 x_1 x_2] \end{bmatrix} =: \mathbf{G}(t, \mathbf{x}). \tag{3.4.1}$$

The results of Lemma 3.B.3 in Appendix 3.B show that periodic solutions can exist for sys-

tem (3.4.1) only if $\delta_2 < 1$, or only if $1 \leq \delta_2 < (1+\delta_4)^2/4\delta_4$ and $\delta_4 > 1$. Hence this guides the region of parameter values for which we look for ρ-periodic solutions to exist for (3.4.1).

Existence

Suppose that $\delta_2 < 1$ and consider the systems

$$\underline{\mathbf{x}}' = \begin{bmatrix} \underline{x}_1' \\ \underline{x}_2' \end{bmatrix} = \begin{bmatrix} \beta_2 \underline{x}_1(1 - \underline{x}_1 - \delta_2 \underline{x}_2) \\ \beta_4[i(t) - \underline{x}_2] \end{bmatrix} =: \underline{\mathbf{G}}(t, \underline{\mathbf{x}}) \tag{3.4.2}$$

and

$$\bar{\mathbf{x}}' = \begin{bmatrix} \bar{x}_1' \\ \bar{x}_2' \end{bmatrix} = \begin{bmatrix} \beta_2 \bar{x}_1(1 - \bar{x}_1) \\ \beta_4[i(t) - \bar{x}_2 - \delta_4 \bar{x}_1 \bar{x}_2] \end{bmatrix} =: \bar{\mathbf{G}}(t, \bar{\mathbf{x}}). \tag{3.4.3}$$

Consider (3.4.1), (3.4.2) and (3.4.3) with a given initial condition $\boldsymbol{\eta} = (\eta_1, \eta_2) \in \mathbb{R}^2_+$. Following the proof of the existence and uniqueness theorem for the full system (3.2.7), it can be shown that a unique solution exists for (3.4.1), (3.4.2) and (3.4.3) that are invariant on the region $[0, \max\{1, \eta_1\}] \times [0, \max\{i_M, \eta_2\}]$. Thus if $\mathbf{x}(0), \underline{\mathbf{x}}(0), \bar{\mathbf{x}}(0) \in [0,1] \times \mathbb{R}_+$, then $\mathbf{x}(t), \underline{\mathbf{x}}(t), \bar{\mathbf{x}}(t) \in [0,1] \times \mathbb{R}_+$ for all $t \in \mathbb{R}_+$.

Note that the solutions for (3.4.2) and (3.4.3) are given by

$$\underline{\mathbf{x}}(t) = \begin{bmatrix} v(t; \beta_2(1 - \delta_2 \underline{x}_2), \beta_2) \\ w(t; \beta_4 i, \beta_4) \end{bmatrix}$$

and

$$\bar{\mathbf{x}}(t) = \begin{bmatrix} v(t; \beta_2, \beta_2) \\ w(t; \beta_4 i, \beta_4(1 + \delta_4 \bar{x}_1)) \end{bmatrix},$$

where w and v are as in Lemmata 3.B.1 and 3.B.2 in Appendix 3.B, respectively.

Let $D = [0,1] \times \mathbb{R}_+$ and $M = \operatorname{diag}(1, -1) = M^{-1}$; assume that $\mathbf{x}(0), \underline{\mathbf{x}}(0), \bar{\mathbf{x}}(0) \in D$ and $M\underline{\mathbf{x}}(0) \leq M\mathbf{x}(0) \leq M\bar{\mathbf{x}}(0)$. We claim that

$$M\underline{\mathbf{x}}(t) \leq M\mathbf{x}(t) \leq M\bar{\mathbf{x}}(t) \quad \text{for all} \quad t \in \mathbb{R}_+. \tag{3.4.4}$$

It is clear that $\mathbf{G}_{\mathbf{x}}', \underline{\mathbf{G}}_{\mathbf{x}}', \bar{\mathbf{G}}_{\mathbf{x}}' \in C(\mathbb{R}_+ \times \mathbb{R}^2, \mathbb{R}^{2^2})$, hence $\mathbf{G}, \underline{\mathbf{G}}, \bar{\mathbf{G}}$ each satisfy a local Lipschitz condition on any $\Omega \subset \mathbb{R}_+ \times \mathbb{R}^4$. It can easily be seen that $M\underline{\mathbf{G}}(t, \boldsymbol{\eta}) \leq M\mathbf{G}(t, \boldsymbol{\eta}) \leq M\bar{\mathbf{G}}(t, \boldsymbol{\eta})$ for all $(t, \boldsymbol{\eta}) \in \mathbb{R}_+ \times D$. Letting $E = [0,1] \times (-\infty, 0]$, we see that the Jacobian matrices

$[M\mathbf{G}(t, M\boldsymbol{\eta})]'_{\boldsymbol{\eta}}$ and $[M\bar{\mathbf{G}}(t, M\boldsymbol{\eta})]'_{\boldsymbol{\eta}}$ are essentially positive (see Remark 3.A.2) on $\mathbb{R}_+ \times E$, meaning $M\mathbf{G}(t, M\boldsymbol{\eta})$ and $M\bar{\mathbf{G}}(t, M\boldsymbol{\eta})$ are quasimonotone increasing (see Definition 3.A.1) on $\mathbb{R}_+ \times E$. Hence by Corollary 3.A.9 the claim is proved true.

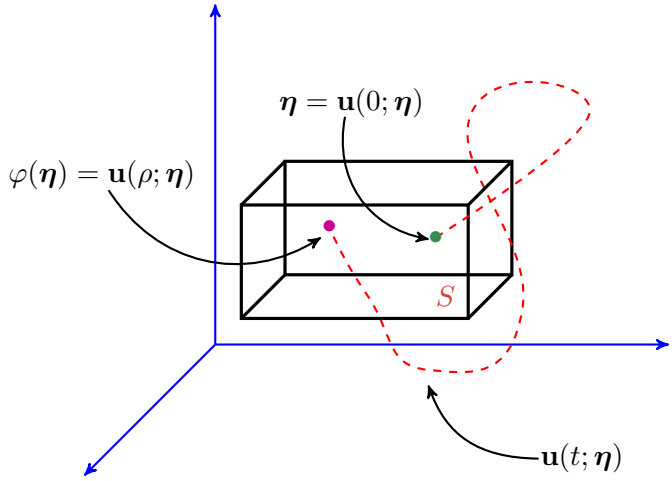

Figure 3.4: Diagram showing solutions $\mathbf{u}$ initially in $S \subset \mathbb{R}^3$ will be in S at time ρ

After having established the time-dependent bounds (3.4.4) on the solution of (3.4.1), we are ready to prove the actual existence of a ρ-periodic solution to (3.4.1). Define the rectangle

$$R = \{\boldsymbol{\eta} \in \mathbb{R}^2_+ : M\underline{\mathbf{x}}(0) \leq M\boldsymbol{\eta} \leq M\bar{\mathbf{x}}(0)\}.$$

Let $\boldsymbol{\eta} = \mathbf{x}(0) \in R$. Denote by $\mathbf{x}(\cdot; \boldsymbol{\eta})$ the solution of (3.4.1) with initial condition $\boldsymbol{\eta} \in R$. Define a map $\varphi : R \to \mathbb{R}^2_+$ by

$$\varphi(\boldsymbol{\eta}) := \mathbf{x}(\rho; \boldsymbol{\eta})$$

for every $\boldsymbol{\eta} \in R$. We wish to apply Brouwer's Fixed Point Theorem to ensure the existence of a fixed point of φ, i.e. we want to show that there is some initial condition $\boldsymbol{\eta}_0 \in R$ for which

$$\varphi(\boldsymbol{\eta}_0) = \mathbf{x}(\rho; \boldsymbol{\eta}_0) = \boldsymbol{\eta}_0.$$

For this particular initial condition, $\mathbf{x}(\rho) = \mathbf{x}(0)$. This idea is illustrated in Figure 3.4 for $\mathbf{u} \in \mathbb{R}^3$. Then a result from [62] will enable us to conclude that $\mathbf{x}(t) = \mathbf{x}(t + \rho)$ for all $t \in \mathbb{R}_+$.

From continuous dependence on initial conditions it is clear that φ is continuous on R. Using

Lemmata 3.B.1 and 3.B.2 in Appendix 3.B, if we pick

$$\underline{\mathbf{x}}(0) = \begin{bmatrix} v(0; \beta_2(1-\delta_2\underline{x}_2), \beta_2) \\ w(0; \beta_4 i, \beta_4) \end{bmatrix} = \begin{bmatrix} \frac{1-\mathrm{e}^{-\int_0^\rho g(s')\,\mathrm{d}s'}}{\beta_2 \int_0^\rho \mathrm{e}^{-\int_s^\rho g(s')\,\mathrm{d}s'}\,\mathrm{d}s} \\ \frac{\beta_4}{\mathrm{e}^{\beta_4\rho}-1}\int_0^\rho \mathrm{e}^{\beta_4 s} i(s)\,\mathrm{d}s \end{bmatrix},$$

where $g(s) = \beta_2[1-\delta_2\underline{x}_2(s)]$, then $\underline{\mathbf{x}}(t+\rho) = \underline{\mathbf{x}}(t) > 0$ for all $t \geq 0$. This is true provided $\int_0^\rho g(s)\,\mathrm{d}s > 0$. From Lemma 3.B.1, we see that

$$\int_0^\rho \underline{x}_2(s)\,\mathrm{d}s = \int_0^\rho i(s)\,\mathrm{d}s = \rho.$$

Recalling that $\delta_2 < 1$, we obtain

$$\delta_2 \int_0^\rho \underline{x}_2(s)\,\mathrm{d}s < \rho, \quad \text{or} \quad \int_0^\rho g(s)\,\mathrm{d}s = \int_0^\rho \beta_2[1-\delta_2\underline{x}_2(s)]\,\mathrm{d}s > 0.$$

Similarly, from Lemmata 3.B.1 and 3.B.2, if we choose

$$\bar{\mathbf{x}}(0) = \begin{bmatrix} v(0; \beta_2, \beta_2) \\ w(0; \beta_4 i, \beta_4(1+\delta_4\bar{x}_1)) \end{bmatrix} = \begin{bmatrix} 1 \\ \frac{\beta_4}{\mathrm{e}^{(1+\delta_4)\beta_4\rho}-1}\int_0^\rho \mathrm{e}^{(1+\delta_4)\beta_4 s} i(s)\,\mathrm{d}s \end{bmatrix},$$

then $\bar{\mathbf{x}}(t+\rho) = \bar{\mathbf{x}}(t) > 0$ for all $t \geq 0$. Furthermore, as $\beta_4 < \beta_4[1+\delta_4\bar{x}_1(t)]$ and $\beta_2[1-\delta_2\underline{x}_2(t)] < \beta_2$ for $t \in \mathbb{R}_+$ we have from Lemmata 3.B.1 and 3.B.2 that $M\underline{\mathbf{x}}(t) \leq M\bar{\mathbf{x}}(t)$ for all $t \in \mathbb{R}_+$. With the above choices for $\underline{\mathbf{x}}(0)$ and $\bar{\mathbf{x}}(0)$ we have that $R \subset \mathrm{int}(\mathbb{R}^2_+)$ and

$$M\underline{\mathbf{x}}(0) = M\underline{\mathbf{x}}(\rho) \leq M\mathbf{x}(\rho;\boldsymbol{\eta}) \leq M\bar{\mathbf{x}}(\rho) = M\bar{\mathbf{x}}(0),$$

that is, $\varphi(\boldsymbol{\eta}) \in R$, which implies that $\varphi(R) \subset R$. By Brouwer's Fixed Point Theorem there is some initial condition $\boldsymbol{\eta}_0 \in R \subset \mathrm{int}(\mathbb{R}^2_+)$ for which

$$\varphi(\boldsymbol{\eta}_0) = \mathbf{x}(\rho;\boldsymbol{\eta}_0) = \boldsymbol{\eta}_0.$$

For this particular initial condition, $\mathbf{x}(\rho) = \mathbf{x}(0)$. Then from [62, Lemma 2.2.1] we have

$$\mathbf{x}(t+\rho) = \mathbf{x}(t) > 0 \quad \text{for all} \quad t \in \mathbb{R}_+,$$

thus showing the existence of a strictly positive ρ-periodic solution to (3.4.1).

Now we prove the uniqueness of the solution constructed above.

Uniqueness

Note that if $\mathbf{u}(t) \geq 0$ and $\mathbf{v}(t) \geq 0$ are solutions to (3.4.1) and $\mathbf{u}(t_0) = \mathbf{v}(t_0)$ at some $t_0 \in \mathbb{R}_+$, then $\mathbf{u}(t) = \mathbf{v}(t)$ for all $t \in \mathbb{R}_+$ by uniqueness.

Now, let $\mathbf{u}(t), \mathbf{v}(t) > 0$ be ρ-periodic solutions of (3.4.1). It will be shown that $u_1(t) = v_1(t)$ for all $t \in \mathbb{R}_+$ if and only if $u_2(t) = v_2(t)$ for all $t \in \mathbb{R}_+$. If $u_1(t) = v_1(t)$ for all $t \in \mathbb{R}_+$, then from (3.4.1) and periodicity it can be seen that

$$0 = \int_0^\rho [u_1(s) - v_1(s)]\,\mathrm{d}s + \delta_2 \int_0^\rho [u_2(s) - v_2(s)]\,\mathrm{d}s = \delta_2 \int_0^\rho [u_2(s) - v_2(s)]\,\mathrm{d}s.$$

Hence by the Mean Value Theorem there exists $t_0 \in (0, \rho)$ such that $u_2(t_0) - v_2(t_0) = 0$ (i.e. $u_2(t_0) = v_2(t_0)$) and since $u_1(t) = v_1(t)$ for all $t \in \mathbb{R}_+$ it follows that $\mathbf{u}(t_0) = \mathbf{v}(t_0)$ which implies $\mathbf{u}(t) = \mathbf{v}(t)$ for all $t \in \mathbb{R}_+$, i.e. $u_2(t) = v_2(t)$ for all $t \in \mathbb{R}_+$. It can be shown similarly that if $u_2(t) = v_2(t)$ for all $t \in \mathbb{R}_+$, then $u_1(t) = v_1(t)$ for all $t \in \mathbb{R}_+$.

Let $\mathbf{u}(t) \geq 0$ and $\mathbf{v}(t) \geq 0$ be distinct ρ-periodic solutions of (3.4.1). It will now be shown that $u_1(t) \leq (\geq) v_1(t)$ for all $t \in \mathbb{R}_+$ and there exists $t_1 \in [0, \rho)$ such that $u_1(t_1) < (>) v_1(t_1)$. Since $\mathbf{u}(t)$ and $\mathbf{v}(t)$ are ρ-periodic it is sufficient to show $u_1(t) \leq (\geq) v_1(t)$ for all $t \in [0, \rho)$.

Assume that there exists $t_2 \in [0, \rho)$ such that $u_1(t_2) = v_1(t_2)$, then as $\mathbf{u}(t)$ and $\mathbf{v}(t)$ are distinct we must have $u_2(t_2) \neq v_2(t_2)$. Assume $u_2(t_2) > (<) u_2(t_2)$, then letting $M = \mathrm{diag}(1, -1)$ we have $M\mathbf{v}(t_2) \geq (\leq) M\mathbf{u}(t_2)$, which shows by Theorem 3.A.8 in Appendix 3.A that $M\mathbf{v}(t) \geq (\leq) M\mathbf{u}(t)$ for all $t \in [t_2, \infty)$ (i.e. $u_1(t) \leq (\geq) v_1(t)$ and $u_2(t) \geq (\leq) v_2(t)$ for all $t \in [t_2, \infty)$), and by periodicity of $\mathbf{u}(t)$ and $\mathbf{v}(t)$ this must hold for all $t \in \mathbb{R}_+$. Furthermore since $u_1(t) = v_1(t)$ for $t \in \mathbb{R}_+$ implies $\mathbf{u}(t)$ and $\mathbf{v}(t)$ are not distinct there must exist $t_1 \in [0, \rho)$ such that $u_1(t_1) < (>) v_1(t_1)$. Now if $u_1(t) \neq v_1(t)$ for any $t \in [0, \rho)$, then as a consequence of the continuity of $\mathbf{u}(t)$ and $\mathbf{v}(t)$ and the Intermediate Value Theorem $u_1(t) < (>) v_1(t)$ for all $t \in \mathbb{R}_+$.

Assume that $\mathbf{u}(t) > 0$ and $\mathbf{v}(t) > 0$ are distinct ρ-periodic solutions to (3.4.1), then as shown previously this implies without loss of generality that $u_1(t) \leq v_1(t)$ for all $t \in \mathbb{R}_+$ and there exists $t_1 \in [0, \rho)$ such that $u_1(t_1) < v_1(t_1)$. From Lemma 3.B.3 in Appendix 3.B, $u_1(t)$ is given by the implicit form

$$u_1(t) = \frac{\delta_4 - 1 + \sqrt{(1+\delta_4)^2 + 4\delta_4[f(t) - \delta_2 i(t)]}}{2\delta_4}, \quad f(t) = \frac{\mathrm{d}}{\mathrm{d}t} V(\mathbf{u}(t)) \tag{3.4.5}$$

and $v_1(t)$ is given by the implicit form

$$v_1(t) = \frac{\delta_4 - 1 + \sqrt{(1+\delta_4)^2 + 4\delta_4[g(t) - \delta_2 i(t)]}}{2\delta_4}, \quad g(t) = \frac{\mathrm{d}}{\mathrm{d}t}V(\mathbf{v}(t)), \tag{3.4.6}$$

noting that f and g must be continuous by the continuity of $\mathbf{u} > 0$ and $\mathbf{v} > 0$. Since $u_1(t) \leq v_1(t)$ for all $t \in \mathbb{R}_+$ and there exists $t_1 \in [0, \rho)$ such that $u_1(t_1) < v_1(t_1)$, then (3.4.5) and (3.4.6) implies $f(t) \leq g(t)$ for all $t \in \mathbb{R}_+$ and $f(t_1) < g(t_1)$. By continuity this implies

$$\int_0^\rho [g(s) - f(s)]\,\mathrm{d}s > 0.$$

However by the periodicity of $\mathbf{u}(t)$ and $\mathbf{v}(t)$

$$\int_0^\rho [g(s) - f(s)]\,\mathrm{d}s = 0,$$

which is a contradiction, hence $u_1(t)$ and $v_1(t)$ cannot be distinct (i.e. $u_1(t) = v_1(t)$) which implies that $u_2(t)$ and $v_2(t)$ are not distinct (i.e. $u_2(t) = v_2(t)$).

We have therefore proved the following theorem:

Theorem 3.4.1. *Suppose that* $0 < \delta_2 < 1$. *Then* (3.4.1) *has a unique solution* $\mathbf{x}$ *that satisfies*

$$\mathbf{x}(t+\rho) = \mathbf{x}(t) > 0 \quad \textit{for all} \quad t \in \mathbb{R}_+.$$

Stability

Here we prove the stability of the strictly positive ρ-periodic solution of (3.4.1) by utilising [62, Theorem 4.2.1]. We summarise the required results of [62] below.

Let

$$\mathbf{u}' = \mathbf{F}(t, \mathbf{u}), \tag{3.4.7}$$

where $\mathbf{F} \in C(\mathbb{R} \times X, \mathbb{R}^n)$, $\mathbf{F}'_{\mathbf{u}} \in C(\mathbb{R} \times X, \mathbb{R}^{n^2})$, X is an open connected subset of $\mathbb{R}^n$ and $\mathbf{F}(t, \cdot) = \mathbf{F}(t + \rho, \cdot)$. Let $\mathbf{u} : \mathbb{R} \to X$ be a non-constant ρ-periodic solution to (3.4.7). Then making the coordinate transformation $\mathbf{z} = \mathbf{u} - \mathbf{p}(t)$ we have

$$\mathbf{z}' = \mathbf{F}(t, \mathbf{z} + \mathbf{p}(t)) - \mathbf{F}(t, \mathbf{p}(t)) = \mathbf{F}'_{\mathbf{u}}(t, \mathbf{p}(t))\mathbf{z} + o(|\mathbf{z}|).$$

Hence the linearisation of (3.4.7) at $\mathbf{p}(t)$ is given by

$$\mathbf{y}' = \mathbf{F}'_{\mathbf{u}}(t, \mathbf{p}(t))\mathbf{y}. \tag{3.4.8}$$

If $\Phi(t)$ represents the fundamental matrix solution of (3.4.8), then the "characteristic multipliers" of (3.4.8) are given by the eigenvalues of $\Phi(\rho)$.

From [62, Theorem 4.2.1], if all the characteristic multipliers of system (3.4.8) are in modulus less than 1 (i.e. the spectral radius of $\Phi(\rho)$ is less than 1), then $\mathbf{p}$ is a uniformly asymptotically stable solution of (3.4.7); if (3.4.8) has at least one characteristic multiplier with modulus greater than 1 (i.e. the spectral radius of $\Phi(\rho)$ is greater than 1), then $\mathbf{p}$ is unstable.

Consider (3.4.1), which when linearised about a strictly positive ρ-periodic solution $\mathbf{x}$ produces the system

$$\frac{\mathrm{d}\mathbf{z}}{\mathrm{d}t} = \begin{bmatrix} \beta_2[1 - 2x_1(t) - \delta_2 x_2(t)] & -\beta_2\delta_2 x_1(t) \\ -\beta_4\delta_4 x_2(t) & -\beta_4[1 + \delta_4 x_1(t)] \end{bmatrix} \mathbf{z} =: A(t)\mathbf{z}. \tag{3.4.9}$$

The fundamental matrix $\Phi(t)$ of this system satisfies

$$\frac{\mathrm{d}\Phi}{\mathrm{d}t} = A(t)\Phi, \quad \Phi(0) = I.$$

Let P be a 2×2 invertible, differentiable matrix function such that $P(t + \rho) = P(t)$ for all $t \in \mathbb{R}_+$. If we let $\mathbf{y}(t) = P(t)\mathbf{z}(t)$, then $\mathbf{y}$ satisfies

$$\frac{\mathrm{d}\mathbf{y}}{\mathrm{d}t} = [P'(t) + P(t)A(t)]P^{-1}(t)\mathbf{y} =: B(t)\mathbf{y}. \tag{3.4.10}$$

The fundamental matrix $\Psi(t)$ of this system satisfies

$$\frac{\mathrm{d}\Psi}{\mathrm{d}t} = B(t)\Psi, \quad \Psi(0) = I,$$

where I is the identity matrix. It can easily be shown that $P(t)\Phi(t)P^{-1}(0)$ is a fundamental matrix solution of (3.4.10), that is, $\Psi(t) = P(t)\Phi(t)P^{-1}(0)$. Since $P(t + \rho) = P(t)$, it is clear that $\Psi(\rho) = P(\rho)\Phi(\rho)P^{-1}(\rho)$ (i.e. $\Psi(\rho)$ is similar to $\Phi(\rho)$), hence $\Psi(\rho)$ and $\Phi(\rho)$ have the same eigenvalues. This demonstrates the requirement for P to be ρ-periodic.

We let

$$P(t) = \begin{bmatrix} p_{11}(t) & 0 \\ 0 & p_{22}(t) \end{bmatrix}$$

for some ρ-periodic functions p_{11} and p_{22} to be determined, which implies

$$B = \begin{bmatrix} \frac{p_{11}'}{p_{11}} + a_{11} & \frac{p_{11}a_{12}}{p_{22}} \\ \frac{p_{22}a_{21}}{p_{11}} & \frac{p_{22}'}{p_{22}} + a_{22} \end{bmatrix}.$$

We want $p_{11}(t)p_{22}(t) < 0$ so that $b_{12}(t) > 0$ and $b_{21}(t) > 0$ (i.e. B is essentially positive). Since $B(t)$ is essentially positive for all $t \in \mathbb{R}_+$, the same argument as that used in [62, p. 190] shows that each entry of $\Psi(t)$ is positive for $t \in [0, \rho]$. In particular, each entry of $\Psi(\rho)$ is positive. Let λ_1, λ_2 denote the eigenvalues of $\Psi(\rho)$, that is, the characteristic multipliers of (3.4.10).

By Perron's Theorem, $\Psi(\rho)$ has a unique largest positive eigenvalue λ_2, say, with a corresponding eigenvector $\mathbf{v} = [v_1 \quad v_2]^{\mathrm{T}}$ having strictly positive components such that $|\lambda_1| < \lambda_2$. Hence for $\mathbf{x}$ to be stable, we need to show that $\lambda_2 < 1$.

Let $\mathbf{y}(t) = \Psi(t)\mathbf{v}$, where $\mathbf{v}$ is such that $\Psi(\rho)\mathbf{v} = \lambda_2\mathbf{v}$. Then $\mathbf{y}$ satisfies $\mathrm{d}\mathbf{y}/\mathrm{d}t = B(t)\mathbf{y}$. If $\mathbf{y}(t) = [y_1(t) \quad y_2(t)]^{\mathrm{T}}$, it follows that $\mathbf{y}(t) > 0$ for all $t \in [0, \rho]$. Suppose that for the moment that we can find a ρ-periodic function $\boldsymbol{\xi}(t) = [\xi_1(t) \quad \xi_2(t)]^{\mathrm{T}}$ such that

$$\langle \boldsymbol{\xi}(0), \mathbf{y}(0) \rangle > 0 \quad \text{and} \quad \int_0^\rho \frac{\mathrm{d}}{\mathrm{d}t} \langle \boldsymbol{\xi}(t), \mathbf{y}(t) \rangle \, \mathrm{d}t < 0.$$

Then $\langle \boldsymbol{\xi}(\rho), \mathbf{y}(\rho) \rangle < \langle \boldsymbol{\xi}(0), \mathbf{y}(0) \rangle$; however $\mathbf{y}(\rho) = \Psi(\rho)\mathbf{v} = \lambda_2\mathbf{v}$, so that $\langle \boldsymbol{\xi}(0), \lambda_2\mathbf{v} \rangle < \langle \boldsymbol{\xi}(0), \mathbf{v} \rangle$ and this would show that $\lambda_2 < 1$. We now proceed to find the desired function $\boldsymbol{\xi}(t)$. We have

$$\begin{aligned} \langle \boldsymbol{\xi}, \mathbf{y} \rangle' &= \langle \boldsymbol{\xi}', \mathbf{y} \rangle + \langle \boldsymbol{\xi}, \mathbf{y}' \rangle = \langle \boldsymbol{\xi}', \mathbf{y} \rangle + \langle \boldsymbol{\xi}, B\mathbf{y} \rangle \\ &= \langle \boldsymbol{\xi}', \mathbf{y} \rangle + \langle B^{\mathrm{T}}\boldsymbol{\xi}, \mathbf{y} \rangle = \langle \boldsymbol{\xi}' + B^{\mathrm{T}}\boldsymbol{\xi}, \mathbf{y} \rangle \\ &= \left[\xi_1' + \left(\frac{p_{11}'}{p_{11}} + a_{11} \right) \xi_1 + \frac{p_{22}a_{21}}{p_{11}} \xi_2 \right] y_1 \\ &\quad + \left[\xi_2' + \frac{p_{11}a_{12}}{p_{22}} \xi_1 + \left(\frac{p_{22}'}{p_{22}} + a_{22} \right) \xi_2 \right] y_2. \end{aligned}$$

Take

$$p_{11}(t) = \frac{1}{x_1(t)}, \quad p_{22}(t) = -\beta_2\delta_2, \quad \xi_1(t) = \beta_4[1 + \delta_4 x_1(t)], \quad \xi_2(t) = 1$$

for example, which are all ρ-periodic and $p_{11}(t)p_{22}(t) < 0$ for all $t \in \mathbb{R}_+$. We also note that $\langle \boldsymbol{\xi}(0), \mathbf{y}(0) \rangle > 0$. This makes the coefficient of y_2 equal to zero, so that

$$\langle \boldsymbol{\xi}, \mathbf{y} \rangle' = \beta_2 \beta_4 x_1 (\delta_4 - 1 - 2\delta_4 x_1) y_1$$

after some algebra.

Suppose that $\delta_2 < 1$. Then from Lemma 3.B.3 in Appendix 3.B

$$x_1(t) = \frac{(\delta_4 - 1) + \sqrt{(\delta_4 - 1)^2 + 4\delta_4[1 - \delta_2 i(t) + h(t)]}}{2\delta_4}, \quad \text{where} \quad h(t) = \frac{\mathrm{d}}{\mathrm{d}t} V(\mathbf{x}(t)),$$

which implies that

$$\delta_4 - 1 - 2\delta_4 x_1(t) = -\sqrt{(1 - \delta_4)^2 + 4\delta_4[1 - \delta_2 i(t) + h(t)]} \leq 0.$$

Moreover, from the periodicity of $\mathbf{x}$ it can be seen that $(1/\rho) \int_0^\rho [\delta_2 i(s) - h(s)] \, \mathrm{d}s = \delta_2$. Thus from the Mean Value Theorem there exists $t^* \in (0, \rho)$ such that

$$(1 - \delta_4)^2 + 4\delta_4[1 - \delta_2 i(t^*) + h(t^*)] = (1 - \delta_4)^2 + 4\delta_4(1 - \delta_2).$$

Since $\delta_2 < 1$, it follows that $(1 - \delta_4)^2 + 4\delta_4(1 - \delta_2) > 0$ and then by continuity, there exists $\epsilon > 0$ such that

$$(1 - \delta_4)^2 + 4\delta_4[1 - \delta_2 i(t) + h(t)] > 0 \quad \text{for all} \quad t \in (t^* - \epsilon, t^* + \epsilon).$$

This yields, by the strict positivity of $\mathbf{x}$ and $\mathbf{y}$,

$$\int_{t^* - \epsilon}^{t^* + \epsilon} x_1(t)[\delta_4 - 1 - 2\delta_4 x_1(t)] y_1(t) \, \mathrm{d}t < 0.$$

Thus,

$$\begin{aligned}\int_0^\rho \frac{\mathrm{d}}{\mathrm{d}t}\langle \boldsymbol{\xi}(t), \mathbf{y}(t)\rangle \,\mathrm{d}t &= \int_0^\rho \beta_2\beta_4 x_1(t)[\delta_4 - 1 - 2\delta_4 x_1(t)]y_1(t)\,\mathrm{d}t \\ &= \int_0^{t^*-\epsilon} \beta_2\beta_4 x_1(t)[\delta_4 - 1 - 2\delta_4 x_1(t)]y_1(t)\,\mathrm{d}t \\ &\quad + \int_{t^*-\epsilon}^{t^*+\epsilon} \beta_2\beta_4 x_1(t)[\delta_4 - 1 - 2\delta_4 x_1(t)]y_1(t)\,\mathrm{d}t \\ &\quad + \int_{t^*+\epsilon}^{\rho} \beta_2\beta_4 x_1(t)[\delta_4 - 1 - 2\delta_4 x_1(t)]y_1(t)\,\mathrm{d}t \\ &< 0.\end{aligned}$$

The above argument then shows that if $\delta_2 < 1$ and a strictly positive ρ-periodic solution exists to (3.4.1), then $|\lambda_1| < \lambda_2 < 1$ (i.e. $\mathbf{x}$ is asymptotically stable). Therefore the unique ρ-periodic solution of (3.4.1) found in Section 3.4.1 is asymptotically stable.

Remark 3.4.2. As a result of Lemma 3.B.3 any strictly positive ρ-periodic solution $\mathbf{x}$ to (3.4.1) must satisfy the implicit form

$$x_1(t) = \frac{(\delta_4 - 1) \pm \sqrt{(\delta_4+1)^2 - 4\delta_4[\delta_2 i(t) - h(t)]}}{2\delta_4}, \quad \text{where} \quad h(t) = \frac{\mathrm{d}}{\mathrm{d}t}V(\mathbf{x}(t)). \quad (3.4.11)$$

By a similar argument to the above it can be concluded that if $\delta_2 < 1$ or if $1 \leq \delta_2 < (1+\delta_4)^2/4\delta_4$ and $\delta_4 > 1$ and a strictly positive ρ-periodic solution exists for (3.4.1) that satisfies the "plus" case of (3.4.11), then $|\lambda_1| < \lambda_2 < 1$ (i.e. $\mathbf{x}$ is asymptotically stable). Similarly, it can be concluded that if a strictly positive ρ-periodic solution exists for (3.4.1) that satisfies the "minus" case of (3.4.11), then $\lambda_2 > 1$ (i.e. $\mathbf{x}$ is unstable).

3.4.2 Existence of co-existence periodic solution

The existence of a strictly positive ρ-periodic solution to the full system (3.2.7) will be shown in this section.

Note that (3.2.7) is invariant on $\mathbb{R}^4_+$. Consider the systems

$$\underline{\mathbf{u}}' = \begin{bmatrix}\underline{u}_1' \\ \underline{u}_2' \\ \underline{u}_3' \\ \underline{u}_4'\end{bmatrix} = \begin{bmatrix}\underline{u}_1(1 - \underline{u}_1 - \alpha_1\underline{u}_2 - \delta_1\underline{u}_3) \\ \beta_2\underline{u}_2(1 - \underline{u}_2 - \delta_2\underline{u}_4) \\ \beta_3(\underline{u}_2 - \underline{u}_3) \\ \beta_4[i(t) - \underline{u}_4 - \delta_4\underline{u}_4\underline{u}_2]\end{bmatrix} =: \underline{\mathbf{F}}(t, \underline{\mathbf{u}}), \quad (3.4.12)$$

and

$$\bar{\mathbf{u}}' = \begin{bmatrix} \bar{u}_1' \\ \bar{u}_2' \\ \bar{u}_3' \\ \bar{u}_4' \end{bmatrix} = \begin{bmatrix} \bar{u}_1(1 - \bar{u}_1 - \alpha_1\bar{u}_2) \\ \beta_2\bar{u}_2(1 - \bar{u}_2 - \alpha_2\bar{u}_1 - \delta_2\bar{u}_4) \\ \beta_3(\bar{u}_2 - \bar{u}_3) \\ \beta_4[i(t) - \bar{u}_4] \end{bmatrix} =: \bar{\mathbf{F}}(t, \bar{\mathbf{u}}). \tag{3.4.13}$$

Similarly to (3.2.7) the solutions to (3.4.12) and (3.4.13) can be shown to be unique and invariant on $\mathbb{R}^4_+$.

We now wish to establish the existence of strictly positive ρ-periodic solutions to (3.4.12) and (3.4.13). First consider (3.4.12) and let $\underline{\mathbf{u}}(t)$ denote a solution, where $\underline{\mathbf{u}}(0) \in \mathbb{R}^4_+$. From the analysis of the normal-tissue free system, if $\delta_2 < 1$ there is a unique strictly positive ρ-periodic solution to $\underline{u}_2' = \underline{F}_2(t, \underline{\mathbf{u}})$ and $\underline{u}_4' = \underline{F}_4(t, \underline{\mathbf{u}})$. Then from Lemma 3.B.1 there exists a unique ρ-periodic solution to $\underline{u}_3' = \underline{F}_3(t, \underline{\mathbf{u}})$, where $\underline{u}_3(t) = w(t; \beta_3\underline{u}_2, \beta_3)$ with initial condition given by (3.B.3). Using these ρ-periodic solutions and Lemma 3.B.2 if $\int_0^\rho [1 - \alpha_1\underline{u}_2(s) - \delta_1\underline{u}_3(s)]\,\mathrm{d}s > 0$, there exists a unique strictly positive ρ-periodic solution to $\underline{u}_1' = \underline{F}_1(t, \underline{\mathbf{u}})$, where $\underline{u}_1(t) = v(t; 1 - \alpha_1\underline{u}_2 - \delta_1\underline{u}_3, 1)$ with initial condition given by (3.B.6). Consider

$$\int_0^\rho [1 - \alpha_1\underline{u}_2(s) - \delta_1\underline{u}_3(s)]\,\mathrm{d}s = \int_0^\rho [1 - (\alpha_1 + \delta_1)\underline{u}_2(s)]\,\mathrm{d}s \geq 1 - (\alpha_1 + \delta_1)\hat{u}_{2+}$$

from Lemmata 3.B.1 and 3.B.3 in Appendix 3.B. Hence if $\delta_2 < 1$ and $1 - (\alpha_1 + \delta_1)\hat{u}_{2+} > 0$, then there exists a unique strictly positive ρ-periodic solution to (3.4.12).

Now consider system (3.4.13) and let $\bar{\mathbf{u}}(t)$ denote a solution, where $\bar{\mathbf{u}}(0) \in \mathbb{R}^4_+$. From the analysis of the normal-tissue free problem it is known that there exists a unique strictly positive ρ-periodic solution to $\bar{u}_4' = \bar{F}_4(t, \bar{\mathbf{u}})$. Then from [94, Prop. 36.1 and 36.3] there exists a unique strictly positive ρ-periodic solution to $\bar{u}_1' = \bar{F}_1(t, \bar{\mathbf{u}})$ and $\bar{u}_2' = \bar{F}_2(t, \bar{\mathbf{u}})$ if

$$1 < (>)\alpha_1\frac{1}{\rho}\int_0^\rho [1 - \delta_2\bar{u}_4(s)]\,\mathrm{d}s = \alpha_1(1 - \delta_2)$$

and

$$\frac{1}{\rho}\int_0^\rho [1 - \delta_2\bar{u}_4(s)]\,\mathrm{d}s = 1 - \delta_2 < (>)\alpha_2.$$

Noting $\bar{u}_2(t) > 0$ for all $t \in \mathbb{R}_+$, we have from Lemma 3.B.1 that $\bar{u}_3' = \bar{F}_3(t, \bar{\mathbf{u}})$ has a unique strictly positive ρ-periodic solution given by $\bar{u}_3(t) = w(t; \beta_3\bar{u}_2, \beta_3)$ with initial condition given

by (3.B.3).

Assume that the parameter conditions

$$\delta_2 < 1, \quad 1 - (\alpha_1 + \delta_1)\hat{u}_{2+} > 0, \quad 1 < (>)\alpha_1(1 - \delta_2) \quad \text{and} \quad 1 - \delta_2 < (>)\alpha_2 \tag{3.4.14}$$

are satisfied, then there exists unique strictly positive ρ-periodic solutions to (3.4.12) and (3.4.13) denoted by $\underline{\mathbf{u}}(t)$ and $\bar{\mathbf{u}}(t)$, respectively. Letting $M = \operatorname{diag}(1, -1, -1, 1) = M^{-1}$, we wish to show that $M\underline{\mathbf{u}}(t) \leq M\bar{\mathbf{u}}(t)$ for all $t \in \mathbb{R}_+$. It was shown in the analysis of the normal-tissue free ρ-periodic solution that $\underline{u}_4(t) \leq \bar{u}_4(t)$ for all $t \in \mathbb{R}_+$. Consider the ρ-periodic solutions $\underline{u}_2(t)$ and $\bar{u}_2(t)$ that satisfy

$$\underline{u}_2' = \beta_2\underline{u}_2[1 - \underline{u}_4(t) - \underline{u}_2] \quad \text{and} \quad \bar{u}_2' = \beta_2\bar{u}_2[1 - \alpha_2\bar{u}_1(t) - \delta_2\bar{u}_4(t) - \bar{u}_2].$$

Note that $1 - \delta_2\bar{u}_4(t) - \alpha_2\bar{u}_1(t) < 1 - \delta_2\underline{u}_4(t)$ for all $t \in \mathbb{R}_+$ and by Lemma 3.B.2 it must hold that $\int_0^\rho [1 - \delta_2\bar{u}_4(s) - \alpha_2\bar{u}_1(s)]\,\mathrm{d}s > 0$ and moreover, $\underline{u}_2(t) \geq \bar{u}_2(t)$ for all $t \in \mathbb{R}_+$. Considering the evolution of $\underline{u}_3(t) - \bar{u}_3(t)$ it then follows directly from Lemma 3.B.1 that $\underline{u}_3(t) \geq \bar{u}_3(t)$ for all $t \in \mathbb{R}_+$.

Consider $\underline{u}_1(t)$ and $\bar{u}_1(t)$ which satisfy

$$\underline{u}_1' = \underline{u}_1[1 - \alpha_1\underline{u}_2(t) - \delta_1\underline{u}_3(t) - \underline{u}_1] \quad \text{and} \quad \bar{u}_1' = \bar{u}_1[1 - \alpha_1\bar{u}_2(t) - \bar{u}_1].$$

Note that $\int_0^\rho [1 - \alpha_1\underline{u}_2(s) - \delta_1\underline{u}_3(s)]\,\mathrm{d}s > 0$ and that $1 - \alpha_1\underline{u}_2(t) - \delta_1\underline{u}_3(t) < 1 - \alpha_1\bar{u}_2(t)$ for all $t \in \mathbb{R}_+$. Then from Lemma 3.B.2, $\underline{u}_1(t) \leq \bar{u}_1(t)$ for all $t \in \mathbb{R}_+$. Hence it has been shown that $M\underline{\mathbf{u}}(t) \leq M\bar{\mathbf{u}}(t)$ for all $t \in \mathbb{R}_+$.

Assume that $\mathbf{u}(0), \underline{\mathbf{u}}(0), \bar{\mathbf{u}}(0) \in \mathbb{R}_+$ and $M\underline{\mathbf{u}}(0) \leq M\mathbf{u}(0) \leq M\bar{\mathbf{u}}(0)$. We claim that

$$M\underline{\mathbf{u}}(t) \leq M\mathbf{u}(t) \leq M\bar{\mathbf{u}}(t) \quad \text{for all} \quad t \in \mathbb{R}_+. \tag{3.4.15}$$

It is clear that $\mathbf{F}_{\mathbf{u}}', \underline{\mathbf{F}}_{\mathbf{u}}', \bar{\mathbf{F}}_{\mathbf{u}}' \in C(\mathbb{R}_+ \times \mathbb{R}^4, \mathbb{R}^{4^2})$, hence $\mathbf{F}, \underline{\mathbf{F}}, \bar{\mathbf{F}}$ each satisfy a local Lipschitz condition on any $D \subset \mathbb{R}_+ \times \mathbb{R}^4$. It can easily be seen that $M\underline{\mathbf{F}}(t, \boldsymbol{\eta}) \leq M\mathbf{F}(t, \boldsymbol{\eta}) \leq M\bar{\mathbf{F}}(t, \boldsymbol{\eta})$ for all $(t, \boldsymbol{\eta}) \in \mathbb{R}_+^{1+4}$. Letting $E = \mathbb{R}_+ \times (-\infty, 0]^2 \times \mathbb{R}_+$, we can see that the Jacobian matrices $[M\mathbf{F}(t, M\boldsymbol{\eta})]_{\boldsymbol{\eta}}'$ and $[M\bar{\mathbf{F}}(t, M\boldsymbol{\eta})]_{\boldsymbol{\eta}}'$ are essentially positive on $\mathbb{R}_+ \times E$, meaning $M\mathbf{F}(t, M\boldsymbol{\eta})$ and $M\bar{\mathbf{F}}(t, M\boldsymbol{\eta})$ are quasimonotone increasing on $\mathbb{R}_+ \times E$. Hence by Corollary 3.A.9 the claim is

proved true.

Theorem 3.4.3. *If* (3.4.14) *is satisfied, then there exists a strictly positive ρ-periodic solution to* (3.2.7).

Proof. Under the given parameter restrictions there exist strictly positive ρ-periodic solutions to (3.4.12) and (3.4.13). Let $\underline{\mathbf{u}}(t)$ and $\bar{\mathbf{u}}(t)$ denote the strictly positive ρ-periodic solutions for systems (3.4.12) and (3.4.13), respectively. Note that it was shown $M\underline{\mathbf{u}}(t) \leq M\bar{\mathbf{u}}(t)$ for all $t \in \mathbb{R}_+$. Construct the box

$$R = \{\boldsymbol{\eta} \in \mathbb{R}^4_+ : M\underline{\mathbf{u}}(0) \leq M\boldsymbol{\eta} \leq M\bar{\mathbf{u}}(0)\} \subset \text{int}(\mathbb{R}^4_+)$$

and define the solution of (3.2.7) with initial condition $\boldsymbol{\eta} \in R$ as $\mathbf{u}(t;\boldsymbol{\eta})$, i.e. $\mathbf{u}(0;\boldsymbol{\eta}) = \boldsymbol{\eta}$. Define the map $\varphi : R \to \mathbb{R}^4_+$ by

$$\varphi(\boldsymbol{\eta}) = \mathbf{u}(\rho, \boldsymbol{\eta}) \quad \text{for} \quad \boldsymbol{\eta} \in R.$$

Note from continuous dependence on initial conditions that φ is clearly continuous. If $\boldsymbol{\eta} \in R$, then from (3.4.15) it is clear that

$$M\underline{\mathbf{u}}(t) \leq M\mathbf{u}(t;\boldsymbol{\eta}) \leq M\bar{\mathbf{u}}(t) \quad \text{for all} \quad t \in \mathbb{R}_+. \tag{3.4.16}$$

Then from the periodicity of $\underline{\mathbf{u}}(t)$ and $\bar{\mathbf{u}}(t)$ it follows that

$$M\underline{\mathbf{u}}(0) = M\underline{\mathbf{u}}(\rho) \leq M\mathbf{u}(\rho;\boldsymbol{\eta}) \leq M\bar{\mathbf{u}}(\rho) = M\bar{\mathbf{u}}(0),$$

that is, $\mathbf{u}(\rho;\boldsymbol{\eta}) \in R$ which implies $\varphi(R) \subset R$. Hence by Brouwer's Fixed Point Theorem there exists $\boldsymbol{\eta}_0 \in R$ such that $\boldsymbol{\eta}_0 = \varphi(\boldsymbol{\eta}_0)$, i.e. $\mathbf{u}(0;\boldsymbol{\eta}_0) = \mathbf{u}(\rho;\boldsymbol{\eta}_0)$. Therefore by [62, Lemma 2.2.1] for initial condition $\mathbf{u}(0) = \boldsymbol{\eta}_0$ the solution $\mathbf{u}(t)$ must be ρ-periodic and from (3.4.16) that solution must be strictly positive. □

3.4.3 Special periodic solutions of the full system

We now classify all the special periodic solutions to system (3.2.7) and determine the stability of each solution. With a slight abuse of notation, the special periodic solutions are of the form:

PS1. $(0, 0, 0, u_4(t))$;

PS2. $(u_1(t), 0, 0, u_4(t))$;

PS3. $(0, u_2(t), u_3(t), u_4(t))$;

PS4. $(u_1(t), u_2(t), u_3(t), u_4(t))$.

Here, $u_j(t+\rho) = u_j(t) > 0$ for all $t \geq 0$ and $j = 1, 2, 3, 4$.

PS1

For PS1 we see that u_4 satisfies the ODE

$$\frac{\mathrm{d}u_4}{\mathrm{d}t} = \beta_4[i(t) - u_4].$$

From Lemma 3.B.1 we deduce that this has the ρ-periodic solution $u_4(t) = w(t; \beta_4 i, \beta_4)$ for all $t \in \mathbb{R}_+$ with initial condition given by (3.B.3).

PS2

For PS2 we see that u_1 and u_2 satisfy the system of equations

$$\frac{\mathrm{d}u_1}{\mathrm{d}t} = u_1(1 - u_1), \quad \frac{\mathrm{d}u_4}{\mathrm{d}t} = \beta_4[i(t) - u_4].$$

Since the equation for u_1 is autonomous, the only nontrivial periodic solution is $u_1(t) = 1$ for all $t \in \mathbb{R}_+$. Again from Lemma 3.B.1 we conclude that the u_4 equation has ρ-periodic solution $u_4(t) = w(t; \beta_4 i, \beta_4)$ for all $t \in \mathbb{R}_+$ with initial condition given by (3.B.3).

PS3

For PS3 the system of ODEs is

$$\begin{aligned}
\frac{\mathrm{d}u_2}{\mathrm{d}t} &= \beta_2 u_2(1 - u_2 - \delta_2 u_4), \\
\frac{\mathrm{d}u_3}{\mathrm{d}t} &= \beta_3(u_2 - u_3), \\
\frac{\mathrm{d}u_4}{\mathrm{d}t} &= \beta_4[i(t) - u_4 - \delta_4 u_2 u_4].
\end{aligned}$$

It suffices to consider the reduced system (3.4.1) since from Lemma 3.B.1 in Appendix 3.B if u_2 is positive and ρ-periodic, then a positive ρ-periodic solution of the u_3 equation is $u_3(t) = w(t; \beta_3 u_2, \beta_3)$ for all $t \in \mathbb{R}_+$ with initial condition given by (3.B.3). From Theorem 3.4.1 we know that there exists a unique strictly positive ρ-periodic solution (u_2, u_4) to (3.4.1) if $\delta_2 < 1$.

PS4

For PS4 the system of ODEs is

$$\begin{aligned}
\frac{\mathrm{d}u_1}{\mathrm{d}t} &= u_1(1-u_1-\alpha_1 u_2-\delta_1 u_3),\\
\frac{\mathrm{d}u_2}{\mathrm{d}t} &= \beta_2 u_2(1-u_2-\alpha_2 u_1-\delta_2 u_4),\\
\frac{\mathrm{d}u_3}{\mathrm{d}t} &= \beta_3(u_2-u_3),\\
\frac{\mathrm{d}u_4}{\mathrm{d}t} &= \beta_4[i(t)-u_4-\delta_4 u_2 u_4].
\end{aligned}$$

From Theorem 3.4.3 it is known there exists a strictly positive ρ-periodic solution to this system if $\delta_2 < 1$, $1-(\alpha_1+\delta_1)\hat{u}_{2+} > 0$, $1 < (>)\alpha_1(1-\delta_2)$ and $1-\delta_2 < (>)\alpha_2$.

3.4.4 Stability of special periodic solutions to the full system

We begin by determining the stability of PS1. Recall that PS1 is $(0,0,0,u_4(t))$, where $u_4(t) = w(t;\beta_4 i,\beta_4)$. Linearising (3.2.7) about PS1, we obtain

$$\frac{\mathrm{d}\mathbf{y}}{\mathrm{d}t} = \begin{bmatrix} 1 & 0 & 0 & 0\\ 0 & \beta_2[1-\delta_2 u_4(t)] & 0 & 0\\ 0 & \beta_3 & -\beta_3 & 0\\ 0 & -\beta_4\delta_4 u_4(t) & 0 & -\beta_4 \end{bmatrix}\mathbf{y}.$$

This has a fundamental matrix $\Phi(t) = (\phi_{ij}(t))_{1\le i,j\le 4}$ given by

$$\Phi(t) = \begin{bmatrix} \mathrm{e}^{t} & 0 & 0 & 0\\ 0 & \mathrm{e}^{\beta_2\int_0^t[1-\delta_2 u_4(s)]\,\mathrm{d}s} & 0 & \\ 0 & \beta_3\int_0^t \mathrm{e}^{-\beta_3(t-s)}\phi_{22}(s)\,\mathrm{d}s & \mathrm{e}^{-\beta_3 t} & 0\\ 0 & -\beta_4\delta_4\int_0^t \mathrm{e}^{-\beta_4(t-s)}u_4(s)\phi_{22}(s)\,\mathrm{d}s & 0 & \mathrm{e}^{-\beta_4 t} \end{bmatrix}.$$

Since this matrix is lower triangular, the characteristic multipliers (i.e. the eigenvalues of $\Phi(\rho)$) are

$$\mathrm{e}^{\rho},\quad \mathrm{e}^{\beta_2\int_0^\rho[1-\delta_2 u_4(s)]\,\mathrm{d}s},\quad \mathrm{e}^{-\beta_3\rho},\quad \mathrm{e}^{-\beta_4\rho}.$$

As $|\mathrm{e}^{\rho}| > 1$, we conclude that PS1 is unstable.

Next we consider the stability of PS2, given by $(1,0,0,u_4(t))$, where $u_4(t) = w(t;\beta_4 i,\beta_4)$.

Linearising (3.2.7) about PS2 gives

$$\frac{\mathrm{d}\mathbf{y}}{\mathrm{d}t} = \begin{bmatrix} -1 & -\alpha_1 & -\delta_1 & 0 \\ 0 & \beta_2[1-\alpha_2-\delta_2 u_4(t)] & 0 & 0 \\ 0 & \beta_3 & -\beta_3 & 0 \\ 0 & -\beta_4\delta_4 u_4(t) & 0 & -\beta_4 \end{bmatrix} \mathbf{y}.$$

With a slight abuse of notation, a fundamental matrix $\Phi(t) = (\phi_{ij}(t))_{1\le i,j\le 4}$ is

$$\Phi(t) = \begin{bmatrix} \mathrm{e}^{-t} & -\int_0^t \mathrm{e}^{-(t-s)}[\alpha_1\phi_{22}(s)+\delta_1\phi_{32}(s)]\,\mathrm{d}s & -\delta_1\int_0^t \mathrm{e}^{-(t-s)}\mathrm{e}^{-\beta_3 s}\mathrm{d}s & 0 \\ 0 & \mathrm{e}^{\beta_2\int_0^t[1-\alpha_2-\delta_2 u_4(s)]\,\mathrm{d}s} & 0 & 0 \\ 0 & \beta_3\int_0^t \mathrm{e}^{-\beta_3(t-s)}\phi_{22}(s)\,\mathrm{d}s & \mathrm{e}^{-\beta_3 t} & 0 \\ 0 & -\beta_4\delta_4\int_0^t \mathrm{e}^{-\beta_4(t-s)}u_4(s)\phi_{22}(s)\,\mathrm{d}s & 0 & \mathrm{e}^{-\beta_4 t} \end{bmatrix}.$$

The characteristic multipliers are then

$$\mathrm{e}^{-\rho}, \quad \mathrm{e}^{\beta_2\int_0^\rho[1-\alpha_2-\delta_2 u_4(s)]\,\mathrm{d}s}, \quad \mathrm{e}^{-\beta_3\rho}, \quad \mathrm{e}^{-\beta_4\rho}.$$

Thus the stability properties of PS2 will depend on the sign of $\int_0^\rho[1-\alpha_2-\delta_2 u_4(s)]\,\mathrm{d}s$. Note that the ODE for u_4 in PS2 is

$$\frac{\mathrm{d}u_4}{\mathrm{d}t} = \beta_4[i(t)-u_4(t)].$$

Integrating from 0 to ρ gives

$$\int_0^\rho u_4(s)\,\mathrm{d}s = \int_0^\rho i(s)\,\mathrm{d}s = \rho,$$

so that

$$\int_0^\rho[1-\alpha_2-\delta_2 u_4(s)]\,\mathrm{d}s = (1-\alpha_2)\rho - \delta_2\rho = \rho(1-\alpha_2-\delta_2).$$

Therefore if $\alpha_2+\delta_2 > 1$, then PS2 is stable. On the other hand, if $\alpha_2+\delta_2 < 1$, then PS2 is unstable.

Finally, we look at the stability of PS3. Recall that PS3 is of the form $(0, u_2(t), u_3(t), u_4(t))$, where $(u_2(t), u_4(t))$ is a periodic solution of (3.4.1) and $u_3(t) = w(t;\beta_3 u_2, \beta_3)$. Linearising (3.2.7) about PS3 gives

$$\frac{\mathrm{d}\mathbf{y}}{\mathrm{d}t} = A(t)\mathbf{y}, \tag{3.4.17}$$

where

$$A(t) = \begin{bmatrix} 1-\alpha_1 u_2(t) - \delta_1 u_3(t) & 0 & 0 & 0 \\ -\alpha_2\beta_2 u_2(t) & \beta_2[1-2u_2(t)-\delta_2 u_4(t)] & 0 & -\beta_2\delta_2 u_2(t) \\ 0 & \beta_3 & -\beta_3 & 0 \\ 0 & -\beta_4\delta_4 u_4(t) & 0 & -\beta_4[1+\delta_4 u_2(t)] \end{bmatrix}.$$

Let $\Theta(t) = (\theta_{ij}(t))_{1\le i,j\le 3}$ be the fundamental matrix that satisfies $\Theta' = C(t)\Theta';\ \Theta(0) = I$, where $C(t) = (a_{ij}(t))_{2\le i,j\le 4}$. Define

$$\boldsymbol{\gamma}(t) = \Theta(t)\int_0^t \Theta^{-1}(s)\boldsymbol{\zeta}(s)\,\mathrm{d}s, \quad \text{where} \quad \boldsymbol{\zeta}(t) = \begin{bmatrix} a_{21}(t)\mathrm{e}^{\int_0^t a_{11}(s)\,\mathrm{d}s} & 0 & 0 \end{bmatrix}^{\mathrm{T}}.$$

Furthermore, let $\Psi(t) = (\psi_{ij}(t))_{1\le i,j\le 2}$ be a fundamental matrix solution of (3.4.9), then the fundamental matrix solution of (3.4.17) is

$$\Phi(t) = \begin{bmatrix} \mathrm{e}^{\int_0^t [1-\alpha_1 q_2(s)-\delta_1 q_3(s)]\,\mathrm{d}s} & 0 & 0 & 0 \\ \gamma_1(t) & \psi_{11}(t) & 0 & \psi_{12}(t) \\ \gamma_2(t) & \beta_3\mathrm{e}^{\beta_3 t}\int_0^t \psi_{11}(t)\mathrm{e}^{\beta_3 s}\,\mathrm{d}s & \mathrm{e}^{-\beta_3 t} & \beta_3\mathrm{e}^{\beta_3 t}\int_0^t \psi_{12}(t)\mathrm{e}^{\beta_3 s}\,\mathrm{d}s \\ \gamma_3(t) & \psi_{21}(t) & 0 & \psi_{22}(t) \end{bmatrix}.$$

The characteristic multipliers are then $\mathrm{e}^{\int_0^\rho [1-\alpha_1 u_2(s)-\delta_1 u_3(s)]\,\mathrm{d}s}$, $\mathrm{e}^{-\beta_3\rho}$ and the eigenvalues of $\Psi(\rho)$ which were shown in Section 3.4.1 to have modulus less that 1 if $\delta_2 < 1$. It is clear that $|\mathrm{e}^{-\beta_3\rho}| < 1$, hence it is required that

$$|\mathrm{e}^{\int_0^\rho [1-\alpha_1 u_2(s)-\delta_1 u_3(s)]\,\mathrm{d}s}| < (>)1 \quad \Longleftrightarrow \quad \int_0^\rho [1-\alpha_1 u_2(s)-\delta_1 u_3(s)]\,\mathrm{d}s < (>)0$$

for the solution PS3 to be stable (unstable). From Lemmata 3.B.1 and 3.B.3

$$\int_0^\rho [1-\alpha_1 u_2(s)-\delta_1 u_3(s)]\,\mathrm{d}s = \int_0^\rho [1-(\alpha_1+\delta_1)u_2(s)]\,\mathrm{d}s \ge \rho[1-(\alpha_1+\delta_1)\hat{u}_{2+}],$$

therefore if $1-(\alpha_1+\delta_1)\hat{u}_{2+} > 0$, then the solution is unstable. Now, from (3.4.1) it can be shown that

$$\frac{1}{\rho}\int_0^\rho u_2(s)\,\mathrm{d}s = 1 - \delta_2\frac{1}{\rho}\int_0^\rho u_4(s)\,\mathrm{d}s.$$

Furthermore, by the periodicity of u_4 and the positivity of u_2 and u_4, it can be obtained from (3.4.1)

that

$$\frac{1}{\rho}\int_0^\rho u_4(s)\,\mathrm{d}s = 1 - \frac{1}{\rho}\int_0^\rho u_2(s)u_4(s)\,\mathrm{d}s < 1$$

and as a result we can conclude

$$\begin{aligned}\frac{1}{\rho}\int_0^\rho 1-\alpha_1 u_2(s)-\delta_1 u_3(s)\,\mathrm{d}s &= 1-(\alpha_1+\delta_1)\frac{1}{\rho}\int_0^\rho u_2(t)\,\mathrm{d}s\\ &= 1-(\alpha_1+\delta_1)\left(1-\delta_2\frac{1}{\rho}\int_0^\rho u_4(t)\,\mathrm{d}s\right)\\ &< 1-(\alpha_1+\delta_1)(1-\delta_2) < 0\end{aligned}$$

if $\delta_2 < (\alpha_1+\delta_1-1)/(\alpha_1+\delta_1)$. Noting that $(\alpha_1+\delta_1-1)/(\alpha_1+\delta_1) < 1$, it can then be concluded that if $\delta_2 < (\alpha_1+\delta_1-1)/(\alpha_1+\delta_1)$, then PS3 is a stable.

3.5 Discussion

It is first noted that the results obtained for the model proposed by Byrne [30], corresponding to system (3.4.1), have been further extended, that is, an examination of the behaviour of the model when $i(t)$ is an arbitrary continuous time-periodic function has been presented. In the analysis conducted by Byrne [30], i was given by (3.2.8) and it was assumed that $x_2 \equiv i$, as a result (3.4.1) reduced to a single Bernoulli equation that could be readily solved. Here, no assumptions were made about x_2, rather the model was considered for all $i \in C(\mathbb{R}_+, [0, i_M])$, where $i(t) = i(t+\rho)$ for some $\rho > 0$ and all $t \in \mathbb{R}_+$. It was found that there exist ρ-periodic solutions to (3.4.1) that were stable for different parameter values. The trivial tumour-tissue free solution (i.e. $x_1 \equiv 0$) was found to exist for all parameter values and was found to be asymptotically stable for $\delta_2 > 1$ and unstable for $\delta_2 < 1$. This is the same result observed for the analogous SS (i.e. RS1) of the model using the constant infusion function. Hence this suggests that using a different method of drug delivery will not change the conditions in which the tumour can be removed from the system, rather it is only required that the same total amount of drug is delivered over each treatment period. For system (3.4.1) a ρ-periodic solution of the form $\mathbf{x}(t) = [x_1(t) \quad x_2(t)]^{\mathrm{T}} > 0$ was found to exist for $\delta_2 < 1$. Furthermore, this solution was shown to be asymptotically stable if $\delta_2 < 1$. It is also noted that if $\delta_2 > (1+\delta_4)^2/4\delta_4$, then no ρ-periodic solution of this form can exist, as is the case for the analogous SS of the constant infusion model (i.e. RS2). It was also shown that if $1 \leq \delta_2 \leq (1+\delta_4)^2/4\delta_4$ and $\delta_4 < 1$, then no biologically meaningful ρ-periodic solution of this form could exist. Once again, this condition is the same as for the analogous SS of the constant

infusion model.

Considering the trivial periodic solution given by PS1, this solution, as in the constant infusion model, is unconditionally unstable and as a result this suggests that the model should always contain normal tissue or tumour tissue. This behaviour is to be expected and is consistent with cell models. The less trivial state PS2, that represents the tumour-free state, is shown to be stable when $\alpha_2 + \delta_2 > 1$ (similarly, unstable if $\alpha_2 + \delta_2 < 1$). Note that this is the condition for stability of the analogous SS in the constant infusion case (i.e. SS2). Whilst it should naturally follow that the periodic stability conditions should imply when the SSs of the constant infusion model are stable (respectively, unstable), it should be noted that these conditions are independent of $i(t)$ and are identical for all non-negative continuous periodic functions. Hence these conditions suggest that for the normal tissue to remain within the system, at the least, there needs to be sufficiently strong population competition and treatment strength. Should there not be significant competition provided by the normal tissue or large enough treatment strength cannot be obtained, for example, if the required dose to do so is unsafe, then this state will be unstable and this would provide the ideal conditions for tumour invasion. Hence if the competition that is provided by the normal tissue is able to be increased, then this would enable the tumour-free solution to become stable and improve the potential efficacy of the treatment. It is clear from this result alone that population competition has a potentially important role to play in treating tumour invasion. Furthermore, if a treatment somehow indirectly weakens the effective competition that normal-tissue can provide without lowering the tumour-tissue competition a proportional amount, then this can actually be harmful to the potential efficacy of the treatment. In a case like this, the assessment would need to be made of whether the relative benefit gained in fighting the tumour with the specific treatment outweighs the loss incurred from the damaged competition that the normal tissue provides.

The normal-tissue free periodic solution (i.e. PS3) was shown to exist if $\delta_2 < 1$ and furthermore could not exist if $\delta_2 > (1+\delta_4)^2/4\delta_4$, or if $1 \leq \delta_2 < (1+\delta_4)^2/4\delta_4$ and $\delta_4 \leq 1$. Hence these represent the parameter conditions in which it can be assured that an invasive tumour will not exist. In this state, the concentration of chemotherapy drug is lower than the tumour-free state, as would be expected due to the model assumption that interaction with the tumour causes some portion of the drug to decay. From the stability analysis in Section 3.4.4, it can be seen that the normal-tissue free periodic solution is unstable if

$$1 - (\alpha_1 + \delta_1)\hat{u}_{2+} > 0.$$

Hence there is a sufficiently large treatment strength that needs to be obtained in order prevent this invasive normal-tissue free state from being able to invade. Furthermore, from this condition it can be concluded that should $\alpha_1 + \delta_1 \leq 1$, then the state is unstable. Therefore if the combined strength of the tumour-tissue competition and the destructive influence of the acid is low, then the tumour will not be invasive. This is consistent with the results obtained for the constant infusion model considered in Section 3.3 and for the spatially heterogeneous model considered by McGillen et al. [140]. This further demonstrates the potential importance of the acid-mediation hypothesis, in that, should a tumour provide low population competition, then invasion may still be achieved provided a sufficiently strong destructive influence of the acid. This once again is consistent with the results of the model proposed by McGillen et al. [140].

It was shown in Section 3.4.4 that if $\delta_2 < (\alpha_1 + \delta_1 - 1)/(\alpha_1 + \delta_1)$, then the normal-tissue free solution (i.e. PS3) is asymptotically stable. Hence for sufficiently small treatment strength and sufficiently large tumour population competition and tumour aggressiveness, the invasive tumour state will be stable. It should be noted that the normal-tissue free solution could still be stable for larger values of δ_2, however the conducted analysis was unable to confirm stability for values of δ_2 outside of this set of values. If the normal-tissue population competition is sufficiently low, then the invasive tumour state will be the only stable solution. This will result in the tumour successfully invading and the treatment being unsuccessful. If however the normal-tissue population competition is sufficiently strong, i.e. if $\alpha_2 + \delta_2 > 1$, then the tumour-tissue free solution will be stable and hence the system will be bistable. Should this be the case, the size of the initial tumour will alter the efficacy of the treatment protocol which, as expected, is consistent with the results of the constant infusion model and the decreased likelihood of a cure associated with more established tumours [164]. From this it can be seen that the population competition, that is, the relative interaction between different cell types, can have a significant impact on the efficacy of the tumour treatment.

It was shown that a strictly positive ρ-periodic coexistence solution exists for (3.2.7) (i.e. PS4). Moreover, numerical simulations, using (3.2.8) for i, suggest that this solution is stable for particular parameter values. It is noted that this state exists and moreover, is stable, when the tumour aggressiveness, tumour-tissue population competition, normal-tissue population competition and destructive influence of the chemotherapy is low (i.e. $\delta_1, \alpha_1, \alpha_2, \delta_2$ are "small"). This is consistent with the results obtained for the constant infusion model. Should any of these parameters increase, the properties of the model change dramatically. If the tumour aggressiveness increases, then the

tumour would become invasive as the normal-tissue free periodic solution would become stable while the tumour-tissue free solution would remain unstable. Conversely, should the destructive influence of the chemotherapy be increased, by way of increased drug infusion (say), the coexistence state would become unstable and the tumour-free periodic solution would become stable resulting in the tumour being removed from the system.

3.6 Concluding remarks

A model for the acid-mediation hypothesis in the presence of a chemotherapy treatment has been proposed and considered. The proposed model is a simple ODE model that is comprised of the normal tissue, tumour tissue, acid concentration and chemotherapy drug concentration in a spatially homogeneous setting. The model was based on the model proposed by McGillen et al. [140] in combination with that proposed by Byrne [30] and has been considered to obtain an understanding of the reaction dynamics governing the system and to provide insights required before considering this in a spatially heterogeneous setting. The model was considered mathematically for different treatment methods using both numerical and analytical techniques.

The model has been considered with constant drug infusion which produced an autonomous system that was studied using a SS analysis. The model was also considered assuming the use of treatment occurring in cycles, which was characterised by time-periodic infusion functions. This resulted in a non-autonomous system that could be examined using an analysis of time-periodic solutions. The results from each analysis draw similar, if not the same, conclusions about the effect of competition, the treatment strength and the destructive influence of acid on the overall system dynamics. This suggests that the method of drug delivery is not a significant factor when trying to treat a tumour, rather it is the average rate of delivery which is the important factor. Hence much more focus can be placed on ensuring the safest method of delivery is used. Moreover, from a modelling standpoint this suggests, at least in a spatially homogeneous model, that the choice of infusion function is not as influential to the overall behaviour of the system as may be intuitively thought. This however only relates to the long term behaviour of the system, whereas the short term dynamics may still vary largely based on the choice of infusion function. Furthermore, this does not consider the potential dynamics that could be displayed in a spatially heterogeneous setting in which spatial variation and associated mechanisms must be considered.

Since the model considered in this chapter assumes spatially homogeneous populations, that is,

well-mixed populations, there are natural limitations to the conclusions that can be drawn from this analysis. However analysis conducted of this spatially homogeneous model provides insights into the potential long-term behaviour of a spatially heterogeneous version of this model, particularly in the situations of monostable solutions for the system. Hence analysis of a model that considers a spatially heterogeneous setting will be considered in the following chapter to further understand the dynamics of the acid-mediation hypothesis with chemotherapy intervention. We also note that the model considered here has assumed a small effect of chemotherapy on normal tissue and as such reduces the applicability of the results presented within this Chapter. Hence an extension of this model that removes this assumption can potentially be considered in further work to increase the usefulness of the model.

3.A Auxiliary definitions and results

We include for the convenience of the reader a collection of definitions and results required for this analysis of model considered in this chapter.

Definition 3.A.1 (Quasimonotonicity, see [201, §10, XII])**.** The function $\mathbf{F} : D \subset \mathbb{R}^{n+1} \to \mathbb{R}^n$ is said to be quasimonotone increasing on D if for $i = 1, \ldots, n$,

$$\mathbf{u} \leq \mathbf{v},\ u_i = v_i,\ (t, \mathbf{u}), (t, \mathbf{v}) \in D \quad \Longrightarrow \quad F_i(t, \mathbf{u}) \leq F_i(t, \mathbf{v}).$$

Remark 3.A.2. A matrix $C = (c_{ij})$ is said to be "essentially positive" if $c_{ij} \geq 0$ for all $i \neq j$. A function $\mathbf{F} : D \subset \mathbb{R}^{n+1} \to \mathbb{R}^n$ is quasimonotone increasing on a set $D \subset \mathbb{R}^{n+1}$ if the Jacobian matrix $\mathbf{F}'_{\mathbf{u}}(t, \mathbf{u})$ is essentially positive for all $(t, \mathbf{u}) \in D$.

Definition 3.A.3 (Invariant Sets in $\mathbb{R}^n$, see [201, §10, XV])**.** A set $D \subset \mathbb{R}^n$ is said to be invariant with respect to the system $\mathbf{u}' = \mathbf{F}(t, \mathbf{u})$ if for any solution $\mathbf{u}$, $\mathbf{u}(t_0) \in D$ implies $\mathbf{u}(t) \in D$ for $t > t_0$ (as long as the solution exists).

Definition 3.A.4 (Tangent Condition, see [201, §10, XV])**.** Let $D \subset \mathbb{R}^n$ and $\mathbf{F} : E \supset J \times \overline{D} \to \mathbb{R}^n$, where $J \subset \mathbb{R}$ is an interval. The tangent condition is given by

$$\langle \mathbf{n}(\mathbf{u}), \mathbf{F}(t, \mathbf{u}) \rangle \leq 0, \quad \text{for} \quad t \in J,\ \mathbf{u} \in \partial D,$$

where $\mathbf{n}(\mathbf{u})$ is the outer normal to D at $\mathbf{u}$.

Definition 3.A.5 (Local Lipschitz Condition, see [201, §6, IV]). Let $J \subset \mathbb{R}$, $D \subset \mathbb{R}^n$ and $E = J \times D$. Then the function $\mathbf{F} : E \to \mathbb{R}^n$ is said to satisfy a local Lipschitz condition with respect to $\mathbf{u}$ in E if for every $(t_0, \mathbf{u}_0) \in E$ there exists a neighbourhood $U = U(t_0, \mathbf{u}_0)$ and an $L = L(t_0, \mathbf{u}_0) < \infty$ such that for all $(t, \mathbf{u}_1), (t, \mathbf{u}_2) \in U \cap E$ the function $\mathbf{F}$ satisfies the Lipschitz condition

$$\|\mathbf{F}(t, \mathbf{u}_1) - \mathbf{F}(t, \mathbf{u}_2)\| \leq L\|\mathbf{u}_1 - \mathbf{u}_2\|.$$

Remark 3.A.6. If D is open and if $\mathbf{F} \in C(E, \mathbb{R}^n)$ has continuous derivative $\mathbf{F}'_{\mathbf{u}}(t, \mathbf{u})$ in E, then $\mathbf{F}$ satisfies a local Lipschitz condition with respect to $\mathbf{u}$ in E.

Theorem 3.A.7 (Invariance Theorem, see [201, §10, XVI]). *Let $D \subset \mathbb{R}^n$ be closed, $\mathbf{F} : [t_0, \infty) \times D \to \mathbb{R}^n$ bounded and continuous and consider the system $\mathbf{u}' = \mathbf{F}(t, \mathbf{u})$. Suppose that $\mathbf{F}$ satisfies the tangent condition (see Definition 3.A.4) and the one-sided Lipschitz condition on D, that is*

$$\langle \mathbf{u}_1 - \mathbf{u}_2, \mathbf{F}(t, \mathbf{u}_1) - \mathbf{F}(t, \mathbf{u}_2) \rangle \leq L\|\mathbf{u}_1 - \mathbf{u}_2\|^2 \quad \textit{for all} \quad t \in [t_0, \infty),\ \mathbf{u}_1, \mathbf{u}_2 \in D.$$

Then for any $\mathbf{u}(t_0) \in D$ a unique solution $\mathbf{u}(t)$ exists for all $t \in [t_0, \infty)$ which is invariant on D.

Theorem 3.A.8 (Comparison Theorem, see [201, §10, Comparison Theorem]). *Let $D \subset \mathbb{R}^n$ and $J = [t_0, t_0 + a]$; assume that $\mathbf{F} : J \times D \to \mathbb{R}^n$ is quasimonotone increasing and that $\mathbf{F}(t, \mathbf{u})$ satisfies a local Lipschitz condition with respect to $\mathbf{u}$ in $J \times D$. Suppose that $\mathbf{u}' = \mathbf{F}(t, \mathbf{u})$ and $\mathbf{v}' \leq \mathbf{F}(t, \mathbf{v})$, if $\mathbf{u}(t)$ and $\mathbf{v}(t)$ are differentiable on J and $\mathbf{v}(t_0) \leq \mathbf{u}(t_0)$, then $\mathbf{v}(t) \leq \mathbf{u}(t)$ for all $t \in J$.*

As a consequence of Theorem 3.A.8 we have the following corollary.

Corollary 3.A.9. *Let $D \subset \mathbb{R}^n$, $J = [t_0, t_0 + a]$ and $\mathbf{F} : J \times D \to \mathbb{R}^n$; assume that $\mathbf{F}(t, \mathbf{u})$ satisfies a local Lipschitz condition with respect to $\mathbf{u}$ on $J \times D$ and that $\mathbf{u}$ satisfies $\mathbf{u}' = F(t, \mathbf{u})$. Suppose that there exists an invertible $n \times n$ matrix M such that $M\mathbf{v}' \leq M\mathbf{F}(t, \mathbf{v})$ and $M\mathbf{F}(t, M^{-1}\boldsymbol{\eta})$ is quasimonotone increasing on $J \times \{\boldsymbol{\eta} \in \mathbb{R}^n : M^{-1}\boldsymbol{\eta} \in D\}$. If $\mathbf{u}(t)$ and $\mathbf{v}(t)$ are differentiable on J and $M\mathbf{v}(t_0) \leq M\mathbf{u}(t_0)$, then $M\mathbf{v}(t) \leq M\mathbf{u}(t)$ for all $t \in J$.*

Proof. It is well known that for any linear operator $T : \Omega \subset \mathbb{R}^n \to \mathbb{R}^n$ there exists a constant $c \in \mathbb{R}$ such that $\|T\mathbf{x}\| \leq c\|\mathbf{x}\|$ for all $\mathbf{x} \in \Omega$ [201, p. 58]. Hence there exists $c \in \mathbb{R}$ such that $\|M\mathbf{F}(t, \mathbf{u}_1) - M\mathbf{F}(t, \mathbf{u}_2)\| = \|M(\mathbf{F}(t, \mathbf{u}_1) - \mathbf{F}(t, \mathbf{u}_2))\| \leq c\|\mathbf{F}(t, \mathbf{u}_1) - \mathbf{F}(t, \mathbf{u}_2)\|$ for all

$(t, \mathbf{u}_1), (t, \mathbf{u}_2) \in J \times D$. Then as $\mathbf{F}(t, \mathbf{u})$ satisfies a local Lipschitz condition on $J \times D$ it easily follows that so too does $M\mathbf{F}(t, \mathbf{u})$.

Let $\bar{\mathbf{u}}(t) = M\mathbf{u}(t)$ and $\bar{\mathbf{v}}(t) = M\mathbf{v}(t)$, then we have $\bar{\mathbf{u}}' = M\mathbf{F}(t, M^{-1}\bar{\mathbf{u}})$ and $\bar{\mathbf{v}}' \leq M\mathbf{F}(t, M^{-1}\bar{\mathbf{v}})$ on $J \times E$, where $E = \{\boldsymbol{\eta} \in \mathbb{R}^n : M^{-1}\boldsymbol{\eta} \in D\}$. Note $M\mathbf{F}(t, M^{-1}\bar{\mathbf{u}})$ is quasi-monotone increasing on $J \times E$ and if $\mathbf{u}(t)$ and $\mathbf{v}(t)$ are differentiable on J, so too are $\bar{\mathbf{u}}(t)$ and $\bar{\mathbf{v}}(t)$. Therefore by Theorem 3.A.8 if $\bar{\mathbf{v}}(t_0) \leq \bar{\mathbf{u}}(t_0)$, then $\bar{\mathbf{v}}(t) \leq \bar{\mathbf{u}}(t)$ for all $t \in J$, that is, if $M\mathbf{v}(t_0) \leq M\mathbf{u}(t_0)$, then $M\mathbf{v}(t) \leq M\mathbf{u}(t)$ for all $t \in J$. □

3.B Results for specific ODEs and corresponding periodic solutions

Lemma 3.B.1. *Consider the equation*

$$\frac{\mathrm{d}w}{\mathrm{d}t} = f(t) - g(t)w, \tag{3.B.1}$$

where $f, g \in C(\mathbb{R}_+)$ are ρ-periodic. Suppose that

$$\int_0^\rho g(s)\,\mathrm{d}s \neq 0, \quad f(t) \geq (>)0 \quad \textit{for all} \quad t \in \mathbb{R}_+.$$

Then the following statements hold:

(i) *The function*

$$w(t; f, g) = w(0)\mathrm{e}^{-\int_0^t g(s)\,\mathrm{d}s} + \int_0^t \mathrm{e}^{-\int_s^t g(s')\,\mathrm{d}s'} f(s)\,\mathrm{d}s \tag{3.B.2}$$

is the unique solution of (3.B.1) *for any initial condition $w(0) \in \mathbb{R}$. Note that $w(t; f, g) > 0$ for all $t \geq 0$ if and only if $w(0) > 0$.*

(ii) *If*

$$w(0) = \frac{\int_0^\rho \mathrm{e}^{-\int_s^\rho g(s')\,\mathrm{d}s'} f(s)\,\mathrm{d}s}{1 - \mathrm{e}^{-\int_0^\rho g(s)\,\mathrm{d}s}}, \tag{3.B.3}$$

then (3.B.2) *is the unique ρ-periodic solution, where*

$$\int_0^\rho g(t)w(t)\,\mathrm{d}t = \int_0^\rho f(t)\,\mathrm{d}t.$$

Moreover, $w(0) \geq (>)0$ if and only if $\int_0^\rho g(s)\,\mathrm{d}s > 0$.

(iii) *Suppose that $g_1(t) \geq g_2(t)$ for all $t \in \mathbb{R}_+$ and $\int_0^\rho g_2(s)\,\mathrm{d}s > 0$. If $w(t; f, g_1)$ and $w(t; f, g_2)$ have initial conditions given by* (3.B.3)*, then $w(t; f, g_1) \leq w(t; f, g_2)$ for all $t \in \mathbb{R}_+$.*

Proof. (i) The unique solution $w = w(\cdot; f, g)$ of the linear ODE (3.B.1) for any initial condition is given by (3.B.2). Since $f(t) \geq 0$ for all $t \in \mathbb{R}_+$ it is straightforward to see that $w(t; f, g) > 0$ for all $t \geq 0$ if and only if $w(0) > 0$.

(ii) If the initial condition is given by (3.B.3), then $w(\rho) = w(0)$. Furthermore, the ρ-periodicity of f and g implies that

$$w'(t) = f(t) - g(t)w(t), \quad w'(t+\rho) = f(t) - g(t)w(t+\rho) \quad \text{for all } t \geq 0.$$

Then $\bar{w}(t) = w(t+\rho) - w(t)$ satisfies the initial value problem

$$\frac{\mathrm{d}\bar{w}}{\mathrm{d}t} = -g(t)\bar{w}, \quad \bar{w}(0) = 0.$$

Hence $\bar{w} \equiv 0$ and $w(t+\rho) = w(t)$ for all $t \geq 0$. Since $f(t) \geq (>)0$ for all $t \in \mathbb{R}_+$ it is clear that if $w(0)$ is given by (3.B.3), then $w(0) \geq (>)0$ if and only if $\int_0^\rho g(s)\,\mathrm{d}s > 0$. To show that the solution for (3.B.3) is the unique ρ-periodic solution we consider two distinct ρ-periodic solutions for (3.B.1) denoted by $w_1(t)$ and $w_2(t)$. Due to uniqueness to initial conditions $w_1(t) \neq w_2(t)$ for all $t \in \mathbb{R}_+$, so without loss of generality we assume $w_1(t) > w_2(t)$ for all $t \in \mathbb{R}_+$. Then $\varepsilon(t) = w_1(t) - w_2(t) = w_1(t+\rho) - w_2(t+\rho) = \varepsilon(t+\rho) > 0$ for all $t \in \mathbb{R}_+$ satisfies

$$\frac{\mathrm{d}\varepsilon}{\mathrm{d}t} = -g(t)\varepsilon \quad \Longrightarrow \quad 0 = \int_0^\rho \frac{1}{\varepsilon(s)}\frac{\mathrm{d}\varepsilon}{\mathrm{d}s}\,\mathrm{d}s = -\int_0^\rho g(s)\,\mathrm{d}s,$$

which is a contradiction. Therefore the ρ-periodic solution for initial condition (3.B.3) must be unique.

(iii) Suppose that $g_1(t) \geq g_2(t)$ for all $t \in \mathbb{R}_+$ and $\int_0^\rho g_2(s)\,\mathrm{d}s > 0$, then $\int_0^\rho g_1(s)\,\mathrm{d}s \geq \int_0^\rho g_2(s)\,\mathrm{d}s > 0$. If $w(t; f, g_1)$ and $w(t; f, g_2)$ have initial conditions given by (3.B.3), then $w(t; f, g_1)$ and $w(t; f, g_2)$ are unique ρ-periodic solutions and $w(t; f, g_1), w(t; f, g_2) \geq 0$ for all $t \in \mathbb{R}_+$. Let $\varepsilon(t) = w(t; f, g_2) - w(t; f, g_1) = w(t+\rho; f, g_2) - w(t+\rho; f, g_1) = \varepsilon(t+\rho)$ which satisfies

$$\varepsilon' = [g_1(t) - g_2(t)]w(t; f, g_2) - g_1(t)\varepsilon.$$

Now $[g_1(t) - g_2(t)]w(t; f, g_2) \geq 0$ for all $t \in \mathbb{R}_+$, hence by the previous results the ρ-periodic solution $\varepsilon(t) \geq 0$ for all $t \in \mathbb{R}_+$, i.e. $w(t; f, g_1) \leq w(t; f, g_2)$ for all $t \in \mathbb{R}_+$.

□

Lemma 3.B.2. *Consider the equation*

$$\frac{\mathrm{d}v}{\mathrm{d}t} = g(t)v - f(t)v^2, \tag{3.B.4}$$

where $f, g \in C(\mathbb{R}_+)$ are ρ-periodic. Suppose that

$$\int_0^\rho g(s)\,\mathrm{d}s \neq 0, \quad f(t) > 0 \quad \textit{for all} \quad t \in \mathbb{R}_+.$$

Then the following statements hold:

(i) *The function*

$$v(t; f, g) = \left[v(0)^{-1}\mathrm{e}^{-\int_0^t g(s)\,\mathrm{d}s} + \int_0^t \mathrm{e}^{-\int_s^t g(s')\,\mathrm{d}s'} f(s)\,\mathrm{d}s\right]^{-1} \tag{3.B.5}$$

is the unique solution of (3.B.4) *for any initial condition $v(0) > 0$. Note that $v(t; f; g) > 0$ for all $t \in \mathbb{R}_+$ if and only if $v(0) > 0$.*

(ii) *If $\int_0^\rho g(s)\,\mathrm{d}s > 0$ and*

$$v(0) = \frac{1 - \mathrm{e}^{-\int_0^\rho g(s')\,\mathrm{d}s'}}{\int_0^\rho \mathrm{e}^{-\int_s^\rho g(s')\,\mathrm{d}s'} f(s)\,\mathrm{d}s}, \tag{3.B.6}$$

then (3.B.5) *is a unique strictly positive ρ-periodic solution. Moreover, $v(0) > 0$ if and only if $\int_0^\rho g(s)\,\mathrm{d}s > 0$.*

(iii) *Suppose that $g_1(t) \geq g_2(t)$ for all $t \in \mathbb{R}_+$ and $\int_0^\rho g_2(s)\,\mathrm{d}s > 0$. If $v(t; f, g_1)$ and $v(t; f, g_2)$ have initial conditions given by* (3.B.6)*, then $v(t; f, g_1) \geq v(t; f, g_2)$ for all $t \in \mathbb{R}_+$.*

Proof. (i) Set $v = v(\cdot; f, g)$ in the Bernoulli equation (3.B.4) to $v(t) = u(t)^{-1}$. Then u satisfies the linear ODE

$$\frac{\mathrm{d}u}{\mathrm{d}t} = f(t) - g(t)u,$$

whose solution for any initial condition is

$$u(t) = u(0)\mathrm{e}^{-\int_0^t g(s)\,\mathrm{d}s} + \int_0^t \mathrm{e}^{-\int_s^t g(s')\,\mathrm{d}s'} f(s)\,\mathrm{d}s.$$

Hence (3.B.5) follows.

(ii) Since $f(t) > 0$ for all $t \in \mathbb{R}_+$ it is clear that if $v(0)$ is given by (3.B.6), then $v(0) > 0$ if and only if $\int_0^\rho g(s)\,\mathrm{d}s > 0$. If $\int_0^\rho g(s)\,\mathrm{d}s > 0$ and the initial condition is given by (3.B.6), then $u(\rho) = u(0) > 0$ and a similar analysis as in the proof of Lemma 3.B.1 shows that v is a unique strictly positive ρ-periodic solution.

(iii) Suppose that $g_1(t) \geq g_2(t)$ for all $t \in \mathbb{R}_+$ and $\int_0^\rho g_2(s)\,\mathrm{d}s > 0$. If the initial conditions for $v(t; f, g_1)$ and $v(t; f, g_2)$ are given by (3.B.6), then Lemma 3.B.1(iii) shows that $u(t; f, g_1) \leq u(t; f, g_2)$ for all $t \in \mathbb{R}_+$, which implies $v(t; f, g_1) \geq v(t; f, g_2)$ for all $t \in \mathbb{R}_+$.

□

Lemma 3.B.3. *Suppose that there exists a solution* $\mathbf{x}(t) = [x_1(t) \quad x_2(t)]^{\mathrm{T}} > 0$ *for all* $t \in \mathbb{R}_+$ *to system* (3.4.1)*, then it follows that*

$$\delta_4 x_1(t)^2 + (1 - \delta_4)x_1(t) + \delta_1 i(t) - 1 = \frac{\mathrm{d}}{\mathrm{d}t}V(\mathbf{x}(t)),$$

where $V(\mathbf{x}) = -(\delta_4/\beta_2)x_1 + (\delta_2/\beta_4)x_2 - (1/\beta_2)\ln x_1$*. Moreover, it is a necessary condition that*

$$\delta_2 i(t) - \tfrac{\mathrm{d}}{\mathrm{d}t}V(\mathbf{x}(t)) \leq \frac{(1+\delta_4)^2}{4\delta_4}.$$

If the solution is ρ*-periodic, then*

(i) *The solution exists only if* $\delta_2 < 1$ *or only if* $1 \leq \delta_2 \leq (1+\delta_4)^2/4\delta_4$ *and* $\delta_4 > 1$*. Moreover,*

$$0 \leq \frac{1}{\rho}\int_0^\rho x_1(s)\,\mathrm{d}s \leq \hat{u}_{2+}.$$

(ii) *If* $\delta_2 < 1$*, then*

$$x_1(t) = \frac{\delta_4 - 1 + \sqrt{(\delta_4+1)^2 - 4\delta_4[\delta_2 i(t) - h(t)]}}{2\delta_4},$$

where $h(t) = \frac{\mathrm{d}}{\mathrm{d}t}V(\mathbf{x}(t))$.

Proof. We wish to find a function $V = V(\mathbf{x})$ such that

$$\frac{\mathrm{d}}{\mathrm{d}t}V(\mathbf{x}(t)) = A(t)x_1(t)^2 + B(t)x_1(t) + C(t),$$

where A, B and C are appropriate ρ-periodic functions. Note the right-hand side is independent

of x_2. By considering (3.4.1), we can try the ansatz

$$V(\mathbf{x}) = ax_1 + bx_2 + c\log x_1,$$

where a, b and c are constants. Then

$$\begin{aligned}\frac{\mathrm{d}}{\mathrm{d}t}V(\mathbf{x}(t)) &= \left[a + \frac{c}{x_1(t)}\right] x_1'(t) + bx_2'(t) \\ &= -a\beta_2 x_1(t)^2 + (a-c)\beta_2 x_1(t) + c\beta_2 + b\beta_4 i(t) \\ &\quad - (a\beta_2\delta_2 + b\beta_4\delta_4)x_1(t)x_2(t) - (c\beta_2\delta_2 + b\beta_4)x_2(t).\end{aligned}$$

To eliminate the terms involving x_2, we set

$$a = -\frac{\delta_4}{\beta_2}, \quad b = \frac{\delta_2}{\beta_4}, \quad c = -\frac{1}{\beta_2}.$$

This gives

$$\frac{\mathrm{d}}{\mathrm{d}t}V(\mathbf{x}(t)) = \delta_4 x_1(t)^2 + (1-\delta_4)x_1(t) + \delta_2 i(t) - 1, \tag{3.B.7}$$

i.e. $A(t) = \delta_4$, $B(t) = 1 - \delta_4$ and $C(t) = \delta_2 i(t) - 1$. Rewriting (3.B.7), we obtain

$$\begin{aligned}x_1(t) &= \frac{(\delta_4 - 1) \pm \sqrt{(\delta_4-1)^2 + 4\delta_4[1 - \delta_2 i(t) + h(t)]}}{2\delta_4} \\ &= \frac{(\delta_4 - 1) \pm \sqrt{(\delta_4+1)^2 - 4\delta_4[\delta_2 i(t) - h(t)]}}{2\delta_4},\end{aligned}$$

where $h(t) = \frac{\mathrm{d}}{\mathrm{d}t}V(u_2(t), u_4(t))$. If $x_1(t) > 0$ for all $t \in \mathbb{R}_+$, a necessary condition is that

$$\delta_2 i(t) - h(t) \leq \frac{(\delta_4+1)^2}{4\delta_4}. \tag{3.B.8}$$

Suppose that the solution $\mathbf{x}(t) > 0$ is ρ-periodic:

(i) Integrating both sides of (3.B.8) with respect to t from 0 to ρ and using the periodicity of $\mathbf{x}$, we have

$$\frac{(\delta_4+1)^2}{4\delta_4} \geq \frac{1}{\rho}\int_0^\rho [\delta_2 i(t) - h(t)]\ \mathrm{d}t = \delta_2.$$

Moreover, by the Mean Value Theorem, there exists $t^* \in (0, \rho)$ such that

$$\frac{1}{\rho}\int_0^\rho [\delta_2 i(t) - h(t)]\,\mathrm{d}t = \delta_2 i(t^*) - h(t^*).$$

We therefore deduce that

$$x_1(t^*) = \frac{(\delta_4 - 1) \pm \sqrt{(\delta_4+1)^2 - 4\delta_4\delta_2}}{2\delta_4},$$

which has at least one strictly positive value if and only if $\delta_2 < 1$, or if $1 \leq \delta_2 \leq (1+\delta_4)^2/4\delta_4$ and $\delta_4 > 1$, hence if these parameter conditions are not satisfied, then it is not possible for $x_1(t) > 0$ for all $t \in \mathbb{R}_+$.

Moreover, the Cauchy-Schwarz inequality gives

$$\begin{aligned}
&\frac{1}{\rho}\int_0^\rho \sqrt{(\delta_4+1)^2 - 4\delta_4[\delta_2 i(s) - h(s)]}\,\mathrm{d}s \\
&\qquad \leq \left[\frac{1}{\rho}\int_0^\rho \{(\delta_4+1)^2 - 4\delta_4[\delta_2 i(s) - h(s)]\}\,\mathrm{d}s\right]^{1/2} \\
&\qquad = \sqrt{(\delta_4+1)^2 - 4\delta_4\delta_2}.
\end{aligned}$$

Hence

$$\begin{aligned}
0 \leq \frac{1}{\rho}\int_0^\rho x_1(s)\,\mathrm{d}s &\leq \max\left\{\frac{1}{\rho}\int_0^\rho \frac{(\delta_4 - 1) \pm \sqrt{(\delta_4+1)^2 - 4\delta_4[\delta_2 i(s) - h(s)]}}{2\delta_4}\,\mathrm{d}s\right\} \\
&\leq \hat{u}_{2+}
\end{aligned}$$

(ii) If $\delta_2 < 1$, we further deduce that

$$(\delta_4 - 1)^2 + 4\delta_4[1 - \delta_2 i(t^*) + h(t^*)] > (\delta_4 - 1)^2$$

and as a result

$$x_1(t) = \frac{(\delta_4 - 1) + \sqrt{(\delta_4 - 1)^2 + 4\delta_4[1 - \delta_2 i(t) + h(t)]}}{2\delta_4},$$

otherwise x_1 can become negative at t^*.

□

3.C Details of steady-state analysis

Lemma 3.C.1. *The system of equations given by* (3.3.1) *has the following SS solutions and respective linear stability conditions:*

SS1. $\mathbf{u}^* = (0, 0, 0, 1)$ *is unconditionally unstable.*

SS2. $\mathbf{u}^* = (1, 0, 0, 1)$ *is stable if and only if* $\alpha_2 + \delta_2 > 1$.

SS3. $\mathbf{u}^* = (0, \hat{u}_{2\pm}, \hat{u}_{2\pm}, [1 + \delta_4 \hat{u}_{2\pm}]^{-1})$, *where* $\hat{u}_{2\pm} = \left[\delta_4 - 1 \pm \sqrt{(1+\delta_4)^2 - 4\delta_2\delta_4}\right]/2\delta_4$. *The SS corresponding to* $\hat{u}_{2-}$ *is unconditionally unstable and the SS corresponding to* $\hat{u}_{2+}$ *will be stable if and only if*

$$\delta_2 < \frac{(\alpha_1 + \delta_1 + \delta_4)(\alpha_1 + \delta_1 - 1)}{(\alpha_1 + \delta_1)^2},$$

or if

$$\frac{(\alpha_1 + \delta_1 + \delta_4)(\alpha_1 + \delta_1 - 1)}{(\alpha_1 + \delta_1)^2} \leq \delta_2 < \frac{(1+\delta_4)^2}{4\delta_4} \quad \textit{and} \quad \frac{1}{\delta_4} < \frac{\alpha_1 + \delta_1 - 2}{\alpha_1 + \delta_1}.$$

SS4. $\mathbf{u}^* = (1 - [\alpha_1 + \delta_1]\tilde{u}_{2\pm}, \tilde{u}_{2\pm}, \tilde{u}_{2\pm}, [1 + \delta_4 \tilde{u}_{2\pm}]^{-1})$, *where*

$$\tilde{u}_{2\pm} = \frac{-(1 - \alpha_2(\alpha_1 + \delta_1)) - \delta_4(\alpha_2 - 1)}{2\delta_4(1 - \alpha_2(\alpha_1 + \delta_1))} \pm \frac{\sqrt{[1 - \alpha_2(\alpha_1 + \delta_1) - \delta_4(\alpha_2 - 1)]^2 - 4\delta_2\delta_4(1 - \alpha_2(\alpha_1 + \delta_1))}}{2\delta_4(1 - \alpha_2(\alpha_1 + \delta_1))}.$$

The SS corresponding to $\tilde{u}_{2-}$ *has no biologically meaningful values for which it is stable. The SS corresponding to* $\tilde{u}_{2+}$ *is stable if and only if*

$$0 < (\alpha_1 + \delta_1)\tilde{u}_{2+} < 1, \quad 0 < \delta_2 < \frac{[1 - \alpha_2(\alpha_1 + \delta_1) - \delta_4(\alpha_2 - 1)]^2}{4\delta_4[1 - \alpha_2(\alpha_1 + \delta_1)]}$$

and

$$c_1 c_2 c_3 > c_3^2 c_0 + c_1^2,$$

where

$$
\begin{aligned}
c_3 &= 1-(\alpha_1+\delta_1)\tilde{u}_2+\beta_3+\beta_2\tilde{u}_2+\beta_4(1+\delta_4\tilde{u}_2),\\
c_2 &= \beta_3[\beta_2\tilde{u}_2+\beta_4(1+\delta_4\tilde{u}_2)]+[1-(\alpha_1+\delta_1)\tilde{u}_2][\beta_3+\beta_4(1+\delta_4\tilde{u}_2)+\beta_2\tilde{u}_2(1-\alpha_2\alpha_1)]\\
&\quad+\frac{\beta_2\beta_4\tilde{u}_2}{1+\delta_4\tilde{u}_2}[(1+\delta_4\tilde{u}_2)^2-\delta_2\delta_4],\\
c_1 &= [1-(\alpha_1+\delta_1)\tilde{u}_2]\left[\frac{\beta_2\beta_4\tilde{u}_2}{1+\delta_4\tilde{u}_2}[(1+\delta_4\tilde{u}_2)^2(1-\alpha_2\alpha_1)-\delta_2\delta_4]+\beta_3\beta_4(1+\delta_4\tilde{u}_2)\right]\\
&\quad+\beta_2\beta_3\tilde{u}_2[1-(\alpha_1+\delta_1)\tilde{u}_2][1-\alpha_2(\alpha_1+\delta_1)]+\frac{\beta_2\beta_3\beta_4\tilde{u}_2}{1+\delta_4\tilde{u}_2}[(1+\delta_4\tilde{u}_2)^2-\delta_2\delta_4],
\end{aligned}
$$

$$
c_0 = \frac{\beta_2\beta_3\beta_4\tilde{u}_2}{1+\delta_4\tilde{u}_2}\left[1-(\alpha_1+\delta_1)\tilde{u}_2\right]\left[(1+\delta_4\tilde{u}_2)^2(1-\alpha_2(\alpha_1+\delta_1))-\delta_2\delta_4\right].
$$

Proof. We consider the system of equations given by (3.3.1), set the derivatives to zero (i.e. $\mathbf{u}' = \mathbf{0}$) and solve for u_1, u_2, u_3, u_4 to obtain the SS solutions. We obtain the solutions

$$
(0,0,0,1),(1,0,0,1),\left(0,\hat{u}_2,\hat{u}_2,\frac{1}{1+\delta_4\hat{u}_2}\right),\left(1-(\alpha_1+\delta_1)\tilde{u}_2,\tilde{u}_2,\tilde{u}_2,\frac{1}{1+\delta_4\tilde{u}_2}\right),
$$

where $\hat{u}_2$ solves

$$
\delta_4\hat{u}_2^2+(1-\delta_4)\hat{u}_2+\delta_2-1=0 \tag{3.C.1}
$$

and $\tilde{u}_2$ solves

$$
\delta_4[1-\alpha_2(\alpha_1+\delta_1)]\tilde{u}_2^2+[1-\alpha_2(\alpha_1+\delta_1)+\delta_4(\alpha_2-1)]\tilde{u}_2+\delta_2+\alpha_2-1=0. \tag{3.C.2}
$$

We wish to determine the stability of these solutions by performing a linear stability analysis. Consider the following vector:

$$
\mathbf{F}(\mathbf{u}) = \begin{bmatrix} u_1(1-u_1-\alpha_1u_2-\delta_1u_3)\\ \beta_2u_2(1-u_2-\alpha_2u_1-\delta_2u_4)\\ \beta_3(u_2-u_3)\\ \beta_4(1-u_4-\delta_4u_4u_2)\end{bmatrix}.
$$

The Jacobian matrix of $\mathbf{F}$ is then given by

$$\mathbf{F}'_{\mathbf{u}}(\mathbf{u}) = \begin{bmatrix} 1-2u_1-\alpha_1u_2-\delta_1u_3 & -\alpha_1u_1 & -\delta_1u_1 & 0 \\ -\beta_2\alpha_2u_2 & \beta_2(1-2u_2-\alpha_2u_1-\delta_2u_4) & 0 & -\beta_2\delta_2u_2 \\ 0 & \beta_3 & -\beta_3 & 0 \\ 0 & -\beta_4\delta_4u_4 & 0 & -\beta_4(1+\delta_4u_2) \end{bmatrix}.$$

SS1. Now if we consider the SS solution $(0,0,0,1)$ we have the Jacobian matrix

$$\mathbf{F}'_{\mathbf{u}}(0,0,0,1) = \begin{bmatrix} 1 & 0 & 0 & 0 \\ 0 & \beta_2(1-\delta_2) & 0 & 0 \\ 0 & \beta_3 & -\beta_3 & 0 \\ 0 & -\beta_4\delta_4 & 0 & -\beta_4 \end{bmatrix}$$

which has eigenvalues $\lambda = 1, \beta_2(1-\delta_2), -\beta_3, -\beta_4$. Hence we can see this is unstable for all parameter values as $\lambda = 1 > 0$.

SS2. The SS $(1,0,0,1)$ has Jacobian matrix

$$\mathbf{F}'_{\mathbf{u}}(1,0,0,1) = \begin{bmatrix} -1 & -\alpha_1 & -\delta_1 & 0 \\ 0 & \beta_2(1-\alpha_2-\delta_2) & 0 & 0 \\ 0 & \beta_3 & -\beta_3 & 0 \\ 0 & -\beta_4\delta_4 & 0 & -\beta_4 \end{bmatrix}$$

with eigenvalues $\lambda = -1, \beta_2(1-\alpha_2-\delta_2), -\beta_3, -\beta_4$. Therefore we can see that all $\mathrm{Re}(\lambda) < 0$ if and only if $\alpha_2+\delta_2 > 1$. Hence we have that $(1,0,0,1)$ is linearly stable if $\alpha_2+\delta_2 > 1$.

SS3. We consider the SS solution $\mathbf{u}^* = (0, \hat{u}_2, \hat{u}_2, [1+\delta_4\hat{u}_2]^{-1})$ noting from $\mathbf{F}(\mathbf{u}) = \mathbf{0}$ we have $1-u_2-\alpha_2u_1-\delta_2u_4 = 0$. Hence we have the Jacobian matrix

$$\mathbf{F}'_{\mathbf{u}}(\mathbf{u}^*) = \begin{bmatrix} 1-(\alpha_1+\delta_1)\hat{u}_2 & 0 & 0 & 0 \\ -\beta_2\alpha_2\hat{u}_2 & -\beta_2\hat{u}_2 & 0 & -\beta_2\delta_2\hat{u}_2 \\ 0 & \beta_3 & -\beta_3 & 0 \\ 0 & -\beta_4\delta_4(1+\delta_4\hat{u}_2)^{-1} & 0 & -\beta_4(1+\delta_4\hat{u}_2) \end{bmatrix}$$

with eigenvalues that satisfy $\lambda = 1-(\alpha_1+\delta_1)\hat{u}_2, -\beta_3$ and $\lambda^2 + [\beta_2\hat{u}_2 + \beta_4(1+\delta_4\hat{u}_2)]\lambda + \beta_2\beta_4\hat{u}_2[(1+\delta_4\hat{u}_2)^2 - \delta_4\delta_2]/(1+\delta_4\hat{u}_2) = 0$. Therefore using the Routh–Hurwitz conditions

[145, pp. 507–509], we have Re$(\lambda) < 0$ if $1 - (\alpha_1 + \delta_1)\hat{u}_2 < 0$, $\delta_4\delta_2 < (1 + \delta_4\hat{u}_2)^2$ and $\hat{u}_2 > 0$. Note that if $1 - (\alpha_1 + \delta_1)\hat{u}_2 < 0$, then it follows that $\hat{u}_2 > 0$. Since $\hat{u}_2$ satisfies (3.C.1), we have that $\delta_2 = 1 - \delta_4\hat{u}_2^2 + (\delta_4 - 1)\hat{u}_2$ and as a result

$$(1 + \delta_4\hat{u}_2)^2 - \delta_4\delta_2 = (1 + \delta_4\hat{u}_2)(2\delta_4\hat{u}_2 + 1 - \delta_4).$$

Therefore if $2\delta_4\hat{u}_2 + 1 - \delta_4 > 0$, then it follows that $\delta_4\delta_2 < (1 + \delta_4\hat{u}_2)^2$. Consider (3.C.1), solving for $\hat{u}_2$ we obtain

$$\hat{u}_{2\pm} = \frac{\delta_4 - 1 \pm \sqrt{(1 - \delta_4)^2 + 4\delta_4(1 - \delta_2)}}{2\delta_4} = \frac{\delta_4 - 1 \pm \sqrt{(1 + \delta_4)^2 - 4\delta_4\delta_2}}{2\delta_4}$$

and note that $\hat{u}_{2\pm} \in \mathbb{R}$ if and only if $\delta_2 \leq (1 + \delta_4)^2/4\delta_4$. Therefore

$$2\delta_4\hat{u}_{2\pm} + 1 - \delta_4 = \pm\sqrt{(1 + \delta_4)^2 - 4\delta_4\delta_2}$$

and as a result we can see that if $\delta_2 < (1 + \delta_4)^2/4\delta_4$, then $2\delta_4\hat{u}_{2+} + 1 - \delta_4 > 0$ and $2\delta_4\hat{u}_{2-} + 1 - \delta_4 < 0$. Hence SS3 with $\hat{u}_{2-}$ will be unstable for all parameter values and we only require that $1 - (\alpha_1 + \delta_1)\hat{u}_{2+} < 0$ for SS3 with $\hat{u}_{2+}$ to be linearly stable. Consider

$$\begin{aligned}
&(\alpha_1 + \delta_1)\hat{u}_{2+} - 1 \\
&\quad = \frac{(\alpha_1 + \delta_1)(\delta_4 - 1) - 2\delta_4 + (\alpha_1 + \delta_1)\sqrt{(1 - \delta_4)^2 + 4\delta_4(1 - \delta_2)}}{2\delta_4} \\
&\quad = \frac{(\alpha_1 + \delta_1)(\delta_4 - 1) - 2\delta_4}{2\delta_4} \\
&\qquad + \frac{\sqrt{[(\alpha_1 + \delta_1)(\delta_4 - 1) - 2\delta_4]^2 + 4\delta_4[(\alpha_1 + \delta_1 + \delta_4)(\alpha_1 + \delta_1 - 1) - \delta_2(\alpha_1 + \delta_1)^2]}}{2\delta_4}
\end{aligned}$$

Hence we can see that if

$$\delta_2 < \frac{(\alpha_1 + \delta_1 + \delta_4)(\alpha_1 + \delta_1 - 1)}{(\alpha_1 + \delta_1)^2},$$

then $1 - (\alpha_1 + \delta_1)\hat{u}_{2+} < 0$ and as a result SS3 with $\hat{u}_{2+}$ is stable. If

$$\frac{(\alpha_1 + \delta_1 + \delta_4)(\alpha_1 + \delta_1 - 1)}{(\alpha_1 + \delta_1)^2} \leq \delta_2 < \frac{(1 + \delta_4)^2}{4\delta_4} \quad \text{and} \quad \frac{1}{\delta_4} < \frac{\alpha_1 + \delta_1 - 2}{\alpha_1 + \delta_1},$$

then $1-(\alpha_1+\delta_1)\hat{u}_{2+}<0$ and as a result SS3 with $\hat{u}_{2+}$ is linearly stable.

SS4. We consider the SS solution $\mathbf{u}^* = (1-(\alpha_1+\delta_1)\tilde{u}_2, \tilde{u}_2, \tilde{u}_2, [1+\delta_4\tilde{u}_2]^{-1})$ noting from $\mathbf{F}(\mathbf{u})=\mathbf{0}$ we have $1-u_2-\alpha_2u_1-\delta_2u_4=0$ and $1-u_1-\alpha_1u_2-\delta_1u_3=0$. Hence we have the Jacobian matrix

$$\mathbf{F}'_{\mathbf{u}}(\mathbf{u}^*) = \begin{bmatrix} (\alpha_1+\delta_1)\tilde{u}_2-1 & \alpha_1[(\alpha_1+\delta_1)\tilde{u}_2-1] & \delta_1[(\alpha_1+\delta_1)\tilde{u}_2-1] & 0 \\ -\beta_2\alpha_2\tilde{u}_2 & -\beta_2\tilde{u}_2 & 0 & -\beta_2\delta_2\tilde{u}_2 \\ 0 & \beta_3 & -\beta_3 & 0 \\ 0 & -\beta_4\delta_4(1+\delta_4\tilde{u}_2)^{-1} & 0 & -\beta_4(1+\delta_4\tilde{u}_2) \end{bmatrix}$$

that has a characteristic equation

$$\lambda^4+c_3\lambda^3+c_2\lambda^2+c_1\lambda+c_0=0,$$

where

$$\begin{aligned} c_3 &= 1-(\alpha_1+\delta_1)\tilde{u}_2+\beta_3+\beta_2\tilde{u}_2+\beta_4(1+\delta_4\tilde{u}_2), \\ c_2 &= \beta_3[\beta_2\tilde{u}_2+\beta_4(1+\delta_4\tilde{u}_2)]+[1-(\alpha_1+\delta_1)\tilde{u}_2][\beta_3+\beta_4(1+\delta_4\tilde{u}_2)+\beta_2\tilde{u}_2(1-\alpha_2\alpha_1)] \\ &\quad +\frac{\beta_2\beta_4\tilde{u}_2}{1+\delta_4\tilde{u}_2}[(1+\delta_4\tilde{u}_2)^2-\delta_2\delta_4], \\ c_1 &= [1-(\alpha_1+\delta_1)\tilde{u}_2]\left[\frac{\beta_2\beta_4\tilde{u}_2}{1+\delta_4\tilde{u}_2}[(1+\delta_4\tilde{u}_2)^2(1-\alpha_2\alpha_1)-\delta_2\delta_4]+\beta_3\beta_4(1+\delta_4\tilde{u}_2)\right] \\ &\quad +\beta_2\beta_3\tilde{u}_2[1-(\alpha_1+\delta_1)\tilde{u}_2][1-\alpha_2(\alpha_1+\delta_1)]+\frac{\beta_2\beta_3\beta_4\tilde{u}_2}{1+\delta_4\tilde{u}_2}[(1+\delta_4\tilde{u}_2)^2-\delta_2\delta_4], \\ c_0 &= \frac{\beta_2\beta_3\beta_4\tilde{u}_2}{1+\delta_4\tilde{u}_2}[1-(\alpha_1+\delta_1)\tilde{u}_2]\left[(1+\delta_4\tilde{u}_2)^2(1-\alpha_2(\alpha_1+\delta_1))-\delta_2\delta_4\right] \end{aligned}$$

From the Routh–Hurwitz conditions [145, pp. 507–509], $c_0,c_1,c_2,c_3>0$ and $c_1c_2c_3>c_3^2c_0+c_1^2$ if and only if $\mathrm{Re}(\lambda)<0$. Hence we require $c_0,c_1,c_2,c_3>0$ and $c_1c_2c_3>c_3^2c_0+c_1^2$ for $\tilde{u}_2$ to be linearly stable. Note that if

$$\tilde{u}_2>0, \quad 1-(\alpha_1+\delta_1)\tilde{u}_2>0 \quad \text{and} \quad 0<\delta_2\delta_4<(1+\delta_4\tilde{u}_2)^2(1-\alpha_2(\alpha_1+\delta_1)),$$

then $c_0 > 0$. Note that

$$(1+\delta_4\tilde{u}_2)^2(1-\alpha_2(\alpha_1+\delta_1)) < (1+\delta_4\tilde{u}_2)^2(1-\alpha_2\alpha_1) < (1+\delta_4\tilde{u}_2)^2,$$

therefore these conditions will imply that $c_0, c_1, c_2, c_3 > 0$. Since $\tilde{u}_2$ satisfies (3.C.2) we have

$$-\delta_2 = (1+\delta_4\tilde{u}_2)[(1-\alpha_2(\alpha_1+\delta_1))\tilde{u}_2 + \alpha_2 - 1].$$

Hence we can show that

$$(1+\delta_4\tilde{u}_2)^2(1-\alpha_2(\alpha_1+\delta_1))-\delta_2\delta_4 = (1+\delta_4\tilde{u}_2)[(1-\alpha_2(\alpha_1+\delta_1))(2\delta_4\tilde{u}_2+1)+\delta_4(\alpha_2-1)], \tag{3.C.3}$$

and as a result

$$c_0 = \beta_2\beta_3\beta_4\tilde{u}_2\left[1-(\alpha_1+\delta_1)\tilde{u}_2\right]\left[(1-\alpha_2(\alpha_1+\delta_1))(2\delta_4\tilde{u}_2+1)+\delta_4(\alpha_2-1)\right]. \tag{3.C.4}$$

Now consider (3.C.2) and solve for $\tilde{u}_2$ to obtain

$$\begin{aligned}\tilde{u}_{2\pm} &= \frac{-(1-\alpha_2(\alpha_1+\delta_1))-\delta_4(\alpha_2-1)}{2\delta_4(1-\alpha_2(\alpha_1+\delta_1))} \\ &\quad \pm \frac{\sqrt{[1-\alpha_2(\alpha_1+\delta_1)+\delta_4(\alpha_2-1)]^2-4\delta_4(1-\alpha_2(\alpha_1+\delta_1))(\delta_2+\alpha_2-1)}}{2\delta_4(1-\alpha_2(\alpha_1+\delta_1))} \\ &= \frac{-(1-\alpha_2(\alpha_1+\delta_1))-\delta_4(\alpha_2-1)}{2\delta_4(1-\alpha_2(\alpha_1+\delta_1))} \\ &\quad \pm \frac{\sqrt{[1-\alpha_2(\alpha_1+\delta_1)-\delta_4(\alpha_2-1)]^2-4\delta_2\delta_4(1-\alpha_2(\alpha_1+\delta_1))}}{2\delta_4(1-\alpha_2(\alpha_1+\delta_1))},\end{aligned} \tag{3.C.5}$$

and note that $\tilde{u}_{2\pm} \in \mathbb{R}$ if and only if

$$0 < \delta_2 \leq \frac{[1-\alpha_2(\alpha_1+\delta_1)-\delta_4(\alpha_2-1)]^2}{4\delta_4[1-\alpha_2(\alpha_1+\delta_1)]} \quad \text{or} \quad 1-\alpha_2(\alpha_1+\delta_1) < 0.$$

Using (3.C.5), we have

$$\begin{aligned}&(1-\alpha_2(\alpha_1+\delta_1))(2\delta_4\tilde{u}_{2\pm}+1)+\delta_4(\alpha_2-1) \\ &\quad = \pm\sqrt{[(1-\alpha_2(\alpha_1+\delta_1))-\delta_4(\alpha_2-1)]^2-4\delta_2\delta_4(1-\alpha_2(\alpha_1+\delta_1))}\end{aligned} \tag{3.C.6}$$

and therefore when $\tilde{u}_{2\pm} \in \mathbb{R}$ we have that (3.C.6) will be positive for $\tilde{u}_{2+}$ and negative

for $\tilde{u}_{2-}$. We first note from (3.C.6) and (3.C.3) that we require either $\tilde{u}_{2-} < 0$ or $\tilde{u}_{1-} = 1-[\alpha_1+\delta_1]\tilde{u}_{2-} < 0$ so that $c_0 > 0$. Hence we can conclude that there will be no biologically meaningful values of SS4 with $\tilde{u}_{2-}$ that are stable. If $1 - \alpha_2(\alpha_1 + \delta_1) < 0$, we can see that (3.C.3) is negative: noting that (3.C.6) will be positive for $\tilde{u}_{2+}$ in this case then (3.C.3) implies that $1+\delta_4\tilde{u}_{2+} < 0$. Hence we can conclude that $\tilde{u}_{2+} < 0$ and as a result, from (3.C.4) we have that $c_0 < 0$ if $1 - \alpha_2(\alpha_1 + \delta_1) < 0$ for $\tilde{u}_{2+}$. Therefore if $1 - \alpha_2(\alpha_1 + \delta_1) < 0$, then SS4 with $\tilde{u}_{2+}$ is unstable. If $1-\alpha_2(\alpha_1+\delta_1) > 0$ and $\tilde{u}_{2+} < 0$, then we can see from (3.C.6) that (3.C.4) will be negative for $\tilde{u}_{2+}$ and hence SS4 with $\tilde{u}_{2+}$ will be unstable. Therefore we can see that for SS4 with $\tilde{u}_{2+}$ to be stable it is necessary that

$$\tilde{u}_{2+} > 0, \quad 1 - (\alpha_1 + \delta_1)\tilde{u}_{2+} > 0 \quad \text{and} \quad 0 < \delta_2 < \frac{[1 - \alpha_2(\alpha_1 + \delta_1) - \delta_4(\alpha_2 - 1)]^2}{4\delta_4[1 - \alpha_2(\alpha_1 + \delta_1)]}.$$

□

Lemma 3.C.2. *The system of equations given by* (3.3.2) *has the following SS solutions and respective linear stability conditions:*

RS1. $\mathbf{x}^* = (0, 1)$ *is stable if and only if* $\delta_2 > 1$.

RS2. $\mathbf{x}^* = (\hat{u}_{2\pm}, [1 + \delta_4\hat{u}_{2\pm}]^{-1})$ *where* $\hat{u}_{2\pm} = \left[\delta_4 - 1 \pm \sqrt{(1 + \delta_4)^2 - 4\delta_2\delta_4}\right]/2\delta_4$. *The SS corresponding to* $\hat{u}_{2-}$ *is unconditionally unstable and the SS corresponding to* $\hat{u}_{2+}$ *will be stable if and only if*

$$\delta_2 < 1 \quad \textit{or} \quad 1 \leq \delta_2 < \frac{(1 + \delta_4)^2}{4\delta_4} \quad \textit{and} \quad \delta_4 > 1.$$

Proof. We consider the system of equations given by (3.3.2), set the derivatives to zero (i.e. $\mathbf{x}' = \mathbf{0}$) and solve for x_1 and x_2 to obtain the SS solutions. We obtain the solutions

$$(0, 1) \quad \text{and} \quad \left(\hat{u}_2, \frac{1}{1 + \delta_4\hat{u}_2}\right),$$

where $\hat{u}_2$ solves

$$\delta_4\hat{u}_2^2 + (1 - \delta_4)\hat{u}_2 + \delta_2 - 1 = 0.$$

We wish to determine the stability of these solutions by performing a linear stability analysis.

Consider the following vector:

$$\mathbf{G}(\mathbf{x}) = \begin{bmatrix} \beta_2 x_1(1 - x_1 - \delta_2 x_2) \\ \beta_4(1 - x_2 - \delta_4 x_1 x_2) \end{bmatrix}.$$

The Jacobian matrix of $\mathbf{G}$ is then given by

$$\mathbf{G}'_{\mathbf{x}}(\mathbf{x}) = \begin{bmatrix} \beta_2(1 - 2x_1 - \delta_2 x_2) & -\beta_2\delta_2 x_1 \\ -\beta_4\delta_4 x_2 & -\beta_4(1 + \delta_4 x_2) \end{bmatrix}$$

RS1. Now if we consider the SS solution $\mathbf{x}* = (0, 1)$ we have the Jacobian matrix

$$\mathbf{G}'_{\mathbf{x}}(0, 1) = \begin{bmatrix} \beta_2(1 - \delta_2) & 0 \\ -\beta_4\delta_4 & -\beta_4 \end{bmatrix}$$

with eigenvalues $\lambda = \beta_2(1 - \delta_2), -\beta_4$ which we can see implies $\mathbf{x}^* = (0, 1)$ will be stable if and only if $\delta_2 > 1$.

RS2. We consider the SS solution $\mathbf{x}^* = (\hat{u}_2, [1 + \delta_4\hat{u}_2]^{-1})$ noting from $\mathbf{G}(\mathbf{x}) = \mathbf{0}$ we have $1 - x_1 - \delta_2 x_2 = 0$. Hence we have the Jacobian matrix

$$\mathbf{G}'_{\mathbf{x}}(\mathbf{x}^*) = \begin{bmatrix} -\beta_2\hat{u}_2 & -\beta_2\delta_2\hat{u}_2 \\ -\beta_4\delta_4(1 + \delta_4\hat{u}_2)^{-1} & -\beta_4(1 + \delta_4\hat{u}_2) \end{bmatrix}$$

with characteristic equation given by

$$\lambda^2 + [\beta_2\hat{u}_2 + \beta_4(1 + \delta_4\hat{u}_2)]\lambda + \frac{\beta_2\beta_4\hat{u}_2}{1 + \delta_4\hat{u}_2}[(1 + \delta_4\hat{u}_2)^2 - \delta_4\delta_2] = 0.$$

We note that this is the same quadratic obtained for SS3. Following the proof considered in Lemma 3.C.1 for SS3 we require

$$c_1 = \beta_2\hat{u}_2 + \beta_4(1 + \delta_4\hat{u}_2) > 0 \quad \text{and} \quad c_0 = \frac{\beta_2\beta_4\hat{u}_2}{1 + \delta_4\hat{u}_2}[(1 + \delta_4\hat{u}_2)^2 - \delta_4\delta_2] > 0.$$

In the proof for Lemma 3.C.1 for SS3 we saw that in the case of $\hat{u}_{2-}$ that $c_0 \leq 0$ for all parameter values, hence RS2 with $\hat{u}_{2-}$ is unconditionally unstable. Moreover it was required that $\delta_2 < (1 + \delta_4)^2/4\delta_4$ for $c_0 > 0$ in the $\hat{u}_{2+}$ case. Note that if $\hat{u}_{2+} > 0$ then it follows

that $c_1 > 0$. Examining the solution for $\hat{u}_{2+}$ as in Lemma 3.C.1 we see that for $\hat{u}_{2+} \in \mathbb{R}$ we require $\delta_2 \leq (1+\delta_4)^2/4\delta_4$. Then we see that for $\hat{u}_{2+} > 0$ and $\delta_2 < (1+\delta_4)^2/4\delta_4$ (i.e. $(\hat{u}_{2+}, [1+\delta_4\hat{u}_{2+}]^{-1})$ is a stable SS) we require

$$\delta_2 < 1 \quad \text{or} \quad 1 \leq \delta_2 < \frac{(1+\delta_4)^2}{4\delta_4} \quad \text{and} \quad \delta_4 > 1.$$

□

Chapter 4

Acid-mediated tumour invasion with chemotherapy intervention: spatially heterogeneous populations

4.1 Introduction

This chapter seeks to extend the model proposed in Chapter 3, that considers the acid-mediation hypothesis with the added interaction of a tumour treatment protocol, to a spatially heterogeneous setting. The model considered in Chapter 3, which examined the acid-mediation hypothesis with chemotherapy by the use of a system of ODEs, is primarily based on the models proposed in [71, 76] combined with the model given in [30]. We wish to consider a spatially heterogeneous model that extends this simpler spatially homogeneous model due to two key reasons, the first of which being the unrealistic nature of the assumption underpinning a spatially homogeneous model. The use of a spatially homogeneous model assumes that the populations considered are well mixed and hence have no significant spatial variations. However we are proposing to consider tumour and normal tissue populations and, in a reductionist view, tumours form as insular masses surrounded by normal cells [89, 90]. Hence the assumption that these populations are well mixed is not realistic. The second important consideration in using a spatially heterogeneous model is the extra insight that can be gained about the key processes governing the dynamic behaviour of the system, an example of this being the acid-mediation hypothesis. Should the model considered in [71] have been modelled in a spatially homogeneous setting with no influence of spatial variances, then due to the governing dynamics of the production of H^+ ions, one would determine very similar

behaviour between a model that considers acid-mediation and one that considers purely population competition. One could conclude that the additional tumour aggressiveness associated with the acid concentration as being attributed to the tumour population having more dominant population competition dynamics. However in the spatio-temporal model as considered by McGillen et al. [140] this confusion could not so easily be made with behaviours such as the development of an interstitial gap only being possible with inclusion of the acid-mediation hypothesis. Whilst we still acknowledge that much insight can be gained from the spatially homogeneous model, much of which can be used to predict behaviour in a spatially heterogenous setting, we feel that to truly determine the behaviour of the system and the important components that govern it, the model must be considered in a spatio-temporal setting.

Similarly to Chapter 3, this chapter seeks to determine the conditions in our model when the treatment is effective/ineffective and whether the presence of normal cells can alter the perceived effectiveness of chemotherapy. Moreover, an aim of this chapter is to determine how treatment affects the strength of the acid-mediated invasion and if a treatment can slow, stop or reverse the invasion of a tumour.

This chapter is organised as follows. In Section 4.2 we discuss the formulation of our model and provide details of a corresponding non-dimensionalisation. In Section 4.3 we examine the model numerically and present some analytical and heuristic analysis of the results. Section 4.4 presents the arguments for the determination of asymptotic approximations to the solutions of a special case of the model. A discussion of results and some concluding remarks are presented in Section 4.5.

4.2 Model formulation

Here, the basic assumptions used to develop the model in Chapter 3 are recalled along with additional assumptions required due to the spatially heterogeneous populations.

(i) Both normal and tumour cells are governed by logistic growth in the absence of any kind of intervention [48, 49, 71];

(ii) Normal cells and tumour cells undergo cell diffusion. Furthermore, the diffusion coefficients may be dependent on the other respective cell density [71];

(iii) There is a population competition relationship between the normal and tumour tissues [140];

(iv) The tumour tissue produces H^+ ions as a result of aerobic glycolysis [71, 140] at a rate proportional to the tumour cell density;

(v) The normal tissue interacts with the excess H^+ ions, leading to a death rate proportional to the H^+ ion concentration [71, 140];

(vi) Excess H^+ ions diffuse chemically with a constant diffusion rate and are produced at a rate proportional to the tumour cell density. Moreover, an uptake term is included to take account of mechanisms for increasing pH [71];

(vii) The chemotherapy drug is infused equally across the system at a rate given by a function of time. A term is included for removal of drug from the system by metabolic processes [30, 49] and the drug is assumed to diffuse chemically with a constant rate of diffusion;

(viii) The tumour tissue interacts with the chemotherapy drug leading to destruction of tumour tissue at a rate proportional to the concentration of drug [30, 49];

(ix) The chemotherapy drug concentration is decreased as a result of interaction with the tumour tissue [30].

Let the populations at time s (in s) and position $\mathbf{y}$ (in cm) be denoted by:

- $N_1(\mathbf{y}, s)$, normal cell density (in $\mathrm{cells\,cm^{-3}}$);
- $N_2(\mathbf{y}, s)$, tumour cell density (in $\mathrm{cells\,cm^{-3}}$);
- $L(\mathbf{y}, s)$, excess H^+ ion concentration (in M);
- $C(\mathbf{y}, s)$, chemotherapy drug concentration (in M).

Consider the following model

$$\frac{\partial N_1}{\partial s} = \underbrace{\nabla \cdot [D_1(N_2)\nabla N_1]}_{\text{cell movement}} + \underbrace{r_1 N_1 \left(1 - \frac{N_1}{K_1} - \alpha_1 \frac{N_2}{K_2}\right)}_{\text{logistic growth with cellular competition}} - \underbrace{d_1 L N_1}_{\substack{\text{normal cell death by} \\ \text{acid}}}, \quad (4.2.1)$$

$$\frac{\partial N_2}{\partial s} = \underbrace{\nabla \cdot [D_2(N_1)\nabla N_2]}_{\text{cell movement}} + \underbrace{r_2 N_2 \left(1 - \frac{N_2}{K_2} - \alpha_2 \frac{N_1}{K_1}\right)}_{\text{logistic growth with cellular competition}} - \underbrace{d_2 C N_2}_{\substack{\text{tumour death by} \\ \text{drug}}}, \quad (4.2.2)$$

$$\frac{\partial L}{\partial s} = \underbrace{D_3 \nabla^2 L}_{\text{acid diffusion}} + \underbrace{r_3 N_2}_{\text{acid production}} - \underbrace{m_3 L}_{\text{acid uptake}}, \quad (4.2.3)$$

$$\frac{\partial C}{\partial s} = \underbrace{D_4 \nabla^2 C}_{\text{drug diffusion}} + \underbrace{r_I(s)}_{\text{drug infusion}} - \underbrace{m_4 C}_{\text{drug decomposition}} - \underbrace{d_4 N_2 C}_{\substack{\text{drug-tumour} \\ \text{interaction removal}}}. \quad (4.2.4)$$

We have used the convention of the subscripts for each parameter corresponding to the relevant equation: r represents growth rate; K represents carrying capacity; α represents population competition strength; d represents rate of decrease due to interaction; D is diffusion coefficient; m represents decrease through system mechanisms. A question then arises: What do we choose for $D_1(N_2)$, $D_2(N_1)$ and $r_I(s)$? In the models considered in [71, 140] and Chapter 2 the following diffusion coefficients were used

$$D_1(N_2) = 0, \quad D_2(N_1) = D\left(1 - \frac{N_1}{K_1}\right); \quad D > 0.$$

These were chosen since it was assumed that the normal cells were well regulated and hence the motility would be negligible. Furthermore, it was assumed that the presence of normal cells inhibited the motility of the tumour cells, hence these terms achieved this effect. It was seen in [63, 140] that for a sufficiently aggressive tumour the coefficient $D_2(N_1)$ could be approximated by the constant D. In the models examined in [70, 76], that consider tumour-host competition interactions, constant diffusion coefficients were used (i.e. with an abuse of notation we let $D_1(N_2) = D_1$ and $D_2(N_1) = D_2$). Whilst this has not proven to be the most effective mechanism of modelling cellular movement, we note it is still unclear what governs cellular motility and as such a complete model for cellular motion remains elusive. With this in mind and noting that cellular movement is small in comparison to other dynamics associated with this model, we will consider constant diffusion coefficients

$$D_1(N_2) = D_1 \quad \text{and} \quad D_2(N_1) = D_2$$

in order to approximate and account for any cellular movement that is present. We also note that to model cellular motion effectively the inclusion of chemical signalling to cause chemotaxis and interactions with the extracellular matrix would need to be considered, which would further complicate the model and take us beyond the aims of our analysis. The inclusion of a more robust model for cellular movement represents a potential extension to this model, however the currently proposed system will still be able to provide insight into the dynamics of these interacting populations.

As in Chapter 3, the most natural choice of functions to use for r_I are ones that are periodic with respect to time as these correspond to treatments that occur in repeated cycles. Alternatively, to enable a higher level of analysis, r_I can be chosen to be constant. Potential infusion functions and corresponding treatment techniques include periodic uses of a weighted Dirac delta function to represent treatment with pills:

$$r_I(s) = r_4 \sum_{n=0}^{N-1} \delta(s - nP), \tag{4.2.5}$$

where P is the length of the treatment cycle and N is the number of treatment cycles. Periodic uses of a weighted boxcar function to represent intravenous infusion of cytotoxic drug occurring in repeated cycles:

$$r_I(s) = r_4 \sum_{n=0}^{N-1} [H(s - nP) - H(s - nP - s_0)], \tag{4.2.6}$$

where P is the length of the treatment cycle, s_0 is the infusion time, N is the number of treatment cycles and $H(s)$ is the Heaviside function.

For simplicity we will consider the system given by (4.2.1)–(4.2.4) in only one spatial dimension, i.e. $\mathbf{y} = y \in \mathbb{R}$. Considering the function $r_I(s)$ with period P we let

$$\bar{r} = \frac{1}{P} \int_0^P r_I(s)\,\mathrm{d}s$$

and then $\bar{r}$ is used to non-dimensionalise the equations given by (4.2.1)–(4.2.4). Make the following substitutions

$$u_1 = \frac{N_1}{K_1}, \quad u_2 = \frac{N_2}{K_2}, \quad u_3 = \frac{m_3}{r_3 K_2} L, \quad u_4 = \frac{m_4}{\bar{r}} C, \quad x = \sqrt{\frac{r_1}{D_3}}\, y, \quad t = r_1 s,$$

with

$$\beta_2 = \frac{r_2}{r_1}, \quad \beta_3 = \frac{m_3}{r_1}, \quad \beta_4 = \frac{m_4}{r_1}, \quad \eta_1 = \frac{D_1}{D_3}, \quad \eta_2 = \frac{D_2}{D_3},$$
$$\eta_4 = \frac{D_4}{D_3}, \quad \delta_1 = \frac{r_3 K_2 d_1}{r_1 m_3}, \quad \delta_2 = \frac{d_2 \bar{r}}{r_2 m_4}, \quad \delta_4 = \frac{d_4 K_2}{m_4}$$

and

$$i(t) = \frac{r_I(t/r_1)}{\bar{r}}, \quad \rho = r_1 P.$$

We then obtain the following system of non-dimensionalised equations

$$\frac{\partial u_1}{\partial t} = \eta_1 \frac{\partial^2 u_1}{\partial x^2} + u_1(1 - u_1 - \alpha_1 u_2 - \delta_1 u_3), \tag{4.2.7}$$
$$\frac{\partial u_2}{\partial t} = \eta_2 \frac{\partial^2 u_2}{\partial x^2} + \beta_2 u_2(1 - u_2 - \alpha_2 u_1 - \delta_2 u_4), \tag{4.2.8}$$
$$\frac{\partial u_3}{\partial t} = \frac{\partial^2 u_3}{\partial x^2} + \beta_3(u_2 - u_3), \tag{4.2.9}$$
$$\frac{\partial u_4}{\partial t} = \eta_4 \frac{\partial^2 u_4}{\partial x^2} + \beta_4[i(t) - u_4 - \delta_4 u_4 u_2]. \tag{4.2.10}$$

We point out that

$$\bar{i} = \frac{1}{\rho} \int_0^\rho i(t)\, \mathrm{d}t = 1$$

and thus we now have that the average rate of infusion over each treatment cycle has been normalised to be equal to one. As is noted in Chapter 3, if different infusion functions are used this non-dimensionalisation enables us to effectively compare these models when the same non-dimensionalised parameter values are used as this assumes that the same amount of drug is infused over each treatment cycle.

Note that the parameters η_1 and η_2 are typically small, i.e. $0 < \eta_1, \eta_2 \ll 1$. This is the case as $\eta_1 = D_1/D_3$ and $\eta_2 = D_2/D_3$ and since we expect chemical diffusion to be much faster than the cellular motility, i.e. $D_1, D_2 \ll D_3$, the assumption follows.

We remark that under this non-dimensionalisation the functions (4.2.5) and (4.2.6) become

$$i(t) = \rho \sum_{n=0}^{N-1} \delta(t - n\rho)$$

and

$$i(t) = \frac{\rho}{\tau} \sum_{n=0}^{N-1} [H(t - n\rho) - H(t - n\rho - \tau)]; \quad \tau = r_1 s_0, \tag{4.2.11}$$

respectively.

We have presented a summary of potential non-dimensional parameter values/range of values and included an interpretation of their meaning in Table 4.2 found in Appendix 4.B. Note the primary parameter that can be controlled is δ_2 since an increase in the amount of drug infused will cause δ_2 to increase.

In order to examine the model (4.2.7)–(4.2.10) we require the results of the analysis of the corresponding spatially homogeneous model that was considered in Chapter 3. As such, some important results about the spatially homogeneous model will be summarised here. Consider the homogeneous system

$$\frac{\mathrm{d}\mathbf{u}}{\mathrm{d}t} = \frac{\mathrm{d}}{\mathrm{d}t}\begin{bmatrix} u_1 \\ u_2 \\ u_3 \\ u_4 \end{bmatrix} = \begin{bmatrix} u_1(1-u_1-\alpha_1 u_2-\delta_1 u_3) \\ \beta_2 u_2(1-u_2-\alpha_2 u_1-\delta_2 u_4) \\ \beta_3(u_2-u_3) \\ \beta_4[i(t)-u_4-\delta_4 u_4 u_2] \end{bmatrix} =: \mathbf{F}(t,\mathbf{u}). \tag{4.2.12}$$

If constant infusion is used, that is, the function $i \equiv 1$, then (4.2.12) has the following SS solutions:

SS1. $\mathbf{u}^* = (0,0,0,1)$;

SS2. $\mathbf{u}^* = (1,0,0,1)$;

SS3. $\mathbf{u}^* = (0,\hat{u}_2,\hat{u}_2,[1+\delta_4\hat{u}_2]^{-1})$, where

$$\hat{u}_2 = \frac{1-\delta_4 \pm \sqrt{(1+\delta)^2-4\delta_2\delta_4}}{2\delta_4}.$$

SS4. $\mathbf{u}^* = (1-(\alpha_1+\delta_1)\tilde{u}_2,\tilde{u}_2,\tilde{u}_2,[1+\delta_4\tilde{u}_2]^{-1})$, where

$$\tilde{u}_2 = \frac{-(1-\alpha_2(\alpha_1+\delta_1))-\delta_4(\alpha_2-1)}{2\delta_4(1-\alpha_2(\alpha_1+\delta_1))} \pm \frac{\sqrt{[1-\alpha_2(\alpha_1+\delta_1)-\delta_4(\alpha_2-1)]^2-4\delta_2\delta_4(1-\alpha_2(\alpha_1+\delta_1))}}{2\delta_4(1-\alpha_2(\alpha_1+\delta_1))}.$$

From this point onwards, we let $\hat{u}_2$ be given by the "plus" case only, as the "minus" case was shown in Chapter 3 to be unconditionally unstable. If a continuous positive periodic infusion function is used, that is, $i(t) = i(t+\rho) \geq 0$ for all $t \in [0,\infty)$, then (4.2.12) has periodic solutions (i.e. $\mathbf{u}(t) = \mathbf{u}(t+\rho)$ for all $t \in [0,\infty)$) of the form:

PS1. $(0,0,0,u_4(t))$;

PS2. $(1,0,0,u_4(t))$;

PS3. $(0, u_2(t), u_3(t), u_4(t))$;

PS4. $(u_1(t), u_2(t), u_3(t), u_4(t))$.

Here, $u_j(t+\rho) = u_j(t) > 0$ for all $t \geq 0$ and $j = 1, 2, 3, 4$. We will refer to the results of Chapter 3 throughout this chapter when more specific results concerning system (4.2.12) are required.

4.3 Numerical simulations

Performing numerical simulations of (4.2.7)–(4.2.10) can give insights into the expected dynamics to be obtained from the system. We consider the system with both constant infusion (i.e. $i(t) = 1$) and a periodic infusion function (i.e. $i(t) = i(t+\rho)$). We perform these simulations using a forward centred finite difference scheme, as is explained in [4]. Since we do not have defined boundary conditions (BCs) we will choose to have homogeneous Neumann BCs at the values $x = -2$ and $x = 2$. The initial conditions are given by step functions as shown in Figure 4.1. The initial conditions show that the tumour population is close to carrying capacity and then decreases to zero at the point $x = 0$, whereas the normal tissue is initially present at a low density in the tumour region and then increases to carrying capacity in the tumour vacant region. The acid and chemotherapy drug concentrations are initially set to zero. Note that these initial conditions will be used for the simulations of (4.2.7)–(4.2.10) for both constant and periodic infusion.

4.3.1 Constant infusion

The case of constant infusion corresponds to using the non-dimensional infusion function $i(t) = 1$ in the system of equations given by (4.2.7)–(4.2.10). In this case the dynamics associated to the spatially homogeneous version of the model with constant infusion considered in Chapter 3 can be used to predict potential behaviour of (4.2.7)–(4.2.10) given knowledge of the initial conditions. For example, should we apply the model (4.2.7)–(4.2.10) with $\delta_2 > 1$ and $\delta_4 < 1$, or $\delta_2 > (1 + \delta_4)^2/4\delta_4$, then the analysis of the spatially homogeneous model predicts that the tumour will be eradicated from the system provided the treatment is applied for a sufficiently large period of time.

It is expected that for certain parameters TW solutions will exist: in the simplest case, a TW solution is a function of the form $u(x, t) = \varphi(x - \theta t)$. These waves have a fixed profile that propagate along the real line with constant speed θ, where the sign of θ determines the direction the wave travels. Moreover, TWs connect SSs of the corresponding spatially homogeneous system.

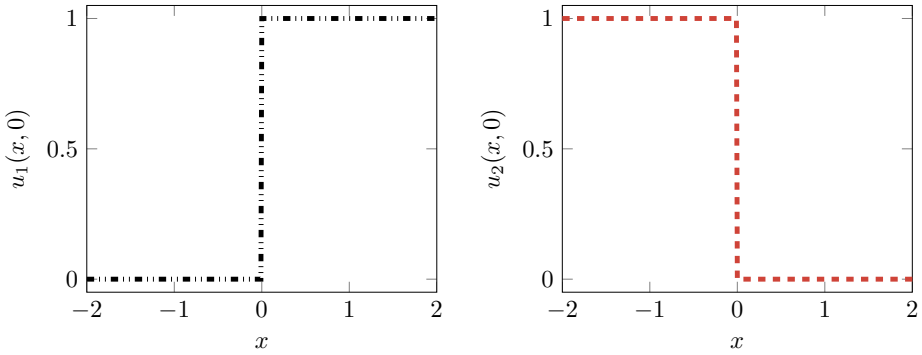

(a) Initial condition for u_1

(b) Initial condition for u_2

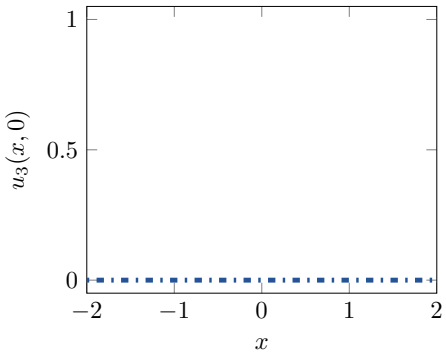

(c) Initial condition for u_3

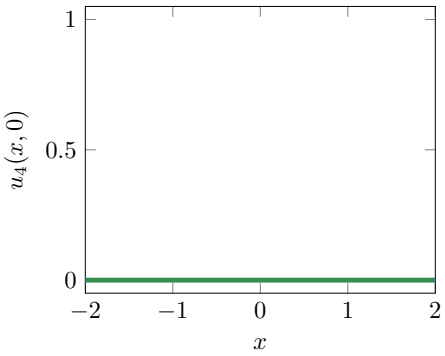

(d) Initial condition for u_4

Figure 4.1: Initial conditions used for the numerical solutions

As such, knowledge of the properties of these SSs allows us to predict the direction in which the respective waves will travel and enables potential estimation and bounds on the speed at which these waves can propagate. Travelling waves for the system (4.2.7)–(4.2.10) with $i(t) = 1$ can be represented mathematically as solutions $(u_1, u_2, u_3, u_4)(x,t) = (\varphi_1, \varphi_2, \varphi_3, \varphi_4)(z)$, where $z = x - \theta t$; the functions $\varphi_1, \varphi_2, \varphi_3$ and φ_4 satisfy

$$\eta_1\varphi_1'' + \theta\varphi_1' + \varphi_1(1 - \varphi_1 - \alpha_1\varphi_2 - \delta_1\varphi_3) = 0, \tag{4.3.1}$$

$$\eta_2\varphi_2'' + \theta\varphi_2' + \beta_2\varphi_2(1 - \varphi_2 - \alpha_2\varphi_1 - \delta_2\varphi_4) = 0, \tag{4.3.2}$$

$$\varphi_3'' + \theta\varphi_3' + \beta_3(\varphi_2 - \varphi_3) = 0, \tag{4.3.3}$$

$$\eta_4\varphi_4'' + \theta\varphi_4' + \beta_4(1 - \varphi_4 - \delta_4\varphi_2\varphi_4) = 0, \tag{4.3.4}$$

where $(\,)'$ denotes differentiation with respect to z and the boundary conditions at $z = \pm\infty$ are distinct and given by the steady-states SS1–SS4.

Travelling wave solutions are expected since they are commonly observed solutions for reaction-diffusion systems. Furthermore, system (4.2.1)–(4.2.4) is based on the model considered in [140], which exhibits TW solutions. Due to the form of the initial conditions, should TW solutions occur

then it will be apparent that the model is not sensitive to initial conditions.

Tumour clearance

From the results of Chapter 3 it can be concluded that it is possible for the tumour to be removed from the system by the reaction dynamics alone. That is, provided a sufficiently strong treatment protocol is used, then only the tumour free SS (i.e. SS2) is stable and furthermore, the normal-tissue free SS (i.e. SS3) will not be biologically meaningful, that is, if $1 < \delta_2 \leq (1+\delta_4)^2/4\delta_4$ and $\delta_4 < 1$, or if $\delta_2 > (1+\delta_4)^2/4\delta_4$. Hence the tumour population will be removed from the system purely as a result of treatment. See Figure 4.2 for an example of the solution obtained in the case $\delta_2 > (1+\delta_4)^2/4\delta_4$. As predicted, given a sufficiently large treatment period, we have that the tumour population is removed from the system.

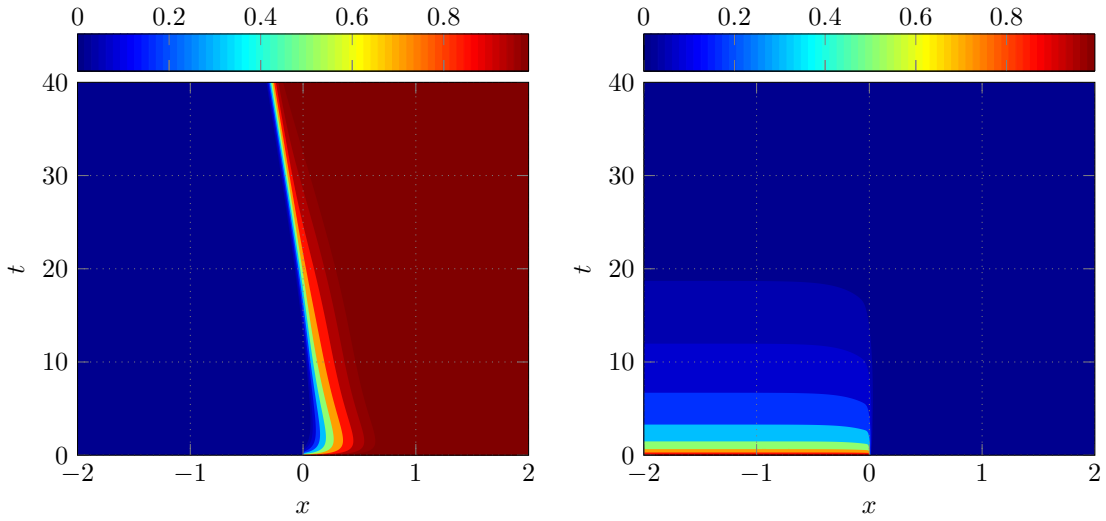

(a) Contour plot of u_1 for $T = 40$

(b) Contour plot of u_2 for $T = 40$

Figure 4.2: Contour plots u_1 and u_2 from simulations of (4.2.7)–(4.2.10) with parameters $\alpha_1 = 1$, $\alpha_2 = 0.5$, $\beta_2 = 1$, $\beta_3 = 70$, $\beta_4 = 20$, $\delta_1 = 12.5$, $\delta_2 = 1.1$, $\delta_4 = 0.6$

Note that given certain parameter conditions when SS2 is stable it is possible to witness a "splitting" behaviour from the solutions of (4.2.7)–(4.2.10). By splitting behaviour it is meant that two sets of fronts appear to emerge that travel at different speeds, respectively, in the same direction. In this case we see that the fronts associated to the tumour, acid and drug concentration (i.e. u_2, u_3 and u_4, respectively) are travelling at a faster speed away from the normal tissue (u_1) such that the waves appear to split from one another. This behaviour can be observed when SS3 exists and is unstable, or when SS2 and SS3 are both stable, as is the case displayed in Figure 4.3.

We now wish to show by a heuristic argument that we at least require the parameter conditions

$1 \leq \delta_2 < (1+\delta_4)^2/4\delta_4$ and $\delta_4 > 1$ and the speed of the receding tumour front to be greater than $\theta_r = 2\sqrt{\eta_1}$ for the splitting behaviour to occur. Intuitively, the long term behaviour of this model when splitting behaviour occurs is that the tumour population and normal tissue population will no longer interact with each other directly since the population of one will be small (i.e. $\simeq 0$) in any region predominantly occupied by the other population. As such we should have that (4.2.7)–(4.2.10) will reduce to a situation in which the normal cells are governed by the Fisher-KPP equation and the model originally proposed by Byrne [30] with the inclusion of diffusion terms such that we have the normal tissue decouples from the tumour and acid equations. Assuming that β_3 is sufficiently large to enable efficient removal of excess acid from the body such that acid only appears in minute concentrations in the regions occupied primarily by normal tissue, this would lead to the system being governed by the equations.

$$\frac{\partial u_1}{\partial t} = \eta_1 \frac{\partial^2 u_1}{\partial x^2} + u_1(1-u_1), \tag{4.3.5}$$

$$\frac{\partial u_2}{\partial t} = \eta_2 \frac{\partial^2 u_2}{\partial x^2} + \beta_2 u_2(1-u_2-\delta_2 u_4), \tag{4.3.6}$$

$$\frac{\partial u_3}{\partial t} = \frac{\partial^2 u_3}{\partial x^2} + \beta_3(u_2-u_3), \tag{4.3.7}$$

$$\frac{\partial u_4}{\partial t} = \eta_4 \frac{\partial^2 u_4}{\partial x^2} + \beta_4(1-u_4-\delta_4 u_4 u_2). \tag{4.3.8}$$

We note that in this system the presence of the acid has no effect on the evolution of the tumour or normal tissue. As such we can ignore (4.3.7) which results in considering only (4.3.5), (4.3.6) and (4.3.8) noting that we have (4.3.5) decoupled from (4.3.6) and (4.3.8). Note (4.3.5) is simply the Fisher-KPP equation which from [66, 112] has a known TW solution of the form $u_1(x,t) = \varphi_1(z+\theta t)$, where $\theta \geq 2\sqrt{\eta_1}$, connecting the points $\varphi_1(-\infty) = 0$ and $\varphi_1(\infty) = 1$. Hence we can see that this equation suggests that the normal population will advance into the tumour region with a minimum speed of $\theta = 2\sqrt{\eta_1}$. This also suggests that in order to guarantee that the splitting behaviour is obtained, the speed of the retracting tumour front (θ_r) needs to at least be greater than the minimal speed of the normal tissue front (i.e. $\theta_r > 2\sqrt{\eta_1}$).

When considering the system given by (4.3.6) and (4.3.8), note that if $\delta_2 > 1$ and $\delta_4 < 1$, or if $\delta_2 > (1+\delta_4)^2/4\delta_4$ then there exists only one biologically meaningful SS for this system: namely $(u_2^*, u_4^*) = (0,1)$, hence we cannot have a front form that connects two distinct SSs of the system. As such, from Chapter 3, we require that $\delta_4 > 1$ and $1 \leq \delta_2 < (1+\delta_4)^2/4\delta_4$, or $\delta_2 < 1$ in order to have multiple SSs for the system, thus permitting fronts to form. Should we have that $\delta_2 < 1$

then we will have that $(u_2^*, u_4^*) = (0, 1)$ will be unstable and the SS $(u_2^*, u_4^*) = (\hat{u}_2, [1 + \delta_4 \hat{u}_2]^{-1})$ will be stable. Therefore this will imply that a wave will propagate in which the tumour free state will be invaded by the tumour, i.e. $(u_2, u_4)(x, t) = (\varphi_2, \varphi_4)(z)$ where $z = x - \theta t$, $\theta > 0$, $(\varphi_2, \varphi_4)(-\infty) = (\hat{u}_2, [1 + \delta_2 \hat{u}_2]^{-1})$ and $(\varphi_2, \varphi_4)(\infty) = (0, 1)$.

Now since we are considering (4.3.6) and (4.3.8) with the splitting behaviour in mind we require that our wave is one in which the tumour free state replaces the state with non-zero tumour population. Hence we require that $\delta_2 > 1$ such that the tumour free state is stable. Therefore it would appear that the splitting behaviour should only occur in conditions under which the system (4.3.6) and (4.3.8) is bistable as when $(\hat{u}_2, [1+\delta_4 \hat{u}_2]^{-1})$ is unstable it is biologically unmeaningful. When considering the implications of this on the full system given by (4.2.7)–(4.2.10), we have that it can be bistable or have a stable tumour-tissue free state connecting the unstable normal-tissue free state.

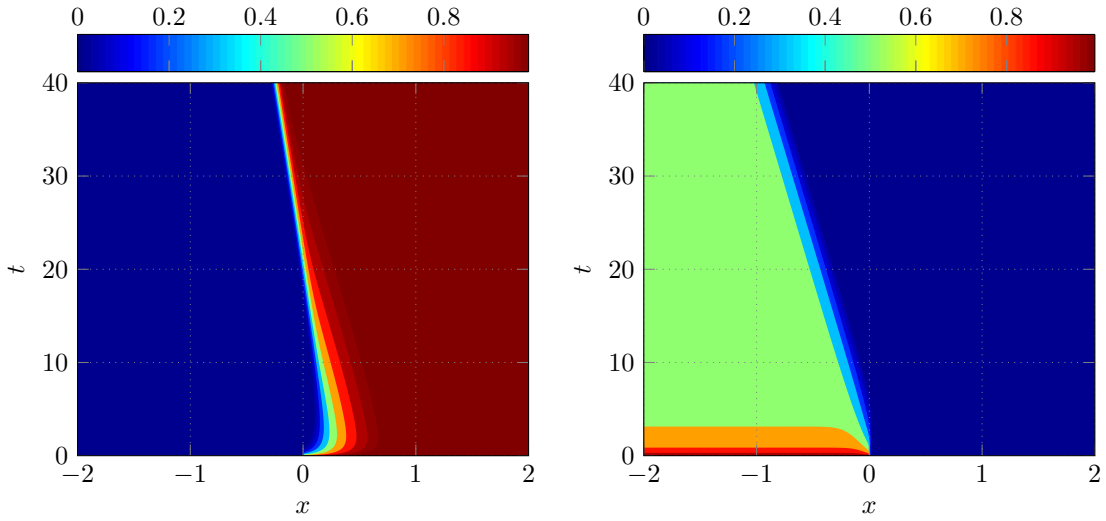

(a) Contour plot of u_1 for $T = 40$

(b) Contour plot of u_2 for $T = 40$

Figure 4.3: Contour plots u_1 and u_2 from simulations of (4.2.7)–(4.2.10) with parameters $\alpha_1 = 1$, $\alpha_2 = 0.5$, $\beta_2 = 1$, $\beta_3 = 70$, $\beta_4 = 20$, $\delta_1 = 12.5$, $\delta_2 = 3$, $\delta_4 = 11$

Note that in addition to the complete tumour clearance and splitting wave behaviour, traditional TW solutions in which the tumour recedes are also observed. We see from Figure 4.4 that a TW forms in which the normal tissue invades the tumour tissue. Note that this typically occurs at a slow rate and hence the assessment may be made that the treatment is not sufficiently effective. As such, an alternative treatment method or stronger dose may be used to try remove the tumour more effectively. Insights for potential parameter values for which this can occur will be obtained in the asymptotic analysis to be conducted in Section 4.4.2.

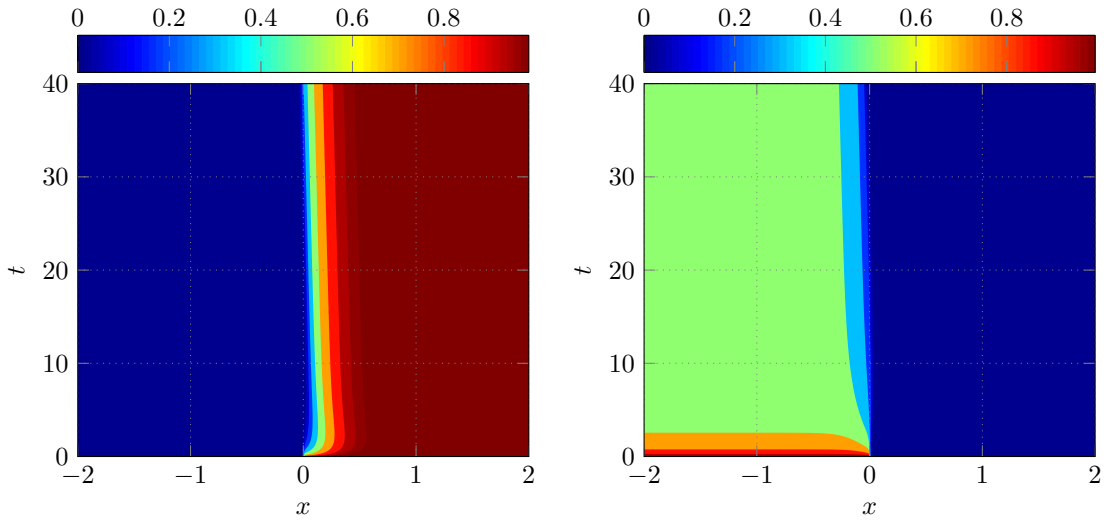

(a) Contour plot of u_1 for $T = 40$

(b) Contour plot of u_2 for $T = 40$

Figure 4.4: Contour plots u_1 and u_2 from simulations of (4.2.7)–(4.2.10) with parameters $\alpha_1 = 1$, $\alpha_2 = 3$, $\beta_2 = 1$, $\beta_3 = 70$, $\beta_4 = 20$, $\delta_1 = 5$, $\delta_2 = 1.25$, $\delta_4 = 3.5$

Tumour invasion

Figure 4.5 displays a TW solution where SS3 is invading SS2. We can identify the TW by the constant front width and constant rate of progression of the solutions along the x-axis. This particular wave can occur under two sets of conditions: when the system is bistable with SS2 and SS3 both being stable; or when SS3 is stable and SS2 is unstable. In the latter case we know from Chapter 3 that we must have $\alpha_2 + \delta_2 < 1$. Furthermore, in this case we are able to obtain the class of speeds under which these waves can form. Since we have that a TW will propagate we then make the substitution $(u_1, u_2, u_3, u_4)(x, t) = (\varphi_1, \varphi_2, \varphi_3, \varphi_4)(z)$ where $z = x - \theta t$, $\theta > 0$, $(\varphi_1, \varphi_2, \varphi_3, \varphi_4)(-\infty) = (0, \hat{u}_2, \hat{u}_2, [1 + \delta_4 \hat{u}_2]^{-1})$ and $(\varphi_1, \varphi_2, \varphi_3, \varphi_4)(\infty) = (1, 0, 0, 1)$. Then linearising about the leading edge of the wave (i.e. $(\varphi_1, \varphi_2, \varphi_3, \varphi_4) = (1, 0, 0, 1)$) as in [146] we decouple the equation for the tumour from the system to give

$$\eta_2 \varphi_2'' + \theta \varphi_2' + \beta_2(1 - \alpha_2 - \delta_2)\varphi_2 = 0,$$

which has solutions

$$\varphi_2(z) \propto \exp\left(\frac{-\theta \pm \sqrt{\theta^2 - 4\beta_2\eta_2(1 - \alpha_2 - \delta_2)}}{2\eta_2} z\right).$$

Since we require that $\varphi_2(z) \to 0$ as $z \to \infty$ with $\varphi_2(z) > 0$ then we cannot have solutions oscillate, otherwise $\varphi_2(z) < 0$ for some z. Hence in order to have a TW exist we require that

the wave speed satisfies $\theta \geq 2\sqrt{\beta_2\eta_2(1-\alpha_2-\delta_2)}$. Therefore we can see that when the tumour free state is unstable, the tumour will invade with a speed of invasion necessarily greater than the minimal value $\theta_m = 2\sqrt{\beta_2\eta_2(1-\alpha_2-\delta_2)}$. It will be seen in Section 4.4 from an estimate for the minimal speed, obtained from an asymptotic analysis, that the minimal speed obtained from this linearisation technique does not necessarily reflect the speed of invasion of the solution to the system. However the minimal speed θ_m does still provide a lower bound on the speeds for which this type of invasive wave will exist. Furthermore, it will be seen that the estimates obtained for the speed from the asymptotic analysis are greater than θ_m as required.

Considering the situation in which we have invasion in the bistable system is more complicated and does not lend itself to the same techniques for estimating the speed of the wave as in the case of a stable state advancing into an unstable state. As has already been noted, the bistable system admits varying behaviour with splitting wave fronts, receding waves and invading waves all being observed. The bistable case will be further analysed in Section 4.4 when (4.3.1)–(4.3.4) is analysed using asymptotic techniques.

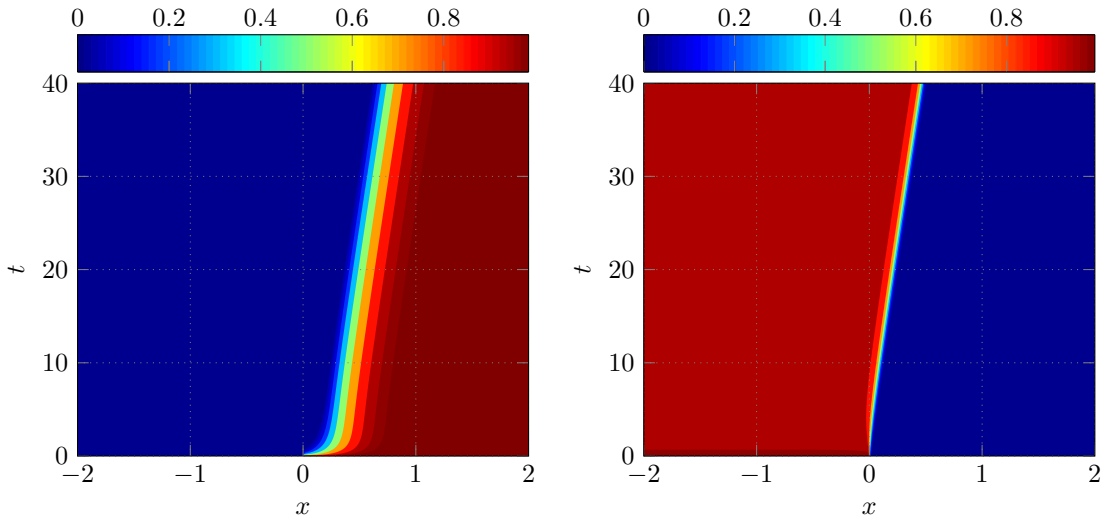

(a) Contour plot of u_1 for $T = 40$

(b) Contour plot of u_2 for $T = 40$

Figure 4.5: Contour plots u_1 and u_2 from simulations of (4.2.7)–(4.2.10) with parameters $\alpha_1 = 1$, $\alpha_2 = 0.5$, $\beta_2 = 1$, $\beta_3 = 70$, $\beta_4 = 20$, $\delta_1 = 12.5$, $\delta_2 = 0.1$, $\delta_4 = 1$

Co-existence is the behaviour in which the tumour and normal tissue populations occupy the same space in a stable equilibrium, an example of this behaviour can been seen in Figure 4.6. Gatenby and Gawlinski [71] categorised this state as benign tumour growth. This behaviour still allows the tumour to invade, in a sense, as the tumour will continue to increase its total cell population and the front will move further out from its initial position. This behaviour will always occur

in the co-existence state as this requires the tumour free state to be unstable. Due to this fact we find that the co-existence state will invade into the tumour free state with speed necessarily greater than or equal to $\theta_m = 2\sqrt{\beta_2\eta_2(1-\alpha_2-\delta_2)}$ by the same argument that we considered for the invasive tumour state considered previously. However we note that for the co-existence behaviour to be observed we require that the normal-tissue free state also be unstable, hence this does not represent an aggressively invading tumour and would not necessarily represent a state in which strong treatment would be required to remove this tumour.

Whilst this state may represent benign behaviour, as suggested in [71], the tumour cells will still remain in the system and be able to undergo further phenotypic mutation that will enable the cells to achieve an invasive state. We do however concede that this model does not explicitly consider an immune response that the body has for tumour cells such as with cytotoxic T lymphocytes and natural killer cells [49, 114, 136], which may be able to clear these non-aggressive tumour cells from the body as suggested by [49].

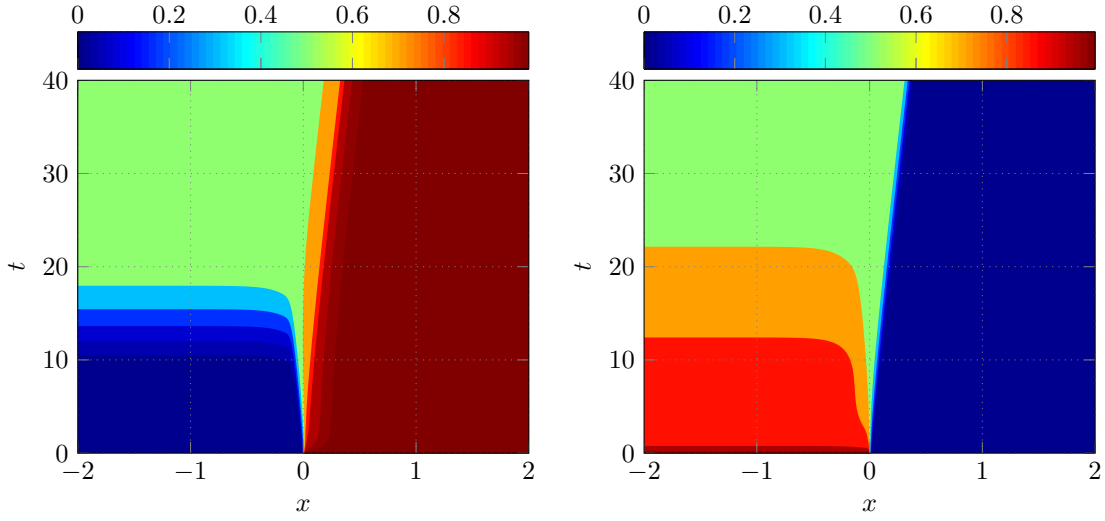

(a) Contour plot of u_1 for $T = 40$

(b) Contour plot of u_2 for $T = 40$

Figure 4.6: Contour plots u_1 and u_2 from simulations of (4.2.7)–(4.2.10) with parameters $\alpha_1 = 0.25$, $\alpha_2 = 0.25$, $\beta_2 = 1$, $\beta_3 = 70$, $\beta_4 = 20$, $\delta_1 = 0.25$, $\delta_2 = 0.25$, $\delta_4 = 1$

4.3.2 Periodic infusion

The use of periodic infusion corresponds, mathematically, to using a non-dimensionalised infusion function of the form $i(t) = i(t+\rho) \geq 0$ in the system (4.2.7)–(4.2.10). To obtain an understanding of how this model behaves when periodic infusion is utilised, numerical simulations will be run of (4.2.7)–(4.2.10) with the infusion function given by the periodic function (4.2.11), where we

let $\rho = 2.8$ (P approximately 1 week) and $\tau = 1.2$ (s_0 approximately 3 days). We remark that the dynamics of the spatially homogeneous version of the model with periodic infusion function considered in Chapter 3 can be used to predict potential behaviour of (4.2.7)–(4.2.10); this will be discussed further in the following sections.

It is expected that for particular parameter conditions, time-periodic travelling wave (TPTW) solutions will exist. A TPTW is a fixed surface that can be parameterised above a cylinder: the surface propagates in the direction of the real line with constant speed θ, where the sign of θ determines the direction the wave travels. Moreover, TPTWs connect periodic solutions of the corresponding spatially homogeneous system. Hence knowledge of the periodic solutions to the spatially homogeneous system enable us to predict the direction in which the respective waves will travel and make predictions about the speed of propagation. Mathematically, TPTWs correspond to the existence of solutions of the form $(u_1, u_2, u_3, u_4)(x,t) = (\varphi_1, \varphi_2, \varphi_3, \varphi_4)(x-\theta t, t) = (\varphi_1, \varphi_2, \varphi_3, \varphi_4)(x-\theta t, t+\rho)$ to the system (4.2.7)–(4.2.10). Hence if we let $(u_1, u_2, u_3, u_4)(x,t) = (\varphi_1, \varphi_2, \varphi_3, \varphi_4)(z,t)$, where $z = x - \theta t$, system (4.2.7)–(4.2.10) becomes

$$\frac{\partial \varphi_1}{\partial t} = \eta_1 \frac{\partial^2 \varphi_1}{\partial z^2} + \theta \frac{\partial \varphi_1}{\partial z} + \varphi_1(1 - \varphi_1 - \alpha_1 \varphi_2 - \delta_1 \varphi_3), \tag{4.3.9}$$

$$\frac{\partial \varphi_2}{\partial t} = \eta_2 \frac{\partial^2 \varphi_2}{\partial z^2} + \theta \frac{\partial \varphi_1}{\partial z} + \beta_2 \varphi_2(1 - \varphi_2 - \alpha_2 \varphi_1 - \delta_2 \varphi_4), \tag{4.3.10}$$

$$\frac{\partial \varphi_3}{\partial t} = \frac{\partial^2 \varphi_3}{\partial z^2} + \theta \frac{\partial \varphi_1}{\partial z} + \beta_3(\varphi_2 - \varphi_3), \tag{4.3.11}$$

$$\frac{\partial \varphi_4}{\partial t} = \eta_4 \frac{\partial^2 \varphi_4}{\partial z^2} + \theta \frac{\partial \varphi_1}{\partial z} + \beta_4(i(t) - \varphi_4 - \delta_4 \varphi_4 \varphi_2), \tag{4.3.12}$$

with "initial" conditions

$$(\varphi_1, \varphi_2, \varphi_3, \varphi_4)(z,0) = (\varphi_1, \varphi_2, \varphi_3, \varphi_4)(z,\rho)$$

and BCs given by the periodic solutions PS1–PS4.

Time-periodic TWs are expected to form due to the existence and stability of periodic solutions of the spatially homogeneous system that was considered in Chapter 3. Furthermore, TPTWs are expected since this system is similar to the well-known Lotka–Volterra reaction-diffusion equations with time-periodic coefficients for which the existence of TPTWs has been shown [10, 212].

Tumour clearance

If $i \in C(\mathbb{R}_+, [0, i_M])$, where $i_M > 0$, then from the results of Chapter 3 it can be concluded that it is possible to remove the tumour from the system by the reaction dynamics alone. Provided a sufficiently strong treatment protocol (i.e. if $1 \leq \delta_2 \leq (1+\delta_4)^2/4\delta_4$ and $\delta_4 < 1$, or if $\delta_2 > (1+\delta_4)^2/4\delta_4$), only the tumour-free periodic solution (i.e. PS2) is stable and furthermore, no other biologically meaningful solutions exist. Hence the tumour will be removed from the system by the treatment alone. See Figure 4.7 for an example of this behaviour.

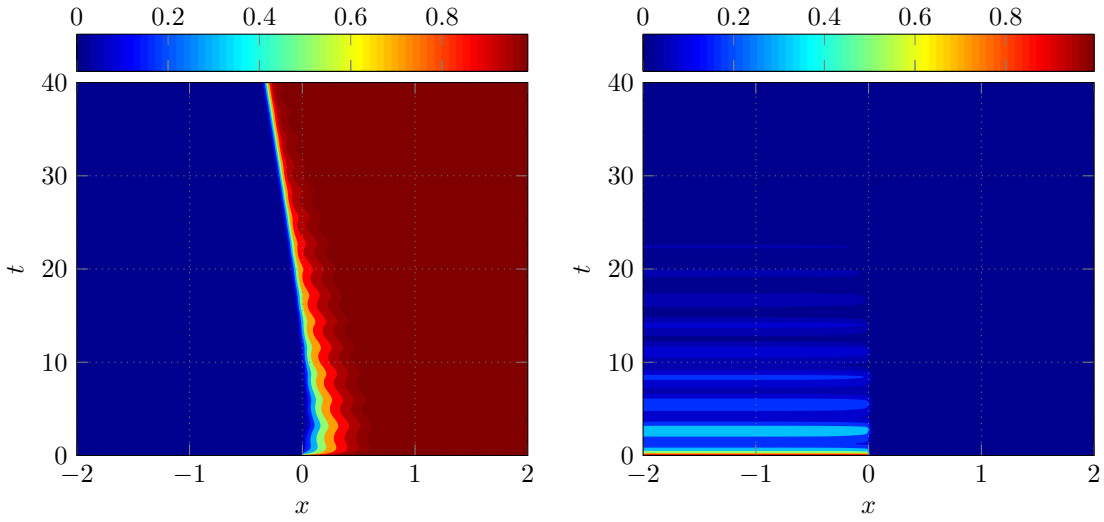

(a) Contour plot of u_1 for $T = 40$

(b) Contour plot of u_2 for $T = 40$

Figure 4.7: Contour plots u_1 and u_2 from simulations of (4.2.7)–(4.2.10) with periodic infusion and parameters $\alpha_1 = 1$, $\alpha_2 = 0.5$, $\beta_2 = 1$, $\beta_3 = 70$, $\beta_4 = 20$, $\delta_1 = 12.5$, $\delta_2 = 1.1$, $\delta_4 = 0.6$

Similarly to the constant infusion case, it is possible to witness a splitting behaviour, as displayed in Figure 4.8, from the solutions of (4.2.7)–(4.2.10) when a periodic infusion function is used. This behaviour is characterised by two sets of surfaces, which are TPTW-like, where each set of surfaces travel at different speeds causing the surfaces to "split" apart over time. In addition to the increasing distances between the surfaces, we note that oscillations in the normal tissue density gradually decrease and disappear whilst the oscillations in the tumour tissue density remain. This indicates the interaction between the populations gradually decreases further signalling splitting behaviour is occurring. This behaviour is only possible when the boundary at $z = \infty$ is given by stable PS2 and the boundary at $z = -\infty$ is given by PS3, which can be stable or unstable. This will reduce the long-term behaviour of the normal tissue to being governed by a Fisher–KPP equation and suggests that the added effect of chemical diffusion will make the treatment strong enough to remove the tumour from the system without the assistance from any other anti-tumour

mechanisms.

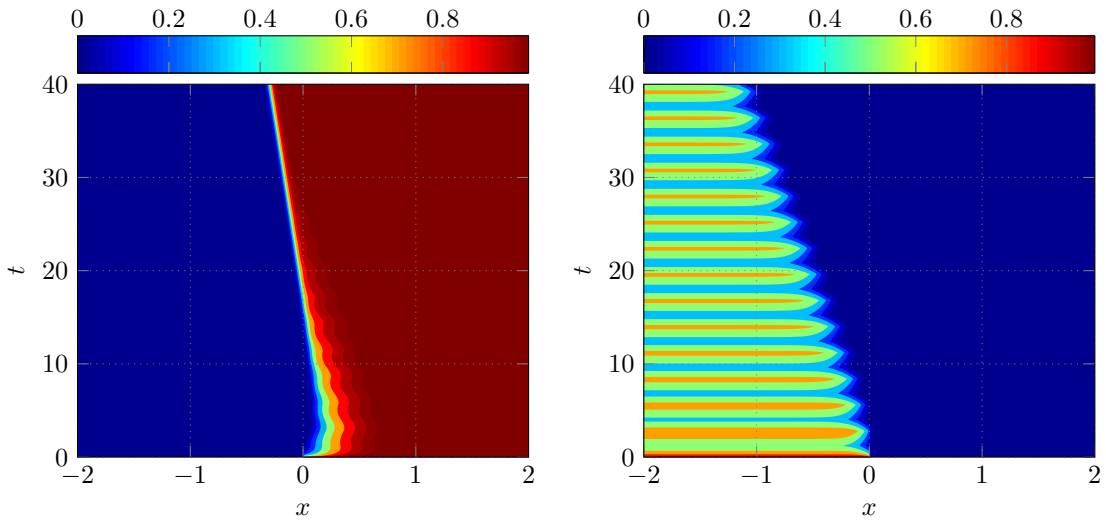

(a) Contour plot of u_1 for $T = 40$

(b) Contour plot of u_2 for $T = 40$

Figure 4.8: Contour plots u_1 and u_2 from simulations of (4.2.7)–(4.2.10) with periodic infusion and parameters $\alpha_1 = 1$, $\alpha_2 = 0.5$, $\beta_2 = 1$, $\beta_3 = 70$, $\beta_4 = 20$, $\delta_1 = 12.5$, $\delta_2 = 3$, $\delta_4 = 11$

As in the constant infusion case, in addition to the tumour clearance and splitting wave behaviour, TPTW solutions in which the tumour recedes are also observed. In Figure 4.9 we see that a TPTW forms that connects PS2 at $z = \infty$ to PS3 at $z = -\infty$, where the wave travels in the direction of PS3. Note that the speed of propagation is very slow and this suggests that the combination of treatment and normal-tissue competition is only marginally stronger than the tumour defences. In this scenario, in practice, the assessment may be made to increase the treatment dose or to utilise an alternative treatment as a means of treating the tumour more effectively.

We remark that under the infusion function (4.2.11), the treatments are marginally more effective in fighting the tumour than in the corresponding constant infusion examples. This can be seen by faster clearance of the tumour from the system and slightly faster wave speeds of the receding tumour for certain parameter values than in the constant infusion case.

Tumour invasion

It can be seen in Figure 4.10 that TPTWs form in which PS3 invades PS2, that is, the tumour is invading the normal tissue. This can occur when the system is bistable, that is, both PS2 and PS3 are stable, or when the system is monostable, where only PS3 is stable. In the latter case it is possible to obtain a class of speeds under which TPTWs can form.

Linearise (4.3.9)–(4.3.12) about the periodic solution PS2 by considering the evolution of

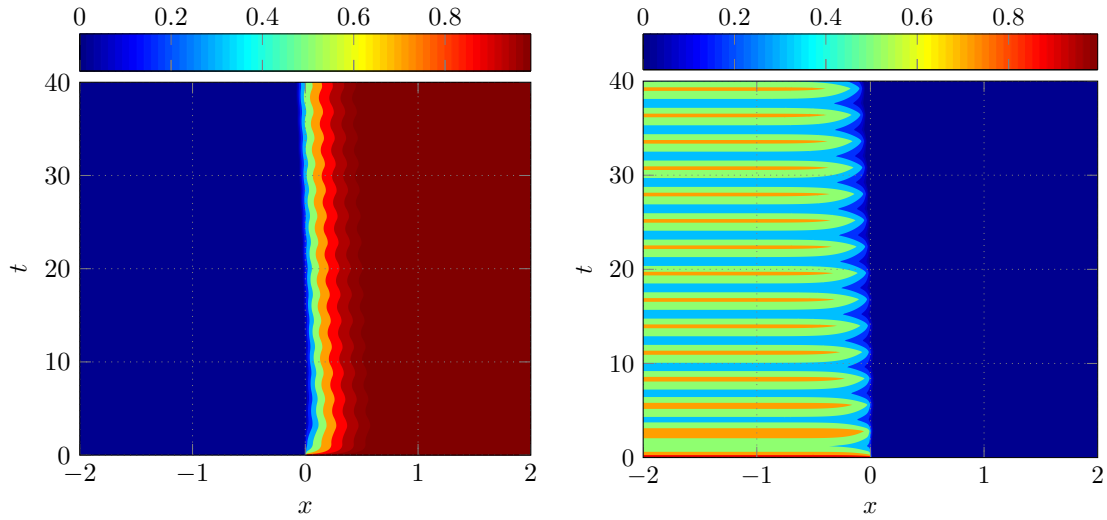

(a) Contour plot of u_1 for $T = 40$

(b) Contour plot of u_2 for $T = 40$

Figure 4.9: Contour plots u_1 and u_2 from simulations of (4.2.7)–(4.2.10) with periodic infusion and parameters $\alpha_1 = 1$, $\alpha_2 = 3$, $\beta_2 = 1$, $\beta_3 = 70$, $\beta_4 = 20$, $\delta_1 = 5$, $\delta_2 = 1.25$, $\delta_4 = 3.5$

$\mathbf{v}(z,t) = (v_1, v_2, v_3, v_4)(z,t) = (\varphi_1, \varphi_2, \varphi_3, \varphi_4)(z,t) - (u_1, u_2, u_3, u_4)(t)$ for large z which gives

$$\frac{\partial \mathbf{v}}{\partial t} = \operatorname{diag}(\eta_1, \eta_2, 1, \eta_4)\frac{\partial^2 \mathbf{v}}{\partial z^2} + \theta\frac{\partial \mathbf{v}}{\partial z} + \mathbf{F}'_{\mathbf{u}}(t, \mathbf{u}(t))\mathbf{v}, \quad \mathbf{v}(\infty, t) = \mathbf{0}, \quad \mathbf{v}(z,0) = \mathbf{v}_0(z).$$

In this system we have that v_2 is decoupled from the other variables and is governed by

$$\frac{\partial v_2}{\partial t} = \eta_2\frac{\partial^2 v_2}{\partial z^2} + \theta\frac{\partial v_2}{\partial z} + \beta_2[1 - \alpha_2 - \delta_2 u_4(t)]v_2, \quad v_2(\infty, t) = 0, \quad v_2(z,0) = v_{2,0}(z).$$

From Lemma 4.A.1 this has the solution

$$\begin{aligned} v_2(z,t) &= \frac{1}{2\sqrt{\pi\eta_2 t}}\int_{-\infty}^{\infty} v_{2,0}(y)\exp\left(-\frac{(z-y)^2}{4\eta_2 t} - \frac{\theta(z-y)}{2\eta_2} - \frac{\theta^2 t}{4\eta_2} + \int_0^t f(s)\,\mathrm{d}s\right)\mathrm{d}y \\ &= \frac{1}{2\sqrt{\pi\eta_2 t}}\exp\left(\int_0^t f(s)\,\mathrm{d}s - \frac{\theta^2 t}{4\eta_2}\right)\int_{-\infty}^{\infty} v_{2,0}(y)\exp\left(-\frac{(z-y)^2}{4\eta_2 t} - \frac{\theta(z-y)}{2\eta_2}\right)\mathrm{d}y, \end{aligned}$$

where $f(s) = \beta_2[1 - \alpha_2 - \delta_2 u_4(s)]$.

Let $G(t) = \exp\left(\int_0^t f(s)\,\mathrm{d}s - \frac{\theta^2 t}{4\eta_2}\right)$, then for $v_2(\infty, t) = 0$ to be satisfied for all $t \in \mathbb{R}_+$ we

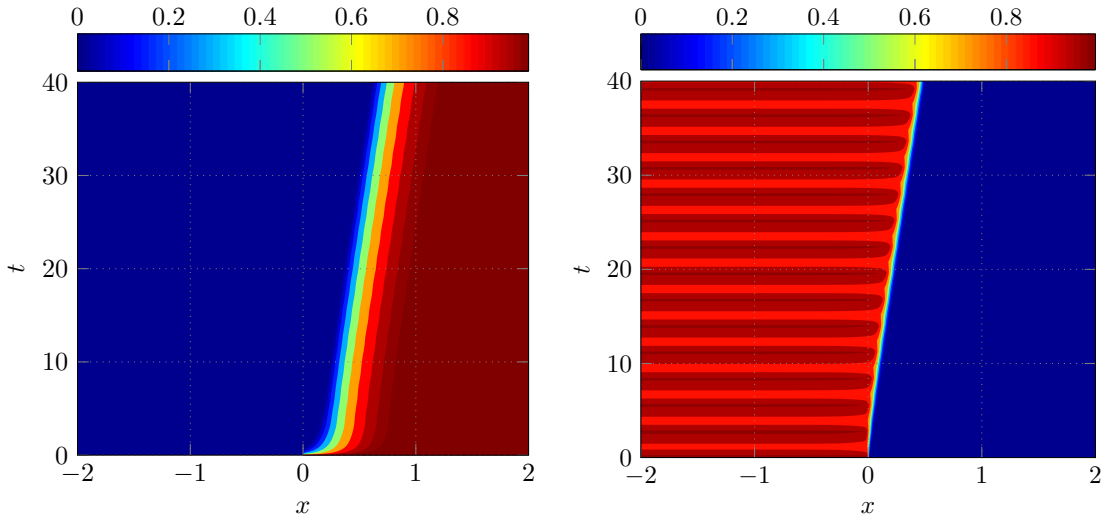

(a) Contour plot of u_1 for $T = 40$

(b) Contour plot of u_2 for $T = 40$

Figure 4.10: Contour plots u_1 and u_2 from simulations of (4.2.7)–(4.2.10) with periodic infusion and parameters $\alpha_1 = 1$, $\alpha_2 = 0.5$, $\beta_2 = 1$, $\beta_3 = 70$, $\beta_4 = 20$, $\delta_1 = 12.5$, $\delta_2 = 0.1$, $\delta_4 = 1$

require that G is bounded. Consider

$$\begin{aligned} G(t+\rho) &= \exp\left(\int_0^{t+\rho} f(s)\,\mathrm{d}s - \frac{\theta^2(t+\rho)}{4\eta_2}\right) \\ &= \exp\left(\int_0^{t} f(s)\,\mathrm{d}s - \frac{\theta^2 t}{4\eta_2} + \left\{\int_t^{t+\rho} f(s)\,\mathrm{d}s - \frac{\theta^2\rho}{4\eta_2}\right\}\right) \\ &= G(t)G(\rho), \end{aligned}$$

by the periodicity of the continuous function f. Hence it easily follows that $G(t)$ is bounded if and only if $G(\rho) \leq 1$, that is, if and only if $|\theta| \geq 2\sqrt{\eta_2 \bar{f}}$, where

$$\bar{f} = \frac{1}{\rho}\int_0^{\rho} \beta_2[1 - \alpha_2 - \delta_2 u_4(s)]\,\mathrm{d}s = \beta_2(1 - \alpha_2 - \delta_2),$$

by Lemma 3.B.1 in Chapter 3. Moreover, since we have a TPTW that is travelling forward we require $\theta > 0$, hence for TPTWs to exist that connects a wave moving from stable PS3 at $z = -\infty$ towards unstable PS2 at $z = \infty$, then we require $\theta \geq 2\sqrt{\eta_2\beta_2(1 - \alpha_2 - \delta_2)}$. Note this gives the same minimum speed of invasion for the tumour tissue as was determined in the system with constant infusion when a front connected stable SS3 at $z = -\infty$ to unstable SS2 at $z = \infty$.

As in the case of the constant infusion, the bistable system presents a far more challenging scenario and does not permit the same speed estimation techniques to be utilised. We remark that similar overall qualitative behaviour of the bistable systems in the constant infusion and periodic

infusion cases was observed. Splitting waves, receding tumour waves and invading tumour waves were observed in both the constant infusion and periodic infusion cases. We remark that splitting and receding behaviour could be observed with slightly smaller values for the parameters α_2 and δ_2 in the periodic infusion case than in the constant infusion case. Similarly, the same is true for marginally larger values of α_1 and δ_1 in the periodic infusion case than in the constant infusion case. This indicates that periodic infusion may be a slightly more effective method for tumour removal than constant infusion.

A TPTW exists in which the coexistence periodic solution PS4 at $z = -\infty$ advances towards the unstable tumour free periodic solution PS2 at $z = \infty$. See Figure 4.11 for an example of a TPTW that connects PS4 to PS2. As PS2 is unstable for TPTWs of this form, the analysis of the speed of the wave connecting stable PS3 to unstable PS2 can be used. Hence TPTWs that connects a wave moving from stable PS4 at $z = -\infty$ towards unstable PS2 at $z = -\infty$ are compatible for the speeds $\theta \geq 2\sqrt{\eta_2\beta_2(1-\alpha_2-\delta_2)}$. Note that from the work in Chapter 3 we required low population competition, tumour aggressiveness and treatment strength (i.e. $\alpha_1, \alpha_2, \delta_1, \delta_2 \ll 1$) in order for the periodic solution PS4 to exist and be stable. Hence this system has the capacity to become either an aggressively invading tumour or one in which the tumour recedes by either increasing α_1 and δ_1, or by increasing α_2 and δ_2, respectively. Furthermore, should an alternative treatment be used, or the treatment dose be increased, then it may be possible to remove the tumour.

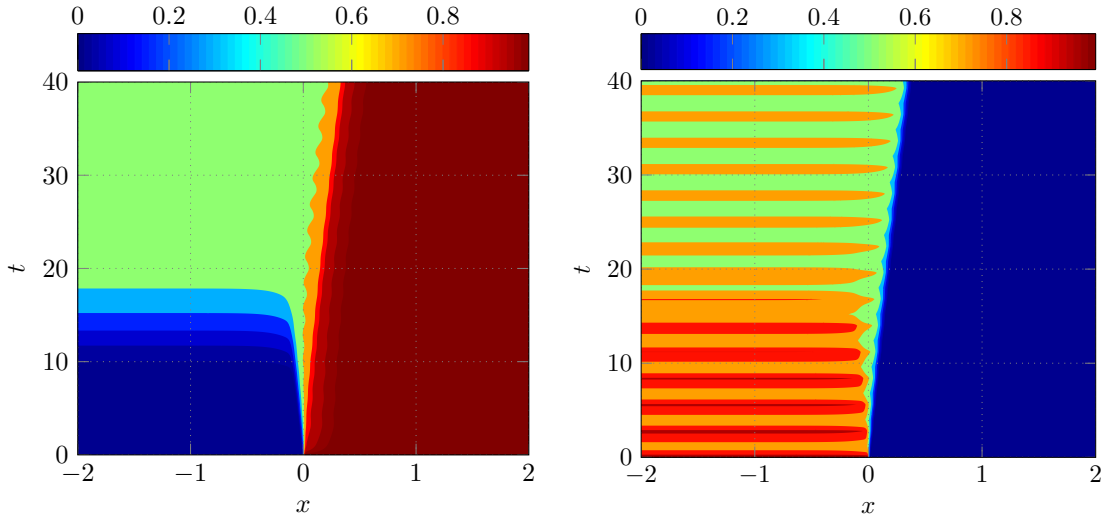

(a) Contour plot of u_1 for $T = 40$

(b) Contour plot of u_2 for $T = 40$

Figure 4.11: Contour plots u_1 and u_2 from simulations of (4.2.7)–(4.2.10) with periodic infusion and parameters $\alpha_1 = 0.25$, $\alpha_2 = 0.25$, $\beta_2 = 1$, $\beta_3 = 70$, $\beta_4 = 20$, $\delta_1 = 0.25$, $\delta_2 = 0.25$, $\delta_4 = 1$

4.4 Asymptotic analysis

In this section we present the arguments required for an asymptotic analysis of the constant infusion model (4.3.1)-(4.3.4).

4.4.1 Analysis for invading tumour

For the convenience of the reader we have provided a summary of results at the end of this section.

We note in the non-dimensional equations (4.2.7)–(4.2.10) that we have small parameters in the form of $0 < \eta_1, \eta_2 \ll 1$. We remark that for the TW formed in the case of the stable normal-tissue free state invading into the unstable tumour-tissue free state the minimal speed of existence, obtained in Section 4.3.1, is $\theta = O(\eta_1^{1/2})$, where θ is the speed parameter used in the substitution $z = x - \theta t$. As noted in [146] for typical initial conditions we expect a TW will form that travels close to or at the minimal wave speed. Hence as in [63, 140] and Chapter 2 we will assume that the speed θ is slow and utilise the theory of matched asymptotic expansions [16, pp. 335–350] in order to obtain an approximation for the solutions to this system of equations connecting the boundary conditions SS3 at $z = -\infty$ to SS2 at $z = \infty$. This technique assumes that there are "outer" regions in which the solution's derivatives undergo small variations and "inner" regions in which the solution's derivatives vary largely. It is noted that $\theta = O(\eta_1^{1/2})$ and furthermore, from Table 4.2 in Appendix 4.B, typically $\eta_1 = O(\eta_2)$, hence we make the substitution $\varepsilon = \eta_2^{1/2}$ and assume

$$\eta_1 = \eta_{10}\varepsilon^2 \quad \text{and} \quad \theta = \theta_0\varepsilon \tag{4.4.1}$$

where $\theta_0, \eta_{10} > 0$ and $\theta_0, \eta_{10} = O(1)$ as $\varepsilon \to 0^+$. Substituting (4.4.1) and

$$(u_1, u_2, u_3, u_4)(x, t; \varepsilon) = (\varphi_1, \varphi_2, \varphi_3, \varphi_4)(z; \varepsilon),$$

where $z = x - \theta t$, into (4.2.7)–(4.2.10) we obtain:

$$\eta_{10}\varepsilon^2\varphi_1'' + \theta_0\varepsilon\varphi_1' + \varphi_1(1 - \varphi_1 - \alpha_1\varphi_2 - \delta_1\varphi_3) = 0, \tag{4.4.2}$$

$$\varepsilon^2\varphi_2'' + \theta_0\varepsilon\varphi_2' + \beta_2\varphi_2(1 - \varphi_2 - \alpha_2\varphi_1 - \delta_2\varphi_4) = 0, \tag{4.4.3}$$

$$\varphi_3'' + \theta_0\varepsilon\varphi_3' + \beta_3(\varphi_2 - \varphi_3) = 0, \tag{4.4.4}$$

$$\eta_4\varphi_4'' + \theta_0\varepsilon\varphi_4' + \beta_4(1 - \varphi_4 - \delta_4\varphi_4\varphi_2) = 0, \tag{4.4.5}$$

with BCs

$$(\varphi_1, \varphi_2, \varphi_3, \varphi_4)(-\infty) = (0, \hat{u}_2, \hat{u}_2, [1 + \delta_4 \hat{u}_2]^{-1})$$

and

$$(\varphi_1, \varphi_2, \varphi_3, \varphi_4)(\infty) = (1, 0, 0, 1),$$

where $(\,)'$ represents differentiation with respect to z. We note that from Chapter 3 the BC at $z = -\infty$ is stable if and only if

$$\delta_2 < \frac{(\alpha_1 + \delta_1 + \delta_4)(\alpha_1 + \delta_1 - 1)}{(\alpha_1 + \delta_1)^2},$$

or if

$$\frac{(\alpha_1 + \delta_1 + \delta_4)(\alpha_1 + \delta_1 - 1)}{(\alpha_1 + \delta_1)^2} \leq \delta_2 < \frac{(1 + \delta_4)^2}{4\delta_4} \quad \text{and} \quad \frac{1}{\delta_4} < \frac{\alpha_1 + \delta_1 - 2}{\alpha_1 + \delta_1}.$$

Moreover, the BC at $z = \infty$ is stable if and only if

$$\alpha_2 + \delta_2 > 1.$$

Uniform approximation for the drug concentration

From the theory of matched asymptotic expansions, we look for outer solutions, in which the solutions undergo gradual changes, and inner solutions, in which the solutions undergo steep changes. We define the outer solution by

$$(\varphi_{1\text{out}}, \varphi_{2\text{out}}, \varphi_{3\text{out}}, \varphi_{4\text{out}})(z) = (\varphi_1, \varphi_2, \varphi_3, \varphi_4)(z; 0).$$

Hence letting $\varepsilon \to 0^+$ in (4.4.2)–(4.4.5) gives

$$\varphi_{1\text{out}}(1 - \varphi_{1\text{out}} - \alpha_1 \varphi_{2\text{out}} - \delta_1 \varphi_{3\text{out}}) = 0, \tag{4.4.6}$$

$$\beta_2 \varphi_{2\text{out}}(1 - \varphi_{2\text{out}} - \alpha_2 \varphi_{1\text{out}} - \delta_2 \varphi_{4\text{out}}) = 0, \tag{4.4.7}$$

$$\varphi''_{3\text{out}} + \beta_3(\varphi_{2\text{out}} - \varphi_{3\text{out}}) = 0, \tag{4.4.8}$$

$$\eta_4 \varphi''_{4\text{out}} + \beta_4(1 - \varphi_{4\text{out}} - \delta_4 \varphi_{4\text{out}} \varphi_{2\text{out}}) = 0, \tag{4.4.9}$$

where

$$(\varphi_{1\text{out}}, \varphi_{2\text{out}}, \varphi_{3\text{out}}, \varphi_{4\text{out}})(-\infty) = (0, \hat{u}_2, \hat{u}_2, [1 + \delta_4 \hat{u}_2]^{-1})$$

and

$$(\varphi_{1\text{out}}, \varphi_{2\text{out}}, \varphi_{3\text{out}}, \varphi_{4\text{out}})(\infty) = (1, 0, 0, 1).$$

Set $z = 0$ to be the region in which φ_2 undergoes a sudden change and introduce the stretched inner variable $\xi = z/\varepsilon$ into (4.4.2)–(4.4.5) to consider the change in this region. Let the inner solution be denoted by

$$(\varphi_{1\text{in}}, \varphi_{2\text{in}}, \varphi_{3\text{in}}, \varphi_{4\text{in}})(\xi) = \lim_{\varepsilon \to 0^+} (\varphi_1, \varphi_2, \varphi_3, \varphi_4)(\varepsilon\xi; \varepsilon).$$

Hence making the substitution $\xi = z/\varepsilon$ into (4.4.2)–(4.4.5) and letting $\varepsilon \to 0^+$ we obtain

$$\begin{aligned}
\eta_{10}\ddot{\varphi}_{1\text{in}} + \theta_0\dot{\varphi}_{1\text{in}} + \varphi_{1\text{in}}(1 - \varphi_{1\text{in}} - \alpha_1\varphi_{2\text{in}} - \delta_1\varphi_{3\text{in}}) &= 0, \\
\ddot{\varphi}_{2\text{in}} + \theta_0\dot{\varphi}_{2\text{in}} + \beta_2\varphi_{2\text{in}}(1 - \varphi_{2\text{in}} - \alpha_2\varphi_{1\text{in}} - \delta_2\varphi_{4\text{in}}) &= 0, \\
\ddot{\varphi}_{3\text{in}} &= 0, \qquad (4.4.10) \\
\ddot{\varphi}_{4\text{in}} &= 0 \qquad (4.4.11)
\end{aligned}$$

where $\dot{(\,)}$ denotes differentiation with respect to ξ. The boundary conditions for the inner solutions are obtained from the matching conditions

$$(\varphi_{1\text{out}}, \varphi_{2\text{out}}, \varphi_{3\text{out}}, \varphi_{4\text{out}})(0\pm) = (\varphi_{1\text{in}}, \varphi_{2\text{in}}, \varphi_{3\text{in}}, \varphi_{4\text{in}})(\pm\infty). \qquad (4.4.12)$$

First considering the outer region governed by (4.4.6)–(4.4.9), we have that $\varphi_{1\text{out}}(z) = 0$ for $z < 0$ satisfies (4.4.6). If we also have that $1 - \delta_2\varphi_{4\text{out}}(z) > 0$ for $z < 0$ then

$$\varphi_{2\text{out}}(z) = \begin{cases} 1 - \delta_2\varphi_{4\text{out}}(z) & \text{if } z < 0, \\ 0 & \text{if } z > 0, \end{cases} \qquad (4.4.13)$$

will satisfy (4.4.7). Then (4.4.9) becomes

$$0 = \eta_4\varphi''_{4\text{out}} + \beta_4 \begin{cases} 1 - (1 + \delta_4)\varphi_{4\text{out}} + \delta_2\delta_4\varphi^2_{4\text{out}} & \text{if } z < 0, \\ 1 - \varphi_{4\text{out}} & \text{if } z > 0, \end{cases}$$

where $\varphi_{4\text{out}}(-\infty) = [1 + \delta_4\hat{u}_2]^{-1}$ and $\varphi_{4\text{out}}(\infty) = 1$. For convenience of notation we define $\hat{u}_4 := [1 + \delta_4\hat{u}_2]^{-1}$ and furthermore, we note that $\hat{u}_2 = 1 - \delta_2\hat{u}_4$.

Before solving this we note that $\ddot{\varphi}_{4\text{in}} = 0$, hence to satisfy bounded BCs at $\xi = \pm\infty$ we must have that $\varphi_{4\text{in}}(\xi) = B_1$ a constant. Then from the matching conditions (4.4.12) we have that

$$\varphi_{4\text{in}}(\pm\infty) = B_1 = \varphi_{4\text{out}}(0\pm) \tag{4.4.14}$$

and as a result we can can see that we require $\varphi_{4\text{out}}(z)$ to be continuous at $z = 0$. We also set the derivatives of $\varphi_{4\text{out}}(z)$ to be continuous at $z = 0$, i.e. $\varphi'_{4\text{out}}(0-) = \varphi'_{4\text{out}}(0+)$, to determine the remaining constant of integration.

The calculations have been omitted, however (4.4.9) can be solved for $z < 0$ by making the substitution $\varphi_4 = \hat{u}_4 + f$ and then solving for f by a simple reduction of order technique and for $z > 0$ (4.4.9) is simply a second order linear ODE. Given this and the continuity conditions we have a solution that satisfies (4.4.9) is

$$\varphi_{4\text{out}}(z) = \begin{cases} \hat{u}_4 + \dfrac{3c_2}{2\delta_2\delta_4}\operatorname{sech}^2\left(\dfrac{c_3}{2}[z - z_0]\right) & \text{if } z < 0, \\ 1 + \left[\hat{u}_4 - 1 + \dfrac{3c_2}{2\delta_2\delta_4}\operatorname{sech}^2\left(\dfrac{c_3}{2}z_0\right)\right]\exp\left(-\sqrt{\dfrac{\beta_4}{\eta_4}}z\right) & \text{if } z > 0. \end{cases} \tag{4.4.15}$$

where $c_2 = \sqrt{(1+\delta_4)^2 - 4\delta_2\delta_4}$, $c_3 = \sqrt{c_2\beta_4/\eta_4}$ and z_0 satisfies

$$\left[\tanh^2\left(\frac{c_3}{2}z_0\right) - 1\right]\left[\sqrt{c_2}\tanh\left(\frac{c_3}{2}z_0\right) + 1\right] + \frac{2\delta_2\delta_4(1-\hat{u}_4)}{3c_2} = 0. \tag{4.4.16}$$

We know *a priori* that c_2 exists (i.e. $(1+\delta_4)^2 - 4\delta_2\delta_4 \geq 0$) as this is the condition for existence of the normal-tissue free SS (i.e. SS3). The uniform approximation is obtained by adding the corresponding outer and inner solutions and subtracting the common value in the overlap region [16]. Now given that we found $\varphi_{4\text{in}}(\xi) = \varphi_{4\text{out}}(0\pm)$ we have that the common value φ_{4c} is $\varphi_{4c} = \varphi_{4\text{out}}(0\pm) = \varphi_{4\text{in}}(\xi)$. Therefore

$$\begin{aligned} \varphi_4(z;\varepsilon) &\simeq \varphi_{4\text{out}}(z) + \varphi_{4\text{in}}(z/\varepsilon) - \varphi_{4c} \\ &= \begin{cases} \hat{u}_4 + \dfrac{3c_2}{2\delta_2\delta_4}\operatorname{sech}^2\left(\dfrac{c_3}{2}[z - z_0]\right) & \text{if } z < 0, \\ 1 + \left[\hat{u}_4 - 1 + \dfrac{3c_2}{2\delta_2\delta_4}\operatorname{sech}^2\left(\dfrac{c_3}{2}z_0\right)\right]\exp\left(-\sqrt{\dfrac{\beta_4}{\eta_4}}z\right) & \text{if } z > 0. \end{cases} \end{aligned} \tag{4.4.17}$$

If we require the solution for the drug concentration to be bound between the boundary values, which we note is demonstrated in the numerical solutions, then we require $\hat{u}_4 < \varphi_4(z) < 1$

and as a result the further condition $z_0 > 0$. We note that the condition $z_0 > 0$ is equivalent to requiring that $0 < \tanh(c_3 z_0/2) < 1$. Moreover, as (4.4.16) is cubic in $\tanh(c_3 z_0/2)$, we can see that $z_0 > 0$ is only possible if the cubic equation $f(x) = (x^2-1)(\sqrt{c_2}x + 1) + c_4$, where $c_4 = 2\delta_2\delta_4(1-\hat{u}_4)/3c_2 > 0$, has a root in the interval $(0,1)$. Note that $f(1) = c_4 > 0$ and that $f(0) = c_4 - 1$, where it is straightforward to show that for δ_2 "small" enough we have $c_4 - 1 < 0$. Hence by the Intermediate Value Theorem, for δ_2 small there exists $x^* \in (0,1)$ such that $f(x^*) = 0$, which implies that for δ_2 small there exists $z_0 > 0$. Therefore we know there exists parameter values for which $z_0 > 0$ is realisable.

Uniform approximation for the H^+ ion concentration

We now wish to obtain the uniform approximation of φ_3. Consider (4.4.8) for the outer solution of φ_3. We note that we can solve this using [63, Lemma 2.1] to obtain

$$\varphi_{3\mathrm{out}}(z) = \frac{\sqrt{\beta_3}}{2}\left[\int_z^\infty \mathrm{e}^{\sqrt{\beta_3}(z-s)}\varphi_{2\mathrm{out}}(s)\,\mathrm{d}s + \int_{-\infty}^z \mathrm{e}^{-\sqrt{\beta_3}(z-s)}\varphi_{2\mathrm{out}}(s)\,\mathrm{d}s\right]$$

and then using (4.4.13) for $\varphi_{2\mathrm{out}}$ in this equation gives the outer solution

$$\varphi_{3\mathrm{out}}(z) = \begin{cases} \hat{u}_2 - \dfrac{\hat{u}_2}{2}\mathrm{e}^{\sqrt{\beta_3}z} - \dfrac{3c_2\sqrt{\beta_3}}{4\delta_4}\left[\displaystyle\int_z^0 \mathrm{e}^{\sqrt{\beta_3}(z-s)}\mathrm{sech}^2\left(\frac{c_3}{2}[s-z_0]\right)\mathrm{d}s\right. & \\ \qquad\qquad \left. + \displaystyle\int_{-\infty}^z \mathrm{e}^{-\sqrt{\beta_3}(z-s)}\mathrm{sech}^2\left(\frac{c_3}{2}[s-z_0]\right)\mathrm{d}s\right] & \text{if } z<0, \\ \left[\dfrac{\hat{u}_2}{2} - \dfrac{3c_2\sqrt{\beta_3}}{4\delta_4}\displaystyle\int_{-\infty}^0 \mathrm{e}^{\sqrt{\beta_3}s}\mathrm{sech}^2\left(\frac{c_3}{2}[s-z_0]\right)\mathrm{d}s\right]\mathrm{e}^{-\sqrt{\beta_3}z} & \text{if } z>0. \end{cases} \tag{4.4.18}$$

We note that $\varphi_{3\mathrm{out}}(0+) = \varphi_{3\mathrm{out}}(0-)$ and consider the inner solution for φ_3. We see from (4.4.10) that $\varphi_{3\mathrm{in}}$ is governed by $\ddot{\varphi}_{3\mathrm{in}} = 0$, hence for a bounded solution to satisfy BCs at $\xi = \pm\infty$ we require $\varphi_{3\mathrm{in}}(\xi) = B_2$ a constant. Therefore from the matching conditions $\varphi_{3\mathrm{out}}(0\pm) = \varphi_{3\mathrm{in}}(\pm\infty)$ we have that

$$\varphi_{3\mathrm{in}}(\xi) = \varphi_{3\mathrm{out}}(0\pm). \tag{4.4.19}$$

We obtain the common value in the overlap region φ_{3c} where $\varphi_{3c} = \varphi_{3\text{out}}(0\pm) = \varphi_{3\text{in}}(\xi)$. Therefore the uniform approximation for φ_3 is,

$$\begin{aligned}\varphi_3(z;\varepsilon) &\simeq \varphi_{3\text{out}}(z) + \varphi_{3\text{in}}(z/\varepsilon) - \varphi_{3c},\\ &= \begin{cases} \hat{u}_2 - \dfrac{\hat{u}_2}{2}\mathrm{e}^{\sqrt{\beta_3}z} - \dfrac{3c_2\sqrt{\beta_3}}{4\delta_4}\left[\displaystyle\int_z^0 \mathrm{e}^{\sqrt{\beta_3}(z-s)}\mathrm{sech}^2\left(\frac{c_3}{2}[s-z_0]\right)\mathrm{d}s\right. & \\ \qquad\qquad \left. + \displaystyle\int_{-\infty}^z \mathrm{e}^{-\sqrt{\beta_3}(z-s)}\mathrm{sech}^2\left(\frac{c_3}{2}[s-z_0]\right)\mathrm{d}s\right] & \text{if } z<0,\\ \left[\dfrac{\hat{u}_2}{2} - \dfrac{3c_2\sqrt{\beta_3}}{4\delta_4}\displaystyle\int_{-\infty}^0 \mathrm{e}^{\sqrt{\beta_3}s}\mathrm{sech}^2\left(\frac{c_3}{2}[s-z_0]\right)\mathrm{d}s\right]\mathrm{e}^{-\sqrt{\beta_3}z} & \text{if } z>0. \end{cases}\end{aligned} \tag{4.4.20}$$

Uniform approximation for the tumour and normal tissue cell density for low tumour aggressiveness

We now wish to determine the uniform approximation of the tumour and normal tissue cell densities. Consider the case in which both the tumour and normal tissue undergo a sudden and steep change in the same location. It will be seen that this approximation corresponds to "low tumour aggressiveness", that is, normal cell populations are still able to exist in a small region occupied by the tumour cells. We have already determined the outer solution for φ_2 given by (4.4.13). Using this and (4.4.6), provided $1-\delta_1\varphi_{3\text{out}}(z) > 0$ for $z > 0$, we obtain the outer solution for φ_1 given by

$$\varphi_{1\text{out}}(z) = \begin{cases} 0 & \text{if } z<0,\\ 1-\delta_1\varphi_{3\text{out}}(z) & \text{if } z>0. \end{cases}$$

Note we require that $1-\delta_1\varphi_{3\text{out}}(z) > 0$ for $z > 0$ and $1-\delta_2\varphi_{4\text{out}}(z) > 0$ for $z < 0$. Since we have that $\varphi_{3\text{out}}$ is decreasing for $z > 0$, then $1-\delta_1\varphi_{3\text{out}}(z) > 0$ for $z > 0$ if $1-\delta_1\varphi_{3c} > 0$. Moreover, since $z_0 > 0$ we have that $\varphi_{4\text{out}}$ is increasing for $z < 0$, then $1-\delta_2\varphi_{4\text{out}}(z) > 0$ for $z < 0$ if $1-\delta_2\varphi_{4c} > 0$. Hence the conditions $1-\delta_1\varphi_{3c} > 0$ and $1-\delta_2\varphi_{4c} > 0$ need to be met for this solution to be valid. We have determined the inner solutions for φ_4 and φ_3 given by $\varphi_{4\text{in}}(\xi) = \varphi_{4c}$ and $\varphi_{3\text{in}}(\xi) = \varphi_{3c}$, respectively. The governing equations for $\varphi_{1\text{in}}$ and $\varphi_{2\text{in}}$ become

$$\eta_{10}\ddot{\varphi}_{1\text{in}} + \theta_0\dot{\varphi}_{1\text{in}} + \varphi_{1\text{in}}(1-\delta_1\varphi_{3c} - \varphi_{1\text{in}} - \alpha_1\varphi_{2\text{in}}) = 0, \tag{4.4.21}$$

$$\ddot{\varphi}_{2\text{in}} + \theta_0\dot{\varphi}_{2\text{in}} + \beta_2\varphi_{2\text{in}}(1-\delta_2\varphi_{4c} - \varphi_{2\text{in}} - \alpha_2\varphi_{1\text{in}}) = 0, \tag{4.4.22}$$

with BCs

$$(\varphi_{1\text{in}}, \varphi_{2\text{in}})(-\infty) = (0, 1-\delta_2\varphi_{4c}) \quad \text{and} \quad (\varphi_{1\text{in}}, \varphi_{2\text{in}})(\infty) = (1-\delta_1\varphi_{3c}, 0) \tag{4.4.23}$$

which are determined by the matching conditions (4.4.12). Therefore this represents a traditional competition-diffusion system as considered in [99, 102, 106, 107, 145, 179, 214] among others. From the results in [99, 107], if $1-\delta_1\varphi_{3c}-\alpha_1(1-\delta_2\varphi_{4c}) < 0$ and $1-\delta_2\varphi_{4c}-\alpha_2(1-\delta_1\varphi_{3c}) > 0$, then there exists a class of monotone TW solutions to (4.4.21)–(4.4.23) for speeds of invasion $\theta_0 \geq 2\sqrt{\beta_2[1-\delta_2\varphi_{4c}-\alpha_2(1-\delta_1\varphi_{3c})]}$. If $1-\delta_1\varphi_{3c}-\alpha_1(1-\delta_2\varphi_{4c}) < 0$ and $1-\delta_2\varphi_{4c}-\alpha_2(1-\delta_1\varphi_{3c}) < 0$ then from the results in [106], we have that there exists a class of monotone TW solutions for (4.4.21)–(4.4.23) with minimal speed $\theta_0 = \theta_m(\alpha_1, \alpha_2, \beta_2, \beta_3, \beta_4, \delta_1, \delta_2, \delta_4, \eta_4)$, where $-2\sqrt{\eta_{10}(1-\delta_1\varphi_{3c})} < \theta_m < 2\sqrt{\beta_2(1-\delta_2\varphi_{4c})}$. We note that our asymptotic approximation assumes that $\theta_0 > 0$ hence we cannot have solutions with a negative speed. Therefore we can only say that $\theta_0 > 0$ with certainty when we have $1-\delta_2\varphi_{4c}-\alpha_2(1-\delta_1\varphi_{3c}) > 0$.

We now obtain our uniform approximation for φ_1 and φ_2. The common values in the overlap regions for the normal and tumour tissue are given by φ_{1c} and φ_{2c}, respectively. The obtained values are:

$$\varphi_{1c} = \begin{cases} \varphi_{1\text{in}}(-\infty) = \varphi_{1\text{out}}(0-) = 0 & \text{if } z < 0, \\ \varphi_{1\text{in}}(\infty) = \varphi_{1\text{out}}(0+) = 1-\delta_1\varphi_{3c} & \text{if } z > 0 \end{cases}$$

and

$$\varphi_{2c} = \begin{cases} \varphi_{2\text{in}}(-\infty) = \varphi_{2\text{out}}(0-) = 1-\delta_2\varphi_{4c} & \text{if } z < 0, \\ \varphi_{2\text{in}}(\infty) = \varphi_{2\text{out}}(0+) = 0 & \text{if } z > 0. \end{cases}$$

Therefore the uniform approximation for φ_1 and φ_2 in the case $1-\delta_1\varphi_{3c} > 0$, $1-\delta_2\varphi_{4c} > 0$ and $1-\delta_1\varphi_{3c}-\alpha_1(1-\delta_2\varphi_{4c}) < 0$ are

$$\begin{aligned} \varphi_1(z;\varepsilon) &\simeq \varphi_{1\text{out}}(z) + \varphi_{1\text{in}}(z/\varepsilon) - \varphi_{1c}, \\ &= \phi_1(z/\varepsilon;\theta_0) \\ &\quad + \delta_1 \begin{cases} 0 & \text{if } z < 0, \\ \left[\dfrac{\hat{u}_2}{2} - \dfrac{3c_2\sqrt{\beta_3}}{4\delta_4}\displaystyle\int_{-\infty}^{0} \mathrm{e}^{\sqrt{\beta_3}s}\operatorname{sech}^2\left(\frac{c_3}{2}[s-z_0]\right)\,\mathrm{d}s\right]\left(1-\mathrm{e}^{-\sqrt{\beta_3}z}\right) & \text{if } z > 0 \end{cases} \end{aligned}$$

and

$$\begin{aligned}\varphi_2(z;\varepsilon) &\simeq \varphi_{2\text{out}}(z) + \varphi_{2\text{in}}(z/\varepsilon) - \varphi_{2c},\\ &= \phi_2(z/\varepsilon;\theta_0) + \frac{3c_2}{2\delta_4}\begin{cases}\operatorname{sech}^2\left(\frac{c_3}{2}z_0\right) - \operatorname{sech}^2\left(\frac{c_3}{2}[z-z_0]\right) & \text{if } z<0,\\ 0 & \text{if } z>0,\end{cases}\end{aligned}$$

where $(\varphi_{1\text{in}},\varphi_{2\text{in}})(\xi) = (\phi_1,\phi_2)(\xi;\theta_0)$ solves (4.4.21)–(4.4.23). Furthermore, if $1-\delta_2\varphi_{4c} - \alpha_2(1-\delta_1\varphi_{3c}) > 0$, then the inner solutions have speed $\theta_0 \geq 2\sqrt{\beta_2[1-\delta_2\varphi_{4c}-\alpha_2(1-\delta_1\varphi_{3c})]}$, hence from (4.4.1) our uniform solutions will have speed $\theta \geq 2\sqrt{\eta_2\beta_2[1-\delta_2\varphi_{4c}-\alpha_2(1-\delta_1\varphi_{3c})]}$.

Uniform approximation for the tumour and normal tissue cell density for high tumour aggressiveness

This section will consider "high tumour aggressiveness" in which the normal tissue is destroyed ahead of the invading tumour front such that normal and tumour tissue to do not occupy the same space in significant quantities.

Consider (4.4.21) and (4.4.22) when $1-\delta_2\varphi_{4c} > 0$ and $1-\delta_1\varphi_{3c} < 0$. Note that $1-\delta_1\varphi_{3\text{out}}(0) = 1-\delta_1\varphi_{3c} < 0$ and $1-\delta_1\varphi_{3\text{out}}(\infty) = 1$. It is then straightforward to show by a combination of continuity, the Intermediate Value Theorem and the monotonicity of $\varphi_{3\text{out}}$ that $1-\delta_1\varphi_{3\text{out}}(z) < 0$ for all $z \in (0,z^*)$ and $1-\delta_1\varphi_{3\text{out}}(z) > 0$ for all $z > z^*$, where $z^* > 0$ is such that $1-\delta_1\varphi_{3\text{out}}(z^*) = 0$. Hence to avoid negativity we have that the outer solution satisfying (4.4.6) becomes

$$\varphi_{1\text{out}}(z) = \begin{cases}0 & \text{if } z < z_+,\\ 1-\delta_1\varphi_{3\text{out}}(z) & \text{if } z > z_+,\end{cases}$$

where $z_+ \geq z^*$ is a value to be determined. With this in mind the inner solutions for φ_1 and φ_2 governed by (4.4.21) and (4.4.22) will have BCs

$$(\varphi_{1\text{in}},\varphi_{2\text{in}})(-\infty) = (0, 1-\delta_2\varphi_{4c}) \quad \text{and} \quad (\varphi_{1\text{in}},\varphi_{2\text{in}})(\infty) = (0,0), \tag{4.4.24}$$

which are determined by the matching conditions (4.4.12). We note that the boundary conditions for $\varphi_{1\text{in}}$ are now the same, i.e. $\varphi_{1\text{in}}(\pm\infty) = 0$, and as a result $\varphi_{1\text{in}}$ must form a pulse. Consider the following lemma:

Lemma 4.4.1. *Let* $(\varphi_{1\text{in}},\varphi_{2\text{in}})(\xi)$ *for* $\xi \in \mathbb{R}$ *be solutions of* (4.4.21) *and* (4.4.22) *with* $\varphi_{1\text{in}}(\pm\infty) =$

0, $\varphi_{2\text{in}}(\pm\infty) \in \mathbb{R}$ *and* $1 - \delta_1\varphi_{3c} < 0$. *If we require that* $\varphi_{1\text{in}}, \varphi_{2\text{in}} \geq 0$ *then this implies* $\varphi_{1\text{in}} \equiv 0$.

Proof. First noting that we have $\varphi_{1\text{in}}(\pm\infty) = 0$, $\varphi_{2\text{in}}(\pm\infty) \in \mathbb{R}$, take the limit of (4.4.21) as $\xi \to \pm\infty$ to obtain

$$\lim_{\xi\to\pm\infty} [\eta_{10}\ddot{\varphi}_{1\text{in}}(\xi) + \theta_0\dot{\varphi}_{1\text{in}}(\xi)] = 0$$

and then using the result discussed in [116, 189] we have that $\ddot{\varphi}_{1\text{in}}(\pm\infty) = \dot{\varphi}_{1\text{in}}(\pm\infty) = 0$. Now integrate (4.4.21) over $\mathbb{R}$ to obtain

$$0 = \int_{-\infty}^{\infty} \varphi_{1\text{in}}(s)[\delta_1\varphi_{3c} - 1 + \varphi_{1\text{in}}(s) + \alpha_1\varphi_{2\text{in}}(s)]\,\mathrm{d}s. \tag{4.4.25}$$

Since we require $\varphi_{1\text{in}}, \varphi_{2\text{in}} \geq 0$ then $\varphi_{1\text{in}}(s)[\delta_1\varphi_{3c} - 1 + \varphi_{1\text{in}}(s) + \alpha_1\varphi_{2\text{in}}(s)] \geq 0$ for all $s \in \mathbb{R}$ and as such (4.4.25) is satisfied if and only if $\varphi_{1\text{in}} \equiv 0$. □

As we require nonnegativity of our inner solutions $\varphi_{1\text{in}}$ and $\varphi_{2\text{in}}$ then we can apply Lemma 4.4.1 to (4.4.21) and (4.4.22) with BCs (4.4.24) to obtain that $\varphi_{1\text{in}}(\xi) = 0$. Therefore we have that (4.4.22) reduces to

$$\ddot{\varphi}_{2\text{in}} + \theta_0\dot{\varphi}_{2\text{in}} + \beta_2\varphi_{2\text{in}}(1 - \delta_2\varphi_{4c} - \varphi_{2\text{in}}) = 0, \tag{4.4.26}$$

which is simply the Fisher–KPP equation [66, 112] which has a known solution $\varphi_{2\text{in}}(\xi) = \phi_F(\xi;\theta_0)$ for speed $\theta_0 \geq 2\sqrt{\beta_2(1 - \delta_2\varphi_{4c})}$. We can now obtain the uniform approximation for φ_2 by adding the inner and outer solutions and subtracting the common value in the overlap region. The value in the overlap region φ_{2c} is given by

$$\varphi_{2c} = \begin{cases} \varphi_{2\text{in}}(-\infty) = \varphi_{2\text{out}}(0-) = 1 - \delta_2\varphi_{4c} & \text{if } z < 0, \\ \varphi_{2\text{in}}(\infty) = \varphi_{2\text{out}}(0+) = 0 & \text{if } z > 0. \end{cases}$$

Hence we have the uniform approximation

$$\begin{aligned} \varphi_2(z;\varepsilon) &\simeq \varphi_{2\text{in}}(z/\varepsilon) + \varphi_{2\text{out}}(z) - \varphi_{2c} \\ &= \phi_F(z/\varepsilon;\theta_0) + \frac{3c_2}{2\delta_4} \begin{cases} \operatorname{sech}^2\left(\frac{c_3}{2}z_0\right) - \operatorname{sech}^2\left(\frac{c_3}{2}[z - z_0]\right) & \text{if } z < 0, \\ 0 & \text{if } z > 0, \end{cases} \end{aligned}$$

where $\phi_F(\xi;\theta_0)$ is the solution to the Fisher–KPP equation with BCs $\phi_F(-\infty) = 1 - \delta_2\varphi_{4c}$ and $\phi_F(\infty) = 0$ for speed θ_0. Since we have $1 - \delta_2\varphi_{4c} > 0$ then from (4.4.1) our uniform solutions will have speed $\theta \geq 2\sqrt{\eta_2\beta_2(1 - \delta_2\varphi_{4c})}$.

Consider the behaviour of the solution around the point $z_+ > 0$ where z_+ is to be determined. We define z_+ as the point at which $\varphi_{1\text{out}}(z)$ transitions from $\varphi_{1\text{out}}(z) = 0$ to $\varphi_{1\text{out}}(z) = 1 - \delta_1\varphi_{3\text{out}}(z)$. We note that at z_+ we require $1 - \delta_1\varphi_{3\text{out}}(z_+) \geq 0$ to avoid negativity and since $1-\delta_1\varphi_{3\text{out}}(z)$ is increasing for $z > 0$ we have that $z_+ \geq z^*$ where z^* is such that $1-\delta_1\varphi_{3\text{out}}(z^*) = 0$. We determine z_+ by introducing the stretched variable $\zeta = (z - z_+)/\varepsilon$ into (4.4.2)–(4.4.5) and taking the limit as $\varepsilon \to 0^+$ to consider the inner behaviour of φ_1 about the point z_+. We then obtain the system of equations

$$\eta_{10}\ddot{\varphi}_{1+} + \theta_0\dot{\varphi}_{1+} + \varphi_{1+}(1 - \varphi_{1+} - \alpha_1\varphi_{2+} - \delta_1\varphi_{3+}) = 0, \tag{4.4.27}$$

$$\ddot{\varphi}_{2+} + \theta_0\dot{\varphi}_{2+} + \beta_2\varphi_{2+}(1 - \varphi_{2+} - \alpha_2\varphi_{1+} - \delta_2\varphi_{4+}) = 0,$$

$$\ddot{\varphi}_{3+} = 0, \tag{4.4.28}$$

$$\ddot{\varphi}_{4+} = 0, \tag{4.4.29}$$

where $\dot{(\,)}$ denotes differentiation with respect to ζ and

$$(\varphi_{1+}, \varphi_{2+}, \varphi_{3+}, \varphi_{4+})(\zeta) = \lim_{\varepsilon\to 0^+}(\varphi_1, \varphi, \varphi_3, \varphi_4)(\varepsilon\zeta; \varepsilon).$$

We obtain the BCs for this system from the matching conditions

$$(\varphi_{1\text{out}}, \varphi_{2\text{out}}, \varphi_{3\text{out}}, \varphi_{4\text{out}})(z_+\pm) = (\varphi_{1+}, \varphi_{2+}, \varphi_{3+}, \varphi_{4+})(\pm\infty),$$

which gives

$$(\varphi_{1+}, \varphi_{2+}, \varphi_{3+}, \varphi_{4+})(-\infty) = (0, 0, \varphi_3^*, \varphi_4^*)$$

and

$$(\varphi_{1+}, \varphi_{2+}, \varphi_{3+}, \varphi_{4+})(\infty) = (1 - \delta_1\varphi_3^*, 0, \varphi_3^*, \varphi_4^*),$$

where $\varphi_3^* = \varphi_{3\text{out}}(z_+)$ and $\varphi_4^* = \varphi_{4\text{out}}(z_+)$. Using these BCs with (4.4.28) and (4.4.29) implies that we require $\varphi_{3+}(\zeta) = \varphi_3^*$ and $\varphi_{4+}(\zeta) = \varphi_4^*$. Furthermore, since z_+ is ahead of the advancing wave front of φ_2 in a region in which the outer solution for φ_2 is zero we require for the monotonicity of the system that $\varphi_{2+}(\zeta) = 0$. Hence we have that (4.4.27) reduces to

$$\eta_{10}\ddot{\varphi}_{1+} + \theta_0\dot{\varphi}_{1+} + \varphi_{1+}(1 - \delta_1\varphi_3^* - \varphi_{1+}) = 0, \tag{4.4.30}$$

with BCs $\varphi_{1+}(-\infty) = 0$ and $\varphi_{1+}(\infty) = 1 - \delta_1\varphi_3^*$ where $1 - \delta_1\varphi_3^* \geq 0$. Consider (4.4.30) for $1 - \delta_1\varphi_3^* > 0$ and note that this is simply the Fisher-KPP equation. Note that we have $\theta_0 > 0$ and using a similar argument to the one used in the proof of Lemma 4.4.1 we have $\dot{\varphi}_{1+}(\pm\infty) = 0$. Now multiply (4.4.30) by $\dot{\varphi}_{1+}$ and integrate over $\mathbb{R}$ to obtain

$$\theta_0 \int_{-\infty}^{\infty} \dot{\varphi}_{1+}(s)^2 \, \mathrm{d}s = -\int_{-\infty}^{\infty} \varphi_{1+}(s)[1 - \delta_1\varphi_3^* - \varphi_{1+}(s)]\dot{\varphi}_{1+}(s) \, \mathrm{d}s.$$

then letting $\mu = \varphi_{1+}(s)$ in the integral on the left handside and rearranging to make θ_0 the subject we obtain

$$\theta_0 = -\frac{\int_0^{1-\delta_1\varphi_3^*} \mu(1 - \delta_1\varphi_3^* - \mu) \, \mathrm{d}\mu}{\int_{-\infty}^{\infty} \dot{\varphi}_{1+}(s)^2 \, \mathrm{d}s} = -\frac{1}{6}\frac{(1 - \delta_1\varphi_3^*)^3}{\int_{-\infty}^{\infty} \dot{\varphi}_{1+}(s)^2 \, \mathrm{d}s} < 0$$

which is a contradiction. Hence we require $1 - \delta_1\varphi_3^* = 0$ which corresponds to $z_+ = z^*$ and also reduces (4.4.30) to

$$\eta_{10}\ddot{\varphi}_{1+} + \theta_0\dot{\varphi}_{1+} - \varphi_{1+}^2 = 0.$$

Requiring $\varphi_{1+} \geq 0$ allows us to show by a similar argument used for the proof of Lemma 4.4.1 that $\varphi_{1+}(\zeta) = 0$. We have that the common value in the overlap region given by φ_{1c} is $\varphi_{1c} = \varphi_{1\mathrm{out}}(z^*\pm) = \varphi_{1+}(\pm\infty) = 0$. Hence we have our uniform approximation for φ_1 is

$$\begin{aligned}\varphi_1(z;\varepsilon) &\simeq \varphi_{1\mathrm{out}}(z) + \varphi_{1+}([z - z^*]/\varepsilon) - \varphi_{1c} \\ &= \begin{cases} 0 & \text{if } z < z^*, \\ 1 - \delta_1\left[\dfrac{\hat{u}_2}{2} - \dfrac{3c_2\sqrt{\beta_3}}{4\delta_4}\displaystyle\int_{-\infty}^{0} \mathrm{e}^{\sqrt{\beta_3}s}\mathrm{sech}^2\left(\frac{c_3}{2}[s - z_0]\right) \, \mathrm{d}s\right]\mathrm{e}^{-\sqrt{\beta_3}z} & \text{if } z > z^*, \end{cases}\end{aligned}$$

where z^* is such that $1 - \delta_1\varphi_{3\mathrm{out}}(z^*) = 0$. Note that we do not consider the uniform approximations for φ_2, φ_3 and φ_4 using the solutions obtained for the region around z^* as the solutions will remain unchanged, and similarly we do not need to consider the uniform approximation for φ_1 using the solution obtained in the region around $z = 0$. Note the similarity of the asymptotic approximation for the normal tissue concentration to the solution obtained in [140] for an aggressive tumour. The model proposed in [140] does not consider normal tissue diffusion or the effect of a treatment and obtained their approximation by a different method.

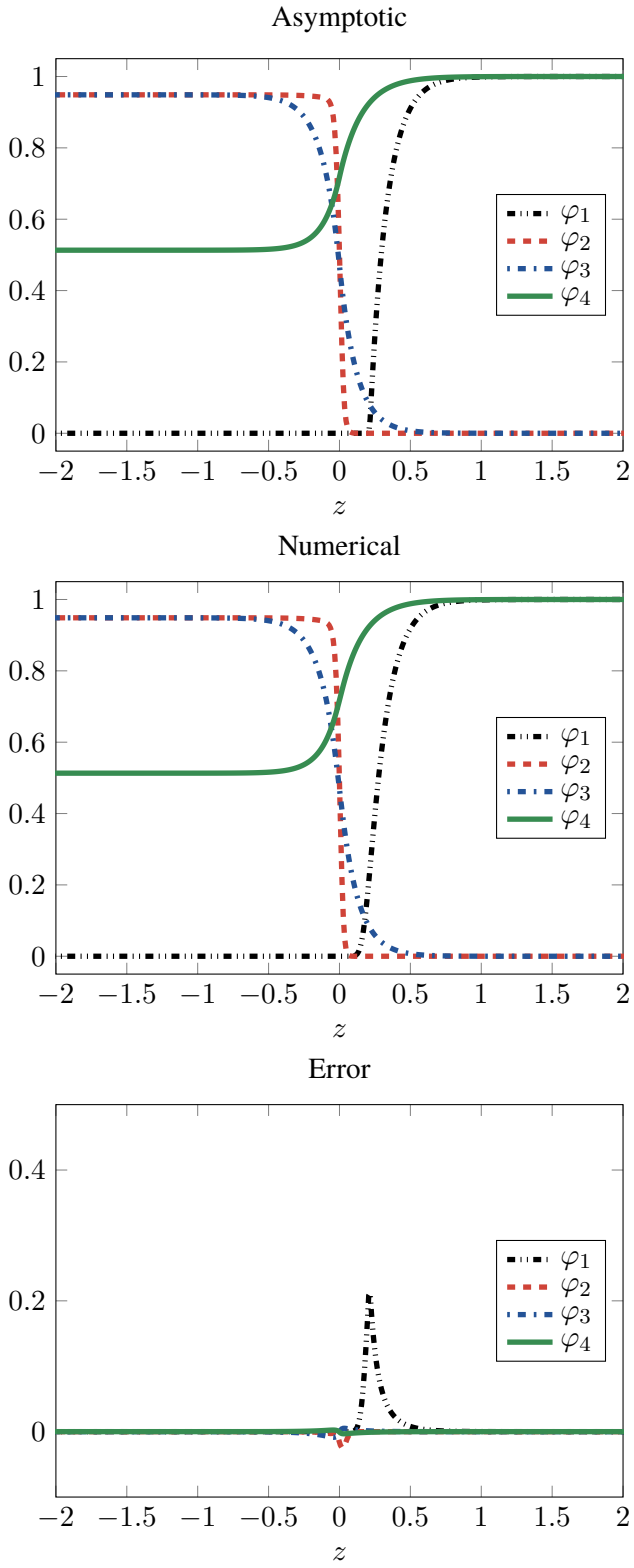

Figure 4.12: Asymptotic, Numerical and Error approximation of (4.2.7)–(4.2.10) with parameters $\alpha_1 = 1$, $\alpha_2 = 0.5$, $\beta_2 = 1$, $\beta_3 = 70$, $\beta_4 = 20$, $\delta_1 = 12.5$, $\delta_2 = 0.1$, $\delta_4 = 1$, $\theta = 0.0122$: The top and centre figures display the asymptotic and numerical solutions, respectively. The bottom figure displays the difference between the numerical and asymptotic solutions (i.e., numerical minus asymptotic). The maximum absolute errors for each solution are $E_1 = 0.2116$, $E_2 = 0.0246$, $E_3 = 0.0086$, $E_4 = 0.0033$

We remark that the value z^* can be calculated by solving $1 - \delta_1 \varphi_{3\text{out}}(z^*) = 0$ for $z^* > 0$ which gives

$$z^* = \frac{1}{\sqrt{\beta_3}} \ln \delta_1 \left[\frac{\hat{u}_2}{2} - \frac{3c_2\sqrt{\beta_3}}{4\delta_4} \int_{-\infty}^{0} \mathrm{e}^{\sqrt{\beta_3}s} \mathrm{sech}^2 \left(\frac{c_3}{2}[s - z_0] \right) \mathrm{d}s \right] = \frac{1}{\sqrt{\beta_3}} \ln \delta_1 \varphi_{3c}.$$

See an example of the asymptotic solution obtain in the case of high tumour aggressiveness in Figure 4.12, where the parameter values used are those utilised in the example displayed in Figure 4.5 and the speed is obtained from the minimal speed for (4.4.26). In Figure 4.12 a comparison of the asymptotic and corresponding numerical solution has been provided. In order to compare the solutions, a value was selected from the front of the numerical solution for φ_4 and matched to the position where the asymptotic solution for φ_4 obtains that value. The asymptotic solution was then subtracted from the numerical solution to obtain the error. It can be seen that there is excellent agreement between the asymptotic and numerical solutions for φ_2, φ_3 and φ_4 with the errors being of $O(\eta_2^{1/2})$ as is expected since the truncated terms in the asymptotic solution are $O(\eta_2^{1/2})$. However we note that the maximum absolute error for the solution to φ_1, located at the point z^*, is an order of magnitude greater than the expected error. This significant error is contained to a small region about z^* which suggests that the particular method used to obtain the solution may need to be refined to capture a steep change that occurs about this point. Outside of this small interval, the asymptotic solution for φ_1 is in excellent agreement with the numerical solution.

Statement of results for invading waves

The results of Section 4.4.1 can be summarised as follows:

Proposition 4.4.2. *Let* $c_2 = \sqrt{(1+\delta_4)^2 - 4\delta_2\delta_4}$, $c_3 = \sqrt{c_2\beta_4/\eta_4}$ *and let* $z_0 > 0$ *satisfy*

$$\left[\tanh^2 \left(\frac{c_3}{2} z_0 \right) - 1 \right] \left[\sqrt{c_2} \tanh \left(\frac{c_3}{2} z_0 \right) + 1 \right] + \frac{2\delta_2\delta_4(1 - \hat{u}_4)}{3c_2} = 0.$$

Furthermore, let

$$\varphi_{3c} = \frac{\hat{u}_2}{2} - \frac{3c_2\sqrt{\beta_3}}{4\delta_4} \int_{-\infty}^{0} \mathrm{e}^{\sqrt{\beta_3}s} \mathrm{sech}^2 \left(\frac{c_3}{2}[s - z_0] \right) \mathrm{d}s$$

and

$$\varphi_{4c} = \hat{u}_4 + \frac{3c_2}{2\delta_2\delta_4} \mathrm{sech}^2 \left(\frac{c_3}{2} z_0 \right).$$

Suppose $\theta = \theta_0 \eta_2^{1/2}$ *and* $\eta_1 = \eta_{10}\eta_2$*, where* $\theta_0, \eta_{10} > 0$ *and that*

$$1 - \delta_1\varphi_{3c} - \alpha_1(1 - \delta_2\varphi_{4c}) < 0, \quad 1 - \delta_2\varphi_{4c} > 0.$$

Let

$$\varphi_3(z;\eta_2) \simeq \begin{cases} \hat{u}_2 - \dfrac{\hat{u}_2}{2}\mathrm{e}^{\sqrt{\beta_3}z} - \dfrac{3c_2\sqrt{\beta_3}}{4\delta_4}\left[\displaystyle\int_z^0 \mathrm{e}^{\sqrt{\beta_3}(z-s)}\mathrm{sech}^2\left(\frac{c_3}{2}[s-z_0]\right)\mathrm{d}s \right. \\ \qquad\qquad \left. + \displaystyle\int_{-\infty}^z \mathrm{e}^{-\sqrt{\beta_3}(z-s)}\mathrm{sech}^2\left(\frac{c_3}{2}[s-z_0]\right)\mathrm{d}s\right] & \text{if } z < 0, \\ \left[\dfrac{\hat{u}_2}{2} - \dfrac{3c_2\sqrt{\beta_3}}{4\delta_4}\displaystyle\int_{-\infty}^0 \mathrm{e}^{\sqrt{\beta_3}s}\mathrm{sech}^2\left(\frac{c_3}{2}[s-z_0]\right)\mathrm{d}s\right]\mathrm{e}^{-\sqrt{\beta_3}z} & \text{if } z > 0. \end{cases} \tag{4.4.31}$$

and

$$\varphi_4(z;\eta_2) \simeq \begin{cases} \hat{u}_4 + \dfrac{3c_2}{2\delta_2\delta_4}\mathrm{sech}^2\left(\dfrac{c_3}{2}[z-z_0]\right) & \text{if } z < 0, \\ 1 + \left[\hat{u}_4 - 1 + \dfrac{3c_2}{2\delta_2\delta_4}\mathrm{sech}^2\left(\dfrac{c_3}{2}z_0\right)\right]\exp\left(-\sqrt{\dfrac{\beta_4}{\eta_4}}z\right) & \text{if } z > 0. \end{cases} \tag{4.4.32}$$

For $1 - \delta_1\varphi_{3c} > 0$ *let*

$$\varphi_1(z;\eta_2) \simeq \phi_1(z/\eta_2^{1/2};\theta_0) + \delta_1 \begin{cases} 0 & \text{if } z < 0, \\ \left[\dfrac{\hat{u}_2}{2} - \dfrac{3c_2\sqrt{\beta_3}}{4\delta_4}\displaystyle\int_{-\infty}^0 \mathrm{e}^{\sqrt{\beta_3}s}\mathrm{sech}^2\left(\frac{c_3}{2}[s-z_0]\right)\mathrm{d}s\right]\left(1 - \mathrm{e}^{-\sqrt{\beta_3}z}\right) & \text{if } z > 0 \end{cases} \tag{4.4.33}$$

and

$$\varphi_2(z;\eta_2) \simeq \phi_2(z/\eta_2^{1/2};\theta_0) + \frac{3c_2}{2\delta_4}\begin{cases} \mathrm{sech}^2\left(\dfrac{c_3}{2}z_0\right) - \mathrm{sech}^2\left(\dfrac{c_3}{2}[z-z_0]\right) & \text{if } z < 0, \\ 0 & \text{if } z > 0, \end{cases} \tag{4.4.34}$$

where $(\phi_1, \phi_2)(\xi;\theta_0)$ *solves the competition-diffusion system given by* (4.4.21)–(4.4.23) *and if* $1 - \delta_2\varphi_{4c} - \alpha_2(1 - \delta_1\varphi_{3c}) > 0$*, then* $\theta_0 \geq 2\sqrt{\beta_2[1 - \delta_2\varphi_{4c} - \alpha_2(1 - \delta_1\varphi_{3c})]}$.

For $1-\delta_1\varphi_{3c}<0$ *let*

$$\varphi_1(z;\eta_2)\simeq\begin{cases}0 & \text{if } z<z^*,\\ 1-\delta_1\left[\dfrac{\hat{u}_2}{2}-\dfrac{3c_2\sqrt{\beta_3}}{4\delta_4}\displaystyle\int_{-\infty}^{0}\mathrm{e}^{\sqrt{\beta_3}s}\mathrm{sech}^2\left(\frac{c_3}{2}[s-z_0]\right)\,\mathrm{d}s\right]\mathrm{e}^{-\sqrt{\beta_3}z} & \text{if } z>z^*,\end{cases} \tag{4.4.35}$$

where $z^*=\beta_3^{-1/2}\ln(\delta_1\varphi_{3c})$ *and*

$$\varphi_2(z;\eta_2)\simeq\phi_F(z/\eta_2^{1/2};\theta_0)+\frac{3c_2}{2\delta_4}\begin{cases}\mathrm{sech}^2\left(\dfrac{c_3}{2}z_0\right)-\mathrm{sech}^2\left(\dfrac{c_3}{2}[z-z_0]\right) & \text{if } z<0,\\ 0 & \text{if } z>0,\end{cases} \tag{4.4.36}$$

where ϕ_F *is the solution to the Fisher-KPP equation* (4.4.26) *with* $\theta_0\geq 2\sqrt{\beta_2[1-\delta_2\varphi_{4c}]}$. *Then* (4.4.31)–(4.4.36) *are asymptotic approximations compatible with solutions of* (4.4.2)–(4.4.5).

Discussed in [63, 71, 140] is the existence of an interstitial gap, which can be defined as an interval I, if any, where $\varphi_1(z;\eta_2)+\varphi_2(z;\eta_2)\ll 1$ for all $z\in I$. If we consider the case when $1-\delta_1\varphi_{3c}<0$ then from (4.4.36) we can see for small η_2 we have for $z\gtrsim 0$ that $\varphi_2(z;\eta_2)\ll 1$ and for $z<z^*$ that $\varphi_1(z;\eta_2)\ll 1$. Hence we see that $I\sim(0,z^*)$ so the width of the interstitial gap is approximately

$$z^*=\frac{1}{\sqrt{\beta_3}}\ln(\delta_1\varphi_{3c});\quad 1-\delta_1\varphi_{3c}<0.$$

Consider the estimates of the minimal speed of invasion obtained from the asymptotic analysis, that is, $\theta\geq 2\sqrt{\eta_2\beta_2[1-\delta_2\varphi_{4c}-\alpha_2(1-\delta_1\varphi_{3c})]}$ for low tumour aggressiveness and $\theta\geq 2\sqrt{\eta_2\beta_2[1-\delta_2\varphi_{4c}]}$ for high tumour aggressiveness. Note that both these speeds are greater than the minimal speed, i.e. $\theta_m=2\sqrt{\beta_2\eta_2(1-\alpha_2-\delta_2)}$, obtained from the linearisation technique used in Section 4.3.1. However, when comparing the asymptotic estimates to the results in [76, 140] for the minimal speed of invasion, for a sufficiently aggressive tumour, we see that the presence of chemotherapy whilst not stopping the invasion of the tumour does decrease the minimal speed and slow the tumour progression as would be expected.

4.4.2 Analysis for receding tumour

For the convenience of the reader a summary of the following results have been provided at the end of the section. Note that if SS2 is stable, SS3 is unstable and assuming a TW solution exists, then the minimum speed for existence of a TW is $\theta=2\sqrt{\eta_1(1-[\alpha_1+\delta_1]\hat{u}_2)}$, which suggests that $\theta=O(\eta_1^{1/2})$. It was noted in Section 4.4.1 that $0<\eta_1,\eta_2\ll 1$, hence we wish to perform

an analysis in which we assume that $\eta_1 = \varepsilon^2$, $\theta = \theta_0\varepsilon$ where $\theta_0 < 0$ and $\theta_0 = O(1)$ as $\varepsilon \to 0^+$. The analysis of receding tumour waves is complicated by the development of splitting fronts for parameters conditions which largely remain uncertain. This splitting behaviour does not meet the requirements of a traditional TW, however through the asymptotic analysis of the receding TW we wish to gain an insight into when this splitting behaviour may occur. As noted for the previous section we have that typically $\eta_2 = O(\eta_1)$, hence we wish to assume that $\eta_2 = \eta_{20}\varepsilon^2$ where $\eta_{20} > 0$ and $\eta_{20} = O(1)$ as $\varepsilon \to 0^+$. Therefore, as previously, we let $z = x - \theta t$, and make these substitutions in (4.2.7)–(4.2.10), with

$$(u_1, u_2, u_3, u_4)(x, t; \varepsilon) = (\varphi_1, \varphi_2, \varphi_3, \varphi_4)(z; \varepsilon),$$

to obtain

$$\varepsilon^2\varphi_1'' + \theta_0\varepsilon\varphi_1' + \varphi_1(1 - \varphi_1 - \alpha_1\varphi_2 - \delta_1\varphi_3) = 0, \tag{4.4.37}$$

$$\eta_{20}\varepsilon^2\varphi_2'' + \theta_0\varepsilon\varphi_2' + \beta_2\varphi_2(1 - \varphi_2 - \alpha_2\varphi_1 - \delta_2\varphi_4) = 0, \tag{4.4.38}$$

$$\varphi_3'' + \theta_0\varepsilon\varphi_3' + \beta_3(\varphi_2 - \varphi_3) = 0, \tag{4.4.39}$$

$$\eta_4\varphi_4'' + \theta_0\varepsilon\varphi_4' + \beta_4(1 - \varphi_4 - \delta_4\varphi_4\varphi_2) = 0, \tag{4.4.40}$$

with BCs

$$(\varphi_1, \varphi_2, \varphi_3, \varphi_4)(-\infty) = (0, \hat{u}_2, \hat{u}_2, [1 + \delta_4\hat{u}_2]^{-1})$$

and

$$(\varphi_1, \varphi_2, \varphi_3, \varphi_4)(\infty) = (1, 0, 0, 1),$$

where $(\,)'$ represents differentiation with respect to z. We once again use the theory of matched asymptotic expansions to obtain approximate solutions.

Uniform approximation for the drug concentration and H^+ ion concentration

We define the outer solution by

$$(\varphi_{1\mathrm{out}}, \varphi_{2\mathrm{out}}, \varphi_{3\mathrm{out}}, \varphi_{4\mathrm{out}})(z) = (\varphi_1, \varphi_2, \varphi_3, \varphi_4)(z; 0).$$

Hence letting $\varepsilon \to 0^+$ in (4.4.37)–(4.4.40) gives

$$\begin{aligned}
\varphi_{1\text{out}}(1 - \varphi_{1\text{out}} - \alpha_1\varphi_{2\text{out}} - \delta_1\varphi_{3\text{out}}) &= 0,\\
\beta_2\varphi_{2\text{out}}(1 - \varphi_{2\text{out}} - \alpha_2\varphi_{1\text{out}} - \delta_2\varphi_{4\text{out}}) &= 0,\\
\varphi''_{3\text{out}} + \beta_3(\varphi_{2\text{out}} - \varphi_{3\text{out}}) &= 0,\\
\eta_4\varphi''_{4\text{out}} + \beta_4(1 - \varphi_{4\text{out}} - \delta_4\varphi_{4\text{out}}\varphi_{2\text{out}}) &= 0,
\end{aligned} \tag{4.4.41}$$

where

$$(\varphi_{1\text{out}}, \varphi_{2\text{out}}, \varphi_{3\text{out}}, \varphi_{4\text{out}})(-\infty) = (0, \hat{u}_2, \hat{u}_2, [1 + \delta_4\hat{u}_2]^{-1})$$

and

$$(\varphi_{1\text{out}}, \varphi_{2\text{out}}, \varphi_{3\text{out}}, \varphi_{4\text{out}})(-\infty) = (1, 0, 0, 1).$$

We set $z = 0$ to be the region in which φ_1 and φ_2 undergo a sudden change and introduce the stretched inner variable $\xi = z/\varepsilon$ into (4.4.37)–(4.4.40) to consider the change in this region. We let the inner solution be denoted by

$$(\varphi_{1\text{in}}, \varphi_{2\text{in}}, \varphi_{3\text{in}}, \varphi_{4\text{in}})(\xi) = \lim_{\varepsilon\to 0^+}(\varphi_1, \varphi_2, \varphi_3, \varphi_4)(\varepsilon\xi; \varepsilon).$$

Hence making the substitution $\xi = z/\varepsilon$ into (4.4.37)–(4.4.40) and letting $\varepsilon \to 0^+$ we obtain

$$\ddot{\varphi}_{1\text{in}} + \theta_0\dot{\varphi}_{1\text{in}} + \varphi_{1\text{in}}(1 - \varphi_{1\text{in}} - \alpha_1\varphi_{2\text{in}} - \delta_1\varphi_{3\text{in}}) = 0, \tag{4.4.42}$$

$$\eta_{20}\ddot{\varphi}_{2\text{in}} + \theta_0\dot{\varphi}_{2\text{in}} + \beta_2\varphi_{2\text{in}}(1 - \varphi_{2\text{in}} - \alpha_2\varphi_{1\text{in}} - \delta_2\varphi_{4\text{in}}) = 0, \tag{4.4.43}$$

$$\begin{aligned}
\ddot{\varphi}_{3\text{in}} &= 0,\\
\ddot{\varphi}_{4\text{in}} &= 0,
\end{aligned}$$

where $\dot{(\,)}$ denotes differentiation with respect to ξ. The boundary conditions for the inner solutions are obtained from the matching conditions

$$(\varphi_{1\text{out}}, \varphi_{2\text{out}}, \varphi_{3\text{out}}, \varphi_{4\text{out}})(0\pm) = (\varphi_{1\text{in}}, \varphi_{2\text{in}}, \varphi_{3\text{in}}, \varphi_{4\text{in}})(\pm\infty). \tag{4.4.44}$$

Consider $\varphi_{2\text{out}}(z) = 0$ for $z > 0$ which we can see satisfies (4.4.41) and moreover, assuming

that $1-\delta_1\varphi_{3\text{out}}(z)>0$ for $z>0$, then the solution

$$\varphi_{1\text{out}}(z)=\begin{cases}0 & \text{if } z<0,\\ 1-\delta_1\varphi_{3\text{out}}(z) & \text{if } z>0,\end{cases}$$

satisfies (4.4.42). Furthermore, assuming that $1-\delta_2\varphi_{4\text{out}}(z)>0$ for $z<0$, then

$$\varphi_{2\text{out}}(z)=\begin{cases}1-\delta_2\varphi_{4\text{out}}(z) & \text{if } z<0,\\ 0 & \text{if } z>0,\end{cases} \tag{4.4.45}$$

satisfies (4.4.41). Using (4.4.45) we note that the equations governing $\varphi_{3\text{out}}$, $\varphi_{4\text{out}}$, $\varphi_{3\text{in}}$, and $\varphi_{4\text{in}}$ are the same as those considered in the asymptotic analysis for the invading tumour, i.e. (4.4.8), (4.4.9), (4.4.10) and (4.4.11), respectively. Hence the outer and inner solutions for φ_3 and φ_4 will be the same as obtained in the invading case, i.e. (4.4.18) and (4.4.15) for the outer solutions and (4.4.19) and (4.4.14) for the inner solutions, respectively. It then follows that the uniform approximations for $\varphi_3(z;\varepsilon)$ and $\varphi_4(z;\varepsilon)$ will be given by (4.4.20) and (4.4.17), respectively.

Uniform approximation for the tumour and normal tissue cell density

Noting that we have $\varphi_{3\text{in}}(\xi)=\varphi_{3\text{out}}(0\pm)=\varphi_{3c}$ and $\varphi_{4\text{in}}(\xi)=\varphi_{4\text{out}}(0\pm)=\varphi_{4c}$, then (4.4.42) and (4.4.43) become

$$\ddot{\varphi}_{1\text{in}}+\theta_0\dot{\varphi}_{1\text{in}}+\varphi_{1\text{in}}(1-\delta_1\varphi_{3c}-\varphi_{1\text{in}}-\alpha_1\varphi_{2\text{in}})=0, \tag{4.4.46}$$

$$\eta_{20}\ddot{\varphi}_{2\text{in}}+\theta_0\dot{\varphi}_{2\text{in}}+\beta_2\varphi_{2\text{in}}(1-\delta_2\varphi_{4c}-\varphi_{2\text{in}}-\alpha_2\varphi_{1\text{in}})=0, \tag{4.4.47}$$

with BCs

$$(\varphi_{1\text{in}},\varphi_{2\text{in}})(-\infty)=(0,1-\delta_2\varphi_{4c})\quad\text{and}\quad(\varphi_{1\text{in}},\varphi_{2\text{in}})(\infty)=(1-\delta_1\varphi_{3c},0), \tag{4.4.48}$$

which have been determined by the matching conditions (4.4.44). By our assumptions we require that $1-\delta_2\varphi_{4c}>0$ and $1-\delta_1\varphi_{3c}>0$. This is a traditional competition-diffusion system and from the results in [99, 107], if $1-\delta_1\varphi_{3c}-\alpha_1(1-\delta_2\varphi_{4c})>0$ and $1-\delta_2\varphi_{4c}-\alpha_2(1-\delta_1\varphi_{3c})<0$, then a class of TWs exist in which $\theta_0\leq-2\sqrt{1-\delta_1\varphi_{3c}-\alpha_1(1-\delta_2\varphi_{4c})}$. If how-

ever $1-\delta_1\varphi_{3c}-\alpha_1(1-\delta_2\varphi_{4c}) < 0$ and $1-\delta_2\varphi_{4c}-\alpha_2(1-\delta_1\varphi_{3c}) < 0$, then from the results in [106] there exists a class of monotone TWs for (4.4.46)–(4.4.48) with minimal speed $\theta_m = \theta_m(\alpha_1,\alpha_2,\beta_2,\beta_3,\beta_4,\delta_1,\delta_2,\delta_4,\eta_4)$, where $-2\sqrt{1-\delta_1\varphi_{3c}} < \theta_m < 2\sqrt{\eta_{20}\beta_2(1-\delta_2\varphi_{4c})}$. As we have assumed that $\theta_0 < 0$, we can only say that $\theta_0 < 0$ with certainty in the case $1-\delta_1\varphi_{3c}-\alpha_1(1-\delta_2\varphi_{4c}) > 0$. We do not exclude the possibility of a negative speed should this condition not be met, however we cannot make a definitive statement about the sign of the speed. We can now obtain the common values in the overlap region for φ_1 and φ_2 denoted by φ_{1c} and φ_{2c}, respectively. We obtain the values

$$\varphi_{1c} = \begin{cases} \varphi_{1\text{in}}(-\infty) = \varphi_{1\text{out}}(0-) = 0 & \text{if } z < 0, \\ \varphi_{1\text{in}}(\infty) = \varphi_{1\text{out}}(0+) = 1-\delta_1\varphi_{3c} & \text{if } z > 0 \end{cases}$$

and

$$\varphi_{2c} = \begin{cases} \varphi_{2\text{in}}(-\infty) = \varphi_{2\text{out}}(0-) = 1-\delta_2\varphi_{4c} & \text{if } z < 0, \\ \varphi_{2\text{in}}(\infty) = \varphi_{2\text{out}}(0+) = 0 & \text{if } z > 0. \end{cases}$$

Therefore the uniform approximation for φ_1 and φ_2 in the case $0 < 1-\delta_2\varphi_{4c} < \alpha_2(1-\delta_1\varphi_{3c})$ are

$$\begin{aligned} \varphi_1(z;\varepsilon) &\simeq \varphi_{1\text{out}}(z) + \varphi_{1\text{in}}(z/\varepsilon) - \varphi_{1c}, \\ &= \psi_1(z/\varepsilon;\theta_0) \\ &\quad + \delta_1 \begin{cases} 0 & \text{if } z < 0, \\ \left[\dfrac{\hat{u}_2}{2} - \dfrac{3c_2\sqrt{\beta_3}}{4\delta_4}\displaystyle\int_{-\infty}^{0} \mathrm{e}^{\sqrt{\beta_3}s}\operatorname{sech}^2\left(\frac{c_3}{2}[s-z_0]\right)\,\mathrm{d}s\right]\left(1-\mathrm{e}^{-\sqrt{\beta_3}z}\right) & \text{if } z > 0 \end{cases} \end{aligned}$$

and

$$\begin{aligned} \varphi_2(z;\varepsilon) &\simeq \varphi_{2\text{out}}(z) + \varphi_{2\text{in}}(z/\varepsilon) - \varphi_{2c}, \\ &= \psi_2(z/\varepsilon;\theta_0) \\ &\quad + \frac{3c_2}{2\delta_4} \begin{cases} \operatorname{sech}^2\left(\dfrac{c_3}{2}z_0\right) - \operatorname{sech}^2\left(\dfrac{c_3}{2}[z-z_0]\right) & \text{if } z < 0, \\ 0 & \text{if } z > 0, \end{cases} \end{aligned}$$

where $(\varphi_{1\text{in}},\varphi_{2\text{in}})(\xi) = (\psi_1,\psi_2)(\xi;\theta_0)$ solve (4.4.46)–(4.4.48). Furthermore, if $1-\delta_1\varphi_{3c}-$

$\alpha_1(1-\delta_2\varphi_{4c}) > 0$, then the inner solutions have speed $\theta_0 \leq -2\sqrt{\beta_2[1-\delta_1\varphi_{3c}-\alpha_1(1-\delta_2\varphi_{4c})]}$ and as $\theta = \theta_0\eta_1^{1/2}$ our uniform solutions will have speed $\theta \leq -2\sqrt{\eta_1[1-\delta_1\varphi_{3c}-\alpha_1(1-\delta_2\varphi_{4c})]}$.

For this analysis we made the assumption that $1-\delta_2\varphi_{4\text{out}}(z) > 0$ for $z < 0$. Without this assumption we would require the use of the outer solution for φ_2 of $\varphi_{2\text{out}}(z) = 0$ for $z > z^*$, where $z^* < 0$, which would result in a similar analysis to that used for the invading tumour in the case of high tumour aggressiveness. This outer solution and the resulting uniform approximation that follows would suggest the existence of an interstitial gap in the case that the wave is receding. We note that we have only observed this behaviour when we see the splitting wave, hence this approximation would seem to be no longer valid since a traditional TW would not exist for the system. Hence we predict that if the splitting wave behaviour occurs then $1-\delta_2\varphi_{4c} < 0$ or $\varphi_{4c} \notin \mathbb{R}$. If we consider the example of the splitting wave in Figure 4.3 we find that z_0 does not satisfy the condition $z_0 > 0$, hence φ_{4c} does not exist (i.e. $\varphi_{4c} \notin \mathbb{R}$). Hence we say that this provides a condition for when the chemotherapy treatment would be able to remove the tumour without natural competition created by the host.

Statement of results for receding waves

The results of Section 4.4.2 can be summarised as follows:

Proposition 4.4.3. *Let $c_2, c_3, z_0, \varphi_{3c}$ and φ_{4c} be as in Proposition 4.4.2. Suppose $0 < 1-\delta_2\varphi_{4c} < \alpha_2(1-\delta_1\varphi_{3c})$, $\theta = \theta_0\eta_1^{1/2}$ and $\eta_2 = \eta_{20}\eta_1$ where $\theta_0 < 0$ and $\eta_{20} > 0$. Let*

$$\varphi_1(z;\eta_1) \simeq \psi_1(z/\eta_1^{1/2};\theta_0) + \delta_1 \begin{cases} 0 & \text{if } z < 0, \\ \left[\dfrac{\hat{u}_2}{2} - \dfrac{3c_2\sqrt{\beta_3}}{4\delta_4}\displaystyle\int_{-\infty}^{0} \mathrm{e}^{\sqrt{\beta_3}s}\operatorname{sech}^2\left(\frac{c_3}{2}[s-z_0]\right)\,\mathrm{d}s\right]\left(1-\mathrm{e}^{-\sqrt{\beta_3}z}\right) & \text{if } z > 0, \end{cases} \tag{4.4.49}$$

$$\varphi_2(z;\eta_1) \simeq \psi_2(z/\eta_1^{1/2};\theta_0) + \frac{3c_2}{2\delta_4}\begin{cases} \operatorname{sech}^2\left(\dfrac{c_3}{2}z_0\right) - \operatorname{sech}^2\left(\dfrac{c_3}{2}[z-z_0]\right) & \text{if } z < 0, \\ 0 & \text{if } z > 0, \end{cases} \tag{4.4.50}$$

where $(\psi_1, \psi_2)(\xi; \theta_0)$ *solve* (4.4.46)–(4.4.48)*,*

$$\varphi_3(z;\eta_1) \simeq \begin{cases} \hat{u}_2 - \dfrac{\hat{u}_2}{2}\mathrm{e}^{\sqrt{\beta_3}z} - \dfrac{3c_2\sqrt{\beta_3}}{4\delta_4}\left[\displaystyle\int_z^0 \mathrm{e}^{\sqrt{\beta_3}(z-s)}\mathrm{sech}^2\left(\frac{c_3}{2}[s-z_0]\right)\mathrm{d}s \right. \\ \qquad\qquad \left. + \displaystyle\int_{-\infty}^z \mathrm{e}^{-\sqrt{\beta_3}(z-s)}\mathrm{sech}^2\left(\frac{c_3}{2}[s-z_0]\right)\mathrm{d}s\right] & \text{if } z<0, \\ \left[\dfrac{\hat{u}_2}{2} - \dfrac{3c_2\sqrt{\beta_3}}{4\delta_4}\displaystyle\int_{-\infty}^0 \mathrm{e}^{\sqrt{\beta_3}s}\mathrm{sech}^2\left(\frac{c_3}{2}[s-z_0]\right)\mathrm{d}s\right]\mathrm{e}^{-\sqrt{\beta_3}z} & \text{if } z>0, \end{cases} \tag{4.4.51}$$

and

$$\varphi_4(z;\eta_1) \simeq \begin{cases} \hat{u}_4 + \dfrac{3c_2}{2\delta_2\delta_4}\mathrm{sech}^2\left(\dfrac{c_3}{2}[z-z_0]\right) & \text{if } z<0, \\ 1 + \left[\hat{u}_4 - 1 + \dfrac{3c_2}{2\delta_2\delta_4}\mathrm{sech}^2\left(\dfrac{c_3}{2}z_0\right)\right]\exp\left(-\sqrt{\dfrac{\beta_4}{\eta_4}}z\right) & \text{if } z>0. \end{cases} \tag{4.4.52}$$

If $1-\delta_1\varphi_{3c}-\alpha_1(1-\delta_2\varphi_{4c})>0$ *then* $\theta_0 \leq -2\sqrt{1-\delta_1\varphi_{3c}-\alpha_1(1-\delta_2\varphi_{4c})}$*. Then* (4.4.49)–(4.4.52) *are asymptotic approximations compatible with solutions of* (4.4.37)–(4.4.40)*.*

Discussed in Section 4.3.1 is the formation of splitting waves which are TW-like solutions with fronts that travel at different speeds. From the asymptotic analysis of the receding wave we predict that if splitting behaviour occurs, then $1-\delta_2\varphi_{4c}<0$ or $\varphi_{4c}\notin\mathbb{R}$. The splitting behaviour can be interpreted as a situation in which chemotherapy is strong enough to destroy the tumour population without the assistance of population competition, hence we say that $1-\delta_2\varphi_{4c}<0$ represents a condition for which treatment will be strong enough to destroy the tumour.

4.5 Discussion and concluding remarks

In this chapter we considered a RD model for acid-mediated invasion that includes the effects of treatment with a cytotoxic chemotherapy drug. The model is an extension of that proposed in Chapter 3 and was developed to add to the quantitative and qualitative results obtained for the original model. Chapter 3 considered the dynamics of a model of spatially homogeneous populations, whereas the model presented in this chapter assumes a spatially heterogeneous distribution of cell populations. The model has been considered using both numerical and analytical techniques.

As in Chapter 3, the effects of both constant infusion and periodic infusion have been examined. Constant infusion resulted in an autonomous system that was examined using techniques for TW solutions and periodic infusion resulted in a model with time-periodic terms that can be analysed using techniques for TPTW solutions. In both cases, interesting behaviour such as split-

ting waves was exhibited and indicated an important influence of the chemical diffusion properties of the chemotherapy drug in removing what would otherwise be a stable tumour population. For highly aggressive tumours in which the acid has a strong destructive effect, the chemotherapy was effective in slowing, often reversing, the tumour's invasion, overcoming the evolutionary advantage the tumour gained over the normal tissue. The destructive influence of the acid could only facilitate invasion when the treatment strength was low or when the treatment required the assistance of normal tissue population competition in order to be effective. In the latter case, provided a sufficiently destructive tumour, the acid would destroy normal cells ahead of the tumour removing the cellular competition which enabled the treatment to be effective.

Comparisons can be drawn between the results obtained here and those obtained by Fasano et al. [63]. This chapter and [63] considered a RD model for the acid mediation hypothesis for which asymptotic approximations were obtained. Important distinctions between the models are that here constant diffusion terms and terms for population competition have been utilised, whereas in [63] a nonlinear diffusion term is used for the tumour motility and population competition is assumed to be negligible. As was noted in the Introduction, the dynamics of the nonlinear diffusion term tends to that of the constant diffusion terms used in this chapter when an aggressive tumour is considered. Moreover, the aggressive tumour creates a region almost devoid of cells that separates the tumour and normal cell populations, thus removing the effects of population competition from the model. Hence we can only effectively compare the results obtained from these models for aggressively invading tumours. In the model considered in this chapter, provided the parameter conditions of Proposition 4.4.2 are met, an aggressively invading tumour occurs under the parameter condition $1 - \delta_1\varphi_{3c} < 0$; under this condition the tumour invades with a minimal wave speed of $\theta = 2\sqrt{\eta_2\beta_2(1 - \delta_2\varphi_{4c})}$. In [63] an aggressively invading tumour occurs for smaller values of δ_1 and also invades at faster speeds. Moreover, for an aggressively invading tumour, as previously mentioned, there exists an interstitial gap between the tumour and normal cell populations. The interstitial gap is estimated to have width $z^* = \beta_3^{-1/2} \ln(\delta_1\varphi_{3c})$, which is less than the estimate for the gap width obtained in [63]. From the comparison of the speed and gap width, it can be seen that even when the chemotherapy is unable to remove the tumour, the speed of invasion will be slowed and the overall destructive influence of the acid will implicitly be decreased due to a reduced capacity to produce acid by preventing tumour cells from reaching carrying capacity. As is noted in Section 2.6, due to the size of the spatial scale of our model in comparison to that of experimentally observed interstitial gaps, the extent to which this prediction of the gap width is

quantitatively useful is limited as the errors in the estimate are likely to be in the order of the size of a realistic gap width. Hence this estimate may be of more use qualitatively to determine the effect of different mechanisms in the model that govern the level of interaction between the normal and tumour tissue, that is, the conditions that predict an interstitial gap imply the conditions in which there is little to no direct interaction between the normal and tumour cell populations.

If we compare the results obtained from the ODE model examined in Chapter 3 to those obtained for the PDE model considered here, it can be seen that many of the insights that the PDE model provided were able to be gained from the ODE model alone. The ODE model had the capacity to predict very general aspects of the tumour behaviour such as if a tumour would invade or if a tumour would be eradicated from the system given particular model parameters. The ODE however was not able to answer questions about the speed of invasion or the speed at which the tumour would recede. In the cases in which the model is bistable, the ability to make definitive predictions about the long-term behaviour is made more difficult in the ODE model. From the PDE model, not only were predictions able to be made about the speed of invasion and recession, but behaviours such as the development of an interstitial gap are observed and predictions about the size of the gap and the parameter conditions in which the gap would develop were able to be made. Behaviours such as splitting waves occurred in the PDE model, which gave greater insights into when drugs are sufficient to remove tumours without the assistance of other population competition.

Finally, we remark that in the article of Gatenby and Gillies [73] they note that tumour acidity has been associated to decreased effectiveness of anthracyclines as a result of greater phenotypic diversity [64] which is enabled by the mutagenic/clastogenic effects of an acidic environment. We concede that this has not been explicitly demonstrated in our model. This is likely due to the fact that our model does not consider a mutagenic process and as such an extension to the model would need to be made to examine this observed behaviour. One possible extension could be for the term $\delta_2 u_2 u_4$ in (4.2.8) to be made a function which decreases proportionally to concentration of acid and the length of time the tumour cells have been exposed to that acid to account for the mutagenic/clastogenic effects.

4.A Auxiliary results

Lemma 4.A.1. *Consider the initial value problem*

$$\frac{\partial u}{\partial \tau} = d\frac{\partial^2 u}{\partial z^2} + \theta\frac{\partial u}{\partial z} + f(\tau)u + g(z,\tau), \quad u(z,0) = u_0(z); \quad -\infty < z < \infty, \tag{4.A.1}$$

where $d, \theta > 0$, $f \in C(\mathbb{R})$ *and* $g \in C(\mathbb{R}^2)$. *Let*

$$u(z,\tau) = \int_{-\infty}^{\infty} u_0(y)\Phi(z-y,\tau,0)\,\mathrm{d}y + \int_0^{\tau}\int_{-\infty}^{\infty} g(y,s)\Phi(z-y,\tau,s)\,\mathrm{d}y\mathrm{d}s, \tag{4.A.2}$$

where

$$\Phi(z,\tau,s) = \frac{1}{2\sqrt{d\pi(\tau-s)}}\exp\left[-\frac{(z+\theta[\tau-s])^2}{4d(\tau-s)} + \int_s^{\tau} f(s')\,\mathrm{d}s'\right]. \tag{4.A.3}$$

Then (4.A.2) *and* (4.A.3) *solves* (4.A.1).

Proof. Let $x = z + \theta\tau$ and

$$u(z,\tau) = \exp\left[\int_0^{\tau} f(s')\,\mathrm{d}s'\right] w(x,\tau),$$

then (4.A.1) reduces to

$$\frac{\partial w}{\partial \tau} = d\frac{\partial^2 w}{\partial x^2} + \exp\left[-\int_0^{\tau} f(s')\,\mathrm{d}s'\right] g(x-\theta\tau,\tau); \quad w(x,0) = u_0(x).$$

The solution for this system is then given by [167, 1.1.2-1]. It is then straightforward to show that u is given by (4.A.2). □

4.B Tables of parameter values

Table 4.1 provides the meaning and potential values of the parameters contained in (4.2.1)–(4.2.3). Table 4.2 provides non-dimensional parameters contained in (4.2.7)–(4.2.10) with an interpretation of their meaning and potential values/range of values.

Table 4.1: Table of parameters and estimated values

Parameter	Units	Description	Value	Source
r_1	s^{-1}	normal cell growth rate	$O(10^{-6})$	[49, 71]
r_2	s^{-1}	tumour cell growth rate	$O(10^{-6})$	[49, 71]
r_3	$\mathrm{M\,cm^3\,s^{-1}cells^{-1}}$	H^+ ion production rate	2.2×10^{-17}	[133]
d_1	$\mathrm{M^{-1}\,s^{-1}}$	fractional normal cell kill by H^+ ions	$O(1)$	[71]
d_2	$\mathrm{M^{-1}\,s^{-1}}$	fractional tumor cell kill by chemotherapy	9.3×10^{-6}	[50]
d_4	$\mathrm{cells^{-1}\,s^{-1}}$	fractional chemotherapy removal by tumour interaction	$O(10^{-13})$–$O(10^{-12})$	estimated
m_3	s^{-1}	H^+ ion removal rate	$O(10^{-4})$	[71]
m_4	s^{-1}	chemotherapy removal rate	$O(10^{-5})$	[49, 104]
K_1	$\mathrm{cells\,cm^{-3}}$	normal cell carrying capacity	5×10^7	[195]
K_2	$\mathrm{cells\,cm^{-3}}$	tumour cell carrying capacity	5×10^7	[195]
D_1	$\mathrm{cm^2\,s^{-1}}$	normal cell diffusion coefficient	$O(10^{-10})$	$O(D_2)$
D_2	$\mathrm{cm^2\,s^{-1}}$	tumour cell diffusion coefficient	2×10^{-10}	[45]
D_3	$\mathrm{cm^2\,s^{-1}}$	H^+ ion diffusion coefficient	5×10^{-6}	[123]
D_4	$\mathrm{cm^2\,s^{-1}}$	chemotherapy diffusion coefficient	5×10^{-6}	estimated
α_1	none	fractional normal cell death due to tumour cell	$O(1)$	chosen freely
α_2	none	fractional tumour cell death due to normal cell	$O(1)$	chosen freely

Table 4.2: Table of non-dimensionalised parameters

Parameter	Interpretation	Value/Range
α_1	fractional normal death due to tumour competition	$O(1)$
α_2	fractional tumour death due to normal competition	$O(1)$
η_1	relative normal-H^+ ion diffusion rate	4×10^{-5}
η_2	relative tumour-H^+ ion diffusion rate	$O(10^{-5})$
η_4	relative chemotherapy-H^+ ion diffusion rate	$O(1)$
δ_1	tumour aggressiveness	$O(1)$
δ_2	chemotherapy aggressiveness	$O(10^{-1})$–$O(1)$
δ_4	fractional removal due to interaction strength	$O(10^{-1})$–$O(1)$
β_2	relative tumour growth rate	1.0
β_3	relative H^+ ion production rate	$O(10^2)$
β_4	relative chemotherapy rate of increase	$O(10)$

Chapter 5

Integration-based parameter estimation

5.1 Introduction

The application of ODEs to modelling the physical world is extensive and widely studied in many fields including physics, engineering and bioinformatics. Using these models to predict the behaviour of important state variables given particular parameter values has been extensively studied. The inverse problem of predicting the parameter values that appear in an ODE based on observed data has been studied considerably less and traditionally only a few methods have been used, many of which approach the problem via a LS fit method (see for example [8, 11, 93, 121] and the references therein). As discussed in Chapter 1, these methods generate a distance function between the system solution and the observed data which is then minimised with respect to the system parameters. If the ODE system can be solved analytically, the distance function is often highly nonlinear making it computationally expensive to find a global minimum [59]. Alternatively, when the model can only be solved numerically, an iterative scheme is used in which a trajectory is found by solving the ODE system for different parameters and comparing the LS distances. This method can be very inefficient and is not guaranteed to return the global minimum, hence much of the focus is on creating stable and efficient algorithms to optimise this approach [59, 172].

There are more recently proposed parameter estimation methods. One such method utilises a hierarchical Bayesian approach to estimate dynamic parameters [9, 100, 169]. Liang and Wu [122] proposed a local kernel smoothing-based approach to estimate constant parameters. Cubic spline interpolation in conjunction with a LS procedure has been used to estimate dynamic parameters [171]. A spline-based smoothing approach has also been considered in [172] to estimate constant parameters. A method based on integrator theory has been considered in [160] in which a

condition is imposed on the ODE to ensure convergence to the true parameter values.

We remark that the ability to estimate parameters accurately and efficiently is very important for tumour modelling as the future behaviour and treatment of a tumour is determined by various parameter values. For example, if we consider the models examined in Chapters 2, 3 and 4 we can see that these models all require knowledge of the values of parameters such as the population carrying capacity, growth rate and population competition values. We also note the ability to effectively estimate parameters is useful for the analysis of RD equations in which TW solutions arise. Travelling wave solutions transform the governing system of PDEs into a system of ODEs with an introduced parameter, a parameter that needs to be determined. Using a parameter estimation technique and the solution obtained from solving the PDE system, with a sufficiently large time domain, the introduced parameter can be estimated, as was performed in Chapter 2.

This chapter will propose an integration-based method that transforms an ODE to an algebraic system of equations for which we solve for the unknown parameters in our ODE. The method will be computationally unintensive, can be extended to systems of differential equations and the number of parameters that can be estimated is not restricted. The method will be demonstrated by simulating data, with and without noise, from a number of biological models described by ODEs and then estimating the parameters via the proposed technique.

This chapter is organised as follows. In Section 5.2 we will outline this procedure in more detail. Section 5.3 will contain applications of this method to some well-studied problems in which simulated data will be used, with and without noise, to demonstrate the viability of the proposed method. We will make some concluding remarks and discuss potential further analysis for this method in Section 5.4.

5.2 Method

The method we propose considers an ODE with m unknown parameters and then multiplies the system by a given weight function that contains a controllable parameter β, that we will call an "equation-generating parameter". The system is then integrated over a finite interval, in what can be thought of as being analogous to a finite Laplace transform, to remove the derivatives contained within the equation. This integration over an interval can also be thought of as taking a weighted average of each term in the system. We will then substitute m values of our controllable parameter β, for example $\beta_1, \ldots, \beta_m$, into our transformed equation to then give us a set of m distinct al-

gebraic equations in the parameters that will have terms which can be approximated by numerical integration using observed data for the values of the state variable.

To simplify the description of the method we consider an ODE of the form

$$\frac{\mathrm{d}x}{\mathrm{d}t} = f(x, t; \boldsymbol{\theta}), \qquad x(0) = x_0, \tag{5.2.1}$$

where $x : \mathbb{R} \to \mathbb{R}$, $f : \mathbb{R}^{m+2} \to \mathbb{R}$, $\boldsymbol{\theta} \in \mathbb{R}^m$, $x_0 \in \mathbb{R}$ and we wish to estimate $\boldsymbol{\theta}$. Assume that the dependent variable x is observed over a time interval I and consider a weight function $\phi : I \times \mathbb{R} \to \mathbb{R}$ such that ϕ and $\dot{\phi}$ are integrable, where $\dot{(\,)}$ represents the derivative with respect to time.

Multiplying (5.2.1) by $\phi(t; \beta)$ and integrating over I, we obtain an equation of the form

$$\phi(t; \beta)x(t)|_I - \int_I \dot{\phi}(t; \beta)x(t)\,\mathrm{d}t = \int_I \phi(t; \beta)f(x(t), t; \boldsymbol{\theta})\,\mathrm{d}t. \tag{5.2.2}$$

We define $k_\beta := \phi(t; \beta)x(t)|_I - \int_I \dot{\phi}(t; \beta)x(t)\,\mathrm{d}t$ and $F_\beta(\boldsymbol{\theta}) := \int_I \phi(t; \beta)f(x(t), t; \boldsymbol{\theta})\,\mathrm{d}t$ for some constant k_β and function F_β, so that (5.2.2) can be represented as $k_\beta = F_\beta(\boldsymbol{\theta})$. Since we have m unknown parameters, we then substitute m distinct values of β, say $\beta_1, \ldots, \beta_m$, in to (5.2.2) to generate a system of equations given by

$$\begin{bmatrix} k_{\beta_1} \\ \vdots \\ k_{\beta_m} \end{bmatrix} = \begin{bmatrix} F_{\beta_1}(\boldsymbol{\theta}) \\ \vdots \\ F_{\beta_m}(\boldsymbol{\theta}) \end{bmatrix}. \tag{5.2.3}$$

Thus we have reformulated the problem of parameter estimation as a problem of finding a root of an algebraic system of nonlinear equations.

A special case of (5.2.1) is when f is of the form

$$f(x, t; \boldsymbol{\theta}) = \theta_1 g_1(x, t) + \cdots + \theta_m g_m(x, t) + g_0(x, t), \tag{5.2.4}$$

where $g_i : \mathbb{R}^2 \to \mathbb{R}$ and $\boldsymbol{\theta} = (\theta_1, \ldots, \theta_m)$. This case is where the parameters appear linearly in the equation so that (5.2.3) becomes a linear system of algebraic equations. This imposes a restriction on the weight function ϕ such that the resulting coefficient matrix of $\boldsymbol{\theta}$ in (5.2.3) is invertible. Assuming relevant data can be observed, this method can be applied to systems of ODEs by applying it to each equation with unknown parameters that appears within the system.

5.3 Applications

In order to demonstrate the viability of our method as an alternative technique, we will apply it to some well-known models, for some of which alternative parameter estimation techniques have been applied, for example [122].

5.3.1 Bernoulli's smallpox model

In his seminal paper [19], Bernoulli proposed a model to determine the prevalence of immune and susceptible individuals, of a certain age, to smallpox and as a result, calculate the gain in life expectancy if this infectious disease were eliminated at birth as a potential cause of death. A review of this paper has been conducted recently in [54]. Importantly, in Bernoulli's paper an estimate was made about certain parameters in his model based on observed data. It is unclear as to how Bernoulli estimated these values, however this gives us a model in which we can test the effectiveness of our method.

The model proposed by Bernoulli for determining the proportion of susceptible individuals x of a population at age a, was given by

$$\frac{\mathrm{d}x}{\mathrm{d}a} = -\lambda(a)x(a)\left[1 - c(a)x(a)\right] \tag{5.3.1}$$

where $\lambda(a)$ is the force of infection and determines the rate at which susceptibles are infected and $c(a)$ is the case fatality rate, which determines the proportion of people that die as a result of the infection. This model has an initial condition of $x(0) = 1$ as it is assumed that all newborns will not be immune to the disease.

According to [20] and [54], when the assumption was made that the parameters in this model were constants, say $\lambda(a) = \lambda$ and $c(a) = c$, Bernoulli was able to calculate parameter values based on data collected by Edmond Halley, which can be found in [20]. Bernoulli estimated that the force of infection was $\lambda = 0.125$ and the case fatality rate was $c = 0.125$.

Under the assumption that the parameters in (5.3.1) are constant, we have

$$\frac{\mathrm{d}x}{\mathrm{d}a} = -\lambda x(a) + \lambda c x(a)^2, \tag{5.3.2}$$

and by letting $\alpha = \lambda c$ and identifying t with a, we have an equation in the form of (5.2.4) and hence we can apply our method to (5.3.2). The data in [20] are of observations made of people

from ages 0 to 24, therefore we will numerically integrate over the interval $I = [0, 24]$. We choose the weight function to be $\phi(a;\beta) = \mathrm{e}^{-\beta a}$, where a is in years. We chose this type of function since, as mentioned in the introduction, we can think of our method as being analogous to applying a finite Laplace transform to an ODE. However it should be noted that we are not limited to this choice of weight function and theoretically the method will work with any choice of ϕ as long as system (5.2.3) is solvable.

The method yields, with $\beta = \beta_1, \beta_2$, the system

$$\begin{bmatrix} \mathrm{e}^{-\beta_1 a}x(a)\big|_0^{24} + \beta_1 \int_0^{24} \mathrm{e}^{-\beta_1 a}x(a)\,\mathrm{d}a \\ \mathrm{e}^{-\beta_2 a}x(a)\big|_0^{24} + \beta_2 \int_0^{24} \mathrm{e}^{-\beta_2 a}x(a)\,\mathrm{d}a \end{bmatrix} = \begin{bmatrix} -\int_0^{24} \mathrm{e}^{-\beta_1 a}x(a)\,\mathrm{d}a & \int_0^{24} \mathrm{e}^{-\beta_1 a}x(a)^2\,\mathrm{d}a \\ -\int_0^{24} \mathrm{e}^{-\beta_2 a}x(a)\,\mathrm{d}a & \int_0^{24} \mathrm{e}^{-\beta_2 a}x(a)^2\,\mathrm{d}a \end{bmatrix} \begin{bmatrix} \lambda \\ \alpha \end{bmatrix}. \tag{5.3.3}$$

The analysis for the appropriate choice of β_1 and β_2 still needs to be conducted, so values were chosen that do not alter the data set by a large amount as to create a potential bias towards particular sections of the data and not to create any numerical errors as a result of having one equation a large factor greater than the other. Hence we let $\beta_1 = 0$ and $\beta_2 = 0.2$ since the choice of $\beta_1 = 0$ will leave the data unchanged and $\beta_2 = 0.2$ is relatively small. Using MATLAB, we calculate the integrals given in (5.3.3) numerically by interpolating the data by a cubic spline method, then integrate and thus calculate the predicted values for λ and α, and as a result c. With these values we obtain that $\lambda = 0.1250$ and $c = 0.1263$ to four significant figures. Hence we have obtained values close to those predicted by Bernoulli in 1766. Note that (5.3.2) can be solved analytically, so as a result the LS method can be used to calculate the parameter values. When this method was used, the parameter values found were $\lambda = 0.1250$ and $c = 0.1257$ and it can be seen that the values obtained via the analytical LS method and the proposed method are very close.

As can been seen in Figure 5.1, these parameter values represent an approximation that generates a solution with a strong fit to the data.

5.3.2 HIV dynamic model

Modelling the dynamics of HIV is an important and significant area of study. Models initially considered described the dynamics of the HIV virus and immune cell response. A review of these models has been considered in [149, 161, 194]. A HIV dynamic model [122, 211] in which alter-

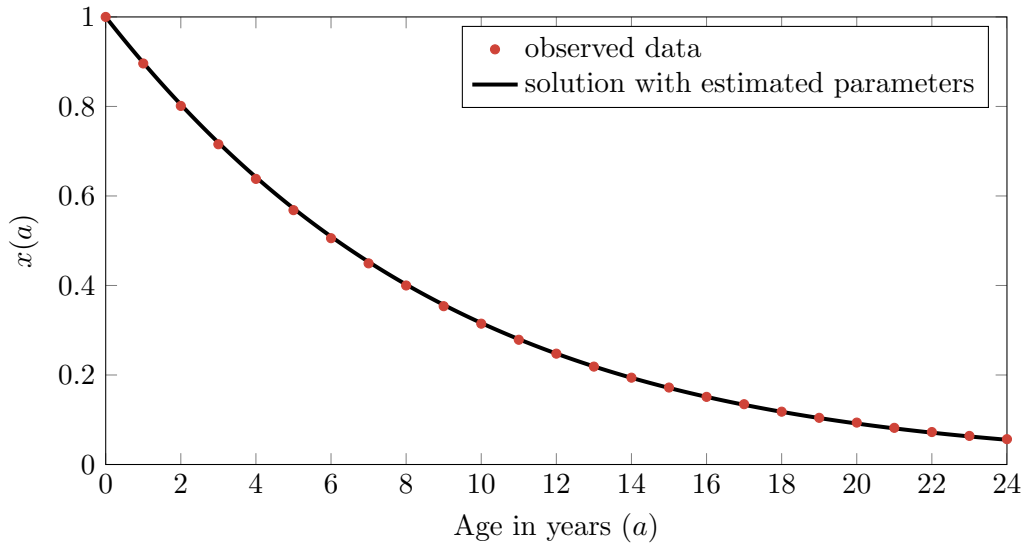

Figure 5.1: Comparison of data observed by Halley with solution to Bernoulli's model with estimated parameters $\lambda = 0.1250$ and $c = 0.1263$ for the prevalence of susceptibles from ages 0 to 24

native parameter estimation techniques were applied, is given by

$$\frac{\mathrm{d}T_{\mathrm{u}}}{\mathrm{d}t} = \lambda - \rho T_{\mathrm{u}} - \eta(t) T_{\mathrm{u}} V, \tag{5.3.4}$$

$$\frac{\mathrm{d}T_{\mathrm{i}}}{\mathrm{d}t} = \eta(t) T_{\mathrm{u}} V - \delta T_{\mathrm{i}}, \tag{5.3.5}$$

$$\frac{\mathrm{d}V}{\mathrm{d}t} = N\delta T_{\mathrm{i}} - cV, \tag{5.3.6}$$

where T_{u} is the concentration of uninfected CD4+ T cells; T_{i} is the concentration of infected CD4+ T cells; V is the concentration of plasma virus (viral load); λ is the rate at which new CD4+ T cells are generated; ρ is the death rate of uninfected CD4+ T cells; $\eta(t)$ is the infection rate of CD4+ T cells; δ is the death rate of infected cells; c is the clearance rate of free virions; N is the number of virions produced from each infected cell.

As is stated in [122], only the total CD4+ T-cell count $T(t) = T_{\mathrm{u}}(t) + T_{\mathrm{i}}(t)$ and the plasma viral load $V(t)$ can be measured. Therefore equations (5.3.4)–(5.3.6) are transformed such that we have an equation for $T(t)$ and $V(t)$ given by

$$V'(t) + cV(t) = \alpha_0 T'(t) + \alpha_1 T(t) + \alpha_2, \tag{5.3.7}$$

where

$$\alpha_0 = \frac{N\delta}{\rho - \delta},\ \alpha_1 = \rho\alpha_0,\ \alpha_2 = -\lambda\alpha_0.$$

See [122] for the full working.

We now have (5.3.7) in which the parameters appear linearly and hence we can apply our parameter estimation technique. As is done in [122], we generate data by solving the system of equations (5.3.4)–(5.3.6) with a particular set of parameters and then apply the technique to (5.3.7) to see if we reobtain those parameters, both with and without noise added to the generated data. We also make the same assumption made in [122] that values of δ and c can be obtained from the literature [162, 163, 209, 210]. We generate data by solving (5.3.4)–(5.3.6), with initial values of $(T_{\mathrm{u}}(0), T_{\mathrm{i}}(0), V(0)) = \left(600, 30, 10^5\right)$, parameter values of

$$(\lambda, \rho, N, \delta, c) = (36, 0.108, 10^3, 0.5, 3), \tag{5.3.8}$$

and dynamic parameter given by $\eta(t) = 9 \times 10^{-5}\left[0.9 - \cos(\pi 10^{-3} t)\right]$, over the interval of time $[0, 20]$ (cf. [122]). Once this data is generated, we add T_{u} and T_{i} together to recreate the conditions in a clinical study and then apply the proposed technique to (5.3.7). Once again we will let $\phi(t;\beta) = \mathrm{e}^{-\beta t}$ and as we are finding the value of three different parameters, we will need to use three distinct values of β which will be $\beta = 0, 0.2, 0.4$. These values were chosen as they are small and will not skew the observed data by large amounts.

Absence of noise

We solve (5.3.4)–(5.3.6) with time-steps $0.1,\ 0.2$ and 0.4, such that we have $201,\ 101$ and 51 observations, respectively, over the time period $[0, 20]$. In the absence of noise, when we apply our technique, we obtain parameter values of $(\lambda_{0.1}, \rho_{0.1}, N_{0.1}) = (36.00, 0.1080, 1000)$, $(\lambda_{0.2}, \rho_{0.2}, N_{0.2}) = (35.94, 0.1077, 1000)$ and $(\lambda_{0.4}, \rho_{0.4}, N_{0.4}) = (35.00, 0.1029, 996.8)$, respectively. By comparing these values with (5.3.8) we can see that without noise there are small errors in the cases with fewer observations which can be accounted for by a less accurate approximation for our integrals as a result of using larger time-steps.

In the presence of noise

To simulate the effect of applying this technique to real data, we will follow the method used in [122] in which noise is added to the numerically generated solution. The noise will be normally distributed with different variances. We will then run this simulation several times, recording the average and the standard deviation (SD) of the parameter values given back. We can then compare our results with those obtained in [122]. We will therefore have data at various points in time t_i of the form

$$\widehat{T}_i = T(t_i) + \varepsilon_{T,i}, \qquad \widehat{V}_i = V(t_i) + \varepsilon_{V,i},$$

where $\varepsilon_{T,i}$ and $\varepsilon_{V,i}$ are normally distributed with mean zero and variances of $\sigma_T^2 = 20, 30, 40$ and $\sigma_V^2 = 100, 150, 200$, respectively. Applying this with data generated by using time-steps of 0.1, 0.2 and 0.4, we run the simulations 500 times and then calculate the averages and standard deviations of the parameter estimates produced. The results are summarised in Tables 5.1–5.3 for the time-steps 0.1, 0.2 and 0.4, respectively. We can see that the mean of the estimates obtained in the simulations are very close to the actual parameter values (5.3.8) and that the standard deviations are relatively small. In the presence of a small amount of noise we obtain very accurate approximations for the parameter values for the model (5.3.4)–(5.3.6). When our results are compared to those obtained in [122] by applying the PsLS and SIMEX methods to this model, we can see that this method has obtained more accurate mean approximations for all three parameters and much lower standard deviations for the estimates of λ and ρ and similar standard deviations for the estimates of N. For example, the mean and standard deviation of estimates obtained for the time-step 0.2 and $\sigma_T = 40$ and $\sigma_V = 200$ in [122] were $(\lambda, \rho, N) = (31.1[2.26], 0.090[.22], 935.6[41.9])$ and $(\lambda, \rho, N) = (30.8[9.44], 0.114[.72], 938.1[66.1])$ for the PsLS and SIMEX methods, respectively. Here, the values in square brackets represent the standard deviations. When we compare this to the relevant data in Table 5.2, we can see a much higher level of accuracy has been obtained by the proposed method. If we look at Table 5.3, in which we have used time-steps of 0.4, we can see that we are obtaining results that are as good if not better than those obtained by the methods used in [122] when the time-step is 0.1.

Table 5.1: Means and standard deviations of estimated parameters values from 500 simulations of the HIV model with noise for time-step 0.1

		Mean			Standard Deviation		
σ_T^2	σ_V^2	λ	ρ	N	λ	ρ	N
20	100	36.01	0.1081	1001.0	0.864	0.00492	16.79
	150	35.94	0.1076	999.4	0.814	0.00474	16.49
	200	36.00	0.1082	1001.8	0.853	0.00476	16.80
30	100	35.95	0.1078	1000.6	1.075	0.00593	20.07
	150	35.97	0.1078	1000.6	1.047	0.00619	21.61
	200	36.05	0.1081	999.8	1.021	0.00588	19.78
40	100	35.95	0.1077	1000.2	1.293	0.00719	24.11
	150	36.01	0.1082	1001.9	1.224	0.00699	23.36
	200	36.04	0.1085	1002.9	1.175	0.00687	24.61

Table 5.2: Means and standard deviations of estimated parameters values from 500 simulations of the HIV model with noise for time-step 0.2

		Mean			Standard Deviation		
σ_T^2	σ_V^2	λ	ρ	N	λ	ρ	N
20	100	35.87	0.1072	999.2	1.171	0.00656	18.77
	150	35.89	0.1074	999.8	1.147	0.00637	17.56
	200	35.99	0.1080	1000.9	1.225	0.00670	17.78
30	100	35.97	0.1079	1000.9	1.553	0.00845	22.31
	150	35.90	0.1074	999.7	1.489	0.00827	22.70
	200	35.94	0.1078	1001.4	1.425	0.00783	23.10
40	100	35.96	0.1077	1001.2	1.720	0.00931	26.47
	150	35.97	0.1080	1001.8	1.765	0.00966	26.78
	200	35.88	0.1072	999.4	1.756	0.00963	26.70

5.3.3 Tumour cell and chemotherapy drug interaction model

As noted in Chapter 1, many authors have looked at the growth of tumours by modelling them with ODEs [13, 30] that contain important parameters that need to be determined. Recall the model proposed by Byrne [30], which was used in the development of the models considered in Chapters 3 and 4, that looks at the dynamics of solid tumour cell and chemotherapy drug interaction given by

$$\frac{\mathrm{d}N}{\mathrm{d}t} = kN\left(1 - \frac{N}{\theta}\right) - \mu AN, \tag{5.3.9}$$

$$\frac{\mathrm{d}A}{\mathrm{d}t} = a(t) - \lambda A - \gamma AN, \tag{5.3.10}$$

Table 5.3: Means and standard deviations of estimated parameters values from 500 simulations of the HIV model with noise for time-step 0.4

		Mean			Standard Deviation		
σ_T^2	σ_V^2	λ	ρ	N	λ	ρ	N
20	100	35.02	0.1031	997.6	1.735	0.00929	20.92
	150	34.94	0.1027	997.1	1.724	0.00917	20.21
	200	35.08	0.1034	998.1	1.675	0.00907	20.15
30	100	34.90	0.1027	998.9	2.026	0.01087	24.77
	150	35.03	0.1033	998.8	2.114	0.01142	24.21
	200	35.00	0.1030	998.1	2.266	0.01197	26.03
40	100	34.95	0.1023	995.7	2.437	0.01312	29.28
	150	35.08	0.1033	997.9	2.441	0.01314	29.67
	200	35.01	0.1029	997.6	2.300	0.01273	29.88

with

$$N(0) = N_0 \qquad \text{and} \qquad A(0) = A_0. \tag{5.3.11}$$

In this, $N(t)$ is the number of tumour cells at time t, $A(t)$ is the average concentration of chemotherapeutic drug within the tumour at time t, k is the cell proliferation rate, θ represents the carrying capacity of the cell population, μ denotes the rate at which the drug kills the tumour cells, λ represents the drug's decay rate, γ is the rate at which the drug becomes ineffective as a result of a cell kill and $a(t)$ is the drug delivery rate to the tumour. The dynamic parameter $a(t)$ can be used to represent various drug infusion protocols. However for simplicity we will let it represent continuous drug infusion, that is $a(t) = a_\infty$ for all t, where a_∞ is a positive constant.

Absence of noise

We can see that (5.3.9)–(5.3.11) is a system in which the parameters appear linearly. Hence we can apply our method to this system to estimate the parameters. Since both the number (N) of tumour cells and the average concentration (A) of chemotherapeutic drug can be estimated [142, 215], we do not need to alter the state variables as was done for the HIV model (5.3.4)–(5.3.6). To test the effectiveness of our estimation technique on the model (5.3.9)–(5.3.11), we simulate data from a numerical solution to the system of ODEs with a particular set of parameter values and we assume that a_∞ is known. To estimate the parameters k, θ and μ, we use our technique on (5.3.9) and then

to estimate λ and γ, we need to apply the technique to (5.3.10). We let

$$(k, \theta, \mu, a_\infty, \lambda, \gamma) = (0.8, 1, 1.1, 0.8, 1.2, 0.6), \tag{5.3.12}$$

and use initial values of $N(0) = 1$ and $A(0) = 0.1$. We generate sets of values for N and A over a time period of $[0, 10]$ using time-steps of 0.1, 0.2 and 0.4 to generate sample sizes of 101, 51 and 26, respectively. For both equations we let $\phi(t; \beta) = \mathrm{e}^{-\beta t}$ and take $\beta = 0, 0.4, 0.8$ for (5.3.9) and $\beta = 0, 0.4$ for (5.3.10). These values were chosen as they are small and will not skew the observed data by large amounts. Using the generated data, we obtain estimates for our parameters of $(k_{0.1}, \theta_{0.1}, \mu_{0.1}, \lambda_{0.1}, \gamma_{0.1}) = (0.800, 1.00, 1.10, 1.20, 0.600)$, $(k_{0.2}, \theta_{0.2}, \mu_{0.2}, \lambda_{0.2}, \gamma_{0.2}) = (0.800, 1.00, 1.10, 1.20, 0.600)$ and $(k_{0.4}, \theta_{0.4}, \mu_{0.4}, \lambda_{0.4}, \gamma_{0.4}) = (0.787, 0.993, 1.08, 1.20, 0.602)$ for the data generated with time-steps 0.1, 0.2 and 0.4, respectively. When we compare this with (5.3.12), we can see that the accuracy of the estimation is reduced in the cases with fewer data values as a result of less accurate approximations of the integrals.

In the presence of noise

To test the effectiveness of this model in a clinical situation we will add noise to the data sets generated by solving the system numerically and then estimate our parameters as was done for the HIV model. In the case of the HIV model, noise was added that was normally distributed so that we could compare our results with that of those obtained in [122]. Noise that is normally distributed has the capability of producing large outliers from the data set that would not necessarily be considered for estimation of the parameters. We therefore add noise that is uniformly distributed, say $U(-\sigma_N, \sigma_N)$ and $U(-\sigma_A, \sigma_A)$ for the sets of data produced for N and A, respectively. We will use the sets of data generated previously by using time-steps of 0.1, 0.2 and 0.4 and run 500 simulations with noise added with σ_N and σ_A taking each of the values 0.02 and 0.04, and take the average and standard deviation of the estimates produced for each parameter. The results of this are summarised in Tables 5.4–5.6.

We define the error measures mean absolute error (MAE) and mean absolute value (MAV) as

$$\mathrm{MAE} = \frac{1}{n} \sum_{i=1}^{n} |x(t_i) - y_i|$$

and

$$\text{MAV} = \frac{1}{n}\sum_{i=1}^{n}|a_i|,$$

where $x(t_i)$ is the predicted value at t_i, y_i is the observed value at t_i and a_i is the i-th element of an arbitrary set of n values. For each simulation we also use the parameters estimated to solve the system of equations given by (5.3.9)–(5.3.11) and then calculate the MAE between the solution generated with the estimated parameters and the simulated data with noise and we take the average and standard deviation of the MAEs obtained from the 500 simulations. We also calculate the MAV of the noise added to the original solution in each simulation and then take the average and standard deviation of the MAV from the 500 simulations as a basis for comparison. Since the noise is uniformly distributed the expected MAV of the noise generated for N and A is $\sigma_N/2$ and $\sigma_A/2$, respectively. This data is summarised in Tables 5.7–5.9.

Table 5.4: Means and standard deviations of estimated parameter values from 500 simulations of the tumour cell and chemotherapy drug interaction model with noise for time-step 0.1

		Mean					Standard Deviation				
σ_N	σ_A	k	θ	μ	λ	γ	k	θ	μ	λ	γ
0.02	0.02	0.801	0.992	1.10	1.20	0.600	0.164	0.072	0.213	0.0144	0.0335
	0.04	0.810	0.995	1.11	1.20	0.601	0.176	0.078	0.232	0.0319	0.0743
0.04	0.02	0.791	0.959	1.09	1.20	0.600	0.310	0.156	0.403	0.0162	0.0381
	0.04	0.816	0.965	1.12	1.20	0.608	0.320	0.163	0.415	0.0307	0.0727

Table 5.5: Means and standard deviations of estimated parameter values from 500 simulations of the tumour cell and chemotherapy drug interaction model with noise for time-step 0.2

		Mean					Standard Deviation				
σ_N	σ_A	k	θ	μ	λ	γ	k	θ	μ	λ	γ
0.02	0.02	0.803	0.991	1.10	1.20	0.602	0.182	0.082	0.241	0.0212	0.0515
	0.04	0.817	0.993	1.12	1.20	0.597	0.229	0.103	0.308	0.0426	0.1031
0.04	0.02	0.796	0.943	1.10	1.20	0.600	0.360	0.226	0.477	0.0209	0.0506
	0.04	0.826	0.959	1.14	1.20	0.603	0.375	0.205	0.497	0.0394	0.0947

We can see from the data contained in Tables 5.7–5.9 that the averages produced are close to the actual parameter values (5.3.12), with the error increasing as the number of observations decreases. However for some of the parameters, the respective standard deviations are large relative to the parameter value, which suggest there is significant probability of obtaining values that can have significant relative errors to the actual parameter values. However if we look at the MAEs of

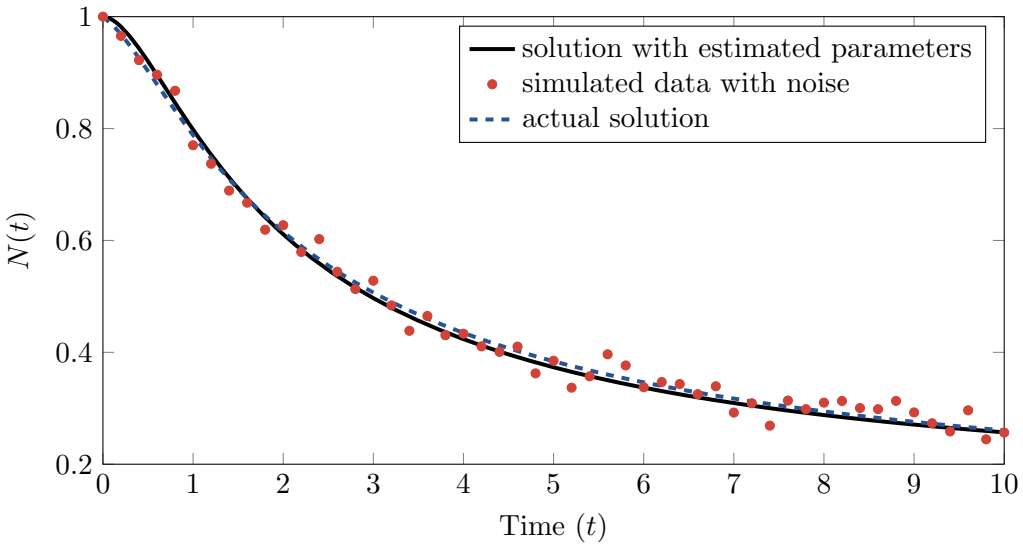

(a) Plots of number of tumour cells

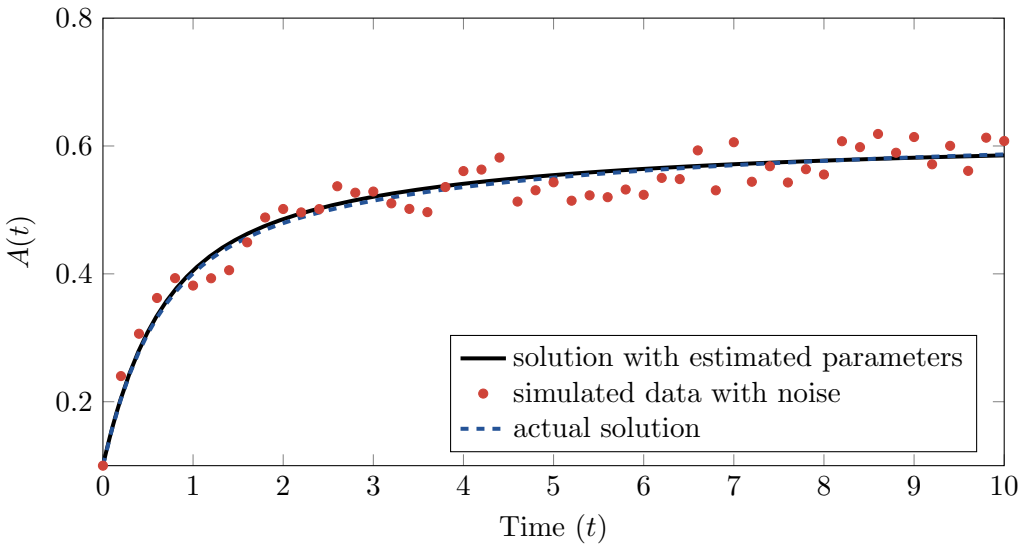

(b) Plots of average drug concentration

Figure 5.2: Comparison of simulated data with noise, model solution and model solution with estimated parameters given by $(k_{0.2}, \theta_{0.2}, \mu_{0.2}, \lambda_{0.2}, \gamma_{0.2}) = (1.12, 1.15, 1.57, 1.23, 0.527)$

Table 5.6: Means and standard deviations of estimated parameter values from 500 simulations of the tumour cell and chemotherapy drug interaction model with noise for time-step 0.4

		Mean					Standard Deviation				
σ_N	σ_A	k	θ	μ	λ	γ	k	θ	μ	λ	γ
0.02	0.02	0.797	0.981	1.10	1.20	0.596	0.219	0.110	0.295	0.0288	0.0710
	0.04	0.817	0.984	1.12	1.20	0.601	0.276	0.131	0.380	0.0540	0.1351
0.04	0.02	0.815	0.898	1.12	1.20	0.601	0.401	1.127	0.543	0.0296	0.0740
	0.04	0.806	0.917	1.11	1.20	0.610	0.459	0.301	0.622	0.0557	0.1354

Table 5.7: Means and standard deviations of MAE of simulated data and solution obtained with estimated parameters and MAV of noise from simulated data for time-step 0.1

		MAE		MAV		SD of MAE		SD of MAV	
σ_N	σ_A	N	A	ε_N	ε_A	N	A	ε_N	ε_A
0.02	0.02	0.0102	0.0099	0.0099	0.0099	0.00073	0.00058	0.00057	0.00057
	0.04	0.0102	0.0197	0.0099	0.0199	0.00080	0.00117	0.00058	0.00058
0.04	0.02	0.0202	0.0099	0.0198	0.0099	0.00144	0.00058	0.00111	0.00111
	0.04	0.0203	0.0197	0.0198	0.0198	0.00146	0.00111	0.00113	0.00113

the solutions generated by using the estimated parameters, we can see that these values are close to the MAVs of the noise and this suggests that the approximated solutions fit the data on average as well as the solution used to generate the noisy data, which one would assume would be close to the solution of best fit. We can see that if we plot the solution of the ODEs with the estimated parameter values with significant relative errors, we find that the solutions produced still fits the data well. An example of this is shown in Figure 5.2, in which we can see there is a 40% error in the value of k and a 43% error in the estimated value of μ, however the solution still represents a good fit to the data. This shows that due to the fact this system has a large number of parameters to be estimated, there is a greater set of values of the parameters that will generate solutions for the ODE that will represent a good fit to the observed data. This suggests that for certain systems our method will not always be appropriate. However our method could potentially be used in conjunction with an alternative method that requires an initial estimate of the parameters values to work, such as the numerical LS method [93], in order to save computation time by producing a set of values that are close to the values that generate the solution of best fit.

Table 5.8: Means and standard deviations of MAE of simulated data and solution obtained with estimated parameters and MAV of noise from simulated data for time-step 0.2

		MAE		MAV		SD of MAE		SD of MAV	
σ_N	σ_A	N	A	ε_N	ε_A	N	A	ε_N	ε_A
0.02	0.02	0.0098	0.0097	0.0097	0.0098	0.00095	0.00079	0.00080	0.00080
	0.04	0.0101	0.0193	0.0098	0.0196	0.00104	0.00167	0.00078	0.00078
0.04	0.02	0.0197	0.0097	0.0196	0.0097	0.00192	0.00085	0.00163	0.00163
	0.04	0.0198	0.0193	0.0197	0.0196	0.00189	0.00168	0.00157	0.00157

Table 5.9: Means and standard deviations of MAE of simulated data and solution obtained with estimated parameters and MAV of noise from simulated data for time-step 0.4

		MAE		MAV		SD of MAE		SD of MAV	
σ_N	σ_A	N	A	ε_N	ε_A	N	A	ε_N	ε_A
0.02	0.02	0.0092	0.0092	0.0096	0.0096	0.00129	0.00114	0.00109	0.00109
	0.04	0.0096	0.0184	0.0096	0.0192	0.00144	0.00239	0.00109	0.00109
0.04	0.02	0.0183	0.0093	0.0193	0.0096	0.00259	0.00114	0.00234	0.00234
	0.04	0.0186	0.0186	0.0192	0.0192	0.00250	0.00227	0.00222	0.00222

5.4 Discussion and concluding remarks

We have presented a method for finding unknown parameters in systems of ODEs, that is integration based. Three model systems have been chosen to demonstrate the validity of this method. We have seen that this method is relatively simple and therefore requires very little computational time. We have noted that this method could be used to obtain an estimate close to the parameter values, where that estimate can then be used for the starting point of a numerical LS procedure to find the parameters that generate the LS best fit to the data. Further work that can be conducted is a review of the class of problems for which this method is appropriate as we have seen that for certain systems, in the presence of noise, this method can become unreliable. A procedure for how to choose appropriate weight functions and equation generating parameters for a particular system is needed. Analysis is needed to determine if certain weight functions are more appropriate for particular sets of data and whether or not certain weight functions can be used to give more weight to sections of the data that is available. An analysis of the errors that are to be expected from this method needs to be conducted to determine the suitability of this method for particular systems of ODEs and the errors that can be expected as a result of non-uniform data.

Chapter 6

Conclusions

This thesis has been primarily concerned with the study of tumour invasion, with particular focus on the effect of the tumour metabolism (i.e. the Warburg effect) on invasion, through the use of mathematical modelling and associated techniques. In Chapter 1 it was noted that tumours have many complex interacting biological mechanisms to ensure cell survival, enhance proliferation and facilitate invasion. These mechanisms include rapid cellular reproduction through proliferative signalling, disrupting negative feedback loops designed to suppress signalling, evading senescence and apoptosis, preventing telomere shortening, inducing angiogenesis, metastasising and altering the normal cellular metabolism, to name a few. Due to this vast array of interacting mechanisms the challenge of modelling tumour growth mathematically can seem intractable and as though it would require far more sophisticated techniques than those that are currently available. However many models have provided excellent predictions and insights despite their relative simplicity. It was with this in mind that we proposed and subsequently examined simple models for the acid-mediation hypothesis.

In Chapter 2 a model was proposed for the acid-mediation hypothesis that was an altered version of that originally proposed by Gatenby and Gawlinski [71]. The model considered the additional hypothesis that H^+ ions are produced at a rate proportional to the tumour cell density until the latter reaches a threshold, after which the production rate decreases as the tumour tissue attains its carrying capacity. This hypothesis was designed to reflect the spatially heterogeneous concentration of acid commonly observed in tumours [92, 117]. Furthermore, the model required the inclusion of tumour population competition, whereas the model in [71] did not. The model considered was a system of RD equations that examined the interaction between normal cells, tumour cells and acid. A numerical and asymptotic analysis was performed that indicated the existence of TW solutions.

The solutions for the tumour and normal densities presented as fronts and the acid concentration presented as a pulse with the primary acid concentration occurring in the region of the tumour host interface, consistent with experimental results observed in [51, 92, 133]. The analysis of this model indicates the requirement for a large production rate of H^+ ions for significant concentrations of acid to occur. This indicates that for tumours to become acidic the cells must be highly reliant on aerobic glycolysis for energy production.

The asymptotic analysis of the model considered in Chapter 2 predicted the existence of an interstitial gap for highly aggressive tumours, consistent with the results in [63, 71]. Similarly to the analysis in [63], an estimate was obtained for the size of the interstitial gap. This gap was found to be dependent on more system parameters than the estimate obtained in [63]. Moreover, the estimate was found to be monotone with respect to the tumour aggressiveness, the relative strength of the pH uptake, the relative tumour-H^+ ion diffusion rate and the relative tumour growth rate.

The model considered in Chapter 2 has the potential to be generalised further, similarly to the model of McGillen et al. [140]. A rigorous proof of existence of solutions still remains to be conducted. The model has the potential to be considered in higher dimensional geometries and to include additional dynamics such as the processes of chemotaxis and haptotaxis. A further possible extension is to consider the effect of an intervention such as an immune response or a cytotoxic treatment.

Chapter 3 considered a model for the acid-mediation hypothesis with chemotherapy intervention based on the work of Byrne [30], Gatenby and Gawlinski [71] and McGillen et al. [140]. The model produced was a simple system of ODEs that examined the interaction of tumour tissue, normal tissue, H^+ ions and a cytotoxic drug, where the infusion of the drug was considered as a function of time. The model was investigated for constant infusion and periodic infusion of chemotherapy drugs. This resulted in an autonomous and time-periodic system, respectively, being examined. Accordingly, a SS analysis was conducted for the constant infusion case and periodic solutions were investigated for the time-periodic system. From each of these analyses, similar, if not the same, overall long term behaviour was found for the constant and periodic infusion models. It was shown that there exists zero population solutions (i.e. SS1 and PS1) which are unconditionally unstable, indicating there should always exist a nonzero cellular population. Tumour-tissue free solutions (i.e. SS2 and PS2) were shown to exist that were stable for sufficiently strong normal tissue population competition and chemotherapy aggressiveness. Normal-tissue free solutions (i.e. SS3 and PS3) were shown to exist and be stable given sufficiently strong tumour population

competition and tumour aggressive and sufficiently low chemotherapy aggressiveness. Moreover, it was shown that there exists a critical value of the chemotherapy aggressiveness after which the normal-tissue free solution could not exist. The existence of a coexistence state, that is, a state in which tumour and normal tissue exist in equilibrium, was confirmed, where the state was stable given sufficiently low population competition, tumour aggressiveness and chemotherapy aggressiveness. We also note that the analysis conducted in Chapter 3 further completed the analysis of the model proposed by Byrne [30]. When considering periodic infusion of a chemotherapy drug, the analysis in [30] assumed that the concentration of drug was equal to the periodic infusion function given by a specific function. In the analysis of our model this assumption was removed and was considered for all positive continuous periodic functions of time.

The work of Chapter 4 extended the model examined in Chapter 3 by considering the effect of spatial variations in the population densities. This resulted in the formulation of a system of RD equations to model the acid-mediation hypothesis with chemotherapy intervention. This model was analysed using numerical and analytical techniques for both constant and periodic infusion functions. This analysis demonstrated the behaviours of tumour clearance and "splitting waves" and indicated the existence of TW and TPTW solutions, for particular parameter values, for constant and periodic infusion, respectively. The tumour clearance behaviour demonstrated that the tumour could be removed from the system by the reaction dynamics alone, provided sufficiently strong treatment was administered. The splitting behaviour indicated an important influence of the chemical diffusion properties of the cytotoxic drug in removing what would otherwise be a stable tumour population. It was shown that chemotherapy slowed, often reversed, the invasion of tumour populations. It was determined that acid only facilitated invasion for low destructive influence of chemotherapy or when the chemotherapy required population competition to be effective. In the latter case, the acid would facilitate invasion by destroying normal tissue, removing competition.

Asymptotic approximations were obtained utilising the theory of matched asymptotic expansions. The asymptotic approximations allowed predictions to be made about when the tumour would be invading or receding. Similarly to [63, 140] and Chapter 2 this analysis predicted the existence of an interstitial gap for particular parameter values and also provided an estimate for the gap width. However it is noted that this estimate and that obtained in Chapter 2 may have more qualitative rather than quantitative value. We note that the analysis predicts that the gap width is decreased by the use of chemotherapy. The asymptotic analysis also provided estimates in terms of the parameter values for minimal speed of invasion of the tumour population, which as noted

above, decreases as a result of the chemotherapy intervention.

The model presented in Chapter 4 has the potential for further analysis with the inclusion of processes such as chemotaxis and haptotaxis. The mutagenic/clastogenic effects of an acidic environment and the resulting effect that this has on chemoresistance also remains to be considered. Furthermore, a rigorous proof of existence of solutions remains to be conducted.

A simple method for the estimation of constant parameters appearing in a class of systems of ODEs was considered in Chapter 5. The method utilised a weight function which contains a controllable parameter, termed the "equation-generating parameter", that was multiplied through the ODE being considered. The ODE was then integrated over a period of observation to create an algebraic expression in terms of the parameters. The equation-generating parameter was then used to generate a system of equations for which the unknown parameters could be solved. Utilising observations of the state variables and numerical integration techniques, parameter estimations were able to be made. The method that was proposed is computationally efficient and simple to implement. The parameter estimation technique was demonstrated by applying it to Bernoulli's smallpox model [19], a HIV dynamic model [122, 211] and Byrne's chemotherapy model [30]. The technique was shown to provide good estimates for the parameter values. We note that this procedure was used to good effect in Chapter 2 to estimate the speed of invasion of the tumour tissue. This represents a highly useful application of this technique relevant to the use of RD equations for mathematical modelling. As with many parameter estimation techniques, the proposed method does not guarantee excellent estimate of the parameters, however due to the computational efficiency of the method, this technique can be used to provide a good initial guess of the parameters for a numerical LS procedure. The parameter estimation technique still requires an appropriate error analysis, an analysis to indicate the suitability of the method for different systems of ODEs and an examination of the weight functions that are most suitable to use to ensure the greatest accuracy of results.

Overall, this thesis has presented new models for the examination of acid-mediated tumour invasion, provided a guide for how these and similar models can be examined by a combination of numerical, analytical and asymptotic techniques and presented a simple technique to the estimate parameters contained in these models, and others, from observations of the states variables. Moreover, it has been displayed that simple ODE and RD systems can provide valuable insights about the underlying mechanisms of tumour invasion and provide predictions about how these mechanisms affect invasion.

List of Symbols

$\in$	Element of
$\subset$	Subset of
$\bigcup$	The union of sets
$\simeq$	Asymptotically equal to
$\ll$	A lot less than
$\gg$	A lot larger than
$\propto$	Proportional to
$O(\cdot)$	Big-O notation, order of magnitude
$o(\cdot)$	Little-o notation
$\circ(\diamond)$	$\circ$ or $\diamond$, where $\circ$ and $\diamond$ are binary relations (e.g. $=, <, >$, $\geq, \leq$). Should multiple uses occur in the same argument, the first terms corresponds to the first term in subsequent uses
$\mathbb{N}$	The natural numbers
$\mathbb{R}$	The real numbers
$\mathbb{R}_+$	The positive real numbers, i.e. $[0, \infty)$
$(\cdot, \cdot)$	An open interval
$[\cdot, \cdot]$	A closed interval
$S \times R$	The cartesian product of the sets S and R
∂S	The boundary of the set S
$\mathrm{int}(S)$	The interior of the set S
S^n	The set of ordered n-tuples with entries in S
S^{n^2}	The set of $n \times n$ matrices with entries in S

$C^n(S)$	The class of n times continuously differentiable functions defined on the set S
$C^n(S, R)$	The class of n times continuously differentiable functions defined on the set S with range in R
$\frac{\mathrm{d}}{\mathrm{d}x}$	Derivative with respect to the variable x
$\frac{\partial}{\partial x}$	Partial derivative with respect to the variable x
∇	Euclidean vector differential operator
$\mathbf{F}'_{\mathbf{u}}$	Derivative of the vector valued function $\mathbf{F}$ with respect to the argument $\mathbf{u}$
$\langle \cdot, \cdot \rangle$	The scalar product
$\| \cdot \|$	The euclidean norm
A^{T}	The transpose of matrix A
$\mathrm{diag}(\mathbf{s})$	A diagonal matrix with diagonal entries given by the respective entries of the n-tuple $\mathbf{s}$

Bibliography

[1] Adams, J. M. and Cory, S. (2007). The Bcl-2 apoptotic switch in cancer development and therapy. *Oncogene*, 26(9):1324–1337. doi:10.1038/sj.onc.1210220.

[2] Aderem, A. and Ulevitch, R. J. (2000). Toll-like receptors in the induction of the innate immune response. *Nature*, 406(6797):782–787. doi:10.1038/35021228.

[3] Alikakos, N., Bates, P. and Chen, X. (1999). Periodic traveling waves and locating oscillating patterns in multidimensional domains. *Transactions of the American Mathematical Society*, 351(7):2777–2805. doi:10.1090/S0002-9947-99-02134-0.

[4] Ames, W. F. (1977). *Numerical Methods for Partial Differential Equations*. Academic Press, New York, NY.

[5] Anderson, A. R. A., Chaplain, M. A. J., Newman, E. L., Steele, R. J. C. and Thompson, A. M. (2000). Mathematical modelling of tumour invasion and metastasis. *Computational and Mathematical Methods in Medicine*, 2(2):129–154. doi:10.1080/10273660008833042.

[6] Araujo, R. P. and McElwain, D. L. S. (2004). A history of the study of solid tumour growth: The contribution of mathematical modelling. *Bulletin of Mathematical Biology*, 66:1039–1091. doi:10.1016/j.bulm.2003.11.002.

[7] Arnold, F. and West, D. C. (1991). Angiogenesis in wound healing. *Pharmacology and Therapeutics*, 52(3):407–422. doi:10.1046/j.1087-0024.2000.00014.x.

[8] Aster, R. C. and Thurber, C. H. (2012). *Parameter Estimation and Inverse Problems*. Academic Press, Waltham, MA.

[9] Banks, H. T., Grove, S., Hu, S. and Ma, Y. (2005). A hierarchical Bayesian approach for parameter estimation in HIV models. *Inverse Problems*, 21(6):1803–1822. doi:10.1088/0266-5611/21/6/001.

[10] Bao, X. and Wang, Z.-C. (2013). Existence and stability of time periodic traveling waves for a periodic bistable Lotka–Volterra competition system. *Journal of Differential Equations*, 255(8):2402–2435. doi:10.1016/j.jde.2013.06.024.

[11] Bard, Y. (1974). *Nonlinear Parameter Estimation*. Academic Press, New York, NY.

[12] Barkan, D., Green, J. E. and Chambers, A. F. (2010). Extracellular matrix: a gatekeeper in the transition from dormancy to metastatic growth. *European Journal of Cancer*, 46(7): 1181–1188. doi:10.1016/j.ejca.2010.02.027.

[13] Bellomo, N. and Adam, J. A. (1997). *A Survey of Models for Tumor-Immune System Dynamics*. Birkhäuser, Boston.

[14] Bellomo, N. and Preziosi, L. (2000). Modelling and mathematical problems related to tumor evolution and its interaction with the immune system. *Mathematical and Computer Modelling*, 32(3):413–452. doi:10.1016/S0895-7177(00)00143-6.

[15] Bellomo, N., Firmani, B. and Guerri, L. (1999). Bifurcation analysis for a nonlinear system of integro-differential equations modelling tumor-immune cells competition. *Applied Mathematics Letters*, 12(2):39–44. doi:10.1016/S0893-9659(98)00146-3.

[16] Bender, C. M. and Orszag, S. A. (1999). *Advanced Mathematical Methods for Scientists and Engineers*. Springer, New York, NY.

[17] Bennasroune, A., Gardin, A., Aunis, D., Crémel, G. and Hubert, P. (2004). Tyrosine kinase receptors as attractive targets of cancer therapy. *Critical Reviews in Oncology/Hematology*, 50(1):23–38. doi:10.1016/j.critrevonc.2003.08.004.

[18] Bergers, G. and Benjamin, L. E. (2003). Tumorigenesis and the angiogenic switch. *Nature Reviews Cancer*, 3(6):401–410. doi:10.1038/nrc1093.

[19] Bernoulli, D. (1766). Essai d'une nouvelle analyse de la mortalité caus'ee par la petite vérole. *Mém. Math. Phys. Acad. Roy. Sci., Paris*. 1. (Reprinted in: L.P. Bouckaert, B.L. van der Waerden (Eds.), Die Werke von Daniel Bernoulli, Bd. 2 Analysis und Wahrscheinlichkeitsrechnung, Birkhhäuser, Basel, 1982, p. 235. English translation entitled "An attempt at a new analysis of the mortality caused by smallpox and of the advantages of inoculation to prevent it" in: L. Bradley, Smallpox Inoculation: An Eighteenth Century Mathematical

Controversy, Adult Education Department, Nottingham, 1971, p. 21. Reprinted in: S. Haberman, T.A. Sibbett (Eds.) History of Actuarial Science, vol. VIII, Multiple Decrement and Multiple State Models, William Pickering, London, 1995, p. 1.).

[20] Bernoulli, D. and Blower, S. (2004). An attempt at a new analysis of the mortality caused by smallpox and of the advantages of inoculation to prevent it. *Reviews in Medical Virology*, 14(5):275–288. doi:10.1002/rmv.443.

[21] Bianchini, L. and Fasano, A. (2009). A model combining acid-mediated tumour invasion and nutrient dynamics. *Nonlinear Analysis: Real World Applications*, 10(4):1955–1975. doi:10.1016/j.nonrwa.2008.03.001.

[22] Bishr, M. and Saad, F. (2013). Overview of the latest treatments for castration-resistant prostate cancer. *Nature Reviews Urology*, 10(9):522–528. doi:10.1038/nrurol.2013.137.

[23] Blasco, M. A. (2005). Telomeres and human disease: ageing, cancer and beyond. *Nature Reviews Genetics*, 6(8):611–622. doi:10.1038/nrg1656.

[24] Boland, C. R. and Goel, A. (2005). Somatic evolution of cancer cells. In *Seminars in Cancer Biology*, volume 15, pages 436–450. Elsevier.

[25] Britton, N. F. (2003). *Essential Mathematical Biology*. Springer, New York, NY.

[26] Brock, A., Chang, H. and Huang, S. (2009). Non-genetic heterogeneity – a mutation-independent driving force for the somatic evolution of tumours. *Nature Reviews Genetics*, 10(5):336–342. doi:10.1038/nrg2556.

[27] Burden, T., Ernstberger, J. and Fister, K. R. (2004). Optimal control applied to immunotherapy. *Discrete and Continuous Dynamical Systems - Series B*, 4(1):135–146. doi:10.3934/dcdsb.2004.4.135.

[28] Burton, A. C. (1966). Rate of growth of solid tumours as a problem of diffusion. *Growth*, 30(2):157–176.

[29] Bussolino, F., Arese, M., Audero, E., Giraudo, E., Marchio, S., Mitola, S., Primo, L. and Serini, G. (2003). Biological aspects of tumour angiogenesis. In Preziosi, L., editor, *Cancer Modelling and Simulation*, Chapman & Hall/CRC Mathematical & Computational Biology, pages 1–22. CRC Press, Boca Raton, FL.

[30] Byrne, H. M. (2003). Modelling avascular tumour growth. In Preziosi, L., editor, *Cancer Modelling and Simulation*, Chapman & Hall/CRC Mathematical & Computational Biology, pages 75–120. CRC Press, Boca Raton, FL.

[31] Byrne, H. M., Owen, M. R., Alarcon, T., Murphy, J. and Maini, P. K. (2006). Modelling the response of vascular tumours to chemotherapy: a multiscale approach. *Mathematical Models and Methods in Applied Sciences*, 16:1219–1241. doi:10.1142/S0218202506001522.

[32] Carmeliet, P. (2005). VEGF as a key mediator of angiogenesis in cancer. *Oncology*, 69(3): 4–10. doi:10.1159/000088478.

[33] Casciari, J. J., Sotirchos, S. V. and Sutherland, R. M. (1992). Variations in tumor cell growth rates and metabolism with oxygen concentration, glucose concentration, and extracellular pH. *Journal of Cell Physiology*, 151:386–394. doi:10.1002/jcp.1041510220.

[34] Chaplain, M. A. J. (1996). Avascular growth, angiogenesis and vascular growth in solid tumours: The mathematical modelling of the stages of tumour development. *Mathematical and Computer Modelling*, 23(6):47–87. doi:10.1016/0895-7177(96)00019-2.

[35] Chaplain, M. A. J. and Anderson, A. R. A. (2003). Mathematical modelling of tissue invasion. In Preziosi, L., editor, *Cancer Modelling and Simulation*, Chapman & Hall/CRC Mathematical & Computational Biology, pages 269–297. CRC Press, Boca Raton, FL.

[36] Chen, H., Treweeke, A. T., West, D. C., Till, K. J., Cawley, J. C., Zuzel, M. and Toh, C. H. (2000). In vitro and in vivo production of vascular endothelial growth factor by chronic lymphocytic leukemia cells. *Blood*, 96(9):3181–3187.

[37] Cheng, N., Chytil, A., Shyr, Y., Joly, A. and Moses, H. L. (2008). Transforming growth factor-β signaling–deficient fibroblasts enhance hepatocyte growth factor signaling in mammary carcinoma cells to promote scattering and invasion. *Molecular Cancer Research*, 6 (10):1521–1533. doi:10.1158/1541-7786.MCR-07-2203.

[38] Christofk, H. R., Vander Heiden, M. G., Harris, M. H., Ramanathan, A., Gerszten, R. E., Wei, R., Fleming, M. D., Schreiber, S. L. and Cantley, L. C. (2008). The M2 splice isoform of pyruvate kinase is important for cancer metabolism and tumour growth. *Nature*, 452 (7184):230–233. doi:10.1038/nature06734.

[39] Coghlin, C. and Murray, G. I. (2010). Current and emerging concepts in tumour metastasis. *The Journal of Pathology*, 222(1):1–15. doi:10.1002/path.2727.

[40] Collado, M. and Serrano, M. (2010). Senescence in tumours: evidence from mice and humans. *Nature Reviews Cancer*, 10(1):51–57. doi:10.1038/nrc2772.

[41] Collado, M., Blasco, M. A. and Serrano, M. (2007). Cellular senescence in cancer and aging. *Cell*, 130(2):223–233. doi:10.1016/j.cell.2007.07.003.

[42] Corrie, P. G. (2011). Cytotoxic chemotherapy: clinical aspects. *Medicine*, 39(12):717–722. doi:10.1383/medc.32.3.25.28619.

[43] Cronin, M., Stanton, R. M., Francis, K. P. and Tangney, M. (2012). Bacterial vectors for imaging and cancer gene therapy: a review. *Cancer Gene Therapy*, 19(11):731–740. doi:10.1038/cgt.2012.59.

[44] Cruveilier, J. (1829). *Anatomie Pathologique du Corps Humain*. Bailliere, Paris.

[45] Dale, P. D., Maini, P. K. and Sherratt, J. A. (1994). Mathematical modeling of corneal epithelial wound healing. *Mathematical Biosciences*, 124(2):127–147. doi:10.1016/0025-5564(94)90040-X.

[46] De Bock, K., Mazzone, M. and Carmeliet, P. (2011). Antiangiogenic therapy, hypoxia, and metastasis: risky liaisons, or not? *Nature Reviews Clinical Oncology*, 8(7):393–404. doi:10.1038/nrclinonc.2011.83.

[47] de Pillis, L., Renee Fister, K., Gu, W., Collins, C., Daub, M., Gross, D., Moore, J. and Preskill, B. (2009). Mathematical model creation for cancer chemo-immunotherapy. *Computational and Mathematical Methods in Medicine*, 10(3):165–184. doi:10.1080/17486700802216301.

[48] de Pillis, L. G. and Radunskaya, A. (2003). A mathematical model of immune response to tumor invasion. In Bathe, K. J., editor, *Proceedings of the Second MIT Conference on Computational Fluid and Solid Mechanics*.

[49] de Pillis, L. G., Gu, W. and Radunskaya, A. E. (2006). Mixed immunotherapy and chemotherapy of tumors: modeling, applications and biological interpretations. *Journal of Theoretical Biology*, 238(4):841–862. doi:10.1016/j.jtbi.2005.06.037.

[50] de Pillis, L. G., Gu, W., Fister, K. R., Head, T., Maples, K., Murugan, A., Neal, T. and Yoshida, K. (2007). Chemotherapy for tumors: An analysis of the dynamics and a study of quadratic and linear optimal controls. *Mathematical Biosciences*, 209(1):292–315. doi:10.1016/j.mbs.2006.05.003.

[51] Dellian, M., Helmlinger, G., Yuan, F. and Jain, R. K. (1996). Fluorescence ratio imaging of interstitial pH in solid tumours: effect of glucose on spatial and temporal gradients. *British Journal of Cancer*, 74(8):1206–1215. doi:10.1038/bjc.1996.518.

[52] Demicheli, R., Retsky, M. W., Hrushesky, W. J. M., Baum, M. and Gukas, I. D. (2008). The effects of surgery on tumor growth: a century of investigations. *Annals of Oncology*, 19(11): 1821–1828. doi:10.1093/annonc/mdn386.

[53] DeVita, V. T., Lawrence, T. S. and Rosenberg, S. A. (2011). *Cancer: Principles and Practice of Oncology*. Lippincott Williams and Wilkins, 9th edition.

[54] Dietz, K. and Heesterbeek, J. A. P. (2002). Daniel Bernoulli's epidemiological model revisited. *Mathematical Biosciences*, 180:1–21. doi:10.1016/S0025-5564(02)00122-0.

[55] Drake, C. G. (2010). Prostate cancer as a model for tumour immunotherapy. *Nature Reviews Immunology*, 10(8):580–593. doi:10.1038/nri2817.

[56] Durand, R. E. (1990). Multicell spheroids as a model for cell kinetic-studies. *Cell and Tissue Kinetics*, 23(3):141–159. doi:10.1111/j.1365-2184.1990.tb01111.x.

[57] Eifel, P. J. (2006). Concurrent chemotherapy and radiation therapy as the standard of care for cervical cancer. *Nature Clinical Practice Oncology*, 3(5):248–255. doi:10.1038/ncponc0486.

[58] Elstrom, R. L., Bauer, D. E., Buzzai, M., Karnauskas, R., Harris, M. H., Plas, D. R., Zhuang, H., Cinalli, R. M., Alavi, A., Rudin, C. M. and Thompson, C. B. (2004). Akt stimulates aerobic glycolysis in cancer cells. *Cancer Research*, 64(11):3892–3899. doi:10.1158/0008-5472.CAN-03-2904.

[59] Esposito, W. R. and Floudas, C. A. (1998). Parameter estimation in nonlinear algebraic models via global optimization. *Computers and Chemical Engineering*, 22:S213–S220. doi:10.1016/S0098-1354(98)00217-8.

[60] Estrella, V., Chen, T., Lloyd, M., Wojtkowiak, J., Cornnell, H. H., Ibrahim-Hashim, A., Bailey, K., Balagurunathan, Y., Rothberg, M., Sloane, B. F., Johnson, J., Gatenby, R. A. and Gillies, R. J. (2013). Acidity generated by the tumor microenvironment drives local invasion. *Cancer Research*, 73:1524–1535. doi:10.1158/0008-5472.CAN-12-2796.

[61] Evan, G. I. and Vousden, K. H. (2001). Proliferation, cell cycle and apoptosis in cancer. *Nature*, 411(6835):342–348. doi:10.1038/35077213.

[62] Farkas, M. (1994). *Periodic Motions*, volume 104 of *Applied Mathematical Sciences*. Springer-Verlag, New York, NY.

[63] Fasano, A., Herrero, M. A. and Rodrigo, M. R. (2009). Slow and fast invasion waves in a model of acid-mediated tumour growth. *Mathematical Biosciences*, 220(1):45–56. doi:10.1016/j.mbs.2009.04.001.

[64] Fearon, E. R. and Vogelstein, B. (1990). A genetic model for colorectal tumorigenesis. *Cell*, 61(5):759–767. doi:10.1016/0092-8674(90)90186-I.

[65] Ferrara, N. (2009). Vascular endothelial growth factor. *Arteriosclerosis, Thrombosis, and Vascular Biology*, 29(6):789–791. doi:10.1161/ATVBAHA.108.179663.

[66] Fisher, R. A. (1937). The wave of advance of advantageous genes. *Annals of Eugenics*, 7 (2):355–369.

[67] Fister, K. R. and Donnelly, J. H. (2005). Immunotherapy: An optimal control theory approach. *Mathematical Biosciences and Engineering*, 2(3):499–510. doi:10.3934/mbe.2005.2.499.

[68] Gambhir, S. S. (2002). Molecular imaging of cancer with positron emission tomography. *Nature Reviews Cancer*, 2(9):683–693. doi:10.1038/nrc882.

[69] Gardner, R. A. (1982). Existence and stability of travelling wave solutions of competition models: A degree theoretic approach. *Journal of Differential Equations*, 44(3):343–364. doi:10.1016/0022-0396(82)90001-8.

[70] Gatenby, R. A. (1995). Models of tumor-host interaction as competing populations: implications for tumor biology and treatment. *Journal of Theoretical Biology*, 176(4):447–455. doi:10.1006/jtbi.1995.0212.

[71] Gatenby, R. A. and Gawlinski, E. T. (1996). A reaction-diffusion model of cancer invasion. *Cancer Research*, 56(24):5745–5753.

[72] Gatenby, R. A. and Gawlinski, E. T. (2003). The glycolytic phenotype in carcinogenesis and tumour invasion: insights through mathematical modelling. *Cancer Research*, 63(24): 3847–3854.

[73] Gatenby, R. A. and Gillies, R. J. (2004). Why do cancers have high aerobic glycolysis? *Nature Reviews Cancer*, 4:891–899. doi:10.1038/nrc1478.

[74] Gatenby, R. A. and Gillies, R. J. (2008). A microenvironmental model of carcinogenesis. *Nature Reviews Cancer*, 8(1):56–61. doi:10.1038/nrc2255.

[75] Gatenby, R. A. and Vincent, T. L. (2003). An evolutionary model of carcinogenesis. *Cancer Research*, 63(19):6212–6220.

[76] Gatenby, R. A., Maini, P. K. and Gawlinski, E. T. (2002). Analysis of tumor as an inverse problem provides a novel theoretical framework for understanding tumor biology and therapy. *Applied Mathematics Letters*, 15(3):339–345. doi:10.1016/S0893-9659(01)00141-0.

[77] Gatenby, R. A., Gawlinski, E. T., Gmitro, A. F., Kaylor, B. and Gillies, R. J. (2006). Acid-mediated tumor invasion: a multidisciplinary study. *Cancer Research*, 66(10):5216–5223. doi:10.1158/0008-5472.CAN-05-4193.

[78] Gatenby, R. A., Smallbone, K., Maini, P. K., Rose, F., Averill, J., Nagle, R. B., Worrall, L. and Gillies, R. J. (2007). Cellular adaptations to hypoxia and acidosis during somatic evolution of breast cancer. *British Journal of Cancer*, 97(5):646–653. doi:10.1038/sj.bjc.6603922.

[79] Gerisch, A. and Chaplain, M. A. J. (2008). Mathematical modelling of cancer cell invasion of tissue: Local and non-local models and the effect of adhesion. *Journal of Theoretical Biology*, 250:684–704. doi:10.1016/j.jtbi.2007.10.026.

[80] Giancotti, F. G. (2014). Deregulation of cell signaling in cancer. *FEBS Letters*, 588(16): 2558–2750. doi:10.1016/j.febslet.2014.02.005.

[81] Gillies, R., Liu, Z. and Bhujwalla, Z. (1994). 31P-MRS measurements of extracellular pH of tumors using 3-aminopropylphosphonate. *American Journal of Physiology - Cell Physiology*, 267(1):C195–C203.

[82] Gompertz, B. (1825). On the nature of the function expressive of the law of human mortality, and on a new mode of determining the value of life contingencies. *Philosophical Transactions of the Royal Society of London*, 115:513–583.

[83] Gottschalk, S., Anderson, N., Hainz, C., Eckhardt, S. G. and Serkova, N. J. (2004). Imatinib (STI571)-mediated changes in glucose metabolism in human leukemia BCR-ABL-positive cells. *Clinical Cancer Research*, 10(19):6661–6668. doi:10.1158/1078-0432.CCR-04-0039.

[84] Gray, L. H., Conger, A. D., Ebert, M., Hornsey, S. and Scott, O. C. (1953). The concentration of oxygen dissolved in tissues at the time of irradiation as a factor in radiotherapy. *The British Journal of Radiology*, 26(312):638–648. doi:10.1259/0007-1285-26-312-638.

[85] Greenspan, H. P. (1976). On the growth and stability of cell cultures and solid tumors. *Journal of Theoretical Biology*, 56(1):229–242. doi:10.1016/S0022-5193(76)80054-9.

[86] Grossfeld, G. D., Ginsberg, D. A., Stein, J. P., Bochner, B. H., Esrig, D., Nichols, P. W., Taylor, C. R., Cote, R. J., Groshen, S., Dunn, M. and Skinner, D. G. (1997). Thrombospondin-1 expression in bladder cancer: Association with p53 alterations, tumor angiogenesis, and tumor progression. *Journal of the National Cancer Institute*, 89(3):219–227. doi:10.1093/jnci/89.3.219.

[87] Gupta, G. P., Minn, A. J., Kang, Y., Siegel, P. M., Serganova, I., Cordon-Cardo, C., Olshen, A. B., Gerald, W. L. and Massagué, J. (2005). Identifying site-specific metastasis genes and functions. In *Cold Spring Harbor Symposia on Quantitative Biology*, volume 70, pages 149–158.

[88] Hanahan, D. and Folkman, J. (1996). Patterns and emerging mechanisms of the angiogenic switch during tumorigenesis. *Cell*, 86(3):353–364. doi:10.1016/S0092-8674(00)80108-7.

[89] Hanahan, D. and Weinberg, R. A. (2000). The hallmarks of cancer. *Cell*, 100(1):57–70. doi:10.1016/S0092-8674(00)81683-9.

[90] Hanahan, D. and Weinberg, R. A. (2011). Hallmarks of cancer: The next generation. *Cell*, 144(5):646–674. doi:10.1016/j.cell.2011.02.013.

[91] Hawkins, R. A. and Phelps, M. E. (1988). PET in clinical oncology. *Cancer and Metastasis Reviews*, 7(2):119–142. doi:10.1007/BF00046482.

[92] Helmlinger, G., Yuan, F., Dellian, M. and Jain, R. K. (1997). Interstitial pH and pO2 gradients in solid tumors in vivo: high-resolution measurements reveal a lack of correlation. *Nature Medicine*, 3(2):177–182. doi:10.1038/nm0297-177.

[93] Hemker, P. W. (1972). Numerical methods for differential equations in system simulation and in parameter estimation. *Analysis and Simulation of Biochemical Systems*, pages 59–80.

[94] Hess, P. (1991). *Periodic-Parabolic Boundary Value Problems and Positivity*, volume 247 of *Pitman Research Notes in Mathematics Series*. Longman Scientific & Technical, Harlow, UK.

[95] Holder, A. B. and Rodrigo, M. R. (2013). An integration-based method for estimating parameters in a system of differential equations. *Applied Mathematics and Computation*, 219: 9700–9708. doi:10.1016/j.amc.2013.03.052.

[96] Holder, A. B. and Rodrigo, M. R. (2014). Model for acid-mediated tumour invasion with chemotherapy intervention I: Homogeneous populations. *eprint arXiv:1412.0748*.

[97] Holder, A. B. and Rodrigo, M. R. (2014). Model for acid-mediated tumour invasion with chemotherapy intervention II: heterogeneous populations. Working paper, University of Wollongong.

[98] Holder, A. B., Rodrigo, M. R. and Herrero, M. A. (2014). A model for acid-mediated tumour growth with nonlinear acid production term. *Applied Mathematics and Computation*, 227C: 176–198. doi:10.1016/j.amc.2013.11.018.

[99] Hosono, Y. (1998). The minimal speed of traveling fronts for a diffusive Lotka–Volterra competition model. *Bulletin of Mathematical Biology*, 60(3):435–448. doi:10.1006/bulm.1997.0008.

[100] Huang, Y., Liu, D. and Wu, H. (2006). Hierarchical Bayesian methods for estimation of parameters in a longitudinal HIV dynamic system. *Biometrics*, 62(2):413–423. doi:10.1111/j.1541-0420.2005.00447.x.

[101] Hubbard, S. R. and Miller, W. T. (2007). Receptor tyrosine kinases: mechanisms of activation and signaling. *Current Opinion in Cell Biology*, 19(2):117–123. doi:10.1016/j.ceb.2007.02.010.

[102] Hung, L.-C. (2012). Exact traveling wave solutions for diffusive Lotka–Volterra systems of two competing species. *Japan Journal of Industrial and Applied Mathematics*, 29(2): 237–251. doi:10.1007/s13160-012-0056-2.

[103] International Agency for Research on Cancer (2014). Globocan 2012: Estimated cancer incidence, mortality and prevalence worldwide in 2012. URL http://globocan.iarc.fr/Pages/fact_sheets_population.aspx.

[104] Jackson, T. L. and Byrne, H. M. (2000). A mathematical model to study the effects of drug resistance and vasculature on the response of solid tumors to chemotherapy. *Mathematical Biosciences*, 164(1):17–38. doi:10.1016/S0025-5564(99)00062-0.

[105] Jones, P. F. and Sleeman, B. D. (2006). Angiogenesis–understanding the mathematical challenge. *Angiogenesis*, 9(3):127–138. doi:10.1007/s10456-006-9039-8.

[106] Kan-On, Y. (1995). Parameter dependence of propagation speed of travelling waves for competition-diffusion equations. *SIAM Journal on Mathematical Analysis*, 26(2):340–363. doi:10.1137/S0036141093244556.

[107] Kan-On, Y. (1997). Fisher wave fronts for the Lotka–Volterra competition model with diffusion. *Nonlinear Analysis: Theory, Methods & Applications*, 28(1):145–164. doi:10.1016/0362-546X(95)00142-I.

[108] Keener, J. P. (1986). A geometrical theory for spiral waves in excitable media. *SIAM Journal on Applied Mathematics*, 46(6):1039–1056. doi:10.1137/0146062.

[109] Kim, M.-Y., Oskarsson, T., Acharyya, S., Nguyen, D. X., Zhang, X. H.-F., Norton, L. and Massague, J. (2009). Tumor self-seeding by circulating cancer cells. *Cell*, 139(7):1315–1326. doi:10.1016/j.cell.2009.11.025.

[110] Kim, P. S. and Lee, P. P. (2012). Modeling protective anti-tumor immunity via preventative cancer vaccines using a hybrid agent-based and delay differential equation approach. *PLoS Computational Biology*, 8(10):e1002742. doi:10.1371/journal.pcbi.1002742.

[111] Klein, C. A. (2009). Parallel progression of primary tumours and metastases. *Nature Reviews Cancer*, 9(4):302–312. doi:10.1038/nrc2627.

[112] Kolmogorov, A. A., Petrovsky, I. G. and Piskunov, N. S. (1937). Study of the diffusion equation with growth of the quantity of matter and its application to a biology problem (Russian). *Bulletin of the Moscow State University*, 17:1–26.

[113] Kraus, M. and Wolf, B. (1996). Implications of acidic tumor microenvironment for neoplastic growth and cancer treatment: A computer analysis. *Tumor Biology*, 17(3):133–154. doi:10.1159/000217977.

[114] Kuznetsov, V. A., Makalkin, I. A., Taylor, M. A. and Perelson, A. S. (1994). Nonlinear dynamics of immunogenic tumors: Parameter estimation and global bifurcation analysis. *Bulletin of Mathematical Biology*, 56(2):295–321. doi:10.1016/S0092-8240(05)80260-5.

[115] Laird, A. K. (1964). Dynamics of tumour growth. *British Journal of Cancer*, 13:490–502. doi:10.1038/bjc.1964.55.

[116] Landau, M. D. and Jones, W. R. (1983). A hardy old problem. *Mathematics Magazine*, 56 (4):230–232. doi:10.2307/2689813.

[117] Lardner, A. (2001). The effects of extracellular pH on immune function. *Journal of Leukocyte Biology*, 69(4):522–530.

[118] Lee, W.-Y., Huang, S.-C., Hsu, K.-F., Tzeng, C.-C. and Shen, W.-L. (2008). Roles for hypoxia-regulated genes during cervical carcinogenesis: Somatic evolution during the hypoxia-glycolysis-acidosis sequence. *Gynecologic Oncology*, 108(2):377–384. doi:10.1016/j.ygyno.2007.10.034.

[119] Lemmon, M. A. and Schlessinger, J. (2010). Cell signaling by receptor tyrosine kinases. *Cell*, 141(7):1117–1134. doi:10.1016/j.cell.2010.06.011.

[120] Lessene, G., Czabotar, P. E. and Colman, P. M. (2008). BCL-2 family antagonists for cancer therapy. *Nature Reviews Drug Discovery*, 7(12):989–1000. doi:10.1038/nrd2658.

[121] Li, Z., Osbourne, M. and Prvan, T. (2005). Parameter estimation of ordinary differential equations. *IMA Journal of Numerical Analysis*, 25:264:264–235. doi:10.1093/imanum/drh016.

[122] Liang, H. and Wu, H. (2008). Parameter estimation for differential equation models using a framework of measurement error in regression models. *Journal of the American Statistical Association*, 103(484):1570–1583. doi:10.1198/016214508000000797.

[123] Lide, D. R. (2001). *CRC Handbook of Physics and Chemistry*. CRC Press, Boca Raton, FL.

[124] Lindner, U., Trachtenberg, J. and Lawrentschuk, N. (2010). Focal therapy in prostate cancer: modalities, findings and future considerations. *Nature Reviews Urology*, 7(10):562–571. doi:10.1038/nrurol.2010.142.

[125] Liotta, L. A., Saidel, G. M. and Kleinerman, J. (1976). Stochastic model of metastases formation. *Biometrics*, 32(3):535–550. doi:10.2307/2529743.

[126] Liotta, L. A., Saidel, G. M. and Kleinerman, J. (1977). Diffusion model of tumor vascularization and growth. *Bulletin of Mathematical Biology*, 39(1):117–128. doi:10.1016/S0092-8240(77)80040-2.

[127] Loeffler, D. A., Juneau, P. L. and Heppner, G. H. (1991). Natural killer-cell activity under conditions reflective of tumor micro-environment. *International Journal of Cancer*, 48(6): 895–899. doi:10.1002/ijc.2910480617.

[128] Loeffler, D. A., Juneau, P. L. and Masserant, S. (1992). Influence of tumour physicochemical conditions on interleukin-2-stimulated lymphocyte proliferation. *British Journal of Cancer*, 66(4):619–622. doi:10.1038/bjc.1992.326.

[129] Lowe, S. W., Cepero, E. and Evan, G. (2004). Intrinsic tumour suppression. *Nature*, 432 (7015):307–315. doi:10.1038/nature03098.

[130] Mac Gabhann, F. and Popel, A. S. (2008). Systems biology of vascular endothelial growth factors. *Microcirculation*, 15(8):715–738. doi:10.1080/10739680802095964.

[131] Mallet, D. G. and de Pillis, L. G. (2006). A cellular automata model of tumor-immune system interactions. *Journal of Theoretical Biology*, 239:334–350. doi:10.1016/j.jtbi.2005.08.002.

[132] Mantzaris, N. V., Webb, S. and Othmer, H. G. (2004). Mathematical modeling of tumor-induced angiogenesis. *Journal of Mathematical Biology*, 49(2):111–187. doi:10.1007/s00285-003-0262-2.

[133] Martin, G. R. and Jain, R. K. (1994). Noninvasive measurement of interstitial pH profiles in normal and neoplastic tissue using fluorescence ratio imaging microscopy. *Cancer Research*, 54(21):5670–5674.

[134] Martin, N. K., Gaffney, E. A., Gatenby, R. A. and Maini, P. K. (2010). Tumour-stromal interactions in acid-mediated invasion: A mathematical model. *Journal of Theoretical Biology*, 267:461–470. doi:10.1016/j.jtbi.2010.08.028.

[135] Martinez-Zaguilan, R., Seftor, E. A., Seftor, R. E. B., Chu, Y.-W., Gillies, R. J. and Hendrix, M. J. C. (1996). Acidic pH enhances the invasive behavior of human melanoma cells. *Clinical and Experimental Metastasis*, 14(2):176–186. doi:10.1007/BF00121214.

[136] Matzavinos, A., Chaplain, M. A. J. and Kuznetsov, V. A. (2004). Mathematical modelling of the spatio-temporal response of cytotoxic t-lymphocytes to a solid tumour. *Mathematical Medicine and Biology*, 21(1):1–34. doi:10.1093/imammb/21.1.1.

[137] Mayer, H., Zaenker, K. S. and an der Heiden, U. (1994). A basic mathematical model of the immune response. *Chaos*, 5(1):155–161. doi:10.1063/1.166098.

[138] Mayneord, W. V. (1932). On a law of growth of Jensen's rat sarcoma. *American Journal of Cancer*, 16:841–846. doi:10.1158/ajc.1932.841.

[139] McGillen, J. B., Martin, N. K., Robey, I. F., Gaffney, E. A. and Maini, P. K. (2012). Applications of mathematical analysis to tumour acidity modelling. *RIMS Kokyuroku Bessatsu*, 31:31–59.

[140] McGillen, J. B., Gaffney, E. A., Martin, N. K. and Maini, P. K. (2014). A general reaction-diffusion model of acidity in cancer invasion. *Journal of Mathematical Biology*, 68:1199–1224. doi:10.1007/s00285-013-0665-7.

[141] McGowan, P. M., Kirstein, J. M. and Chambers, A. F. (2009). Micrometastatic disease and metastatic outgrowth: clinical issues and experimental approaches. *Future Oncology*, 5(7):1083–1098. doi:10.2217/fon.09.73.

[142] Meyskens, Jr, F. L., Thomson, S. P. and Moon, T. E. (1984). Quantitation of the number of cells within tumor colonies in semisolid medium and their growth as oblate spheroids. *Cancer Research*, 44(1):271–277.

[143] Monazzam, A., Razifar, P., Lindhe, Ö., Josephsson, R., Långström, B. and Bergström, M. (2005). A new, fast and semi-automated size determination method (SASDM) for studying multicellular tumor spheroids. *Cancer Cell International*, 5(1):32. doi:10.1186/1475-2867-5-32.

[144] Morita, T., Nagaki, T., Fukuda, I. and Okumura, K. (1992). Clastogenicity of low pH to various cultured mammalian cells. *Mutation Research/Fundamental and Molecular Mechanisms of Mutagenesis*, 268(2):297–305. doi:10.1016/0027-5107(92)90235-T.

[145] Murray, J. D. (2002). *Mathematical Biology I: An Introduction*. Springer, New York, NY, 3rd edition.

[146] Murray, J. D. (2002). *Mathematical Biology II: Spatial Models and Biomedical Applications*, volume II. Springer, New York, NY, 3rd edition.

[147] Nguyen, D. X., Bos, P. D. and Massagué, J. (2009). Metastasis: from dissemination to organ-specific colonization. *Nature Reviews Cancer*, 9(4):274–284. doi:10.1038/nrc2622.

[148] Nolop, K. B., Rhodes, C. G., Brudin, L. H., Beaney, R. P., Krausz, T., Jones, T. and Hughes, J. M. B. (1987). Glucose utilization in vivo by human pulmonary neoplasms. *Cancer*, 60(11):2682–2689. doi:10.1002/1097-0142(19871201)60:11<2682::AID-CNCR2820601118>3.0.CO;2-H.

[149] Nowak, M. A. and May, R. M. (2000). *Virus Dynamics: Mathematical Principles of Immunology and Virology*. Oxford University Press, Oxford.

[150] Orme, M. E. and Chaplain, M. A. J. (1996). A mathematical model of vascular tumour growth and invasion. *Mathematical and Computer Modelling*, 23(10):43–60. doi:10.1016/0895-7177(96)00053-2.

[151] Owen, M. R. and Sherratt, J. A. (1998). Modelling the macrophage invasion of tumours: effects on growth and composition. *IMA Journal of Mathematics Applied in Medicine and Biology*, 15(2):165–185. doi:10.1093/imammb/15.2.165.

[152] Owen, M. R. and Sherratt, J. A. (1999). Mathematical modelling of macrophage dynamics in tumours. *Mathematical Models and Methods in Applied Sciences*, 9(4):513–539. doi:10.1142/S0218202599000270.

[153] Owen, M. and Sherratt, J. (1997). Pattern formation and spatiotemporal irregularity in a model for macrophage-tumour interactions. *Journal of Theoretical Biology*, 189(1):63–80. doi:10.1006/jtbi.1997.0494.

[154] Owonikoko, T. K., Tran, N. L., Ryken, T., Moore, M. K., Egan, K. M., Olson, J. J., Arbiser, J., Zelnak, A., Shu, H. K. G., Shim, H., Robin, A. M., Kalkanis, S. N., Whitsett, T. G. and

Salhia, B. (2014). Current approaches to the treatment of metastatic brain tumours. *Nature Reviews Clincal Oncology*, 11(4):203–222. doi:10.1038/nrclinonc.2014.25.

[155] Painter, K. J. (2009). Continuous models for cell migration in tissues and applications to cell sorting via differential chemotaxis. *Bulletin of Mathematical Biology*, 71(5):1117–1147. doi:10.1007/s11538-009-9396-8.

[156] Panetta, J. and Fister, K. (2000). Optimal control applied to cell-cycle-specific cancer chemotherapy. *SIAM Journal on Applied Mathematics*, 60(3):1059–1072. doi:10.1137/S0036139998338509.

[157] Panetta, J. C. (1997). A mathematical model of breast and ovarian cancer treated with paclitaxel. *Mathematical Biosciences*, 146(2):89–113. doi:10.1016/S0025-5564(97)00077-1.

[158] Park, H. J., Lyons, J. C., Ohtsubo, T. and Song, C. W. (1999). Acidic environment causes apoptosis by increasing caspase activity. *British Journal of Cancer*, 80:1892–1897. doi:10.1038/sj.bjc.6690617.

[159] Patel, A. A., Gawlinski, E. T., Lemieux, S. K. and Gatenby, R. A. (2001). A cellular automaton model of early tumor growth and invasion: the effects of native tissue vascularity and increased anaerobic tumor metabolism. *Journal of Theoretical Biology*, 213(3):315–331. doi:10.1006/jtbi.2001.2385.

[160] Peng, H., Li, L., Yang, Y. and Wang, C. (2009). Parameter estimation of nonlinear dynamical systems based on integrator theory. *Chaos*, 19(3):033130. doi:10.1063/1.3216850.

[161] Perelson, A. S. and Nelson, P. W. (1999). Mathematical analysis of HIV-1 dynamics in vivo. *SIAM Review*, 41(1):3–44. doi:10.1137/S0036144598335107.

[162] Perelson, A. S., Neumann, A. U., Markowitz, M., Leonard, J. M. and Ho, D. D. (1996). HIV-1 dynamics in vivo: virion clearance rate, infected cell life-span, and viral generation time. *Science*, 271(5255):1582–1586. doi:10.1126/science.271.5255.1582.

[163] Perelson, A. S., Essunger, P., Cao, Y., Vesanen, M., Hurley, A., Saksela, K., Markowitz, M. and Ho, D. D. (1997). Decay characteristics of HIV-1-infected compartments during combination therapy. *Nature*, 387(6629):188–191. doi:10.1038/387188a0.

[164] Perry, M. C., editor (2008). *The Chemotherapy Source Book*. Lippincott Williams and Wilkins, fourth edition.

[165] Pierotti, M., Berrino, F., Gariboldi, M., Melani, C., Mogavero, A., Negri, T., Pasanisi, P. and Pilotti, S. (2013). Targeting metabolism for cancer treatment and prevention: metformin, an old drug with multi-faceted effects. *Oncogene*, 32(12):1475–1487. doi:10.1038/onc.2012.181.

[166] Plank, M. J. and Sleeman, B. D. (2003). Tumour-induced angiogenesis: A review. *Journal of Theoretical Medicine*, 5(3-4):137–153. doi:10.1080/10273360410001700843.

[167] Polyanin, A. D. (2002). *Handbook of Linear Partial Differential Equations for Engineers and Scientists*. Chapman & Hall/CRC, Boca Raton, FL.

[168] Preziosi, L. (2003). *Cancer Modelling and Simulation*. Chapman & Hall/CRC Mathematical & Computational Biology. CRC Press, Boca Raton, FL.

[169] Putter, H., Heisterkamp, S. H., Lange, J. M. A. and de Wolf, F. (2002). A Bayesian approach to parameter estimation in HIV dynamical models. *Statistics in Medicine*, 21(15):2199–2214. doi:10.1002/sim.1211.

[170] Raica, M., Cimpean, A. M. and Ribatti, D. (2009). Angiogenesis in pre-malignant conditions. *European Journal of Cancer*, 45(11):1924–1934. doi:10.1016/j.ejca.2009.04.007.

[171] Ramsay, J. O. and Silverman, B. W. (2005). *Functional Data Analysis*. Springer, New York, NY.

[172] Ramsay, J. O., Hooker, G., Campbell, D. and Cao, J. (2007). Parameter estimation for differential equations: A generalized smoothing approach. *Journal of the Royal Statistical Society Series B (Statistical Methodology)*, 69(5):741–796. doi:10.1111/j.1467-9868.2007.00610.x.

[173] Ratner, S. (1990). Lymphocytes stimulated with recombinant human interleukin-2: relationship between motility into protein matrix and in vivo localization in normal and neoplastic tissues of mice. *Journal of the National Cancer Institute*, 82(7):612–616. doi:10.1093/jnci/82.7.612.

[174] Ratner, S. (1992). Motility of IL-2-stimulated lymphocytes in neutral and acidified extracellular matrix. *Cellular Immunology*, 139(2):399–410. doi:10.1016/0008-8749(92)90081-Y.

[175] Redegeld, F., Filippini, A. and Sitkovsky, M. (1991). Comparative studies of the cytotoxic T lymphocyte-mediated cytotoxicity and of extracellular ATP-induced cell lysis. Different requirements in extracellular Mg2+ and pH. *The Journal of Immunology*, 147(10):3638–3645.

[176] Reinacher-Schick, A., Pohl, M. and Schmiegel, W. (2008). Drug insight: antiangiogenic therapies for gastrointestinal cancers–focus on monoclonal antibodies. *Nature Clinical Practice Gastroenterology & Hepatology*, 5(5):250–267. doi:10.1038/ncpgasthep1097.

[177] Rice, J., Ottensmeier, C. H. and Stevenson, F. K. (2008). DNA vaccines: precision tools for activating effective immunity against cancer. *Nature Reviews Cancer*, 8(2):108–120. doi:10.1038/nrc2326.

[178] Rinzel, J. and Keller, J. B. (1973). Traveling wave solutions of a nerve conduction equation. *Biophysical Journal*, 13(12):1313–1337. doi:10.1016/S0006-3495(73)86065-5.

[179] Rodrigo, M. and Mimura, M. (2000). Exact solutions of a competition-diffusion system. *Hiroshima Mathematical Journal*, 30(2):257–270.

[180] Rofstad, E. K., Mathiesen, B., Kindem, K. and Galappathi, K. (2006). Acidic extracellular pH promotes experimental metastasis of human melanoma cells in athymic nude mice. *Cancer Research*, 66(13):6699–6707. doi:10.1158/0008-5472.CAN-06-0983.

[181] Saidel, G. M., Liotta, L. A. and Kleinerman, J. (1976). System dynamics of a metastatic process from an implanted tumor. *Journal of Theoretical Biology*, 56(2):417–434. doi:10.1016/S0022-5193(76)80083-5.

[182] Schlappack, O. K., Zimmermann, A. and Hill, R. P. (1991). Glucose starvation and acidosis: effect on experimental metastatic potential, DNA content and MTX resistance of murine tumour cells. *British Journal of Cancer*, 64(4):663–670. doi:10.1038/bjc.1991.378.

[183] Severin, T., Muller, B., Giese, G., Uhl, B., Wolf, B., Hauschildt, S. and Kreutz, W. (1994). pH-dependent LAK cell cytotoxicity. *Tumor Biology*, 15(5):304–310. doi:10.1159/000217905.

[184] Shay, J. W. and Keith, W. N. (2008). Targeting telomerase for cancer therapeutics. *British Journal of Cancer*, 98(4):677–683. doi:10.1038/sj.bjc.6604209.

[185] Shepard, D. R. and Raghavan, D. (2010). Innovations in the systemic therapy of prostate cancer. *Nature Reviews Clinical Oncology*, 7(1):13–21. doi:10.1038/nrclinonc.2009.187.

[186] Skak, K., Kragh, M., Hausman, D., Smyth, M. J. and Sivakumar, P. V. (2008). Interleukin 21: combination strategies for cancer therapy. *Nature Reviews Drug Discovery*, 7(3):231–240. doi:10.1038/nrd2482.

[187] Smallbone, K., Gavaghan, D. J., Gatenby, R. A. and Maini, P. K. (2005). The role of acidity in solid tumour growth and invasion. *Journal of Theoretical Biology*, 235(4):476–484. doi:10.1016/j.jtbi.2005.02.001.

[188] Smallbone, K., Gatenby, R. A. and Maini, P. K. (2008). Mathematical modelling of tumour acidity. *Journal of Theoretical Biology*, 255(1):106–112. doi:10.1016/j.jtbi.2008.08.002.

[189] Solomon, M. and Kestelman, H. (1978). E2663. *The American Mathematical Monthly*, 85 (8):685–686. doi:10.2307/2320352.

[190] Spencer, S. L., Gerety, R. A., Pienta, K. J. and Forrest, S. (2006). Modeling somatic evolution in tumorigenesis. *PLoS Computational Biology*, 2(8):e108. doi:10.1371/journal.pcbi.0020108.

[191] Stubbs, M., McSheehy, P. M., Griffiths, J. R. and Bashford, C. L. (2000). Causes and consequences of tumour acidity and implications for treatment. *Molecular Medicine Today*, 6 (1):15–19. doi:10.1016/S1357-4310(99)01615-9.

[192] Sutherland, R. M. (1988). Cell and environment interactions in tumor microregions: the multicell spheroid model. *Science*, 240(4849):177–184. doi:10.1126/science.2451290.

[193] Talmadge, J. E. and Fidler, I. J. (2010). AACR centennial series: the biology of cancer metastasis: historical perspective. *Cancer Research*, 70(14):5649–5669. doi:10.1158/0008-5472.CAN-10-1040.

[194] Tan, W. Y. and Wu, H. (2005). *Deterministic and Stochastic Models of AIDS Epidemics and HIV Infections with Intervention*. World Scientific, Hackensack, NJ.

[195] Tracqui, P., Cruywagen, G. C., Woodward, D. E., Bartoo, G. T., Murray, J. D. and Alvord, E. C. (1995). A mathematical model of glioma growth: the effect of chemotherapy on spatio-temporal growth. *Cell Proliferation*, 28(1):17–31. doi:10.1111/j.1365-2184.1995.tb00036.x.

[196] Tsuji, T., Ibaragi, S. and Hu, G.-f. (2009). Epithelial-mesenchymal transition and cell cooperativity in metastasis. *Cancer Research*, 69(18):7135–7139. doi:10.1158/0008-5472.CAN-09-1618.

[197] Tyson, J. J. and Fife, P. C. (1980). Target patterns in a realistic model of the Belousov–Zhabotinskii reaction. *The Journal of Chemical Physics*, 73(5):2224–2237. doi:10.1063/1.440418.

[198] Tyson, J. J. and Novak, B. (2001). Regulation of the eukaryotic cell cycle: molecular antagonism, hysteresis, and irreversible transitions. *Journal of Theoretical Biology*, 210(2): 249–263. doi:10.1006/jtbi.2001.2293.

[199] Vander Heiden, M. G. (2011). Targeting cancer metabolism: a therapeutic window opens. *Nature Reviews Drug Discovery*, 10(9):671–684. doi:10.1038/nrd3504.

[200] Vander Heiden, M. G., Cantley, L. C. and Thompson, C. B. (2009). Understanding the Warburg effect: the metabolic requirements of cell proliferation. *Science*, 324:1029–1033. doi:10.1126/science.1160809.

[201] Walter, W. (1998). *Ordinary Differential Equations*, volume 182 of *Graduate Texts in Mathematics*. Springer, New York, NY.

[202] Warburg, O. (1926). *Über den Stoffwechsel der Tumoren*. Springer, Berlin.

[203] Warburg, O. (1956). On the origin of cancer cells. *Science*, 123:309–314. doi:10.1126/science.123.3191.309.

[204] Warburg, O., Posener, K. and Negelein, E. (1924). Ueber den stoffwechsel der tumoren. *Biochemische Zeitschrift*, 152:319–344.

[205] Weber, W. A., Avril, N. and Schwaiger, M. (1999). Relevance of positron emission tomography (PET) in oncology. *Strahlentherapie und Onkologie*, 175(8):356–372. doi:10.1007/s000660050022.

[206] Werner, J., Combs, S. E., Springfeld, C., Hartwig, W., Hackert, T. and Büchler, M. W. (2013). Advanced-stage pancreatic cancer: therapy options. *Nature Reviews Clinical Oncology*, 10:323–333. doi:10.1038/nrclinonc.2013.66.

[207] Winfree, A. T. (1980). *The Geometry of Biological Time*, volume 8. Springer-Verlag, New York, NY.

[208] World Health Organization (2012). Cancer factsheet. URL http://www.who.int/mediacentre/factsheets/fs297/en/index.html.

[209] Wu, H. and Ding, A. A. (1999). Population HIV-1 dynamics in vivo: Applicable models and inferential tools for virological data from AIDS clinical trials. *Biometrics*, 55(2):410–418. doi:10.1111/j.0006-341X.1999.00410.x.

[210] Wu, H., Ding, A. A. and De Gruttola, V. (1998). Estimation of HIV dynamic parameters. *Statistics in Medicine*, 17(21):2463–2485. doi:10.1002/(SICI)1097-0258(19981115)17:21<2463::AID-SIM939>3.0.CO;2-A.

[211] Wu, H., Zhu, H., Miao, H. and Perelson, A. (2008). Parameter identifiability and estimation of HIV/AIDS dynamic models. *Bulletin of Mathematical Biology*, 70:785–799. doi:10.1007/s11538-007-9279-9.

[212] Zhao, G. and Ruan, S. (2011). Existence, uniqueness and asymptotic stability of time periodic traveling waves for a periodic Lotka–Volterra competition system with diffusion. *Journal de Mathematiques Pures et Appliquees*, 95(6):627–671. doi:10.1016/j.matpur.2010.11.005.

[213] Zhou, B.-B. S., Zhang, H., Damelin, M., Geles, K. G., Grindley, J. C. and Dirks, P. B. (2009). Tumour-initiating cells: challenges and opportunities for anticancer drug discovery. *Nature Reviews Drug Discovery*, 8(10):806–823. doi:10.1038/nrd2137.

[214] Zhou, L. and Pao, C. V. (1982). Asymptotic behavior of a competition-diffusion system in population dynamics. *Nonlinear Analysis: Theory, Methods and Applications*, 6(11): 1163–1184. doi:10.1016/0362-546X(82)90028-1.

[215] Zhou, Q., Guo, P., Kruh, G. D., Vicini, P., Wang, X. and Gallo, J. M. (2007). Predicting human tumor drug concentrations from a preclinical pharmacokinetic model of temozolomide brain disposition. *Clinical Cancer Research*, 13(14):4271–4279. doi:10.1158/1078-0432.CCR-07-0658.

[216] Zuckerman, V., Wolyniec, K., Sionov, R. V., Haupt, S. and Haupt, Y. (2009). Tumour sup-

pression by p53: the importance of apoptosis and cellular senescence. *The Journal of Pathology*, 219(1):3–15. doi:10.1002/path.2584.